UNIVERSITÀ
DEGLI STUDI
DI TORINO

Doctoral Dissertation
Doctoral Program in **Pure and Applied Mathematics** (XXXIV Cycle)

Dipartimento di Matematica "Giuseppe Peano" - Università degli Studi di Torino
Dipartimento di Scienze Matematiche "G.L. lagrange" - Politecnico di Torino

Multiscale studies of the constitutive behaviour of biological media

Academic Field: MAT/07 - Mathematical Physics

Ariel Ramírez Torres

* * * * *

Supervisor
Prof. Alfio Grillo

Doctoral Examination Committee:
Prof. Alessandro MUSESTI – Università Cattolica del Sacro Cuore, Brescia, Italy
Prof. Dušan ZORICA – Mathematical Institute, Serbian Academy of Arts and Sciences, Novi Sad, Serbia
Department of Physics, Faculty of Sciences, University of Novi Sad, Novi Sad, Serbia
Prof. Olga BARRERA – Oxford Brookes University, Oxford, UK

PhD Program Coordinators: Prof. Anna Maria Fino, Prof. Andrea Tosin

Università degli Studi di Torino
Politecnico di Torino
Academic Year 2021/2022

I hereby declare that, the contents and organisation of this dissertation constitute my own original work and does not compromise in any way the rights of third parties, including those relating to the security of personal data.

Ariel Ramírez Torres
Glasgow, June 29, 2022

Summary

This Thesis focuses on the mathematical modelling of some problems of biomechanical interest with particular attention to the influence of spatial interactions due to the heterogeneous and complex environment in which these take place.

The Thesis is divided in three parts. In Part I, we concentrate on the influence of two types of non-local phenomena in the growth and remodelling of biological tissues, with special focus on tumour tissues. In Part II, we investigate non-Fickean diffusion in a two-scale composite by means of the asymptotic homogenisation technique. Finally, in Part III, we report on some studies on the electrophysiology of nerve fibers and propose a reformulation of a recent model based on the notion of fractal measure. In particular, the content of this Thesis is based on the following list of papers and book chapters:

1. **Ramírez–Torres, A.**, Di Stefano, S., Grillo, A. (2021) *Influence of non-local diffusion in avascular tumour growth.* Mathematics and Mechanics of Solids, 26(9):1264–1293. https://doi.org/10.1177/1081286520975086

2. **Ramírez–Torres, A.**, Penta, R., Grillo, A. (2021) *Two-scale, non-local diffusion in homogenized heterogeneous media.* Archive of Applied Mechanics. https://doi.org/10.1007/s00419-020-01880-3

3. Hashlamoun, K., Abusara, Z., **Ramírez–Torres, A.**, Grillo, A., Herzog, W., Federico, S. (2020) *Fluorescence recovery after photobleaching: Direct measurement of diffusion anisotropy.* Biomechanics and Modeling in Mechanobiology, 19(6):2397–2412. https://doi.org/10.1007/s10237-020-01346-z

4. Penta, R., Miller, L., Grillo, A., **Ramírez–Torres, A.**, Mascheroni, P., Rodríguez–Ramos, R. (2020) Constitutive modelling of solid continua (J. Merodio & R. Ogden, Eds.). *Porosity and Diffusion in Biological Tissues. Recent Advances and Further Perspectives.* https://doi.org/10.1007/978-3-030-31547-4

5. Grillo, A., Di Stefano, S., **Ramírez–Torres, A.**, Loverre, M. (2019) *A study of growth and remodeling in isotropic tissues, based on the Anand-Aslan-Chester theory of strain-gradient plasticity.* GAMM-Mitteilungen, 42:e20190 0015. https://doi.org/10.1002/gamm.201900015

6. **Ramírez–Torres, A.**, Napoli, V., Grillo, A. (2022) *Fractional versus fractal formulation of the Poisson–Nernst–Plack model for the propagation of the membrane potential in neurons.* In Preparation.

Among the main results of this Thesis, we mention the following:

Part I:

- The use of a strain-gradient framework to analyse the notion of remodelling at two different length scales and provide an interpretation of benchmark problems in which the accumulated remodelling strain is sufficiently localised.
- The impact that the non-local character of diffusion processes have in the evolution of an avascular tumour. We quantify this influence by hypothesising a non-local constitutive law for the diffusive mass flux vector identifiable with derivatives of fractional type.
- The investigation of the effect of remodelling on diffusion processes by which the nutrients are transported throughout a biological tissue.

Part II:

- The quantification of the impact of a spatially non-local diffusion of chemical substances, resolved at the macro- and at the micro-scale of a composite medium, on the transport of such substances within the medium by employing the asymptotic homogenisation technique.
- The realisation of a numerical scheme capable of putting together FE techniques with the integro-differential spatial operators from Fractional Calculus in a composite medium.

Part III:

- The reformulation of the Poisson–Nernst–Planck model in the context of a fractal geometry to describe the complex arrangement of nerve cells in the nervous system.

Other works, produced during the period of the PhD project and in collaboration with international researchers, are reported below. However, these papers will not be considered in the present Thesis.

1. **Ramírez–Torres, A.**, Penta, R., Rodríguez–Ramos, R., Grillo, A. (2019) *Effective properties of hierarchical fiber-reinforced composites via a three-scale asymptotic homogenization approach.* Mathematics and Mechanics of Solids, 24(11):3554–3574. https://doi.org/10.1177/1081286519847687

2. Rodríguez–Ramos, R., **Ramírez–Torres, A.**, Bravo-Castillero, J., Guinovart–Díaz, R., Guinovart–Sanjuán, D., Cruz–González, O. L., . . . , Penta, R. (2020) Constitutive modelling of solid continua (J. Merodio & R. Ogden, Eds.). *Multiscale Homogenization for Linear Mechanics*. https://doi.org/10.1007/978-3-030-31547-4

3. Cruz–González, O., **Ramírez–Torres, A.**, Rodríguez–Ramos, R., Otero, J., Penta, R., Lebon, F. (2021) *Effective behavior of long and short fiber-reinforced viscoelastic composites*. Applications in Engineering Science, 6:100037. https://doi.org/10.1016/j.apples.2021.100037

4. Cruz–González, O., Rodríguez–Ramos, R., Otero, J., **Ramírez–Torres, A.**, Penta, R., Lebon, F. (2020) *On the effective behavior of viscoelastic composites in three dimensions*. International Journal of Engineering Science, 157:103377. https://doi.org/10.1016/j.ijengsci.2020.103377

5. Cruz–González, O. L., **Ramírez–Torres, A.**, Rodríguez–Ramos, R., Penta, R., Bravo–Castillero, J., Guinovart–Díaz, R., . . . , Lebon, F. (2020) *A hierarchical asymptotic homogenization approach for viscoelastic composites*. Mechanics of Advanced Materials and Structures, 28(21):2190–2201. https://doi.org/10.1080/15376494.2020.1722872

6. Penta, R., **Ramírez–Torres, A.**, Merodio, J., Rodríguez–Ramos, R. (2021) *Effective governing equations for heterogeneous porous media subject to inhomogeneous body forces*. Mathematics in Engineering, 3(4):1–17. https://doi.org/10.3934/mine.2021033

7. Marchena–Menéndez, J., **Ramírez–Torres, A.**, Penta, R., Rodríguez–Ramos, R., Merodio, J. (2019) *Macroscopic thermal profile of heterogeneous cancerous breasts. a three-dimensional multiscale analysis*. International Journal of Engineering Science, 144:103135. https://doi.org/10.1016/j.ijengsci.2019.103135

Acknowledgements

It is a genuine pleasure to express my deep sense of thanks and gratitude to my supervisor Prof. Alfio Grillo, above all, for the friendship. His guidance, dedication, meticulous scrutiny and scientific approach have helped to a very great extent to accomplish this task. I have learned and continue learning a lot from him. I would like to believe that I am a better person and researcher thanks to him.

I would like to thank all the people with whom I collaborated or interacted during my PhD studies at the *Politecnico di Torino*. Especially to Dr Raimondo Penta, Prof. Reinaldo Rodríguez Ramos and Prof. Luigi Preziosi, who helped me enormously during this period.

It is my privilege to thank Dr. Salvatore Di Stefano, who is an exceptional person and researcher. His enthusiasm, dynamism and inspiration were fundamental in the development of this work.

I would also like to thank Dr. Eloy Llevat Soy for his friendship and encouragement during these years.

Finally, I am extremely grateful to my family for their constant support. Especially to my wife for always being by my side on this tortuous path.

To my daughter Sofia, my wife Valentina, my mother Olga, and my brother Daniel for your love and support.

Contents

Introduction

The main scope of this Thesis is to evaluate the impact of the consideration of non-local constitutive laws in the evolution of heterogeneous and complex biological media. In particular, we recourse to non-local tools, such as those provided by strain-gradient plasticity and fractional calculus, for the mathematical description of potential non-local spatial interactions occurring in the systems under investigation. In doing this, we consider fully coupled, highly non-linear problems to model the relationships among growth, remodelling and diffusion.

Part I: In Chapter 1, we start by discussing some general aspects of growth and remodelling and the role of diffusion (being active or passive) in the modelling of these phenomena. Furthermore, we bring attention to the consideration of non-local constitutive laws to account for the effect of the medium's environment in the evolution of the phenomenon under investigation.

Motivated by the increasing interest of the biomechanical community towards the employment of strain-gradient theories for solving biological problems, in Chapter 2, we study the growth and remodelling of a biological tissue on the basis of a strain-gradient formulation of remodelling. Our scope is to evaluate the impact of such an approach on the principal physical quantities that determine the growth of the tissue. For our purposes, we assume that remodelling is characterised by a coarse and a fine length scale and, taking inspiration from a work by L. Anand, O. Aslan, and S. A. Chester [14], we introduce a kinematic variable that resolves the fine scale inhomogeneities induced by remodelling. With respect to this variable, a strain-gradient framework of remodelling is developed. We adopt this formulation in order to investigate how a tumour tissue grows *and* how it remodels *in response* to growth. In particular, we focus on a type of remodelling that manifests itself in two different, but complementary, ways: on the one hand, it finds its expression in a stress-induced reorganisation of the adhesion bonds among the tumour cells, and, on the other hand, it leads to a change of shape of the cells and of the tissue, which is generally not recovered when external loads are removed. To address this situation, we resort to a generalised Bilby-Kröner-Lee decomposition of the deformation gradient tensor. We test our model on a benchmark problem taken from the literature, which we rephrase in two ways: micro-scale remodelling is disregarded

in the first case, and accounted for in the second one. Finally, we compare and discuss the obtained numerical results.

Furthermore, in Chapter 3, we focus on the mathematical description of the availability and evolution of chemical agents in the growth of a tumour. Usually, Fick's law of diffusion is adopted for describing the local character of the evolution of chemicals. However, in a highly complex, heterogeneous medium, as is a tumour, the progression of chemical species could be influenced by non-local interactions. In this respect, our goal is to investigate the influence of such types of diffusion on the growth of a tumour in the avascular stage. For our purposes, we consider a diffusion equation for the evolution of the chemical agents that accounts for the existence of non-local interactions in a non-Fickean manner, and that involves notions of fractional calculus. In particular, the introduction of derivatives or integrals of fractional type of order $\alpha \in \mathbb{R}$ has proven to be an effective mathematical tool in the description of various non-local phenomena. To achieve our goals, we adopt part of the modelling assumptions outlined in previous works, in which the growth of a tumour is described in terms of mass transfer among the tumour's constituents and structural changes that occur in the tumour itself in response to growth. The latter ones are characterised by means of the Bilby–Kröner–Lee decomposition of the deformation gradient tensor. We perform numerical simulations and the results indicate the relevance of embracing a fractional framework in modelling tumour growth. Specifically, the real parameter α 'dominates' the way in which the tumour grows, since it permits the modelling of a variety of growth patterns ranging from the standard growth to no growth at all.

Finally, in Chapter 4, we review the set-up necessary for the formulation of a problem of diffusion in a tissue that undergoes remodelling and the steps leading to the definition of the diffusivity tensor in the case of transverse isotropy. Finally, we consider an existing model of non-local diffusion [195, 105, 252], and we adapt it to our framework with the purpose of suggesting further investigations, possibly of interest for biomechanical problems.

Part II: In this Part, we are interested in the study of diffusion in highly heterogeneous biological media (see Chapter 5). Specifically, we study a problem in which the mass flux of a chemical species in each constituent is related to the species' concentration gradient by means of a spatially non-local constitutive law. We do this by admitting that, in principle, two types of non-locality coexist: one pertains to the micro-scale and is thus associated with each constituent of the composite medium, while the other one is introduced *a priori* to allow for a non-local behaviour at the macro-scale. Note that these two types of non-locality are, in general, independent of each other.

Particularly, in Chapter 6, we prescribe the mass flux to obey a two-scale, non-local constitutive law featuring derivatives of fractional order, and we employ the

asymptotic homogenisation technique [250, 34, 72] to obtain an overall description of the species' evolution. As a result, the non-local effects at the micro-scale are *ciphered* in the effective diffusivity while, at the macro-scale, the homogenised problem features an integro-differential equation of fractional type. In particular, we prove that in the limit case in which the non-local interactions are neglected, classical results of asymptotic homogenisation theory are re-obtained.

In Chapter 7, we address the two types of non-locality (that is, the one at the micro-scale and the one at the macro-scale), through dedicated benchmark problems. We remark that the results presented in Chapter 7 can be adapted in a straightforward manner to the study of thermal diffusion. Still, we shall only discuss diffusion of chemical species because the main problems that we have in mind come from the transport of chemical species in biological tissues (see Chapter 5). In particular, we perform numerical simulations to show the impact of the fractional approach on the overall diffusion of species in a composite medium. Our main result is the quantification of the impact of the spatially non-local diffusion of fractional type of chemical substances, resolved at the macro- and at the micro-scale of a strongly heterogeneous composite medium, on the transport of such substances within the medium.

Finally, in Chapter 8, we report some details of the numerical schemes based on Finite Element (FE) methods. Specifically, we concentrate on the matrices and vectors appearing in the algebraic equations resulting from the discretisation process presented in Chapter 7 and investigate some of their properties.

Part III: We focus on the study of the propagation of the action potential in neuron cells. This Part constitutes a first step towards the conception of mathematical models to investigate neurological pathologies characterised by axon demyelination such as, for example, multiple sclerosis.

First, in Chapter 9, we revisit the more salient aspects of the Poisson–Nernst–Planck (PNP) model considered in [96] for the propagation of action potential and perform numerical simulations based on the Finite Elements method. In doing this, our scope is to highlight the most relevant aspects in the formulation of the PNP model and to introduce some fundamental modelling assumptions, such as the consideration of the Hodgkin & Huxley [147] model for ionic currents through the axon's membrane.

Driven by recent studies investigations concerning the fractal branching behaviour of neurons (see, e.g. [259]), in Chapter 10, we reformulate the PNP model in a fractal context. Wit this aim, we start by reformulating Maxwell's equations in the case of a medium with fractal geometry using the the fractal measures introduced in [266]. In this case, we speak about Maxwell's fractal equations. In particular, to determine the fractal equations for the currents, we study the mass balance equations and the dissipation of the system by adapting the approach presented in [141, 39, 129] to the fractal framework under consideration. We mention

that the topics presented in this chapter are part of our current investigations which include, but are not limited to, numerical simulations for a specific problem. This, however, is a challenging task that requires the conception of dedicated computational algorithms. For this reason, the design of such algorithms and the numerical simulations concerning the fractal PNP model are out of the scope of this Thesis.

Part I

Non-locality in the growth and remodelling of biological tissues

Chapter 1

Growth, remodelling and diffusion in biological tissues

The work reported in this chapter has been previously published in [131, 220, 235].

Among the phenomena that characterise the evolution of biological tissues, growth and remodelling certainly play fundamental roles. Growth manifests itself through the variation of the mass of a tissue and, to occur, a complex family of intermingled interactions has to take place [265]. Remodelling, on the other hand, is usually understood as the evolution of the physical, mechanical, and transport properties of a tissue [265]. It may originate from interactions internal to the tissue, or from interactions of the tissue with its environment. In both cases, remodelling may lead to a rearrangement of the tissue's internal structure or to changes observable from outside [76]. Such types of evolution can contribute to modify the tissue's capability of bearing loads and of conducting fluids as well as its sensitivity to external stimuli. A review of the most acknowledged interactions, and of the theoretical tools for taking these into account, can be found in [116, 242, 265, 50, 76, 102, 86, 120, 176, 198, 23, 51, 12, 80, 228, 24, 129, 126, 127, 237, 91, 78], to mention just a few[1].

The growth of a biological tissue consists of the variation and redistribution of its mass, and is the consequence of processes that influence each other reciprocally in spite of their being characterised by different time and length scales [265, 116, 76]. Besides genetic, bio-chemical, and bio-physical phenomena, which pertain to the molecular and intra-cellular scales, the growth of a tissue also depends on interactions that occur at the inter-cellular level, as well as on those that involve the tissue as a whole. The latter two types of interactions are often studied with

[1]The literature on growth and remodelling—especially on the mechanical aspects of these phenomena—has been proliferating in the last years, and even attempting to provide an adequate list of Authors is not an easy task.

the purpose of describing how a tissue evolves, for instance, by adapting its internal structure and material properties in response to the changes of its environment.

In the literature, the noun "growth" may denote markedly different processes. These can be physiological, as in the case of embryonic development, increase of muscular mass, and healing of bone fractures [265, 76], or they may refer to pathological facts, like aortic aneurysm, hypertrophic cardiomyopathy, hyperplasia and, more specifically, formation of tumours (see e.g. [79] for a comprehensive review). Even though, in principle, all of these events are accompanied by structural adaptations, "remodelling" may also stand on its own and, in fact, it has been extensively investigated also alone, i.e., with or without growth (see e.g. [93, 41, 80, 274, 32, 139, 213]).

In fact, the structural adaptation of a tissue may manifest itself in several different ways, and it may involve one or more classes of phenomena, which are often referred to with the common name of *remodelling*. For the types of problems addressed in this work, in which a tissue is viewed as an aggregate of cells, a reorganisation of its internal structure is assumed to occur through the dissolution and reformation of the adhesion bonds among the cells [10, 227, 124], or through a rearrangement of the position, shape, and orientation of the cells in the aggregate [115, 114]. In both cases, remodelling acquires the character of a *configurational* process at the inter-cellular scale, and may result in an inelastic change of shape of the tissue as a whole. More generally, however, when the extracellular matrix (ECM) is accounted for, or in the case of fibre-reinforced tissues, the structural changes take place through the distortion of the ECM's collagenous network [228], or through the reorientation of the collagen fibres.

The problem of fibre reorientation has been addressed in several works, sometimes in connection with growth, and for different types of tissues, these ranging from blood vessels (see e.g. [93, 139, 197, 213]) to articular cartilage (see e.g. [274, 233, 32, 132, 128, 78]). In other situations, as is the case for bone, the concept of structural adaptation is introduced to interpret the formation of cracks [119], the onset of damage, and the occurrence of inelastic distortions that are remnant of the phenomenon of plasticity in metals (see e.g. [179, 201]).

To describe the processes mentioned so far, a tissue may be viewed as a continuum, or a mixture of continua, and its dynamics may be revealed, at least *partially*, by formulating mathematical models based on the laws of continuum mechanics. Such models should capture the "two-level" nature of the phenomena that they are meant to resolve, thereby trying to connect the visible transformations of a tissue with the chemical, electrical, and mechanical interactions occurring inside it. For instance, in the case of growth, a connection of this kind is established by *mechanotransduction* [71, 191], i.e., the modulation that mechanical stress exerts on the tissue's growth rate due to its interplay with the tissue's mass sources. Mechanotransduction has also been recently discussed by [94] in the context of *"inverse*

poroelasticity" for *"soft biomembranes"* and, in particular, in the case of the interplay between mechanical stress and chemical potential that results in the possibility of driving the variations of osmotic pressure through mechanical loading.

When a tissue is modelled as a mixture of continua —typically a fluid phase and one or more solid phases— [49, 23, 12, 129, 124, 125], its growth is usually identified with an inter-phase exchange of mass. Such process is assumed to yield either an accretion of the solid mass at the expenses of the fluid or a loss of solid mass, induced by the disintegration of the tissue cells, which become necrotic and are then dissolved into the fluid. In such a framework, the solid phase is taken as a representation of the tissue cells (and, where appropriate, of the ECM), and a mathematical model of growth should be able to relate the mass variation of the solid phase with the availability of nutrients and with the structural transformations that possibly accompany growth. As already mentioned above, the latter ones are assumed to have inelastic nature and may refer to the redistribution of the solid mass, to the change of the cells' arrangement inside the tissue, so as to mimic the result of the dissolution and reformation of the cellular adhesion bonds, or to a combination of both phenomena.

Since the growth of a tissue is subordinated to the availability of nourishment, an adequate amount of nutrient substances, like for instance oxygen and sugars, has to be supplied to the tissue cells [205, 204, 58]. Hence, to understand the processes underlying the activation, progression and regulation of growth, it is of fundamental importance to describe the mechanisms by which the nutrient substances reach the cells. These mechanisms, in fact, become even more intriguing when remodelling is accounted for, as it contributes to vary the environment in which the nutrients are transported.

The role of the interstitial fluid is to bring the nutrients to the cells, to take away the byproducts of their metabolic activity, and to remove dead cells from the tissue. From this description, it is clear that the interstitial fluid is far from being "pure water". Rather, it is a mixture of water and other substances of various nature, which are commonly denominated *fluid constituents*. The evolution of these substances follows a dynamics that is governed both by their reciprocal interactions and by the interactions of the fluid with the medium. The latter, in turn, varies its shape and internal structure in response to growth and remodelling, thereby changing the flow domain of the fluid.

1.1 Non-locality in the growth and remodelling of a biological tissue

Because of the intrinsic heterogeneous and complex structure of biological tissues, the consideration of local constitutive laws may not be suitable for describing the several interactions among their constituents. In this respect, an alternative

is to recourse to the introduction of constitutive laws of non-local type to account for the influence of the medium's environment in the description of the phenomena acting on the tissue.

Non-locality is a broad notion [104, 117], which covers a wide spectrum of phenomena, from transport processes [106] to plasticity [4, 134] or visco-elasticity [18, 88], and depends on the intrinsic structure of the system to which it is referred and/or on its response to long-range stimuli. Moreover, non-locality can be introduced in different ways, e.g., by having recourse to higher-order gradient theories, as is the case for plasticity [4, 134, 260], or by assigning constitutive laws that feature integro-differential operators [164, 104].

In the following, we discuss two approaches that will be considered in this Thesis for the description of non-local phenomena that may be influencing the growth and remodelling of a biological tissue of interest.

1.1.1 Strain-gradient non-locality

Understanding how growth and remodelling are related to each other is a necessary step towards the comprehension of the evolution of biological tissues. In this respect, we remark that the coupling of growth and remodelling has been investigated in several papers (see e.g. [10, 125, 191] and the references therein, without considering strain-gradient constitutive laws, while second-order theories have been proposed e.g. by Ciarletta et al. [70, 68, 67] to investigate the transport of mass in the presence of morphogenesis (see also [102] for a discussion on this issue). We note that in the case of growth, a theory of strain-gradient type has been recently proposed in [91], although no remodelling was considered.

The type of remodelling induced by mechanical stress can be viewed as a plastic-like behaviour and, if one assumes plastic response to be triggered by a yield stress (as is the case, for instance, in rate-independent [201, 136] or in Perzyna-like plasticity [201]), one may conclude that remodelling commences in the regions of the tissue in which the stress exceeds a certain threshold. Since in a growing tissue such regions are those in which the growth is predominant and the deformation is inhibited, it is very important to resolve accurately the plastic-like distortions. This exigency becomes stringent when the "plastic" strains accumulate in very narrow zones. In such cases, a useful tool of investigation could be to switch from a local to a *"non-local"* model of plasticity. A possible way of accomplishing this task is supplied by the theory proposed by Anand et al. in [14]. However, before exposing such theory and adapting it to our purposes, we should clarify that the framework within which Anand et al. [135, 15, 14] and Gurtin et al. [135] developed their work is deeply different from ours. Indeed, the *"gradient regularisation"* presented in their paper is introduced for numerical reasons, that is, with the purpose of correctly resolving the accumulated plastic strain in the shear bands that arise in strain-softening materials. Anand et al. [14] justify such regularisation by means

of the concept of *"micro-scale plasticity"* and, by doing this, they actually admit the existence of a physics that cannot be captured by standard theories of plasticity. The Authors, in fact, end up with a yield condition expressed by a partial differential equation in the variable that resolves the fine scale remodelling (*"micro-plasticity"*, in the jargon of Anand et al. [14]). Such equation resolves the length scale over which the plastic strain is accumulated, and allows to recover a yield condition in the style of Aifantis [2, 3]. Starting from the approach suggested by Anand et al. [14], and in spite of the differences between their framework and ours, we investigate how the introduction of a fine scale remodelling affects our growth problem.

As explained by [14], the micro-scale plasticity describes the inhomogeneities that arise, in the plastic regions of a material, at a length scale much smaller than the one at which the standard accumulated plastic strains are resolved. According to the theory of Anand et al. [15, 14], and similarly to what is done in [133] and by [135], the micro-scale plasticity is investigated by enriching the standard kinematics that describes an elasto-plastic body. In this respect, a dedicated kinematic descriptor is introduced, whose task is to capture the fine scale plastic inhomogeneities, and, along with it, a force balance equation is added to the list of balance laws of a classical elasto-plastic problem. Such additional force balance is deduced by the means of the Principle of Virtual Powers and, under suitable hypotheses, the forces featuring in it can be obtained constitutively by exploiting the dissipation inequality of the considered system.

We mention that, as is known from the literature, the non-standard approach is necessary for materials exhibiting strain-softening elasto-plastic behaviour, and when the plastic distortions tend to be markedly localised. The occurrence of the strain-softening behaviour is related to the definition of the yield stress of the considered material, expressed as a monotonically decreasing function of the accumulated plastic strain, whereas the localisation of plastic strains may be strongly problem dependent. Before going further, we should thus clarify that, to the best of our knowledge, no strain-softening behaviour has been observed in the biological tissues under investigation: it might occur or not, and, if it occurs, it is not necessarily ascribable to the accumulated plastic strain. Moreover, in the problem analysed in the sequel, the localisation of the accumulated "plastic" strain is not so pronounced to call at all costs for the non-standard approach. It should also be mentioned that the type of remodelling addressed in our work cannot be employed, as it stands, for any kind of biological tissue. In fact, our model might be adequate for tumours [10], as it describes stress-driven irreversible deformations, which are related to a rearrangement of the cells' shape and of the cellular adhesion network. However, it is very likely inappropriate for tissues capable of bearing loads, such as tendons and blood vessels. For such tissues, indeed, the occurrence of remodelling is put in relation to *"tensional homeostasis"* [79]. Furthermore, we can speak of "irreversibility" only for processes occurring over relatively short time windows.

Indeed, even though plastic-like distortions take place, the tissue may recover its initial shape because cells grow or because the cells move actively towards their original configuration.

1.1.2 Non-locality based on Fractional Calculus

It is worth noting that, although the inelastic distortions accompanying growth play an important role on its evolution [145, 11, 80, 125, 191], which may also be partially self-driven [98, 91], the growth of a tissue (e.g. a tumour) is conditioned by the presence of chemical agents of various nature, such as nutrients. Fick's law of diffusion is largely adopted for this purpose, even though it has often turned out to be inconsistent with the results of some observed transport processes [118, 52, 74], which are thus referred to as *non-Fickean*. In fact, non-Fickean diffusion processes have been recognised in several biological tissues, including cells [118, 74], neuromuscular junctions [166] and brain tissue [52], among others. In particular, the experiments conducted by Danyuo et al. [81] suggest that cancer drug release kinetics in breast cancer is non-Fickean.

A common characteristic of the occurrence of non-Fickean patterns, as suggested in several works [161, 200, 118, 156, 113], is the multi-scale and heterogeneous nature of the environment in which diffusion takes place. Specifically, Lacks [166] shows that geometric factors, such as tortuosity, could cause the diffusion processes occurring in a neuromuscular junction to be non-Fickean. Within this view, in the case of a tumour, although to our knowledge there is no experimental evidence that correlates non-Fickean diffusion with its internal structure, its microvascular network is known to have a strong influence on transport phenomena. In fact, this issue has been discussed in several papers, like e.g. [160, 216] and references therein.

Before going further, we notice that in the literature there exist other non-Fickean diffusion laws that, however, do not rely on the assumption of non-local effects. In particular, the Maxwell-Stefan model [162], which generalises Fick's diffusion by the consideration of *"thermodynamic non-idealities"*[2] and *"influence of external force fields"*, has been postulated in the study of porous media and tumour growth [157].

In general, non-Fickean behaviours can be gathered in two categories:

(i) non-locality in time, which associates the mass flux of a given chemical agent with the concentration gradient of that agent through an integro-differential

[2]According to [273], the thermodynamic non-idealities are related to a phenomenon that pertains to a thermodynamic system, like, for instance, a gas, and that occurs through the *"storage of potential energy"* among the molecules of the system itself as a result of the interactions among such molecules. The main consequence of the non-idealities is that the concentrations of the molecules turn out to be different from those expected in the absence of the energy storage among them.

602 relationship, such as, for example, those involving fractional time derivatives
603 or fractional time integrals [21];

604 (ii) non-locality in space, which means that the mass flux vector of a species *can-*
605 *not* be expressed as a point-wise linear function of the concentration gradient,
606 as Fick's law would prescribe.

607 In particular, the employment of integrals and derivatives of fractional order
608 [224, 21, 22] has demonstrated to be an effective method in the description of
609 various non-local phenomena [19, 45, 55], including non-Fickean diffusion [64, 195,
610 82, 209]. As pointed out in [82], the introduction of Fractional Calculus allows
611 for the description of non-Fickean transport processes in a natural way, because of
612 their close connection with the concept of anomalous diffusion [200].

Chapter 2

A strain-gradient approach to remodelling in growing media

The work reported in this chapter has been previously published in [131].

2.1 Introduction

A number of papers has been produced in which growth and remodelling have been described by adopting the language and formalism of continuum theories (see e.g. [199] and the references therein). In some works devoted to the theoretical foundations of volumetric growth (see e.g. [102, 178, 86]), emphasis is put on the necessity of defining variables that, together with the descriptors of the tissue's *standard* mechanical state, are capable of catching its structural transformations. In [102], this is done by having recourse to the theory of uniformity [99, 100], and introducing the concepts of *"archetype"* and *"transplant operator"* [102, 99, 100]. On the other hand, in several other contexts, the Bilby-Kröner-Lee multiplicative decomposition of the deformation gradient tensor is adopted, along with its generalisations, in order to frame remodelling in terms of "plastic-like distortions" (see e.g. [130]). We use this terminology in order to underline that, in the presence of remodelling, the structural transformations of the tissues considered in this work recall the plastic distortions of non-living, elasto-plastic materials. Sometimes, we use the adjectives "plastic" and "remodelling" interchangeably: we take this liberty when a physical quantity, historically conceived for the theory of plasticity, has to be re-interpreted in compliance with the physical context of the present work. A relevant example is the *accumulated plastic strain*, a variable for which we use both its original name and the name *accumulated remodelling strain*. In other cases, however, we use quotation marks for "plastic" and "plasticity", if we need to recall that we are borrowing terms from the theory of plasticity. For instance, we use this convention when we speak of *micro-scale plasticity*.

To further clarify the type of remodelling addressed in this work, and to contextualise the wording "plastic-like distortions", we provide an explicit example of the inelastic rearrangement of the cells of a tissue. For this purpose, we discuss the results of an experiment commented in [114]. In Figure 2.1 (which corresponds to Figure 7 of [114]), Forgacs et al. [114] show three different stages of a cellular aggregate subjected to a loading history referred to as *"centrifugation"* [114]. The first column of Figure 2.1 reports the configuration of the aggregate *"before centrifugation"*[114], when the cells are *"isodiametric"* and the aggregate is spherical. The second column, instead, shows the aggregate after a 5 minute centrifugation: at this stage, the aggregate is no longer spherical, the cells have changed their shape and are said to be in a *"rapidly relaxing, more elastic phase"* [114]. Finally, the third column depicts the configuration of the aggregate after 36 hour centrifugation. In this configuration, the aggregate is believed to have reached a new state of equilibrium, and its cells seem to have attained a state free of stress. Most importantly, the cells seem to have changed their positions and to have redistributed their shape and orientation in a permanent manner, so that the aggregate does not spontaneously tend to recover its original configuration, regardless of the absence of external loads. Forgacs et al. [114] use the theory of viscoelasticity to model the experiment described so far. To us, however, the inelastic behaviour of the cellular aggregate may also suggest interpretations other than, and perhaps complementary to, viscoelasticity. Indeed, looking at the third column of Figure 2.1, one observes that the internal structure of the aggregate has changed, and this change seems to be due to the fact that the cells, relaxed or not, have modified their shape and arrangement inside the tissue. Therefore, at least in our opinion, viscoelasticity alone may be insufficient to accurately account for the irreversible deformations (distortions) of the tissue. Rather, the interpretation of the just discussed phenomenology may necessitate concepts borrowed from the theories of plasticity or viscoplasticity, since these are able to describe the tissue's internal kinematics in a way that is similar to the motion of the defects in solids. This view seems to be corroborated also by other experiments conducted on tumour spheroids (see e.g. [262] and references therein). In such experiments, a spheroid is allowed to grow and, after growth has occurred, it is cut radially for a length of about the 80% of its diameter: what is observed is a relaxation of the stresses, resulting in the opening of the spheroid, with the edges of the cut drifting away from one another (see Figure 2.1d). This behaviour, in fact, suggests the existence of an incompatible, stress-free state of the tumour, which is consistent with the description of the tumour as an elasto-plastic material. To us, this observation justifies the approach followed in our work, although it does not exclude visco-plastic effects. While bearing this in mind, for simplicity we restrict here our investigations to the case of plasticity alone, and we adopt this approach to model the internal rearrangement, i.e., the remodelling, of the tissues studied in our work.

To move forward in the comprehension of how growth and remodelling interact,

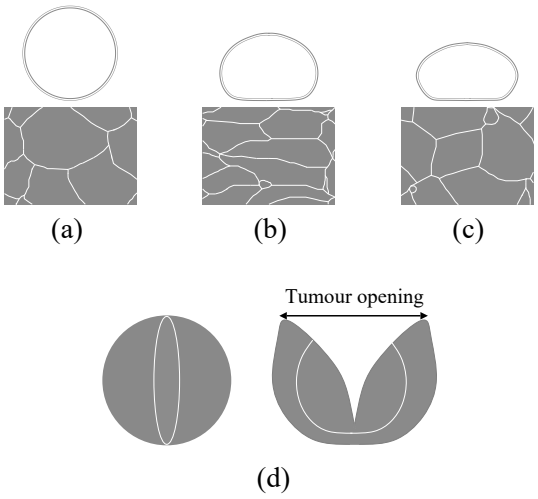

Figure 2.1: First row (redrawn and adapted from Forgacs et al. [114]): Schematic representation of the cells rearrangement in an spherical aggregate (a) before centrifugation, (b) after a 5 minute centrifugation, and (c) after 36 hour centrifugation. Second row (redrawn and adapted from Stylianopoulos et al. [262]): Stress relaxation of a tumour spheroid after a radial cut is performed.

an important question to answer is how to relate mechanical stress with both phenomena (see e.g. [199, 13]). For example, the tearing of the inter-cellular bonds in a tumour, which can be interpreted as an expression of remodelling [10, 227], leads to the relaxation of stress, and stress, apart from mechanotransduction, may play a role on the growth of the tumour. Indeed, a recent result of some of us seems to show that remodelling enhances the growth of a tumour in the avascular stage by increasing the speed at which the tumour's boundary advances in space [191]. Although this result necessitates validations, it may help to estimate qualitatively a possible interplay between remodelling and growth. To this end, Mascheroni et al. [191], drew the conclusion that the observed behaviour was the consequence of the smoothing effect of the plastic-like distortions on mechanical stress, and that such effect was transferred to the term describing growth through the mechanotransduction.

2.1.1 Aim of our work

The main goal of our work is to determine the consequences of a strain-gradient formulation of remodelling on the growth of a biological tissue. Many different paths could be followed to address this question. Indeed, one may adopt the framework developed in [102], in which a constitutive theory is developed that features the first- and second-order gradient of the deformation as well as the first- and second-order *"transplant operators"* [70, 68, 67]. Alternatively, one may turn to a gradient

theory of remodelling in continua with micro-structure by elaborating the Cosserat-type approach put forward in [100]. Another possibility is to have recourse to the higher-order gradient theories presented, for example, by [185] for the case of partially saturated porous media, and by [123] for problems of bone reconstruction (see also [83] for a review).

In this work, we focussed on the approach based on the *"micro-scale plasticity"* of Anand et al. [14] because of its "simplicity". This approach, indeed, is "simple" because it describes the phenomenon of micro-plasticity by means of a *scalar* variable, which makes its use and implementation rather straightforward in the study of growth and remodelling as coupled phenomena.

For our purposes, we consider a benchmark problem taken from the literature [11, 91], and we adapt it to our framework. We elaborate two different formulations of this problem. In the first one, referred to as "standard model" (or approach), we give no room to micro-scale "plasticity", and we adopt the accumulated "plastic" strain, denoted by ε_{p}, as the only measure of the plastic-like distortions representing the tissue's remodelling. In the second formulation, referred to as "non-standard model", we switch on the micro-scale "plasticity" and, as done by [14], we assume that the information about this type of fine scale remodelling is disclosed by a scalar variable, denoted by $\mathfrak{e}_{\mathrm{p}}$. Then, the difference between $\mathfrak{e}_{\mathrm{p}}$ and ε_{p} indicates to what extent remodelling tends to be a two-scale phenomenon.

We emphasise that our leading motivation is to weigh the influence of the strain-gradient approach outlined above on the main descriptors of growth in the considered benchmark problem.

2.1.2 Limitations and novelties

In addition to these considerations, we clarify that, in this work, we study only the case in which growth is inhibited by the lack of nutrients or boosted by their consumption. This hypothesis is typical for tumours, in which cells thrive as long as nourishment is at their disposal. However, more generally, and especially in tissues other than tumours, nutrients are not the only agents responsible for cell proliferation. The latter, indeed, can be repressed or enhanced, depending, for instance, on the presence of physical barriers, lack of space, or the occurrence of contact inhibition mechanisms.

In spite of the limitations outlined above, our approach offers some essential novelties that can improve the interpretation of benchmark problems in which the accumulated remodelling strain is sufficiently localised. This could be the case when the growth of a tissue is strongly promoted by a great availability of nutrients, while its deformation is prohibited by the presence of constraints, like undeformable walls or contact with much stiffer materials. In such situations, indeed, the mechanical stress increases and, when it overcomes a given threshold, a plastic-like remodelling is activated. In the cases in which a confinement of the accumulated "plastic" strain

takes place, e.g. close to an interface separating two materials or at the constrained boundaries of a tissue, the non-standard approach proposed in our work can help to achieve a better resolution of its growth and remodelling.

More in detail, the novelties of the present study with respect to previous publications of some of us [191, 91] are the following: (i) we analyse the coupling between growth and remodelling both theoretically and computationally, and we resolve the remodelling at two different length scales; (ii) with the aid of the theory developed by Anand et al.[14], we formulate remodelling within a strain-gradient framework, thereby generalising our past approaches, which were of "grade zero" in the remodelling variables[1].

Furthermore, the major novelties of our contribution with respect to the work of Anand et al. [14] are the following: (a) in our work, the material is a biphasic medium, featuring a solid and a fluid phase, with the solid phase comprising two populations of cells, and the fluid carrying chemical substances; (b) the interplay between growth and remodelling leads to several interactions that are accounted for in several parts of the mathematical model, and that address, for instance, the evolution of the fluid pressure, of the nutrients, and of the cell populations. Moreover, with reference to point (b), we emphasise the generalisation of the equation for the micro-scale plasticity [14], in which the length associated with the spatial evolution of $\mathfrak{e}_{\mathrm{p}}$, rather than being a constant (cf. [14]), depends on growth and on the coarse scale plastic-like distortions.

2.2 Theoretical background

The problem under investigation involves the motion of the solid phase, the motion of the fluid phase, the distortions related to growth, and plastic-like distortions, which are associated with the reorganisation of the tissue's internal structure. The definitions supplied in this section can be encountered in many works addressing Mixture Theory, and have been recently used for establishing the theoretical framework of previous works of some of us [269, 128, 91, 78]. Such framework, in turn, has been adapted from the kinematic description of biphasic mixtures as developed by [231] and [232].

[1]We remark that, in Grillo et al.[128] and Crevacore et al.[78], we do present a first grade theory for the considered remodelling variable, but such variable does not represent plastic-like distortions. Rather, it is the order parameter describing the mean fibre orientation in a fibre-reinforced biological tissue.

2.2.1 Mass balance laws

Following [191] and [91], the solid phase of the tissue is assumed to comprise only two types of cells, i.e., the proliferating cells and the necrotic ones. Their presence in the tissue is measured by the mass densities $\varphi_\mathrm{s}\rho_\mathrm{s}c_\mathrm{p}$ and $\varphi_\mathrm{s}\rho_\mathrm{s}c_\mathrm{n}$, respectively, where φ_s is the volumetric fraction of the solid phase, ρ_s is its true mass density, while c_p and c_n are the cells' mass fractions, compelled to satisfy the constraint $c_\mathrm{p}+c_\mathrm{n}=1$, everywhere in $\mathscr{C}_t$ and $\mathscr{I}$. Here, $\mathscr{I}\subset\mathbb{R}$ is an interval of time, and $\mathscr{C}_t$ is the subset of the three-dimensional Euclidean space, $\mathscr{S}$, occupied by the biphasic system at time t. Note that the indices "p" and "n" stand for "proliferating" and "necrotic", respectively. Once the composition of the solid phase is specified, it is possible to characterise the mass balance of the solid phase by writing one balance law for each cell population, i.e.,

$$\partial_t(\,\varphi_\mathrm{s}\rho_\mathrm{s}c_\mathrm{p}) + \mathrm{div}\,(\,\varphi_\mathrm{s}\rho_\mathrm{s}c_\mathrm{p}\boldsymbol{v}_\mathrm{s}) = r_\mathrm{fp} + r_\mathrm{pn}, \tag{2.1a}$$

$$\partial_t(\,\varphi_\mathrm{s}\rho_\mathrm{s}c_\mathrm{n}) + \mathrm{div}\,(\,\varphi_\mathrm{s}\rho_\mathrm{s}c_\mathrm{n}\boldsymbol{v}_\mathrm{s}) = r_\mathrm{nf} - r_\mathrm{pn}. \tag{2.1b}$$

As reported by [191] and [91], r_fp describes the transfer of mass from the fluid phase to the solid phase, r_nf measures the dissolution per unit time of the necrotic cells in the fluid, and r_pn is the rate at which the proliferating cells become necrotic. Equations (2.1a) and (2.1b) have been obtained under the assumption that both the proliferating and the necrotic cells move with the velocity of the solid phase, $\boldsymbol{v}_\mathrm{s}$. Moreover, because of the constraint on the mass fractions, they can be rephrased as

$$\partial_t(\,\varphi_\mathrm{s}\rho_\mathrm{s}c_\mathrm{p}) + \mathrm{div}\,(\,\varphi_\mathrm{s}\rho_\mathrm{s}c_\mathrm{p}\boldsymbol{v}_\mathrm{s}) = r_\mathrm{pn} + r_\mathrm{fp}, \tag{2.2a}$$

$$\partial_t(\,\varphi_\mathrm{s}\rho_\mathrm{s}) + \mathrm{div}\,(\,\varphi_\mathrm{s}\rho_\mathrm{s}\boldsymbol{v}_\mathrm{s}) = r_\mathrm{fp} + r_\mathrm{nf} \equiv r_\mathrm{s}. \tag{2.2b}$$

Note that the last equality of Equation (2.2b) defines the overall source/sink of mass of the solid phase, i.e., the term r_s, which describes the variation of the tissue's mass due to growth.

Finally, we relate the occurrence of growth with the presence of nutrients in the tissue. These are conveyed by the fluid phase to the proliferating cells and are believed to activate or inhibit growth depending on whether or not they exceed a certain threshold. To characterise the evolution of the nutrients, we introduce the *nutrients' mass fraction*, c_N, and the mass density $\varphi_\mathrm{f}\rho_\mathrm{f}c_\mathrm{N}$, where φ_f and ρ_f indicate the volumetric fraction and the mass density of the fluid phase, respectively. In addition, we require that the tissue obeys the saturation condition, i.e., $\varphi_\mathrm{f}=1-\varphi_\mathrm{s}$, and we consider the mass balance laws of the nutrients and of the fluid phase as a whole, i.e. [191, 91],

$$\partial_t(\,\varphi_\mathrm{f}\rho_\mathrm{f}c_\mathrm{N}) + \mathrm{div}\,(\,\varphi_\mathrm{f}\rho_\mathrm{f}c_\mathrm{N}\boldsymbol{v}_\mathrm{f} + \boldsymbol{y}_\mathrm{N}) = r_\mathrm{Np}, \tag{2.3a}$$

$$\partial_t(\,\varphi_\mathrm{f}\rho_\mathrm{f}) + \mathrm{div}\,(\,\varphi_\mathrm{f}\rho_\mathrm{f}\boldsymbol{v}_\mathrm{f}) = -r_\mathrm{s}. \tag{2.3b}$$

In (2.3a) and (2.3b), $\boldsymbol{v}_\mathrm{f}$ is the velocity of the fluid phase, $\boldsymbol{y}_\mathrm{N}$ is the mass flux vector associated with the motion of the nutrients relative to $\boldsymbol{v}_\mathrm{f}$, r_Np is the rate at which the nutrients are consumed by the proliferating cells, and the right-hand-side of (2.3b) is taken equal to the negative of r_s in order to ensure the local conservation of mass for the biphasic mixture under study.

Next, we hypothesise that the mass densities of the solid and of the fluid phase can be regarded as constants in the range of interest for the problem at hand. Hence, we set $\rho_\mathrm{s}(x,t) = \rho_\mathrm{s0}$ and $\rho_\mathrm{f}(x,t) = \rho_\mathrm{f0}$ for all $x \in \mathscr{C}_t$ and $t \in \mathscr{I}$, and we summarise (2.2a), (2.2b), (2.3a), and (2.3b) in the following system of equations

$$\varphi_\mathrm{s}\rho_\mathrm{s0}\mathrm{D}_\mathrm{s}c_\mathrm{p} = r_\mathrm{pn} + r_\mathrm{fp} - r_\mathrm{s}c_\mathrm{p}, \tag{2.4a}$$

$$\rho_\mathrm{s0}\mathrm{D}_\mathrm{s}\varphi_\mathrm{s} + \rho_\mathrm{s0}\varphi_\mathrm{s}\,\mathrm{div}\,\boldsymbol{v}_\mathrm{s} = r_\mathrm{s}, \tag{2.4b}$$

$$\varphi_\mathrm{f}\rho_\mathrm{f0}\mathrm{D}_\mathrm{s}c_\mathrm{N} + \varphi_\mathrm{f}\rho_\mathrm{f0}\boldsymbol{w}\,\nabla c_\mathrm{N} + \mathrm{div}\boldsymbol{y}_\mathrm{N} = r_\mathrm{Np} + r_\mathrm{s}c_\mathrm{N}, \tag{2.4c}$$

$$\mathrm{div}\,\boldsymbol{v}_\mathrm{s} + \mathrm{div}\,(\varphi_\mathrm{f}\boldsymbol{w}) = \left(\frac{1}{\rho_\mathrm{s0}} - \frac{1}{\rho_\mathrm{f0}}\right) r_\mathrm{s}, \tag{2.4d}$$

where, for any given physical quantity f, the symbol $\mathrm{D}_\mathrm{s}f \equiv \partial_t f + (\nabla f)\boldsymbol{v}_\mathrm{s}$ denotes the substantial derivative of f with respect to the solid phase velocity, and $\boldsymbol{w} \equiv \boldsymbol{v}_\mathrm{f} - \boldsymbol{v}_\mathrm{s}$ is the velocity of the fluid relative to the solid. Note that the product $\varphi_\mathrm{f}\boldsymbol{w}$ is often referred to as *filtration velocity*[149], although it actually represents a specific mass flux vector [35].

For future use, we remark that the mass balance law (2.4d) can also be recast in the equivalent representation

$$\varphi_\mathrm{s}\mathrm{div}\,\boldsymbol{v}_\mathrm{s} + \varphi_\mathrm{f}\mathrm{div}\,\boldsymbol{v}_\mathrm{f} + (\nabla\varphi_\mathrm{f})\boldsymbol{w} = \left(\frac{1}{\rho_\mathrm{s0}} - \frac{1}{\rho_\mathrm{f0}}\right) r_\mathrm{s}. \tag{2.5}$$

2.2.2 Kinematics

The motion of the solid phase is described by the smooth mapping $\chi : \mathscr{B}\times\mathscr{I} \to \mathscr{S}$, where $\mathscr{B}$ is the tissue's reference configuration. For each pair $(X,t) \in \mathscr{B}\times\mathscr{I}$, the spatial point occupied by the solid phase is given by $x = \chi(X,t) \in \mathscr{S}$. By differentiating χ with respect to its arguments, we obtain the deformation gradient tensor, i.e., the tangent map of χ, defined by $\boldsymbol{F}(X,t) = T\chi(X,t) : T_X\mathscr{B} \to T_{\chi(X,t)}\mathscr{S}$ [189], and the solid phase velocity $\boldsymbol{V}_\mathrm{s}(X,t) = \dot{\chi}(X,t)$. Here, $T_X\mathscr{B}$ and $T_{\chi(X,t)}\mathscr{S}$ are the tangent space of $\mathscr{B}$ at X and the tangent space of $\mathscr{S}$ at $\chi(X,t)$, respectively [189], and the superimposed dot means partial differentiation with respect to time. For completeness, we recall the relationship between $\boldsymbol{V}_\mathrm{s}$ and the Eulerian velocity of the solid phase, i.e., $\boldsymbol{v}_\mathrm{s}(x,t) = \boldsymbol{v}_\mathrm{s}(\chi(X,t),t) = \boldsymbol{V}_\mathrm{s}(X,t)$, so that the composition $\boldsymbol{v}_\mathrm{s}(\,\cdot\,,t)\circ\chi(\,\cdot\,,t) = \boldsymbol{V}_\mathrm{s}(\,\cdot\,,t)$ holds true for all $t \in \mathscr{I}$.

The fluid motion is described by the Eulerian velocity $\boldsymbol{v}_\mathrm{f}(x,t)$, evaluated at every point $x \in \mathscr{S}$ occupied by the fluid and at time $t \in \mathscr{I}$. Note that, since the

system under investigation is a mixture, the fluid co-exists with the solid at every point $x \in \mathscr{S}$ at which the tissue is observed. Thus, the point x can also be viewed as the image of X through the solid motion, i.e., $x = \chi(X,t)$, and the fluid motion can be studied by means of the composition $\boldsymbol{V}_{\mathrm{f}}(\,\cdot\,,t) \equiv \boldsymbol{v}_{\mathrm{f}}(\,\cdot\,,t) \circ \chi(\,\cdot\,,t)$, such that $\boldsymbol{V}_{\mathrm{f}}(X,t) = \boldsymbol{v}_{\mathrm{f}}(\chi(X,t),t)$.

To account for the growth and structural reorganisation of the tissue, we have recourse to the multiplicative decomposition of the deformation gradient tensor, which we propose in the form [10, 155, 125]

$$\boldsymbol{F} = \boldsymbol{F}_{\mathrm{e}}\boldsymbol{F}_{\mathrm{p}}\boldsymbol{F}_{\gamma}. \tag{2.6}$$

In (2.6), $\boldsymbol{F}_{\gamma}$, $\boldsymbol{F}_{\mathrm{p}}$, and $\boldsymbol{F}_{\mathrm{e}}$ describe the distortions associated with the uptake or loss of mass, the distortions accompanying the plastic-like rearrangement of the tissue's internal structure, and the distortions due to the elastic accommodation of the tissue, respectively. In the sequel, $\boldsymbol{F}_{\mathrm{p}}$ and $\boldsymbol{F}_{\gamma}$ will also be referred to as *remodelling tensor*[2] and *growth tensor*, respectively. We notice that, whereas it is rather standard to consider $\boldsymbol{F}_{\mathrm{e}}$ as the first factor of the right-hand-side of (2.6), the order of appearance of $\boldsymbol{F}_{\mathrm{p}}$ and $\boldsymbol{F}_{\gamma}$ is not standard at all. Indeed, it is conceivable to formulate a decomposition of $\boldsymbol{F}$ in which the inelastic contributions to the overall deformation appear in reverse order. In addition, there exist also cases in which the accommodating part of the deformation is put at the end of the decomposition [66]. We adopt the order shown above because, in the present work, we have in mind a tissue that grows *and* that remodels its internal structure *in response* to growth. This statement notwithstanding, we regard growth and structural reorganisation as independent, yet mutually interacting processes. Consequently, we consider $\boldsymbol{F}_{\mathrm{p}}$ and $\boldsymbol{F}_{\gamma}$ as independent kinematic (tensor) variables and, following the same philosophy outlined in some previous publications [60, 86, 213, 129, 91, 78], we associate each of them with degrees of freedom having the same "dignity" as those related to the other kinematic descriptors, i.e., $\boldsymbol{V}_{\mathrm{s}}$ and $\boldsymbol{V}_{\mathrm{f}}$. Finally, we emphasise that the decomposition (2.6) is a generalised Bilby-Kröner-Lee decomposition (see e.g. [201] for similar decompositions in the case of damage or other inelastic processes). Since we have recently discussed the decomposition (2.6) in [91] for the case of growth, here we do not fuss over the physics behind it, and we suggest the reviews [201, 246] for details. However, we recall that, for every $X \in \mathscr{B}$ and $t \in \mathscr{I}$, the product $\boldsymbol{F}_{\mathrm{p}}(X,t)\boldsymbol{F}_{\gamma}(X,t)$ maps vectors of the tangent space $T_X\mathscr{B}$ into vectors of the image vector space $\mathscr{N}_t(X)$, attached at X. By ideally performing such transformation for all $X \in \mathscr{B}$, the solid phase is brought into a relaxed state at time t, the latter being

[2] We use the subscript "p" to emphasise the fact that the distortions associated with remodelling are plastic-like. In this respect, we could have also referred to $\boldsymbol{F}_{\mathrm{p}}$ as "plasticity tensor". However, we prefer to speak here of "remodelling tensor", because the concept of remodelling is more specific for the addressed biological materials.

characterised by the absence of *any* stresses, including the residual ones. Such state is also referred to as *natural state* [201, 126].

Differentiation of $\boldsymbol{F}$ with respect to time and left-multiplication by $\boldsymbol{F}^{-1} = \boldsymbol{F}_\gamma^{-1}\boldsymbol{F}_\mathrm{p}^{-1}\boldsymbol{F}_\mathrm{e}^{-1}$ yield

$$\dot{\boldsymbol{F}}\boldsymbol{F}^{-1} = \dot{\boldsymbol{F}}_\mathrm{e}\boldsymbol{F}_\mathrm{e}^{-1} + \boldsymbol{F}_\mathrm{e}\boldsymbol{L}_\mathrm{p}\boldsymbol{F}_\mathrm{e}^{-1} + \boldsymbol{F}_\mathrm{e}\boldsymbol{F}_\mathrm{p}\boldsymbol{L}_\gamma\boldsymbol{F}_\mathrm{p}^{-1}\boldsymbol{F}_\mathrm{e}^{-1}, \tag{2.7}$$

where we introduced the tensor of *rate of remodelling-induced distortions*, $\boldsymbol{L}_\mathrm{p} \equiv \dot{\boldsymbol{F}}_\mathrm{p}\boldsymbol{F}_\mathrm{p}^{-1}$, and the tensor of *rate of growth-induced distortions*, $\boldsymbol{L}_\gamma \equiv \dot{\boldsymbol{F}}_\gamma\boldsymbol{F}_\gamma^{-1}$. In compliance with (2.6), the *volume ratio* $J \equiv \det\boldsymbol{F}$ can be rewritten as $J = J_\mathrm{e}J_\mathrm{p}J_\gamma$, where $J_\mathrm{e} \equiv \det\boldsymbol{F}_\mathrm{e}$, $J_\mathrm{p} \equiv \det\boldsymbol{F}_\mathrm{p}$, and $J_\gamma \equiv \det\boldsymbol{F}_\gamma$ denote, respectively, the volumetric distortions associated with the elastic, remodelling, and growth part of the deformation gradient tensor. We use these definitions to perform the Piola transformations of (2.4a)–(2.4d), thereby obtaining

$$\rho_{\mathrm{s}0}\Phi_\mathrm{s}\dot{\omega}_\mathrm{p} = R_\mathrm{pn} + R_\mathrm{fp} - R_\mathrm{s}\omega_\mathrm{p}, \tag{2.8a}$$

$$\rho_{\mathrm{s}0}\dot{\Phi}_\mathrm{s} = R_\mathrm{s}, \tag{2.8b}$$

$$\rho_{\mathrm{f}0}\Phi_\mathrm{f}\dot{\omega}_\mathrm{N} + \rho_{\mathrm{f}0}\boldsymbol{Q}\,\mathrm{Grad}\,\omega_\mathrm{N} + \mathrm{Div}\boldsymbol{Y}_\mathrm{N} = R_\mathrm{Np} + R_\mathrm{s}\omega_\mathrm{N}, \tag{2.8c}$$

$$\dot{J} + \mathrm{Div}\,\boldsymbol{Q} = \left(\frac{1}{\rho_{\mathrm{s}0}} - \frac{1}{\rho_{\mathrm{f}0}}\right) R_\mathrm{s}, \tag{2.8d}$$

where, for every $X \in \mathscr{B}$ and $t \in \mathscr{I}$, we denote by

$$\Phi_\alpha(X,t) = J(X,t)\varphi_\alpha(\chi(X,t),t), \qquad \alpha \in \{\mathrm{f},\mathrm{s}\}, \tag{2.9a}$$

$$R_\beta(X,t) = J(X,t)r_\beta(\chi(X,t),t), \qquad \beta \in \{\mathrm{pn},\mathrm{fp},\mathrm{s},\mathrm{Np}\}, \tag{2.9b}$$

$$\omega_\upsilon(X,t) = c_\upsilon(\chi(X,t),t), \qquad \upsilon \in \{\mathrm{p},\mathrm{N}\}, \tag{2.9c}$$

the material volumetric fractions, the material sources/sinks of mass, and the mass fractions expressed as functions of X and time, respectively. Moreover, we introduced the material flux vectors associated with the filtration velocity $\varphi_\mathrm{f}\boldsymbol{w}$ and with the nutrients' mass flux vector $\boldsymbol{y}_\mathrm{N}$, respectively, i.e.,

$$\boldsymbol{Q}(X,t) = \Phi_\mathrm{f}(X,t)\boldsymbol{w}(\chi(X,t),t)\boldsymbol{F}^{-\mathrm{T}}(X,t), \tag{2.10a}$$

$$\boldsymbol{Y}_\mathrm{N}(X,t) = J(X,t)[\boldsymbol{y}_\mathrm{N}(\chi(X,t),t)]\boldsymbol{F}^{-\mathrm{T}}(X,t). \tag{2.10b}$$

In particular, $\boldsymbol{Q}$ will also be referred to as *material filtration velocity* in the sequel.

The kinematic picture of the problem under study is completed with a scalar descriptor, denoted by $\mathrm{e_p} : \mathscr{C}_t \times \mathscr{I} \to \mathbb{R}$. This quantity and its gradient, $\nabla\mathrm{e_p}$, have been introduced by [14] with the purpose of constructing indicators of the inelastic transformations occurring in the body at the scale of its micro-structure. More precisely, [14] speak of $\mathrm{e_p}$ in terms of a *"measure of the inhomogeneity of the microscale plasticity"*. In our framework, it is more appropriate to interpret $\mathrm{e_p}$ as a variable defined to resolve explicitly the inhomogeneities induced by the remodelling of the tissue. To this end, we define the "Lagrangian field" $\mathfrak{e}_\mathrm{p}$, such that $\mathfrak{e}_\mathrm{p}(X,t) = \mathrm{e_p}(\chi(X,t),t)$, and the material gradient $\mathrm{Grad}\mathfrak{e}_\mathrm{p}(X,t) = [\nabla\mathrm{e_p}(\chi(X,t),t)]\boldsymbol{F}(X,t)$.

2.2.3 Constraints on the kinematic variables

By virtue of the presence of growth in our model, the study conducted in this work may be thought of as a slight generalisation of the framework depicted by Anand et al.[14], where the Authors develop a scalar theory of strain-gradient plasticity based on several *ab initio* restrictions on the kinematic variables of their problem. Such restrictions are expressed in terms of the generalised velocities of the proposed theory, and are thus cast in non-holonomic form. To highlight their role on the overall dynamics of the system under investigation, we specify the imposed constraints, and we discuss in detail their impact on the kinematic descriptors that they involve.

For the sake of clarity, we start with rephrasing, in our formalism, the constraints on $\boldsymbol{F}_\mathrm{p}$ and $\dot{\boldsymbol{F}}_\mathrm{p}$ introduced by Anand et al. [14]. On the top of those, we exploit the mass balance laws in order to extract pieces of information that can be interpreted as constraints on the growth tensor, $\boldsymbol{F}_\gamma$, and on its rate $\boldsymbol{L}_\gamma$.

If $\boldsymbol{L}_\mathrm{p}$ is assigned, $\boldsymbol{F}_\mathrm{p}$ can be computed by integrating the ordinary differential equation $\dot{\boldsymbol{F}}_\mathrm{p} = \boldsymbol{L}_\mathrm{p}\boldsymbol{F}_\mathrm{p}$, which can be rewritten as

$$\dot{\boldsymbol{F}}_\mathrm{p} = \left(\boldsymbol{\eta}^{-1}\boldsymbol{D}_\mathrm{p} + \boldsymbol{\eta}^{-1}\boldsymbol{W}_\mathrm{p}\right)\boldsymbol{F}_\mathrm{p}, \tag{2.11}$$

where $\boldsymbol{\eta}$ is the metric tensor associated with the tissue's natural state, while $\boldsymbol{D}_\mathrm{p}$ and $\boldsymbol{W}_\mathrm{p}$ are the symmetric part and the skew-symmetric part of $\boldsymbol{L}_\mathrm{p}$, respectively, i.e.,

$$\boldsymbol{D}_\mathrm{p} = \mathrm{sym}(\boldsymbol{\eta}\boldsymbol{L}_\mathrm{p}) = \tfrac{1}{2}\left(\boldsymbol{\eta}\boldsymbol{L}_\mathrm{p} + \boldsymbol{L}_\mathrm{p}^\mathrm{T}\boldsymbol{\eta}\right), \tag{2.12a}$$

$$\boldsymbol{W}_\mathrm{p} = \mathrm{skew}(\boldsymbol{\eta}\boldsymbol{L}_\mathrm{p}) = \tfrac{1}{2}\left(\boldsymbol{\eta}\boldsymbol{L}_\mathrm{p} - \boldsymbol{L}_\mathrm{p}^\mathrm{T}\boldsymbol{\eta}\right). \tag{2.12b}$$

Following the theory of [14], the *first constraint* on $\boldsymbol{F}_\mathrm{p}$ is supplied by requiring from the outset that the *"plastic" spin tensor*, $\boldsymbol{W}_\mathrm{p}$ vanishes identically, i.e., $\boldsymbol{W}_\mathrm{p} = \boldsymbol{0}$. Hence, we obtain the identity $\boldsymbol{L}_\mathrm{p} = \boldsymbol{\eta}^{-1}\boldsymbol{D}_\mathrm{p}$, and, consequently, Equation (2.11) becomes

$$\dot{\boldsymbol{F}}_\mathrm{p} = \boldsymbol{\eta}^{-1}\boldsymbol{D}_\mathrm{p}\boldsymbol{F}_\mathrm{p}. \tag{2.13}$$

The *second constraint* on $\boldsymbol{F}_\mathrm{p}$ stems from the hypothesis of isochoric remodelling distortions, i.e., $J_\mathrm{p} = \det\boldsymbol{F}_\mathrm{p} = 1$. This relation, in turn, can be put in differential form, i.e., $\dot{J}_\mathrm{p} = J_\mathrm{p}\mathrm{tr}[\dot{\boldsymbol{F}}_\mathrm{p}\boldsymbol{F}_\mathrm{p}^{-1}] = 0$, and implies $\mathrm{tr}[\boldsymbol{\eta}^{-1}\boldsymbol{D}_\mathrm{p}] = 0$, as can be deduced by right-multiplying Equation (2.13) by $\boldsymbol{F}_\mathrm{p}^{-1}$ and taking the trace of the resulting expression. Accordingly, only the deviatoric part of $\boldsymbol{D}_\mathrm{p}$, i.e., $\tilde{\boldsymbol{D}}_\mathrm{p} = \boldsymbol{D}_\mathrm{p} - \frac{1}{3}\mathrm{tr}[\boldsymbol{\eta}^{-1}\boldsymbol{D}_\mathrm{p}]\boldsymbol{\eta}$, is involved in (2.13), which reduces to

$$\dot{\boldsymbol{F}}_\mathrm{p} = \boldsymbol{\eta}^{-1}\tilde{\boldsymbol{D}}_\mathrm{p}\boldsymbol{F}_\mathrm{p}. \tag{2.14}$$

In analogy with [14], we base our model on the further hypothesis that $\tilde{\boldsymbol{D}}_\mathrm{p}$ is *co-directional* with a tensor $\boldsymbol{N}_\nu$, associated with the tissue's natural state, and

obtained by normalising a symmetric tensorial measure of stress, which will be specified later. In formulae, by indicating with $\boldsymbol{\Sigma}_\nu$ such measure of stress, we define $\boldsymbol{N}_\nu$ as

$$\boldsymbol{N}_\nu \equiv \frac{\boldsymbol{\eta}\,\tilde{\boldsymbol{\Sigma}}_\nu\boldsymbol{\eta}}{\|\tilde{\boldsymbol{\Sigma}}_\nu\|_{\boldsymbol{\eta}}}, \tag{2.15}$$

where $\tilde{\boldsymbol{\Sigma}}_\nu \equiv \boldsymbol{\Sigma}_\nu - \frac{1}{3}\mathrm{tr}[\boldsymbol{\eta}\boldsymbol{\Sigma}_\nu]\boldsymbol{\eta}^{-1}$ is the deviatoric part of $\boldsymbol{\Sigma}_\nu$, and $\boldsymbol{\eta}\tilde{\boldsymbol{\Sigma}}_\nu\boldsymbol{\eta}$ is the covariant representation of $\tilde{\boldsymbol{\Sigma}}_\nu$, and we enforce the co-directionality condition as the *third constraint* on $\boldsymbol{F}_\mathrm{p}$, i.e.,

$$\tilde{\boldsymbol{D}}_\mathrm{p} = \|\tilde{\boldsymbol{D}}_\mathrm{p}\|_{\boldsymbol{\eta}^{-1}}\boldsymbol{N}_\nu. \tag{2.16}$$

Equation (2.16) follows from the hypothesis that the distortions associated with remodelling obey an evolution law of the same type as the normality rule of isotropic, associative, finite-strain plasticity. For this reason, the physical quantity that represents them, i.e., $\tilde{\boldsymbol{D}}_\mathrm{p}$, has to be co-directional with $\tilde{\boldsymbol{\Sigma}}_\nu$ (see Sections 95.5 and 98 of Gurtin et al. [136]). In turn, this condition is automatically satisfied by introducing the direction tensor $\boldsymbol{N}_\nu$ and requiring $\tilde{\boldsymbol{D}}_\mathrm{p}$ to be proportional to $\boldsymbol{N}_\nu$. Clearly, this identifies the corresponding proportionality factor with the norm of $\tilde{\boldsymbol{D}}_\mathrm{p}$.

In (2.15) and (2.16), the norms $\|\tilde{\boldsymbol{\Sigma}}_\nu\|_{\boldsymbol{\eta}}$ and $\|\tilde{\boldsymbol{D}}_\mathrm{p}\|_{\boldsymbol{\eta}^{-1}}$ are defined by

$$\|\tilde{\boldsymbol{\Sigma}}_\nu\|_{\boldsymbol{\eta}} = \sqrt{\mathrm{tr}\left[\left(\boldsymbol{\eta}\tilde{\boldsymbol{\Sigma}}_\nu\boldsymbol{\eta}\right)^\mathrm{T}\tilde{\boldsymbol{\Sigma}}_\nu\right]}, \tag{2.17a}$$

$$\|\tilde{\boldsymbol{D}}_\mathrm{p}\|_{\boldsymbol{\eta}^{-1}} = \sqrt{\mathrm{tr}\left[\boldsymbol{\eta}^{-1}\tilde{\boldsymbol{D}}_\mathrm{p}\boldsymbol{\eta}^{-1}\tilde{\boldsymbol{D}}_\mathrm{p}\right]}, \tag{2.17b}$$

and their product coincides with the double contraction $\tilde{\boldsymbol{\Sigma}}_\nu{:}\tilde{\boldsymbol{D}}_\mathrm{p} = \|\tilde{\boldsymbol{\Sigma}}_\nu\|_{\boldsymbol{\eta}}\|\tilde{\boldsymbol{D}}_\mathrm{p}\|_{\boldsymbol{\eta}^{-1}}$. Moreover, to simplify the notation, we invoke the definition of *accumulated plastic strain*[14, 201], ε_p, i.e.,

$$\varepsilon_\mathrm{p}(X,t) \equiv \sqrt{\tfrac{2}{3}}\int_0^t \|\tilde{\boldsymbol{D}}_\mathrm{p}(X,\tau)\|_{\boldsymbol{\eta}^{-1}}\mathrm{d}\tau \quad \Rightarrow \quad \dot{\varepsilon}_\mathrm{p}(X,t) = \sqrt{\tfrac{2}{3}}\,\|\tilde{\boldsymbol{D}}_\mathrm{p}(X,t)\|_{\boldsymbol{\eta}^{-1}}, \tag{2.18}$$

so that Equation (2.16) becomes

$$\tilde{\boldsymbol{D}}_\mathrm{p} = \sqrt{\tfrac{3}{2}}\,\dot{\varepsilon}_\mathrm{p}\boldsymbol{N}_\nu. \tag{2.19}$$

Finally, by substituting (2.19) into (2.14), we obtain

$$\dot{\boldsymbol{F}}_\mathrm{p} = \left(\sqrt{\tfrac{3}{2}}\,\dot{\varepsilon}_\mathrm{p}\boldsymbol{\eta}^{-1}\boldsymbol{N}_\nu\right)\boldsymbol{F}_\mathrm{p} \quad \Rightarrow \quad \boldsymbol{L}_\mathrm{p} = \sqrt{\tfrac{3}{2}}\,\dot{\varepsilon}_\mathrm{p}\boldsymbol{\eta}^{-1}\boldsymbol{N}_\nu. \tag{2.20}$$

Equation (2.20) implies that, once $\boldsymbol{N}_\nu$ is assigned, $\boldsymbol{L}_\mathrm{p}$ has only one independent coefficient, given by $\dot{\varepsilon}_\mathrm{p}$. The important consequence of this result is that the body's structural degrees of freedom, originally represented by the tensorial quantity $\boldsymbol{F}_\mathrm{p}$, condense into the scalar variable ε_p.

Remark 1 (Descriptive adequacy of ε_{p})**.** *According to Equation* (2.18)*,* $\varepsilon_{\mathrm{p}}(X,t)$ *is well-defined for all the tensor fields* $\tilde{\boldsymbol{D}}_{\mathrm{p}}$ *such that the norm* $\|\tilde{\boldsymbol{D}}_{\mathrm{p}}(X,\cdot)\|_{\boldsymbol{\eta}^{-1}}$ *is an integrable function of time over* $[0,t]$*, for every* $X \in \mathscr{B}$ *and* $t \in [0,+\infty[$*. Coherently with this definition,* $\varepsilon_{\mathrm{p}}(X,t)$ *keeps track of all the magnitudes of the rates of inelastic distortions,* $\tilde{\boldsymbol{D}}_{\mathrm{p}}(X,\tau)$*, which have occurred in a given material over* $[0,t]$*. For this reason,* ε_{p} *is a suitable descriptor of the mechanical response of materials that are capable of "perfectly memorising" inelastic distortions, as is the case for metals exhibiting rate-independent plasticity [144]. Biological tissues, on the contrary, are often modelled as viscoelastic materials [115, 114], and show fading memory effects. Nonetheless, as discussed in the Introduction, the experiments on cellular aggregates reported in [114, 262] seem to suggest the existence of inelastic distortions that do not fade away in time, unless some active process restores the original configuration of the aggregates. For these reasons,* ε_{p} *can be regarded as appropriate for describing the inelastic distortions accumulated in a tissue from the beginning of its loading history. Should the active processes be considered, they could be accounted for by introducing another factor, denoted e.g. by* $\boldsymbol{F}_{\mathrm{a}}$*, and representing the active part of the tissue's deformation [223].*

We switch now to the constraints placed on $\boldsymbol{F}_\gamma$, and we analyse their impact on the way in which the mass balance law (2.8b) can be reformulated. Upon using the decomposition $J = J_{\mathrm{e}}J_{\mathrm{p}}J_\gamma$, and recalling the condition $J_{\mathrm{p}} = 1$, we rewrite Φ_{s} as $\Phi_{\mathrm{s}} = J_\gamma \Phi_{\mathrm{s}\nu}$, where $\Phi_{\mathrm{s}\nu}$ is such that $\Phi_{\mathrm{s}\nu}(X,t) = J_{\mathrm{e}}(X,t)\varphi_{\mathrm{s}}(\chi(X,t),t)$, and indicates, thus, the solid phase volumetric fraction with respect to the volume measure of the *natural state*. Hence, Equation (2.8b) becomes

$$\rho_{\mathrm{s}0}\dot{J}_\gamma \Phi_{\mathrm{s}\nu} + \rho_{\mathrm{s}0} J_\gamma \dot{\Phi}_{\mathrm{s}\nu} = R_{\mathrm{s}}. \tag{2.21}$$

A rather standard hypothesis in the mechanics of growth, see e.g. [102, 11, 178, 176], is to choose $\boldsymbol{F}_\gamma$ in such a way that the time derivative of its determinant, $\dot{J}_\gamma$, compensates for the mass source R_{s}. In other words, by exploiting the identity $\dot{J}_\gamma = J_\gamma \mathrm{tr}[\dot{\boldsymbol{F}}_\gamma \boldsymbol{F}_\gamma^{-1}] = J_\gamma \mathrm{tr}[\boldsymbol{L}_\gamma]$, we require the fulfilment of the auxiliary condition

$$\rho_{\mathrm{s}0} J_\gamma \Phi_{\mathrm{s}\nu} \mathrm{tr}[\boldsymbol{L}_\gamma] = R_{\mathrm{s}} \quad \Rightarrow \quad \mathrm{tr}[\boldsymbol{L}_\gamma] = \frac{R_{\mathrm{s}}}{\rho_{\mathrm{s}0}\Phi_{\mathrm{s}\nu}J_\gamma}, \tag{2.22}$$

which constitutes the *first constraint* on $\boldsymbol{F}_\gamma$. Such constraint has, in fact, non-holonomic nature, since it is defined through a non-homogeneous algebraic condition on the generalised (tensorial) velocity $\boldsymbol{L}_\gamma$. Plugging (2.22) into (2.21) yields $\rho_{\mathrm{s}0} J_\gamma \dot{\Phi}_{\mathrm{s}\nu} = 0$, thereby implying that the volumetric fraction $\Phi_{\mathrm{s}\nu}$ is necessarily independent of time.

The *second constraint* on $\boldsymbol{F}_\gamma$ is provided by the phenomenological evidence according to which, for the class of problems under study, growth occurs isotropically[10]. The consequences of this fact on the admissible choices of the growth

tensor can be deduced by looking at the polar decompositions of $\boldsymbol{F}_\gamma$. Indeed, by considering for instance the right decomposition, $\boldsymbol{F}_\gamma = \boldsymbol{\mathcal{R}}_\gamma \boldsymbol{U}_\gamma$, where $\boldsymbol{\mathcal{R}}_\gamma$ is the rotation tensor and $\boldsymbol{U}_\gamma$ is the stretch tensor associated with $\boldsymbol{F}_\gamma$, the isotropy of growth translates to the kinematic restrictions $\boldsymbol{\mathcal{R}}_\gamma = \boldsymbol{I}$ and $\boldsymbol{U}_\gamma = \gamma \boldsymbol{I}$, where $\boldsymbol{I}$ is the identity tensor. Therefore, it holds that $\boldsymbol{F}_\gamma = \gamma \boldsymbol{I}$ and (2.22) can be rephrased as

$$\frac{\dot{\gamma}}{\gamma} = \frac{R_\mathrm{s}}{3\rho_{\mathrm{s}0}\Phi_{\mathrm{s}\nu} J_\gamma} \quad \Rightarrow \quad \dot{\gamma} = \frac{R_\mathrm{s}}{3\rho_{\mathrm{s}0}\Phi_{\mathrm{s}\nu}\gamma^2}. \tag{2.23}$$

Finally, we notice that Equation (2.8d) can be regarded as a constraint on the material filtration velocity, $\boldsymbol{Q}$, expressed through a restriction on its divergence.

2.3 Principle of Virtual Powers

After laying down the kinematic picture that describes the problem under investigation, we select the generalised velocities upon which the system's mechanical power is defined. Summarising the discussion reported above, such velocities may be enlisted in the following collection of fields

$$\mathscr{V} = (\boldsymbol{v}_\mathrm{s}, \nabla \boldsymbol{v}_\mathrm{s}, \mathrm{D_s}\varepsilon_\mathrm{p}, \mathrm{D_s e_p}, \nabla(\mathrm{D_s e_p}) \,|\, \boldsymbol{v}_\mathrm{f}, \nabla \boldsymbol{v}_\mathrm{f}), \tag{2.24}$$

which will be employed to define the internal and the external mechanical powers. We remark that, whereas the fluid phase requires only $\boldsymbol{v}_\mathrm{f}$ and $\nabla \boldsymbol{v}_\mathrm{f}$ for the characterisation of the system's internal power, the solid phase necessitates both *standard* and *non-standard* descriptors. The standard ones, i.e., $\boldsymbol{v}_\mathrm{s}$ and $\nabla \boldsymbol{v}_\mathrm{s}$, account only for the *"visible"* changes of shape of the system (here, the word *"visible"* is meant in the sense of DiCarlo and Quiligotti [86]), while the non-standard terms are the generalised velocities $\mathrm{D_s}\varepsilon_\mathrm{p}$, $\mathrm{D_s e_p}$, and $\nabla(\mathrm{D_s e_p})$, introduced to define the power expended to accomplish the structural changes of the system. As anticipated in the Introduction, the main motivation for taking the approach of Anand et al. [14] and specialising it to our problem is that it allows to develop a strain-gradient formulation of remodelling based on the scalar variable $\mathrm{e_p}$. The latter is defined as the micro-scale counterpart of the accumulated remodelling strain, ε_p, and, as such, it is assumed to "condense" in itself all the information about the inelastic processes that determine the micro-scale remodelling of the tissue under study. Moreover, since it is an "effective" representative of these processes, it prevents from the introduction of a micro-scale, second-order remodelling tensor, which would render the theoretical and numerical analysis of the problem at hand much more complicated. Accordingly, the generalised velocities associated with $\mathrm{e_p}$, i.e., $\mathrm{D_s e_p}$ and $\nabla(\mathrm{D_s e_p})$, are a scalar and a co-vector field, rather than being a second-order and a third-order tensor field, respectively. It follows from these considerations that an inelastic model built on ε_p and $\mathrm{e_p}$ has the right to stand on its own, independently

on any numerical issue, even though Anand et al. [14] have originally introduced $\mathrm{e_p}$ for numerical purposes. Clearly, such a model represents the limit case of more elaborated theories that involve tensor fields, rather than scalar ones.

Coherently with (2.24), we introduce the collection of virtual velocities

$$\mathscr{V}_{\mathrm{v}} = (\boldsymbol{u}_{\mathrm{s}}, \nabla\boldsymbol{u}_{\mathrm{s}}, u_{\varepsilon}, u_{\mathrm{p}}, \nabla u_{\mathrm{p}} | \, \boldsymbol{u}_{\mathrm{f}}, \nabla\boldsymbol{u}_{\mathrm{f}}) \in \mathscr{V}_{\mathrm{v}}, \tag{2.25}$$

where $\mathscr{V}_{\mathrm{v}}$ is referred to as the set of all virtual velocities. The elements $\boldsymbol{u}_{\mathrm{s}}$, $\nabla\boldsymbol{u}_{\mathrm{s}}$, $\boldsymbol{u}_{\mathrm{f}}$, and $\nabla\boldsymbol{u}_{\mathrm{f}}$ are the virtual counterparts of $\boldsymbol{v}_{\mathrm{s}}$, $\nabla\boldsymbol{v}_{\mathrm{s}}$, $\boldsymbol{v}_{\mathrm{f}}$, and $\nabla\boldsymbol{v}_{\mathrm{f}}$, respectively, and the non-standard fields u_{ε}, u_{p}, and ∇u_{p} denote the virtual velocities corresponding to the rates $\mathrm{D_s}\varepsilon_{\mathrm{p}}$, $\mathrm{D_s e_p}$, and $\nabla(\mathrm{D_s e_p})$, respectively.

Once the virtual velocities of the model are identified, it is possible to write the internal and the external virtual powers of the system. These two linear and continuous functionals are defined over $\mathscr{V}_{\mathrm{v}}$, and are specified through the expressions

$$\begin{aligned}\mathscr{W}_{\mathrm{v}}^{(\mathrm{i})}(\mathscr{V}_{\mathrm{v}}) \equiv \int_{\mathscr{C}_t} \big\{ &\boldsymbol{\sigma}_{\mathrm{s}} : \boldsymbol{g}\nabla\boldsymbol{u}_{\mathrm{s}} + \boldsymbol{m}_{\mathrm{s}} . \boldsymbol{u}_{\mathrm{s}} + \boldsymbol{\sigma}_{\mathrm{f}} : \boldsymbol{g}\nabla\boldsymbol{u}_{\mathrm{f}} + \boldsymbol{m}_{\mathrm{f}} . \boldsymbol{u}_{\mathrm{f}} + h_{\varepsilon}^{(\mathrm{i})} u_{\varepsilon} \\ &+ h_{\mathrm{p}}^{(\mathrm{i})} u_{\mathrm{p}} + \boldsymbol{\xi}_{\mathrm{p}} \nabla u_{\mathrm{p}} \big\} \, , \end{aligned} \tag{2.26a}$$

$$\mathscr{W}_{\mathrm{v}}^{(\mathrm{e})}(\mathscr{V}_{\mathrm{v}}) \equiv \int_{\Gamma_t^N} \big\{ \boldsymbol{\tau}_{\mathrm{s}} . \boldsymbol{u}_{\mathrm{s}} + \boldsymbol{\tau}_{\mathrm{f}} . \boldsymbol{u}_{\mathrm{f}} + \zeta_{\mathrm{p}} u_{\mathrm{p}} \big\} + \int_{\mathscr{C}_t} \big\{ h_{\varepsilon}^{(\mathrm{e})} u_{\varepsilon} + h_{\mathrm{p}}^{(\mathrm{e})} u_{\mathrm{p}} \big\} \, , \tag{2.26b}$$

respectively. Here, $\mathscr{C}_t \subset \mathscr{S}$ is the portion of the Euclidean space in which the solid and the fluid phase co-exist, and $\Gamma_t^N \subset \partial\mathscr{C}_t$ is the portion of the boundary of $\mathscr{C}_t$ on which Neumann conditions are imposed. In (2.26a), $\boldsymbol{\sigma}_{\mathrm{s}}$ and $\boldsymbol{\sigma}_{\mathrm{f}}$ are the Cauchy stress tensors of the solid and of the fluid, $\boldsymbol{m}_{\mathrm{s}}$ and $\boldsymbol{m}_{\mathrm{f}}$ are internal forces that describe the gain or loss of momentum of the solid and of the fluid in response to exchange interactions between the two phases, $h_{\varepsilon}^{(\mathrm{i})}$ and $h_{\mathrm{p}}^{(\mathrm{i})}$ are internal generalised forces dual to u_{ε} and u_{p}, respectively, and $\boldsymbol{\xi}_{\mathrm{p}}$ is the generalised stress-like field dual to ∇u_{p}. We notice that, since the virtual velocities u_{ε} and u_{p} are scalar fields, the forces dual to them must be representable by scalars. Following the same logic, supplied by duality, since ∇u_{p} is a co-vector by definition, its power-conjugate force, $\boldsymbol{\xi}_{\mathrm{p}}$, must be a vector-like field. On the same footing, in addition to the standard vector-like contact forces $\boldsymbol{\tau}_{\mathrm{s}}$ and $\boldsymbol{\tau}_{\mathrm{f}}$, in (2.26b) we introduce the contact force ζ_{p} and the "bulk" external forces $h_{\varepsilon}^{(\mathrm{e})}$ and $h_{\mathrm{p}}^{(\mathrm{e})}$, all being scalar-like for the reasons explained above.

By requiring the internal virtual power, $\mathscr{W}_{\mathrm{v}}^{(\mathrm{i})}(\mathscr{V}_{\mathrm{v}})$, to be invariant under the superposition of arbitrary rigid motions, we deduce the symmetry of the total stress tensor, $\boldsymbol{\sigma} = \boldsymbol{\sigma}_{\mathrm{s}} + \boldsymbol{\sigma}_{\mathrm{f}}$, and that the sum of the internal forces $\boldsymbol{m}_{\mathrm{s}}$ and $\boldsymbol{m}_{\mathrm{f}}$ must vanish identically, i.e., we obtain the condition $\boldsymbol{m}_{\mathrm{s}} + \boldsymbol{m}_{\mathrm{f}} = \boldsymbol{0}$ [232]. Consistently with the *a priori* exclusion of all inertial terms from our model, this last result constitutes an approximation of the more general balance of internal forces that, for a biphasic medium with mass exchange between the phases, is given by $\boldsymbol{m}_{\mathrm{s}} + r_{\mathrm{s}}\boldsymbol{v}_{\mathrm{s}} + \boldsymbol{m}_{\mathrm{f}} - r_{\mathrm{s}}\boldsymbol{v}_{\mathrm{f}} =$

$\mathbf{0}$. In fact, the approximation consists of dropping the term $r_{\mathrm{s}}\boldsymbol{v}_{\mathrm{s}} - r_{\mathrm{s}}\boldsymbol{v}_{\mathrm{f}} = -r_{\mathrm{s}}\boldsymbol{w}$, and is based on the argument that the interphase mass transfer, r_{s}, depends on the micro-scale velocity with which the mass passes from the fluid to the solid, and vice versa. Such velocity, multiplied by the relative macro-scale velocity $\boldsymbol{w}$, is assumed to produce a rate of momentum exchange that weighs much less than $\boldsymbol{m}_{\mathrm{s}}$ and $\boldsymbol{m}_{\mathrm{f}}$, thereby leading to the desired approximation.

We emphasise that, in writing the expressions of $\mathscr{W}_{\mathrm{v}}^{(\mathrm{i})}(\mathscr{V}_{\mathrm{v}})$ and $\mathscr{W}_{\mathrm{v}}^{(\mathrm{e})}(\mathscr{V}_{\mathrm{v}})$, we have omitted *all* inertial and long-range (e.g. gravity) forces, which we regard as negligible from the outset. Moreover, the nature of the forces $h_{\mathrm{p}}^{(\mathrm{i})}$ and $\boldsymbol{\xi}_{\mathrm{p}}$ is necessarily coherent with the hypothesis that the kinematics of the solid phase micro-structure is represented by e_{p} and $\nabla\mathrm{e}_{\mathrm{p}}$. In this sense, the model features some important similarities with Gurtin's approach to the derivation of the generalised Allen-Cahn equation [133], in which the scalar field describing the micro-structural kinematics of the considered medium is regarded as an order parameter.

Looking at (2.26a) and (2.26b), we also notice that, in principle, also the velocity and the velocity gradient of the nutrients should be considered, along with their virtual counterparts, in (2.24) and (2.25). However, in view of a comprehensive formulation of the Principle of Virtual Powers, this would call for the definition of the generalised forces expending power on them, and, above all, for the introduction of surface tractions, acting on Γ_t^N. Individuating a physically sound way for expressing such contact forces is not easy and taking them into account leads unavoidably to both theoretical and computational complications (see, e.g., Grillo et al.[129] for an attempt of including these forces, based on a work by Sciarra et al. [254]). For these reasons, we present here a simplified framework in which we account for the nutrients through the balance law (2.3a), while we omit to study their kinematics and dynamics in detail. In other words, due to their tantamount importance for activating growth, we do include them in our model, but we do not treat them systematically. Hence, we do not consider any force balance associated with the nutrients, nor do we investigate their contribution to the dissipation inequality (see Section 2.4). Rather, with reference to (2.3a), we "guess" that the mass flux vector, $\boldsymbol{y}_{\mathrm{N}}$, obeys a diffusion dynamics of Fickean type, so that it is prescribed to have the form $\boldsymbol{y}_{\mathrm{N}} = -\rho_{\mathrm{f}0}\boldsymbol{d}\nabla c_{\mathrm{N}}$ in the Eulerian description and $\boldsymbol{Y}_{\mathrm{N}} = -\rho_{\mathrm{f}0}\boldsymbol{D}\,\mathrm{Grad}\,\omega_{\mathrm{N}}$ in material formalism, with $\boldsymbol{d}$ being the diffusivity tensor and $\boldsymbol{D}$ its material counterpart. Note that the latter is related to $\boldsymbol{d}$ through the backward Piola transformation $\boldsymbol{D}(X,t) = J(X,t)\boldsymbol{F}^{-1}(\chi(X,t),t)\boldsymbol{d}(\chi(X,t),t)\boldsymbol{F}^{-\mathrm{T}}(X,t)$.

By invoking the Principle of Virtual Powers, we enforce the condition $\mathscr{W}_{\mathrm{v}}^{(\mathrm{i})}(\mathscr{V}_{\mathrm{v}}) = \mathscr{W}_{\mathrm{v}}^{(\mathrm{e})}(\mathscr{V}_{\mathrm{v}})$, which is required to be fulfilled for any admissible set of generalised velocities $\mathscr{V}_{\mathrm{v}}$, thereby leading to

$$\int_{\mathscr{C}_t} \big\{[-\mathrm{div}\boldsymbol{\sigma}_{\mathrm{s}} + \boldsymbol{m}_{\mathrm{s}}].\boldsymbol{u}_{\mathrm{s}} + [-\mathrm{div}\boldsymbol{\sigma}_{\mathrm{f}} + \boldsymbol{m}_{\mathrm{f}}].\boldsymbol{u}_{\mathrm{f}} + [h_{\varepsilon}^{(\mathrm{i})} - h_{\varepsilon}^{(\mathrm{e})}]u_{\varepsilon}$$

$$+[h_{\rm p}^{\rm (i)} - {\rm div}\boldsymbol{\xi}_{\rm p} - h_{\rm p}^{\rm (e)}]u_{\rm p}\big\} + \int_{\Gamma_t^N} \{[\boldsymbol{\sigma}_{\rm s}.\boldsymbol{n} - \boldsymbol{\tau}_{\rm s}].\boldsymbol{u}_{\rm s} + [\boldsymbol{\sigma}_{\rm f}.\boldsymbol{n} - \boldsymbol{\tau}_{\rm f}].\boldsymbol{u}_{\rm f}$$
$$+[\boldsymbol{\xi}_{\rm p}.\boldsymbol{n} - \zeta_{\rm p}]u_{\rm p}\big\} = 0. \tag{2.27}$$

By adopting the usual localisation procedure that extracts the local form of the equations of motion from the Principle of Virtual Powers, Equation (2.27) yields the following balances of generalised forces

$$\boldsymbol{m}_{\rm s} - {\rm div}\boldsymbol{\sigma}_{\rm s} = \boldsymbol{0}, \tag{2.28a}$$
$$\boldsymbol{m}_{\rm f} - {\rm div}\boldsymbol{\sigma}_{\rm f} = \boldsymbol{0}, \tag{2.28b}$$
$$h_{\varepsilon}^{\rm (i)} - h_{\varepsilon}^{\rm (e)} = 0, \tag{2.28c}$$
$$h_{\rm p}^{\rm (i)} - {\rm div}\boldsymbol{\xi}_{\rm p} - h_{\rm p}^{\rm (e)} = 0, \tag{2.28d}$$

which hold in $\mathscr{C}_t$, and the balances of contact forces on Γ_t^N

$$\boldsymbol{\sigma}_{\rm s}.\boldsymbol{n} - \boldsymbol{\tau}_{\rm s} = \boldsymbol{0}, \tag{2.29a}$$
$$\boldsymbol{\sigma}_{\rm f}.\boldsymbol{n} - \boldsymbol{\tau}_{\rm f} = \boldsymbol{0}, \tag{2.29b}$$
$$\boldsymbol{\xi}_{\rm p}.\boldsymbol{n} - \zeta_{\rm p} = 0. \tag{2.29c}$$

It is worthwhile to mention that, in general, upon defining the field of *total* contact forces $\boldsymbol{\tau} = \boldsymbol{\tau}_{\rm s} + \boldsymbol{\tau}_{\rm f}$, and the *total* Cauchy stress tensor $\boldsymbol{\sigma} = \boldsymbol{\sigma}_{\rm s} + \boldsymbol{\sigma}_{\rm f}$, it is rather natural to provide on Γ_t^N boundary conditions of the kind $\boldsymbol{\sigma}.\boldsymbol{n} = \boldsymbol{\tau}$ (see [254] for details). Nevertheless, even in that case, the boundary conditions (2.29a) and (2.29b) can be recovered under the assumption that $\boldsymbol{\tau}_{\rm s}$ and $\boldsymbol{\tau}_{\rm f}$ are obtained by partitioning $\boldsymbol{\tau}$ as $\boldsymbol{\tau}_{\rm s} = (\rho_{\rm s0}\varphi_{\rm s}/\rho)\boldsymbol{\tau}$ and $\boldsymbol{\tau}_{\rm f} = (\rho_{\rm f0}\varphi_{\rm f}/\rho)\boldsymbol{\tau}$, respectively.

2.4 Dissipation and Dynamic Equations

To extract constitutive information on the internal forces presented so far, we study the dissipation inequality of the system. For this purpose, we enrich the picture proposed in Grillo et al.[129], which, in turn, was inspired by Hassanizadeh[141] and Benethum et al.[39]. This is done by framing the formulation of Anand et al. [14] in the context of biphasic media and, above all, by rephrasing it in order to account for growth. The first step in this direction is to introduce the dissipation density, $\mathscr{D}$, measured per unit volume of the current configuration of the medium, and defining the dissipation associated with an open subset $\Omega_t \subset \mathscr{C}_t$ as

$$\int_{\Omega_t} \mathscr{D} = -\int_{\Omega_t} \{r_{\rm s}(\psi_{\rm s} - \psi_{\rm f}) + \rho_{\rm s0}\varphi_{\rm s}{\rm D}_{\rm s}\psi_{\rm s} + \rho_{\rm f0}\varphi_{\rm f}{\rm D}_{\rm s}\psi_{\rm f} + (\rho_{\rm f0}\varphi_{\rm f}\nabla\psi_{\rm f})\boldsymbol{w}\}$$
$$+ \int_{\partial\Omega_t} \big\{(\boldsymbol{\sigma}_{\rm s}.\boldsymbol{n}).\boldsymbol{v}_{\rm s} + (\boldsymbol{\sigma}_{\rm f}.\boldsymbol{n}).\boldsymbol{v}_{\rm f} + (\boldsymbol{\xi}_{\rm p}.\boldsymbol{n}){\rm D}_{\rm s}{\rm e}_{\rm p}\big\} + \int_{\Omega_t} \big\{h_{\varepsilon}^{\rm (e)}{\rm D}_{\rm s}\varepsilon_{\rm p}$$

$$+h_{\mathrm{p}}^{(\mathrm{e})}\mathrm{D_s e_p}\big\} + \int_{\Omega_t} \mathscr{D}_\gamma \geq 0. \tag{2.30}$$

As shown in (2.30), the dissipation can be written as the sum of four different contributions: with reference to the first integral of the sum defining $\int_{\Omega_t} \mathscr{D}$, we recognise that, by indicating with ψ_{s} and ψ_{f} the Helmholtz free energies per unit mass of the solid and of the fluid, the term $r_{\mathrm{s}}(\psi_{\mathrm{s}} - \psi_{\mathrm{f}})$ expresses the rate of change of the free energy densities, $\rho_{\mathrm{s}0}\varphi_{\mathrm{s}}\psi_{\mathrm{s}}$ and $\rho_{\mathrm{f}0}\varphi_{\mathrm{f}}\psi_{\mathrm{f}}$, due to the mass exchange between the phases. Moreover, $\rho_{\mathrm{s}0}\varphi_{\mathrm{s}}\mathrm{D_s}\psi_{\mathrm{s}}$ and $\rho_{\mathrm{f}0}\varphi_{\mathrm{f}}\mathrm{D_s}\psi_{\mathrm{f}}$ are the rates of change of the Helmholtz free energy densities measured with respect to the solid phase motion, and $(\nabla\psi_{\mathrm{f}})\boldsymbol{w}$ describes how ψ_{f} is transported due to the motion of the fluid relative to the solid. The terms in the surface integral denote the contributions to the net power expended on Ω_t due to the contact forces with the surrounding medium, while the terms in the third integral represent the part of net power ascribable to the non-standard forces $h_{\varepsilon}^{(\mathrm{e})}$ and $h_{\mathrm{p}}^{(\mathrm{e})}$. Finally, $\mathscr{D}_\gamma$ is a dissipation density introduced to account for the fact that the medium experiences growth (see e.g. [126] for a discussion on this issue).

By applying Gauss Theorem to the surface integral of Equation (2.30), and using the balance laws (2.28a)–(2.28d) and (2.29a)–(2.29c), the dissipation inequality becomes

$$\begin{aligned}\int_{\Omega_t} \mathscr{D} = &- \int_{\Omega_t} \{r_{\mathrm{s}}(\psi_{\mathrm{s}} - \psi_{\mathrm{f}}) + \rho_{\mathrm{s}0}\varphi_{\mathrm{s}}\mathrm{D_s}\psi_{\mathrm{s}} + \rho_{\mathrm{f}0}\varphi_{\mathrm{f}}\mathrm{D_s}\psi_{\mathrm{f}} + (\rho_{\mathrm{f}0}\varphi_{\mathrm{f}}\nabla\psi_{\mathrm{f}})\boldsymbol{w}\} \\ &+ \int_{\Omega_t} \big\{\boldsymbol{m}_{\mathrm{s}}.\boldsymbol{v}_{\mathrm{s}} + \boldsymbol{\sigma}_{\mathrm{s}}:\boldsymbol{g}\nabla\boldsymbol{v}_{\mathrm{s}} + \boldsymbol{m}_{\mathrm{f}}.\boldsymbol{v}_{\mathrm{f}} + \boldsymbol{\sigma}_{\mathrm{f}}:\boldsymbol{g}\nabla\boldsymbol{v}_{\mathrm{f}} + h_{\mathrm{p}}^{(\mathrm{i})}\mathrm{D_s e_p} \\ &+ \boldsymbol{\xi}_{\mathrm{p}}\nabla(\mathrm{D_s e_p}) + h_{\varepsilon}^{(\mathrm{i})}\mathrm{D_s}\varepsilon_{\mathrm{p}}\big\} + \int_{\Omega_t} \mathscr{D}_\gamma \geq 0.\end{aligned} \tag{2.31}$$

By localising Equation (2.31) and invoking the condition $\boldsymbol{m}_{\mathrm{s}} + \boldsymbol{m}_{\mathrm{f}} = \boldsymbol{0}$, we obtain

$$\begin{aligned}\mathscr{D} = &\, r_{\mathrm{s}}(\psi_{\mathrm{f}} - \psi_{\mathrm{s}}) - \rho_{\mathrm{s}0}\varphi_{\mathrm{s}}\mathrm{D_s}\psi_{\mathrm{s}} - \rho_{\mathrm{f}0}\varphi_{\mathrm{f}}\mathrm{D_s}\psi_{\mathrm{f}} + [\boldsymbol{m}_{\mathrm{f}} - \boldsymbol{g}^{-1}(\rho_{\mathrm{f}0}\varphi_{\mathrm{f}}\nabla\psi_{\mathrm{f}})].\boldsymbol{w} \\ &+ \boldsymbol{\sigma}_{\mathrm{s}}:\boldsymbol{g}\nabla\boldsymbol{v}_{\mathrm{s}} + \boldsymbol{\sigma}_{\mathrm{f}}:\boldsymbol{g}\nabla\boldsymbol{v}_{\mathrm{f}} + h_{\mathrm{p}}^{(\mathrm{i})}\mathrm{D_s e_p} + \boldsymbol{\xi}_{\mathrm{p}}\nabla(\mathrm{D_s e_p}) + h_{\varepsilon}^{(\mathrm{i})}\mathrm{D_s}\varepsilon_{\mathrm{p}} + \mathscr{D}_\gamma \geq 0.\end{aligned} \tag{2.32}$$

As a simplifying assumption, we approximate the Helmholtz free energy density of the fluid, ψ_{f}, with a constant, so that $\rho_{\mathrm{f}0}\varphi_{\mathrm{f}}\mathrm{D_s}\psi_{\mathrm{f}}$ and $\nabla\psi_{\mathrm{f}}$ are negligible with respect to all the other terms featuring in the dissipation inequality. Such situation occurs, for instance, when the state variables characterising ψ_{f} are, at the most, the temperature and the mass fraction of the nutrients dissolved in the fluid, and the latter is so low that ψ_{f} can be safely set equal to the (constant) Helmholtz free energy density of water at constant temperature. Under these hypotheses, Equation (2.32) becomes

$$\mathscr{D} = r_{\mathrm{s}}(\psi_{\mathrm{f}} - \psi_{\mathrm{s}}) - \rho_{\mathrm{s}0}\varphi_{\mathrm{s}}\mathrm{D_s}\psi_{\mathrm{s}} + \boldsymbol{m}_{\mathrm{f}}.\boldsymbol{w} + \boldsymbol{\sigma}_{\mathrm{s}}:\boldsymbol{g}\nabla\boldsymbol{v}_{\mathrm{s}} + \boldsymbol{\sigma}_{\mathrm{f}}:\boldsymbol{g}\nabla\boldsymbol{v}_{\mathrm{f}} + h_{\mathrm{p}}^{(\mathrm{i})}\mathrm{D_s e_p}$$

$$+ \boldsymbol{\xi}_{\mathrm{p}} \nabla(\mathrm{D_s e_p}) + h_{\varepsilon}^{(\mathrm{i})} \mathrm{D_s} \varepsilon_{\mathrm{p}} + \mathscr{D}_{\gamma} \geq 0. \tag{2.33}$$

It is convenient to rewrite the dissipation inequality per unit volume of $\mathscr{B}$. To do this, we perform a Piola transformation of (2.33), which yields

$$\begin{aligned} \mathscr{D}_{\mathrm{R}} = {} & R_{\mathrm{s}}(\Psi_{\mathrm{f}} - \Psi_{\mathrm{s}}) - \rho_{\mathrm{s}0} J_{\gamma} \Phi_{\mathrm{s}\nu} \dot{\Psi}_{\mathrm{s}} + \Phi_{\mathrm{f}}^{-1} \boldsymbol{Q} \boldsymbol{M}_{\mathrm{f}} + \boldsymbol{P}_{\mathrm{s}} : \boldsymbol{g} \dot{\boldsymbol{F}} + \boldsymbol{P}_{\mathrm{f}} : \boldsymbol{g} \mathrm{Grad} \boldsymbol{V}_{\mathrm{f}} \\ & + H_{\mathrm{p}}^{(\mathrm{i})} \dot{\mathfrak{e}}_{\mathrm{p}} + \boldsymbol{\Xi}_{\mathrm{p}} \mathrm{Grad} \dot{\mathfrak{e}}_{\mathrm{p}} + H_{\varepsilon}^{(\mathrm{i})} \dot{\varepsilon}_{\mathrm{p}} + J \mathscr{D}_{\gamma} \geq 0, \end{aligned} \tag{2.34}$$

where, as anticipated above, $R_{\mathrm{s}}(X,t) = J(X,t) r_{\mathrm{s}}(\chi(X,t),t)$ is the material form of the source/sink of mass for the solid phase as a whole, and we introduced the notation

$$\Psi_{\alpha}(X,t) = \psi_{\alpha}(\chi(X,t),t), \qquad \alpha \in \{\mathrm{f},\mathrm{s}\}, \tag{2.35a}$$

$$\boldsymbol{P}_{\alpha}(X,t) = J(X,t) \boldsymbol{\sigma}_{\alpha}(\chi(X,t),t) \boldsymbol{F}^{-\mathrm{T}}(X,t), \qquad \alpha \in \{\mathrm{f},\mathrm{s}\}, \tag{2.35b}$$

$$H_{\beta}^{(\mathrm{i})}(X,t) = J(X,t) h_{\beta}^{(\mathrm{i})}(\chi(X,t),t), \qquad \beta \in \{\mathrm{p},\varepsilon\}, \tag{2.35c}$$

$$\boldsymbol{\Xi}_{\mathrm{p}}(X,t) = J(X,t) \boldsymbol{\xi}_{\mathrm{p}}(\chi(X,t),t) \boldsymbol{F}^{-\mathrm{T}}(X,t), \tag{2.35d}$$

$$\boldsymbol{M}_{\mathrm{f}}(X,t) = J(X,t) [\boldsymbol{g}(\chi(X,t)) \boldsymbol{m}_{\mathrm{f}}(\chi(X,t),t)] \boldsymbol{F}(X,t). \tag{2.35e}$$

Here, $\boldsymbol{P}_{\mathrm{f}}$ and $\boldsymbol{P}_{\mathrm{s}}$ indicate the first Piola-Kirchhoff stress tensors of the fluid and the solid phase, $H_{\mathrm{p}}^{(\mathrm{i})}$ and $H_{\varepsilon}^{(\mathrm{i})}$ express, in material form, the internal generalised forces dual to $\dot{\mathfrak{e}}_{\mathrm{p}}$ and $\dot{\varepsilon}_{\mathrm{p}}$, respectively, $\boldsymbol{\Xi}_{\mathrm{p}}$ is the material representation of the stress-like generalised force, $\boldsymbol{\xi}_{\mathrm{p}}$, and is thus dual to $\mathrm{Grad}\dot{\mathfrak{e}}_{\mathrm{p}}$, and $\boldsymbol{M}_{\mathrm{f}}$, re-defined as a covector, is the material counterpart of the momentum exchange rate $\boldsymbol{m}_{\mathrm{f}}$.

Finally, by generalising the Helmholtz free energy density proposed by [14], we prescribe Ψ_{s} to be given by the sum of three terms, i.e.,

$$\begin{aligned} \hat{\Psi}_{\mathrm{s}}(\boldsymbol{F}, \boldsymbol{F}_{\mathrm{p}}, \boldsymbol{F}_{\gamma}, \varepsilon_{\mathrm{p}}, \mathfrak{e}_{\mathrm{p}}, \mathrm{Grad}\mathfrak{e}_{\mathrm{p}}) = {} & \hat{\Psi}_{\mathrm{s}}^{(\mathrm{st})}(\boldsymbol{F} \boldsymbol{F}_{\gamma}^{-1} \boldsymbol{F}_{\mathrm{p}}^{-1}) + \tfrac{1}{2} a_0 [\varepsilon_{\mathrm{p}} - \mathfrak{e}_{\mathrm{p}}]^2 \\ & + \tfrac{1}{2} b_0 \boldsymbol{F}_{\gamma}^{-1} \boldsymbol{B}_{\mathrm{p}} \boldsymbol{F}_{\gamma}^{-\mathrm{T}} : \mathrm{Grad}\mathfrak{e}_{\mathrm{p}} \otimes \mathrm{Grad}\mathfrak{e}_{\mathrm{p}}, \end{aligned} \tag{2.36}$$

with $\boldsymbol{B}_{\mathrm{p}} = \boldsymbol{F}_{\mathrm{p}}^{-1} . \boldsymbol{F}_{\mathrm{p}}^{-\mathrm{T}}$, so that the time derivative of Ψ_{s} reads

$$\begin{aligned} \dot{\Psi}_{\mathrm{s}} = {} & \left(\frac{\partial \hat{\Psi}_{\mathrm{s}}^{(\mathrm{st})}}{\partial \boldsymbol{F}_{\mathrm{e}}} \boldsymbol{F}_{\mathrm{p}}^{-\mathrm{T}} \boldsymbol{F}_{\gamma}^{-\mathrm{T}} \right) : \dot{\boldsymbol{F}} - \frac{1}{3} \frac{\mathrm{tr}(\boldsymbol{\eta}\, \boldsymbol{\Sigma}_{\nu})}{\rho_{\mathrm{s}0} \Phi_{\mathrm{s}\nu}} \frac{R_{\mathrm{s}}}{\rho_{\mathrm{s}0} \Phi_{\mathrm{s}\nu} J_{\gamma}} \\ & - \frac{1}{\rho_{\mathrm{s}0} \Phi_{\mathrm{s}\nu}} \left\{ \sqrt{\tfrac{3}{2}} \| \tilde{\boldsymbol{\Sigma}}_{\nu} \|_{\boldsymbol{\eta}} - A_{\nu} [\varepsilon_{\mathrm{p}} - \mathfrak{e}_{\mathrm{p}}] \right\} \dot{\varepsilon}_{\mathrm{p}} \\ & - \frac{A_{\nu}}{\rho_{\mathrm{s}0} \Phi_{\mathrm{s}\nu}} [\varepsilon_{\mathrm{p}} - \mathfrak{e}_{\mathrm{p}}] \dot{\mathfrak{e}}_{\mathrm{p}} + \frac{B_{\nu}}{\rho_{\mathrm{s}0} \Phi_{\mathrm{s}\nu}} \left[\left(\boldsymbol{F}_{\gamma}^{-1} \boldsymbol{B}_{\mathrm{p}} \boldsymbol{F}_{\gamma}^{-\mathrm{T}} \right) \mathrm{Grad}\mathfrak{e}_{\mathrm{p}} \right] \overline{\dot{\mathrm{Grad}\mathfrak{e}_{\mathrm{p}}}}, \end{aligned} \tag{2.37}$$

where $\hat{\Psi}_{\mathrm{s}}^{(\mathrm{st})}$ is differentiated with respect to $\boldsymbol{F}_{\mathrm{e}} = \boldsymbol{F} \boldsymbol{F}_{\gamma}^{-1} \boldsymbol{F}_{\mathrm{p}}^{-1}$. In (2.37), we introduced the notation

$$\boldsymbol{\Sigma}_{\nu} = \boldsymbol{\eta}^{-1} \boldsymbol{F}_{\mathrm{e}}^{\mathrm{T}} \left(\rho_{\mathrm{s}0} \Phi_{\mathrm{s}\nu} \frac{\partial \hat{\Psi}_{\mathrm{s}}^{(\mathrm{st})}}{\partial \boldsymbol{F}_{\mathrm{e}}} \right)$$

$$+ B_\nu \left[\boldsymbol{\eta}^{-1} \boldsymbol{F}_{\mathrm{p}}{}^{-\mathrm{T}} \boldsymbol{F}_{\gamma}{}^{-\mathrm{T}} \left(\mathrm{Grad}\mathfrak{e}_{\mathrm{p}} \otimes \mathrm{Grad}\mathfrak{e}_{\mathrm{p}} \right) \boldsymbol{F}_{\gamma}{}^{-1} \boldsymbol{F}_{\mathrm{p}}{}^{-1} \boldsymbol{\eta}^{-1} \right], \tag{2.38a}$$

$$\tilde{\boldsymbol{\Sigma}}_\nu = \boldsymbol{\Sigma}_\nu - \tfrac{1}{3}\mathrm{tr}[\boldsymbol{\eta}\boldsymbol{\Sigma}_\nu]\boldsymbol{\eta}^{-1}, \tag{2.38b}$$

$$A_\nu = \rho_{\mathrm{s}0}\Phi_{\mathrm{s}\nu} a_0, \tag{2.38c}$$

$$B_\nu = \rho_{\mathrm{s}0}\Phi_{\mathrm{s}\nu} b_0, \tag{2.38d}$$

where A_ν and B_ν are the counterparts of the strictly positive constants a_0 and b_0, expressed per unit volume of the tissue's natural state, and $\boldsymbol{\Sigma}_\nu$ is a generalised Mandel stress tensor that comprises both the standard definition of the Mandel stress tensor, i.e.,

$$\boldsymbol{\Sigma}_\nu^{(\mathrm{st})} = \boldsymbol{\eta}^{-1} \boldsymbol{F}_{\mathrm{e}}{}^{\mathrm{T}} \left(\rho_{\mathrm{s}0}\Phi_{\mathrm{s}\nu} \frac{\partial \hat{\Psi}_{\mathrm{s}}^{(\mathrm{st})}}{\partial \boldsymbol{F}_{\mathrm{e}}} \right), \tag{2.39}$$

and the non-standard stress-like contribution

$$\boldsymbol{\Sigma}_\nu^{(\text{n-st})} = B_\nu \left[\boldsymbol{\eta}^{-1} \boldsymbol{F}_{\mathrm{p}}{}^{-\mathrm{T}} \boldsymbol{F}_{\gamma}{}^{-\mathrm{T}} \left(\mathrm{Grad}\mathfrak{e}_{\mathrm{p}} \otimes \mathrm{Grad}\mathfrak{e}_{\mathrm{p}} \right) \boldsymbol{F}_{\gamma}{}^{-1} \boldsymbol{F}_{\mathrm{p}}{}^{-1} \boldsymbol{\eta}^{-1} \right]. \tag{2.40}$$

We remark that $\boldsymbol{\Sigma}_\nu^{(\text{n-st})}$ is purely configurational, and it descends from the introduction of the micro-scale plasticity variable $\mathfrak{e}_{\mathrm{p}}$. Moreover, $\boldsymbol{\Sigma}_\nu^{(\text{n-st})}$ is independent of deformation, whereas it does depend on the growth and remodelling distortions, $\boldsymbol{F}_\gamma$ and $\boldsymbol{F}_{\mathrm{p}}$.

Remark 2 (Tensor $\boldsymbol{\Sigma}_\nu$ and co-directionality)**.** *In our work, the deviatoric part of the generalised Mandel stress tensor, $\tilde{\boldsymbol{\Sigma}}_\nu$, is the stress tensor used to define $\boldsymbol{N}_\nu$ in* (2.15)*. Therefore, it is the tensor with which the rate of plastic distortions, $\tilde{\boldsymbol{D}}_{\mathrm{p}}$, is co-directional. By virtue of the definition of $\boldsymbol{N}_\nu$, the direction of $\tilde{\boldsymbol{D}}_{\mathrm{p}}$ in the space of the symmetric second-order tensors is determined, partially, by the deviatoric part of the standard Mandel stress tensor, $\tilde{\boldsymbol{\Sigma}}_\nu^{(st)}$, and partially by $\tilde{\boldsymbol{\Sigma}}_\nu^{(n\text{-}st)}$, which includes the contributions of the micro-scale "plasticity", through* $\mathrm{Grad}\mathfrak{e}_{\mathrm{p}}$*, and of the growth and remodelling distortions through $\boldsymbol{F}_\gamma$ and $\boldsymbol{F}_{\mathrm{p}}$, respectively. In the work of Anand et al. [14], instead, $\boldsymbol{N}_\nu$ is determined by $\boldsymbol{\Sigma}_\nu^{(\mathrm{st})}$ only.*

By substituting (2.37) into (2.34), $\mathscr{D}_{\mathrm{R}}$ becomes

$$\begin{aligned}
\mathscr{D}_{\mathrm{R}} = &\left\{ -J_\gamma \left(\rho_{\mathrm{s}0}\Phi_{\mathrm{s}\nu} \frac{\partial \hat{\Psi}_{\mathrm{s}}^{(\mathrm{st})}}{\partial \boldsymbol{F}_{\mathrm{e}}} \boldsymbol{F}_{\mathrm{p}}{}^{-\mathrm{T}} \boldsymbol{F}_{\gamma}{}^{-\mathrm{T}} \right) + \boldsymbol{g}\boldsymbol{P}_{\mathrm{s}} \right\} : \dot{\boldsymbol{F}} + \left\{ \Psi_{\mathrm{f}} - \Psi_{\mathrm{s}} + \frac{1}{3} \frac{\mathrm{tr}\left(\boldsymbol{\eta}\,\boldsymbol{\Sigma}_\nu\right)}{\rho_{\mathrm{s}0}\Phi_{\mathrm{s}\nu}} \right\} R_{\mathrm{s}} \\
&+ \left\{ H_\varepsilon^{(\mathrm{i})} + J_\gamma \sqrt{\tfrac{3}{2}} \|\tilde{\boldsymbol{\Sigma}}_\nu\|_{\boldsymbol{\eta}} - J_\gamma A_\nu [\varepsilon_{\mathrm{p}} - \mathfrak{e}_{\mathrm{p}}] \right\} \dot{\varepsilon}_{\mathrm{p}} + \left\{ H_{\mathrm{p}}^{(\mathrm{i})} + J_\gamma A_\nu [\varepsilon_{\mathrm{p}} - \mathfrak{e}_{\mathrm{p}}] \right\} \dot{\mathfrak{e}}_{\mathrm{p}} \\
&+ \left\{ \boldsymbol{\Xi}_{\mathrm{p}} - J_\gamma B_\nu \left[\left(\boldsymbol{F}_\gamma{}^{-1} \boldsymbol{B}_{\mathrm{p}} \boldsymbol{F}_\gamma{}^{-\mathrm{T}} \right) \mathrm{Grad}\mathfrak{e}_{\mathrm{p}} \right] \right\} \dot{\overline{\mathrm{Grad}\mathfrak{e}_{\mathrm{p}}}} \\
&+ \Phi_{\mathrm{f}}^{-1} \boldsymbol{Q}\boldsymbol{M}_{\mathrm{f}} + \boldsymbol{P}_{\mathrm{f}} : \boldsymbol{g}\mathrm{Grad}\boldsymbol{V}_{\mathrm{f}} + J\mathscr{D}_\gamma \geq 0\,.
\end{aligned} \tag{2.41}$$

We study the dissipation inequality (2.41) by regarding the mass balance law (2.5) as a constraint [175, 39], and appending it to $\mathscr{D}_{\mathrm{R}}$. To this end, we perform the Piola transformation of (2.5), thereby obtaining (see e.g. [39, 129])

$$\begin{aligned}\mathscr{C}_{\mathrm{R}} \equiv & \Phi_{\mathrm{s}}\boldsymbol{F}^{-\mathrm{T}}\!:\dot{\boldsymbol{F}} + \Phi_{\mathrm{f}}\boldsymbol{F}^{-\mathrm{T}}\!:\mathrm{Grad}\boldsymbol{V}_{\mathrm{f}} + J\Phi_{\mathrm{f}}^{-1}\boldsymbol{Q}\,\mathrm{Grad}(J^{-1}\Phi_{\mathrm{f}}) \\ & - \left(\frac{1}{\rho_{\mathrm{s}0}} - \frac{1}{\rho_{\mathrm{f}0}}\right) R_{\mathrm{s}} = 0, \end{aligned} \tag{2.42}$$

where $\mathscr{C}_{\mathrm{R}}$ stands for "constraint". Then, we multiply (2.42) by a Lagrange multiplier, p, which plays the role of hydrostatic pressure, and we attach the resulting expression to (2.41). This leads to a "new" dissipation function, $\mathscr{D}_{\mathrm{R}}^{\mathrm{new}} \equiv \mathscr{D}_{\mathrm{R}} + p\mathscr{C}_{\mathrm{R}}$, that is equal to $\mathscr{D}_{\mathrm{R}}$, but is put in the form

$$\begin{aligned}\mathscr{D}_{\mathrm{R}}^{\mathrm{new}} = & \left\{ -J_\gamma \left(\rho_{\mathrm{s}0}\Phi_{\mathrm{s}\nu} \frac{\partial \hat{\Psi}_{\mathrm{s}}^{(\mathrm{st})}}{\partial \boldsymbol{F}_{\mathrm{e}}} \boldsymbol{F}_{\mathrm{p}}^{-\mathrm{T}} \boldsymbol{F}_{\gamma}^{-\mathrm{T}} \right) + p\,\Phi_{\mathrm{s}}\boldsymbol{F}^{-\mathrm{T}} + \boldsymbol{g}\boldsymbol{P}_{\mathrm{s}} \right\} : \dot{\boldsymbol{F}} \\ & + \left\{ p\,\Phi_{\mathrm{f}}\boldsymbol{F}^{-\mathrm{T}} + \boldsymbol{g}\boldsymbol{P}_{\mathrm{f}} \right\} : \mathrm{Grad}\boldsymbol{V}_{\mathrm{f}} + \Phi_{\mathrm{f}}^{-1}\boldsymbol{Q}\left\{ \boldsymbol{M}_{\mathrm{f}} + Jp\,\mathrm{Grad}(J^{-1}\Phi_{\mathrm{f}}) \right\} \\ & + \left\{ \left(\Psi_{\mathrm{f}} + \frac{p}{\rho_{\mathrm{f}0}} \right) - \left(\Psi_{\mathrm{s}} + \frac{p}{\rho_{\mathrm{s}0}} \right) + \frac{1}{3}\frac{\mathrm{tr}\,(\boldsymbol{\eta}\,\boldsymbol{\Sigma}_\nu)}{\rho_{\mathrm{s}0}\Phi_{\mathrm{s}\nu}} \right\} R_{\mathrm{s}} + J\mathscr{D}_\gamma \\ & + \left\{ H_\varepsilon^{(\mathrm{i})} + J_\gamma\sqrt{\tfrac{3}{2}}\,\|\tilde{\boldsymbol{\Sigma}}_\nu\|_{\boldsymbol{\eta}} - J_\gamma A_\nu[\varepsilon_{\mathrm{p}} - \mathfrak{e}_{\mathrm{p}}] \right\} \dot{\varepsilon}_{\mathrm{p}} + \left\{ H_{\mathrm{p}}^{(\mathrm{i})} + J_\gamma A_\nu[\varepsilon_{\mathrm{p}} - \mathfrak{e}_{\mathrm{p}}] \right\} \dot{\mathfrak{e}}_{\mathrm{p}} \\ & + \left\{ \boldsymbol{\Xi}_{\mathrm{p}} - J_\gamma B_\nu \left[\left(\boldsymbol{F}_{\gamma}^{-1}\boldsymbol{B}_{\mathrm{p}}\boldsymbol{F}_{\gamma}^{-\mathrm{T}} \right) \mathrm{Grad}\mathfrak{e}_{\mathrm{p}} \right] \right\} \dot{\overline{\mathrm{Grad}\mathfrak{e}_{\mathrm{p}}}} \geq 0. \end{aligned} \tag{2.43}$$

2.4.1 Constitutive Laws

We require that the inequality (2.43) be valid for arbitrary values of $\dot{\boldsymbol{F}}$, $\mathrm{Grad}\boldsymbol{V}_{\mathrm{f}}$, $\dot{\mathfrak{e}}_{\mathrm{p}}$, and $\dot{\overline{\mathrm{Grad}\mathfrak{e}_{\mathrm{p}}}}$. Hence, the Coleman-Noll method implies the following identifications

$$\boldsymbol{P}_{\mathrm{s}} = -\Phi_{\mathrm{s}}p\,\boldsymbol{g}^{-1}\boldsymbol{F}^{-\mathrm{T}} + J_\gamma \left(\rho_{\mathrm{s}0}\Phi_{\mathrm{s}\nu}\boldsymbol{g}^{-1} \frac{\partial \hat{\Psi}_{\mathrm{s}}^{(\mathrm{st})}}{\partial \boldsymbol{F}_{\mathrm{e}}} \boldsymbol{F}_{\mathrm{p}}^{-\mathrm{T}} \boldsymbol{F}_{\gamma}^{-\mathrm{T}} \right), \tag{2.44a}$$

$$\boldsymbol{P}_{\mathrm{f}} = -\Phi_{\mathrm{f}}p\,\boldsymbol{g}^{-1}\boldsymbol{F}^{-\mathrm{T}}, \tag{2.44b}$$

$$H_{\mathrm{p}}^{(\mathrm{i})} = -J_\gamma A_\nu[\varepsilon_{\mathrm{p}} - \mathfrak{e}_{\mathrm{p}}], \tag{2.44c}$$

$$\boldsymbol{\Xi}_{\mathrm{p}} = J_\gamma B_\nu \left[\boldsymbol{F}_{\gamma}^{-1}\boldsymbol{B}_{\mathrm{p}}\boldsymbol{F}_{\gamma}^{-\mathrm{T}} \right] \mathrm{Grad}\mathfrak{e}_{\mathrm{p}}. \tag{2.44d}$$

In (2.44a), and in the sequel, the standard part of the solid phase Helmholtz free energy density, $\hat{\Psi}_{\mathrm{s}}^{(\mathrm{st})}$, is assumed to be of the Holmes-Mow type [149], i.e.,

$$\hat{\Psi}_{\mathrm{s}}^{(\mathrm{st})}(\boldsymbol{F}_{\mathrm{e}}) = \frac{\alpha_0}{\rho_{\mathrm{s}0}\Phi_{\mathrm{s}\nu}} \left\{ \exp\left(\hat{f}(\boldsymbol{C}_{\mathrm{e}}) \right) - 1 \right\}, \tag{2.45}$$

where $\boldsymbol{C}_\mathrm{e} = \boldsymbol{F}_\mathrm{e}^\mathrm{T}.\boldsymbol{F}_\mathrm{e}$ is the elastic Cauchy-Green deformation tensor, α_0 is a material coefficient having physical units of energy per unit volume, and the function $\hat{f}$ is given by

$$\begin{aligned}\hat{f}(\boldsymbol{C}_\mathrm{e}) &= \check{f}(\hat{I}_1(\boldsymbol{C}_\mathrm{e}), \hat{I}_2(\boldsymbol{C}_\mathrm{e}), \hat{I}_3(\boldsymbol{C}_\mathrm{e})) \\ &= \alpha_1[\hat{I}_1(\boldsymbol{C}_\mathrm{e}) - 3] + \alpha_2[\hat{I}_2(\boldsymbol{C}_\mathrm{e}) - 3] - \alpha_3 \ln\left(\hat{I}_3(\boldsymbol{C}_\mathrm{e})\right),\end{aligned} \tag{2.46}$$

with $\hat{I}_1(\boldsymbol{C}_\mathrm{e})$, $\hat{I}_2(\boldsymbol{C}_\mathrm{e})$, and $\hat{I}_3(\boldsymbol{C}_\mathrm{e})$ denoting the first three principal invariants of $\boldsymbol{C}_\mathrm{e}$. The material parameters α_1, α_2, and α_3 are all assumed to be constant in this work. Moreover, it holds that $\alpha_1 + 2\alpha_2 = \alpha_3$ [149], and the following relations connect α_0, α_1, α_2, and α_3 with Lamé's elastic parameters of the material (see e.g. [269]):

$$\alpha_0 = \frac{2\mu + \lambda}{4\alpha_3}, \quad \alpha_1 = \alpha_3 \frac{2\mu - \lambda}{2\mu + \lambda}, \quad \alpha_2 = \alpha_3 \frac{\lambda}{2\mu + \lambda}. \tag{2.47}$$

In the forthcoming calculations, we set $\alpha_3 = 1$, and we give μ and λ the values reported in Table 2.1.

We recognise the dissipative parts of $\boldsymbol{M}_\mathrm{f}$ and $H_\varepsilon^{(\mathrm{i})}$, which we identify with the following quantities

$$\boldsymbol{M}_\mathrm{f}^{(\mathrm{d})} = \boldsymbol{M}_\mathrm{f} + Jp\,\mathrm{Grad}(J^{-1}\Phi_\mathrm{f}), \tag{2.48a}$$

$$H_\varepsilon^{(\mathrm{i,d})} = H_\varepsilon^{(\mathrm{i})} + J_\gamma \sqrt{\tfrac{3}{2}}\, \|\tilde{\boldsymbol{\Sigma}}_\nu\|_{\boldsymbol{\eta}} - J_\gamma A_\nu[\varepsilon_\mathrm{p} - \mathfrak{e}_\mathrm{p}], \tag{2.48b}$$

and the dissipation inequality becomes

$$\begin{aligned}\mathscr{D}_\mathrm{R} =& \Phi_\mathrm{f}^{-1}\boldsymbol{Q}\boldsymbol{M}_\mathrm{f}^{(\mathrm{d})} + H_\varepsilon^{(\mathrm{i,d})}\dot{\varepsilon}_\mathrm{p} \\ &+ \left\{\left(\Psi_\mathrm{f} + \frac{p}{\rho_{\mathrm{f}0}}\right) - \left(\Psi_\mathrm{s} + \frac{p}{\rho_{\mathrm{s}0}}\right) + \frac{1}{3}\frac{\mathrm{tr}\,(\boldsymbol{\eta}\,\boldsymbol{\Sigma}_\nu)}{\rho_{\mathrm{s}0}\Phi_{\mathrm{s}\nu}}\right\} R_\mathrm{s} + J\mathscr{D}_\gamma \geq 0.\end{aligned} \tag{2.49}$$

We notice that, in (2.48b), growth influences the expression of $H_\varepsilon^{(\mathrm{i,d})}$ through the determinant J_γ in the term $J_\gamma A_\nu[\varepsilon_\mathrm{p} - \mathfrak{e}_\mathrm{p}]$.

According to (2.49), our model predicts that the system under study features three independent dissipative processes. The first one is due to the power loss associated with the resistance to the fluid flow and, under the hypothesis of negligible inertial forces, it leads to Darcy's law, i.e.,

$$\boldsymbol{M}_\mathrm{f}^{(\mathrm{d})} = \Phi_\mathrm{f}\boldsymbol{K}^{-1}\boldsymbol{Q}. \tag{2.50}$$

Equation (2.50) represents the material form of Darcy's law and, accordingly, the tensor $\boldsymbol{K}$ is the *material* permeability tensor of the medium, defined by

$$\boldsymbol{K}(X,t) = J(X,t)\boldsymbol{F}(X,t)\boldsymbol{k}(\chi(X,t),t)\boldsymbol{F}^{-\mathrm{T}}(X,t), \tag{2.51}$$

with $\boldsymbol{k}$ being the spatial permeability tensor. Finally, we remark that, in deriving (2.50), we have tacitly assumed that $\boldsymbol{K}$ is invertible, whereas sometimes this may not be necessarily the case. By substituting (2.50) into the first term on the right-hand-side of (2.49), we obtain that the dissipation due to fluid flow is always non-negative, i.e., for all $\boldsymbol{Q}$, it holds that $\Phi_{\mathrm{f}}^{-1}\boldsymbol{Q}\boldsymbol{M}_{\mathrm{f}}^{(\mathrm{d})} = \boldsymbol{K}^{-1} : (\boldsymbol{Q} \otimes \boldsymbol{Q}) \geq 0$, as long as $\boldsymbol{K}$ is positive-definite. Note that, by putting together the results (2.48a) and (2.50), $\boldsymbol{M}_{\mathrm{f}}$ is determined constitutively as

$$\boldsymbol{M}_{\mathrm{f}} = \Phi_{\mathrm{f}}\boldsymbol{K}^{-1}\boldsymbol{Q} - Jp\,\mathrm{Grad}(J^{-1}\Phi_{\mathrm{f}}). \tag{2.52}$$

The second process contributing to the dissipation, $\mathscr{D}_{\mathrm{R}}$, is given by $H_{\varepsilon}^{(\mathrm{i,d})}\dot{\varepsilon}_{\mathrm{p}}$, which represents the power that the solid phase expends in order to remodel its internal structure by accumulating plastic strain ε_{p}. We assume that $H_{\varepsilon}^{(\mathrm{i,d})}\dot{\varepsilon}_{\mathrm{p}}$ is non-negative for all $\dot{\varepsilon}_{\mathrm{p}}$ and, since $\dot{\varepsilon}_{\mathrm{p}}$ is always non-negative by virtue of its own definition (see (2.18)), we conclude that $H_{\varepsilon}^{(\mathrm{i,d})}$ has to be non-negative too. In our work, we hypothesise that the tissue remodels in a rate-dependent way and, in particular, we assign $H_{\varepsilon}^{(\mathrm{i,d})}$ as

$$H_{\varepsilon}^{(\mathrm{i,d})} = J\tau_{\mathrm{p}}\dot{\varepsilon}_{\mathrm{p}}, \tag{2.53}$$

where τ_{p} is here taken as a strictly positive coefficient with the physical units of a generalised viscosity. By plugging (2.53) into (2.48b), we determine $H_{\varepsilon}^{(\mathrm{i})}$ through the constitutive law

$$H_{\varepsilon}^{(\mathrm{i})} = J\tau_{\mathrm{p}}\dot{\varepsilon}_{\mathrm{p}} - J_{\gamma}\sqrt{\tfrac{3}{2}}\,\|\tilde{\boldsymbol{\Sigma}}_{\nu}\|_{\boldsymbol{\eta}} + J_{\gamma}A_{\nu}[\varepsilon_{\mathrm{p}} - \mathfrak{e}_{\mathrm{p}}]. \tag{2.54}$$

The third dissipative phenomenon is given by growth, and is represented by the last two summands on the right-hand-side of (2.49), which we denote by $\mathscr{D}_{\mathrm{g}}$ and refer to as the "growth part of $\mathscr{D}_{\mathrm{R}}$". In contrast to what we have done for the other dissipative processes, and even though the terms between braces in (2.49) may be understood as the generalised force power-conjugate to $\dot{\gamma}/\gamma$ through R_{s}, we do not try to look for information on R_{s} from the requirement that $\mathscr{D}_{\mathrm{g}}$ has to be non-negative. Rather, following [11, 10, 49, 124, 125, 191, 91], we enforce a phenomenological law for R_{s}, which is translated into the kinematic constraint (2.23) on $\dot{\gamma}/\gamma$, and we use $\mathscr{D}_{\gamma}$ to adjust $\mathscr{D}_{\mathrm{g}}$ and guarantee that it remains non-negative. We emphasise that, although this path may seem artificial, it can be justified by noticing that $\mathscr{D}_{\gamma}$ represents processes, related to growth, that are not resolved explicitly by our model but that are necessary for growth to occur. In fact, a motivation for introducing a term like $\mathscr{D}_{\gamma}$ in the dissipation inequality of a growth problem can be found in [126].

2.4.2 Dynamic Equations

By adopting the material form of the momentum balance laws (2.28a) and (2.28b), and by invoking the force balance $\boldsymbol{m}_\mathrm{s} + \boldsymbol{m}_\mathrm{f} = \boldsymbol{0}$, we obtain

$$-\boldsymbol{g}^{-1}\boldsymbol{F}^{-\mathrm{T}}\boldsymbol{M}_\mathrm{f} - \mathrm{Div}\boldsymbol{P}_\mathrm{s} = \boldsymbol{0}, \tag{2.55a}$$

$$\boldsymbol{g}^{-1}\boldsymbol{F}^{-\mathrm{T}}\boldsymbol{M}_\mathrm{f} - \mathrm{Div}\boldsymbol{P}_\mathrm{f} = \boldsymbol{0}, \tag{2.55b}$$

where the constitutive expressions of $\boldsymbol{P}_\mathrm{s}$, $\boldsymbol{P}_\mathrm{f}$, and $\boldsymbol{M}_\mathrm{f}$ are given in (2.44a), (2.44b), and (2.52), respectively. Furthermore, by adding together (2.55a) with (2.55b), and using the explicit expression for $\boldsymbol{M}_\mathrm{f}$ in (2.55b), we find

$$\mathrm{Div}(\boldsymbol{P}_\mathrm{s} + \boldsymbol{P}_\mathrm{f}) = \boldsymbol{0}, \tag{2.56a}$$

$$\boldsymbol{K}^{-1}\boldsymbol{Q} + \mathrm{Grad}\, p = \boldsymbol{0}. \tag{2.56b}$$

We exploit now the generalised force balance (2.28c), which becomes $H_\varepsilon^{(\mathrm{i})} = H_\varepsilon^{(\mathrm{e})}$ in material form and, by replacing $H_\varepsilon^{(\mathrm{i})}$ with the right-hand-side of (2.54), we determine an evolution law for ε_p, i.e.,

$$J\tau_\mathrm{p}\dot{\varepsilon}_\mathrm{p} - J_\gamma\sqrt{\tfrac{3}{2}}\,\|\tilde{\boldsymbol{\Sigma}}_\nu\|_{\boldsymbol{\eta}} + J_\gamma A_\nu[\varepsilon_\mathrm{p} - \mathfrak{e}_\mathrm{p}] = H_\varepsilon^{(\mathrm{e})}. \tag{2.57}$$

To close this equation, we prescribe $H_\varepsilon^{(\mathrm{e})}$ as

$$H_\varepsilon^{(\mathrm{e})} = -\left[J\sigma_\mathrm{th} + J_\gamma Z_\nu[\varepsilon_\mathrm{p} - \mathfrak{e}_\mathrm{p}]\right], \tag{2.58}$$

where σ_th is a threshold stress, and Z_ν is a material parameter [14]. Hence, setting $\lambda_\mathrm{p} = 1/\tau_\mathrm{p}$, Equation (2.57) takes on the form

$$\dot{\varepsilon}_\mathrm{p} = \frac{\lambda_\mathrm{p}}{J}\left\{\left(J_\gamma\sqrt{\tfrac{3}{2}}\,\|\tilde{\boldsymbol{\Sigma}}_\nu\|_{\boldsymbol{\eta}} - J\sigma_\mathrm{th}\right) - J_\gamma(A_\nu + Z_\nu)[\varepsilon_\mathrm{p} - \mathfrak{e}_\mathrm{p}]\right\}. \tag{2.59}$$

The last dynamic equation is supplied by (2.28d). Recalling that, in the present framework, the external force $h_\mathrm{p}^{(\mathrm{e})}$ is zero, the material form of (2.28d) reads

$$H_\mathrm{p}^{(\mathrm{i})} - \mathrm{Div}\,\boldsymbol{\Xi}_\mathrm{p} = 0. \tag{2.60}$$

Hence, by substituting (2.44c) and (2.44d) into (2.60), we obtain

$$-J_\gamma A_\nu[\varepsilon_\mathrm{p} - \mathfrak{e}_\mathrm{p}] - \mathrm{Div}\left(J_\gamma B_\nu\left[\boldsymbol{F}_\gamma{}^{-1}\boldsymbol{B}_\mathrm{p}\boldsymbol{F}_\gamma{}^{-\mathrm{T}}\right]\mathrm{Grad}\mathfrak{e}_\mathrm{p}\right) = 0. \tag{2.61}$$

In particular, since we take $\boldsymbol{F}_\gamma$ as $\boldsymbol{F}_\gamma = \gamma\boldsymbol{I}$, (2.61) acquires the equivalent form

$$-\gamma^3 A_\nu[\varepsilon_\mathrm{p} - \mathfrak{e}_\mathrm{p}] - \mathrm{Div}\left(\gamma B_\nu\boldsymbol{B}_\mathrm{p}\mathrm{Grad}\mathfrak{e}_\mathrm{p}\right) = 0. \tag{2.62}$$

Remark 3 (The equation for $\mathfrak{e}_{\mathrm{p}}$)**.** *The result* (2.62) *is our generalisation to Equation (4.40) of Anand et al. [14], which, in our notation, and assuming constant values for A_ν and B_ν, would read*

$$-A_\nu[\varepsilon_{\mathrm{p}} - \mathfrak{e}_{\mathrm{p}}] - B_\nu \Delta \mathfrak{e}_{\mathrm{p}} = 0 \quad \Rightarrow \quad \mathfrak{e}_{\mathrm{p}} - l_\nu^2 \Delta \mathfrak{e}_{\mathrm{p}} = \varepsilon_{\mathrm{p}}, \quad l_\nu = \sqrt{B_\nu / A_\nu}, \qquad \text{(A)}$$

with Δ being the Laplace operator, and l_ν the characteristic length scale associated with the micro-scale plasticity variable, $\mathfrak{e}_{\mathrm{p}}$. For a given distribution of ε_{p}, Equation (A) *returns a "regularised" version of ε_{p}. In particular, since $\mathfrak{e}_{\mathrm{p}}$ is required to satisfy Neumann-zero boundary conditions, if ε_{p} is constant in $\mathscr{B}$, then the unique solution to* (A) *is the constant solution $\mathfrak{e}_{\mathrm{p}} = \varepsilon_{\mathrm{p}}$. However, when ε_{p} is strongly localised, the output of* (A)*, i.e., $\mathfrak{e}_{\mathrm{p}}$, tends to be a lot more homogeneous, the more l_ν increases.*

Our generalisation to (A) *is twofold: first, the plastic-like distortions determine the evolution of $\mathfrak{e}_{\mathrm{p}}$ both through ε_{p} and through the second-order tensor $\boldsymbol{B}_{\mathrm{p}} = \boldsymbol{F}_{\mathrm{p}}^{-1}.\boldsymbol{F}_{\mathrm{p}}^{-\mathrm{T}}$. While ε_{p} is an input for* (A)*, $\boldsymbol{B}_{\mathrm{p}}$ modulates, together with the growth parameter γ, the non-locality of $\mathfrak{e}_{\mathrm{p}}$, which is thus measured by the tensorial coefficient $\gamma B_\nu \boldsymbol{B}_{\mathrm{p}}$. We notice that the occurrence of this coefficient is due to the last term in the definition of $\hat{\Psi}_{\mathrm{s}}$ given in* (2.36)*. Switching to the Eulerian formalism, and using the identity* $\mathrm{Grad}\mathfrak{e}_{\mathrm{p}}(X,t) = (\nabla \mathrm{e}_{\mathrm{p}}(\chi(X,t),t)\boldsymbol{F}(X,t)$*, this term reads*

$$\tfrac{1}{2} b_0 \boldsymbol{b}_{\mathrm{e}} : \nabla \mathrm{e}_{\mathrm{p}} \otimes \nabla \mathrm{e}_{\mathrm{p}},$$

thereby meaning that, in the spatial description, the non-locality of the micro-"plastic" variable, e_{p}, is modulated by the elastic left Cauchy-Green deformation tensor, $\boldsymbol{b}_{\mathrm{e}} = \boldsymbol{F}_{\mathrm{e}}.\boldsymbol{F}_{\mathrm{e}}^{\mathrm{T}}$. To eliminate $\boldsymbol{B}_{\mathrm{p}}$ from (2.62)*, and obtain a model closer to that of Anand et al. [14], we should substitute $\boldsymbol{b}_{\mathrm{e}}$ with the left Cauchy-Green deformation tensor $\boldsymbol{b} = \boldsymbol{F}.\boldsymbol{F}^{\mathrm{T}}$. Such a choice would lead to replace the last term of* (2.36) *with*

$$\tfrac{1}{2} b_0 \boldsymbol{G}^{-1} : \mathrm{Grad}\mathfrak{e}_{\mathrm{p}} \otimes \mathrm{Grad}\mathfrak{e}_{\mathrm{p}},$$

and would have the consequence of defining the unit tensor $\boldsymbol{N}_\nu$ just in terms of the standard Mandel stress tensor, $\boldsymbol{\Sigma}_\nu^{(st)}$ (see Remark 2). We recall that $\boldsymbol{G}$ denotes here the natural material metric tensor associated with $\mathscr{B}$.

The second aspect of our generalisation is related to the fact that, in our model, the evolution of $\mathfrak{e}_{\mathrm{p}}$ is influenced by the growth parameter, γ, which couples with the coefficients A_ν and B_ν, thereby rescaling the characteristic length scale associated with $\mathfrak{e}_{\mathrm{p}}$ in a generally inhomogeneous way, i.e., as $l_\nu \to l = l_\nu \|\boldsymbol{B}_{\mathrm{p}}\|_{\boldsymbol{G}}^{1/2}/\gamma$, so that, for a given l_ν, the condition $\gamma > 1$ tends to reduce the length scale associated with $\mathfrak{e}_{\mathrm{p}}$. Note that $\|\boldsymbol{B}_{\mathrm{p}}\|_{\boldsymbol{G}} = [\mathrm{tr}(\boldsymbol{G}\boldsymbol{B}_{\mathrm{p}}\boldsymbol{G}\boldsymbol{B}_{\mathrm{p}})]^{1/2}$.

Remark 4 (Choice of $H_\varepsilon^{(\mathrm{e})}$)**.** *In the literature on remodelling (see e.g. [213, 139, 78]), when an external force, like $H_\varepsilon^{(e)}$, is taken into account, it is often chosen in*

such a way that a homeostatic state exists for the system under study. If we had followed such philosophy, we should have admitted homeostatic terms for ε_{p} *and* $\mathfrak{e}_{\mathrm{p}}$*, denoted by* $\varepsilon_{\mathrm{p}}^{(\mathrm{h})}$ *and* $\mathfrak{e}_{\mathrm{p}}^{(\mathrm{h})}$*, and we should have expressed* $H_{\varepsilon}^{(\mathrm{e})}$ *as*

$$H_{\varepsilon}^{(\mathrm{e})} = -J_{\gamma}\sqrt{\tfrac{3}{2}}\,\|\tilde{\boldsymbol{\Sigma}}_{\nu}^{(\mathrm{h})}\|_{\boldsymbol{\eta}} + J_{\gamma}A_{\nu}[\varepsilon_{\mathrm{p}}^{(\mathrm{h})} - \mathfrak{e}_{\mathrm{p}}^{(\mathrm{h})}], \tag{2.63}$$

where $\tilde{\boldsymbol{\Sigma}}_{\nu}^{(\mathrm{h})}$ *is the Mandel-like stress tensor in homeostatic conditions (that is, when its arguments attain the homeostatic state). This consideration notwithstanding, in our work we opted for the expression* (2.58) *because, in order to formulate a proof of concept for our problem, we needed to remain as close as possible to the framework supplied by [14].*

Remark 5 (Evolution law for ε_{p})**.** *Equation* (2.58) *represents an essential difference with respect to the evolution law for* ε_{p} *given by [14]. Indeed, Anand et al. [14] set* $H_{\varepsilon}^{(i)} = H_{\varepsilon}^{(e)} = 0$*, and assign* $H_{\varepsilon}^{(i,d)}$ *constitutively as a law that plays the role of an* effective yield stress*, i.e.,* $H_{\varepsilon}^{(i,d)} = J\sigma_{\mathrm{th}} + J_{\gamma}Z_{\nu}[\varepsilon_{\mathrm{p}} - \mathfrak{e}_{\mathrm{p}}]$*, where* $\sigma_{\mathrm{th}} > 0$ *plays the role of the* "conventional yield stress" *[14][3], while* $Z_{\nu} > 0$ *is a model parameter defining the purely dissipative part of* $H_{\varepsilon}^{(i,d)}$*. By doing this, the Authors rewrite the balance equation* $H_{\varepsilon}^{(i)} = H_{\varepsilon}^{(e)}$ *in terms of a yield function of the type* $\mathfrak{f} = J_{\gamma}\sqrt{\frac{3}{2}}\|\tilde{\boldsymbol{\Sigma}}_{\nu}\|_{\boldsymbol{\eta}} - (J\sigma_{\mathrm{th}} + J_{\gamma}(A_{\nu} + Z_{\nu})[\varepsilon_{\mathrm{p}} - \mathfrak{e}_{\mathrm{p}}])$*. In particular, according to the theory of Anand et al. [14], it occurs that* $\dot{\varepsilon}_{\mathrm{p}} = 0$*, if* $\mathfrak{f} < 0$*, and* $\dot{\varepsilon}_{\mathrm{p}} > 0$*, if* $\mathfrak{f} = 0$*. This approach is equivalent to the elasto-plastic problem in the Karush-Kuhn-Tucker form, i.e.,*

$$\mathfrak{f} \le 0, \qquad \dot{\varepsilon}_{\mathrm{p}} \ge 0, \qquad \mathfrak{f}\,\dot{\varepsilon}_{\mathrm{p}} = 0, \tag{2.64}$$

where $\dot{\varepsilon}_{\mathrm{p}}$ *is determined by means of the consistency condition* $\dot{\varepsilon}_{\mathrm{p}}\dot{\mathfrak{f}} = 0$*, when* $\mathfrak{f} = 0$*. If, in our work, we had followed the approach outlined by Anand et al. [14], we would have found a very complicated evolution law for* ε_{p}*, especially from the computational point of view. To circumvent this technical difficulty, we have proposed a modification to the model, i.e., we have assumed* $H_{\varepsilon}^{(i)} = H_{\varepsilon}^{(e)} \neq 0$ *and, in order to obtain an evolution law for* ε_{p} *of the type* $J\tau_{\mathrm{p}}\dot{\varepsilon}_{\mathrm{p}} = \mathfrak{f}$ *(cf. Equation* (2.57)*), with* $\mathfrak{f}$ *defined as done by Anand et al. [14], we have exploited the "freedom" we have to express* $H_{\varepsilon}^{(e)}$ *as in* (2.58)*. A last comment pertains to the terms* λ_{p}/J *and* $J\sigma_{\mathrm{th}}$ *featuring in Equation* (2.59)*: if* λ_{p} *and* σ_{th} *are such that* $\lambda_{\mathrm{p}}/J_{\mathrm{e}} \equiv \Lambda_{\mathrm{p}}$ *and* $J_{\mathrm{e}}\sigma_{\mathrm{th}} \equiv \Sigma_{\mathrm{th}}$ *are constants, then it holds that* $\lambda_{\mathrm{p}}/J = \Lambda_{\mathrm{p}}/J_{\gamma}$ *and* $J\sigma_{\mathrm{th}} = J_{\gamma}\Sigma_{\mathrm{th}}$*. In this case,* J_{γ} *does not feature explicitly in Equation* (2.59)*, which becomes* $\dot{\varepsilon}_{\mathrm{p}} = \Lambda_{\mathrm{p}}\tilde{\mathfrak{f}}$*, where we*

[3]Note that, differently from what is assumed here, Anand et al. [14] hypothesise that the conventional yield stress is a monotonically decreasing function of ε_{p}, because they are interested in studying the phenomenon of *strain-softening*.

have set $\tilde{\mathfrak{f}} \equiv \mathfrak{f}/J_\gamma$. *In this case,* $\Sigma_{\rm th}$ *acquires the meaning of the yield stress that is used in the yield criteria formulated in terms of the norm of the Mandel stress tensor (see e.g. [136]). We remark, however, that solving* $\dot{\varepsilon}_{\rm p} = \Lambda_{\rm p}\tilde{\mathfrak{f}}$ *in lieu of* (2.59) *leads, in our work, to no appreciable differences in the simulation results.*

2.5 Model Equations and benchmark test

In this section, we summarise all the model equations and their corresponding unknowns, we highlight the fundamental hypotheses adopted to simplify our simulations, and we describe the benchmark problem used for testing our model.

2.5.1 Summary of the model equations

The first equation of the problem is given by (2.56a), i.e., the momentum balance law for the mixture as a whole, and its associated unknown is given by the solid phase motion, χ. The second equation determines the pressure, p, and is supplied by the mass balance law (2.8d), in which, coherently with (2.56b), $\boldsymbol{Q}$ is expressed as $\boldsymbol{Q} = -\boldsymbol{K}\mathrm{Grad}p$. The right-hand-side of (2.8d) is set equal to zero on the basis of the assumption that, in tumours, the mass densities $\rho_{\rm s0}$ and $\rho_{\rm f0}$ are approximately the same. The third equation is the mass balance of the proliferating cells (2.8a), and its corresponding unknown is the mass fraction $\omega_{\rm p}$. The fourth equation is in the mass fraction of the nutrients, $\omega_{\rm N}$, and is obtained from (2.8c) by using the identities $\Phi_{\rm f} = J - J_\gamma\Phi_{{\rm s}\nu}$ and $\boldsymbol{Y}_{\rm N} = -\rho_{\rm f0}\boldsymbol{D}\mathrm{Grad}\,\omega_{\rm N}$. The fifth equation descends for the mass balance law of the solid phase and, by assigning the mass source $R_{\rm s}$ phenomenologically, it puts a constraint on the growth parameter, γ, which is thus bound to comply with (2.23). Except for the sources and sinks of mass, which are defined in a slightly different way in our work, the five equations mentioned so far are the same as those studied by Mascheroni et al.[191] and Di Stefano et al. [91].

The evolution of the plastic distortions is described by the dynamic equation (2.59), which determines $\varepsilon_{\rm p}$, and by the constraint on $\boldsymbol{F}_{\rm p}$ placed by (2.20). These add two more equations to the previous five. Finally, the equation for the micro-scale "plasticity" variable, $\mathfrak{e}_{\rm p}$, is supplied by (2.62).

In conclusion, by putting together all the laws enumerated up to now, we obtain

$$\mathrm{Div}(\boldsymbol{P}_{\rm f} + \boldsymbol{P}_{\rm s}) = \boldsymbol{0}, \tag{2.65a}$$

$$\mathrm{Div}\,(\boldsymbol{K}\mathrm{Grad}p) = \dot{J}, \tag{2.65b}$$

$$\rho_{\rm s0}J_\gamma\Phi_{{\rm s}\nu}\dot{\omega}_{\rm p} = R_{\rm pn} + R_{\rm fp} - R_{\rm s}\omega_{\rm p}, \tag{2.65c}$$

$$\rho_{\rm f0}[J - J_\gamma\Phi_{{\rm s}\nu}]\dot{\omega}_{\rm N} + \rho_{\rm f0}\boldsymbol{Q}\,\mathrm{Grad}\omega_{\rm N} = \mathrm{Div}\,(\rho_{\rm f0}\boldsymbol{D}\,\mathrm{Grad}\,\omega_{\rm N}) + R_{\rm Np} + R_{\rm s}\omega_{\rm N}, \tag{2.65d}$$

$$\dot{\gamma} = \frac{R_{\rm s}}{3\rho_{\rm s0}\Phi_{{\rm s}\nu}\gamma^2}, \tag{2.65e}$$

$$\dot{\varepsilon}_{\mathrm{p}} = \frac{\lambda_{\mathrm{p}}}{J}\left\{\left(J_\gamma\sqrt{\tfrac{3}{2}}\|\tilde{\boldsymbol{\Sigma}}_\nu\|_{\boldsymbol{\eta}} - J\sigma_{\mathrm{th}}\right) - J_\gamma(A_\nu + Z_\nu)[\varepsilon_{\mathrm{p}} - \mathfrak{e}_{\mathrm{p}}]\right\}, \tag{2.65f}$$

$$\dot{\boldsymbol{F}}_{\mathrm{p}} = \left(\sqrt{\tfrac{3}{2}}\,\dot{\varepsilon}_{\mathrm{p}}\boldsymbol{\eta}^{-1}\boldsymbol{N}_\nu\right)\boldsymbol{F}_{\mathrm{p}}, \tag{2.65g}$$

$$\mathrm{Div}\,(\gamma B_\nu \boldsymbol{B}_{\mathrm{p}}\mathrm{Grad}\mathfrak{e}_{\mathrm{p}}) - \gamma^3 A_\nu \mathfrak{e}_{\mathrm{p}} = -\gamma^3 A_\nu \varepsilon_{\mathrm{p}}, \tag{2.65h}$$

which constitutes a system of 18 scalar equations in the 18 unknowns

$$\mathscr{U} = \{\chi, p, \omega_{\mathrm{p}}, \omega_{\mathrm{N}}, \gamma, \varepsilon_{\mathrm{p}}, \boldsymbol{F}_{\mathrm{p}}, \mathfrak{e}_{\mathrm{p}}\}. \tag{2.66}$$

For ensuring the non-negativity of $\dot{\varepsilon}_{\mathrm{p}}$ at all times and at all points, we solve (2.65f) numerically by taking the positive part of its right-hand-side. Moreover, to close the problem, we prescribe the permeability tensor and the diffusion tensor [149, 25, 91, 109],

$$\boldsymbol{K} = Jk_0\boldsymbol{C}^{-1}, \quad k_0 = k_{0\mathrm{R}}\left[\frac{J - J_\gamma\Phi_{\mathrm{s}\nu}}{J_\gamma\varphi_{\mathrm{f}0}}\right]^{m_0}\exp\left(\frac{m_1}{2}\left[\frac{J^2 - J_\gamma^2}{J_\gamma^2}\right]\right), \tag{2.67a}$$

$$\boldsymbol{D} = Jd_0\boldsymbol{C}^{-1}, \quad d_0 = \frac{J - J_\gamma\Phi_{\mathrm{s}\nu}}{J}d_{0\mathrm{R}}, \tag{2.67b}$$

as well as the sources and sinks of mass [191, 91], i.e.,

$$R_{\mathrm{pn}} = -J\zeta_{\mathrm{pn}}\left\langle 1 - \frac{\omega_{\mathrm{N}}}{\omega_{\mathrm{Ncr}}}\right\rangle_+ \frac{J_\gamma\Phi_{\mathrm{s}\nu}}{J}\omega_{\mathrm{p}}, \tag{2.68a}$$

$$R_{\mathrm{fp}} = J\zeta_{\mathrm{fp}}\left\langle \frac{\omega_{\mathrm{N}} - \omega_{\mathrm{Ncr}}}{\omega_{\mathrm{Nenv}} - \omega_{\mathrm{Ncr}}}\right\rangle_+ \left[1 - \frac{\delta_1\langle\wp\rangle_+}{\delta_2 + \langle\wp\rangle_+}\right]\frac{J - J_\gamma\Phi_{\mathrm{s}\nu}}{J\varphi_{\mathrm{f}0}}\frac{J_\gamma\Phi_{\mathrm{s}\nu}}{J}\omega_{\mathrm{p}}, \tag{2.68b}$$

$$R_{\mathrm{s}} = R_{\mathrm{fp}} + R_{\mathrm{nf}}, \tag{2.68c}$$

$$R_{\mathrm{nf}} = -J\zeta_{\mathrm{nf}}[1 - \omega_{\mathrm{p}}]\frac{J_\gamma\Phi_{\mathrm{s}\nu}}{J}, \tag{2.68d}$$

$$R_{\mathrm{Np}} = -J\zeta_{\mathrm{Np}}\frac{\omega_{\mathrm{N}}}{\omega_{\mathrm{N}} + \omega_{\mathrm{N}0}}\frac{J_\gamma\Phi_{\mathrm{s}\nu}}{J}\omega_{\mathrm{p}}. \tag{2.68e}$$

Since the expressions of R_{pn}, R_{fp}, R_{nf}, and R_{Np} have been already commented in previous works [191, 91], we do not spend any more words here on their derivation. We recall, however, that the operator $\langle\,\cdot\,\rangle_+$ returns the positive part of its argument, and that ω_{Ncr} denotes a critical value of the mass fraction of the nutrients, below which the proliferating cells tend to be necrotic (that is, $R_{\mathrm{pn}} < 0$), whereas ω_{Nenv} represents the mass fraction of the nutrients in the "environment". Both ω_{Nenv} and ω_{Ncr} are regarded as constant parameters in our work, and it is assumed that the condition $\omega_{\mathrm{Nenv}} > \omega_{\mathrm{Ncr}}$ is always respected, so that also R_{fp} is deactivated, i.e., $R_{\mathrm{fp}} = 0$, for $\omega_{\mathrm{N}} < \omega_{\mathrm{Ncr}}$. Moreover, looking at the definition of R_{fp}, and bearing in mind that, for $\omega_{\mathrm{N}} > \omega_{\mathrm{Ncr}}$, R_{fp} describes the positive variation of mass of the tissue's

solid phase, we notice that the factor

$$\left[1-\frac{\delta_1\langle\wp\rangle_+}{\delta_2+\langle\wp\rangle_+}\right]$$

accounts for mechanotransduction through the action of the stress $\langle\wp\rangle_+$. Comparing this result with the works of Mascheroni et al. [191] and Di Stefano et al. [91], we notice that our model suggests a slightly different interpretation of mechanotransduction. Indeed, while Mascheroni et al. [191] and Di Stefano et al. [91] prescribe $\wp$ as $\wp=-(1/3)\mathrm{tr}(\boldsymbol{g}\boldsymbol{\sigma}_{\mathrm{sc}})$, where $\boldsymbol{\sigma}_{\mathrm{sc}}=J^{-1}\boldsymbol{P}_{\mathrm{sc}}\boldsymbol{F}^{\mathrm{T}}$ is the constitutive part of the solid phase Cauchy stress, and, accordingly, $\boldsymbol{P}_{\mathrm{sc}}$ is defined by

$$\boldsymbol{P}_{\mathrm{sc}}=J_\gamma\left(\rho_{\mathrm{s}0}\Phi_{\mathrm{s}\nu}\boldsymbol{g}^{-1}\frac{\partial\hat{\Psi}_{\mathrm{s}}^{(\mathrm{st})}}{\partial\boldsymbol{F}_{\mathrm{e}}}(\boldsymbol{F}\boldsymbol{F}_\gamma^{-1}\boldsymbol{F}_{\mathrm{p}}^{-1})\boldsymbol{F}_{\mathrm{p}}^{-\mathrm{T}}\boldsymbol{F}_\gamma^{-\mathrm{T}}\right)\equiv\mathscr{P}_{\mathrm{sc}}(\boldsymbol{F},\boldsymbol{F}_\gamma,\boldsymbol{F}_{\mathrm{p}}),\tag{2.69}$$

in our approach $\wp$ is taken as $\wp=-(1/3)\mathrm{tr}(\boldsymbol{g}\boldsymbol{\sigma}_{\mathrm{eff}})$ (see also [78]), with

$$\begin{aligned}\boldsymbol{\sigma}_{\mathrm{eff}}&=\boldsymbol{\sigma}_{\mathrm{sc}}+\frac{1}{J_{\mathrm{e}}}\boldsymbol{g}^{-1}\boldsymbol{F}_{\mathrm{e}}^{-\mathrm{T}}\boldsymbol{\eta}\boldsymbol{\Sigma}_\nu^{(\mathrm{n\text{-}st})}\boldsymbol{F}_{\mathrm{e}}^{\mathrm{T}}\\&=\frac{1}{J_{\mathrm{e}}}\boldsymbol{g}^{-1}\boldsymbol{F}_{\mathrm{e}}^{-\mathrm{T}}\boldsymbol{\eta}\boldsymbol{\Sigma}_\nu^{(\mathrm{st})}\boldsymbol{F}_{\mathrm{e}}^{\mathrm{T}}+\frac{1}{J_{\mathrm{e}}}\boldsymbol{g}^{-1}\boldsymbol{F}_{\mathrm{e}}^{-\mathrm{T}}\boldsymbol{\eta}\boldsymbol{\Sigma}_\nu^{(\mathrm{n\text{-}st})}\boldsymbol{F}_{\mathrm{e}}^{\mathrm{T}}\\&=\frac{1}{J_{\mathrm{e}}}\boldsymbol{g}^{-1}\boldsymbol{F}_{\mathrm{e}}^{-\mathrm{T}}\boldsymbol{\eta}\boldsymbol{\Sigma}_\nu\boldsymbol{F}_{\mathrm{e}}^{\mathrm{T}}.\end{aligned}\tag{2.70}$$

In other words, while the works done by Mascheroni et al.[191] and Di Stefano et al.[91] the stress used to express the mechanotransduction is the classical $\boldsymbol{\sigma}_{\mathrm{sc}}$, we propose here to adopt the *effective Cauchy stress*, $\boldsymbol{\sigma}_{\mathrm{eff}}$, which captures both $\boldsymbol{\sigma}_{\mathrm{sc}}$ and the non-standard, purely configurational contribution $\boldsymbol{\Sigma}_\nu^{(\mathrm{n\text{-}st})}$. Our point is that, since in our approach $\boldsymbol{\Sigma}_\nu$ is (power-)conjugate to the growth rate $\dot{\gamma}/\gamma$ (through R_{s}) and to $\dot{\varepsilon}_{\mathrm{p}}$ (see (2.37)), it might be a more natural representative of the stress responsible for modulating growth. This consideration notwithstanding, for the parameters chosen in our simulations, the contribution of $\boldsymbol{\Sigma}_\nu^{(\mathrm{n\text{-}st})}$ is very marginal with respect to the standard measures of stress, and its contribution is thus not much appreciable.

2.5.2 Benchmark problem

The benchmark problem is essentially the same as the one computed in Di Stefano et al.[91], with the major difference that we are now considering also plastic distortions and the role of micro-plasticity. Hence, by adapting a study originally designed by Ambrosi and Mollica[11], we consider the case of volumetric growth in a cylindrical sample of isotropic material. For this purpose, we introduce the systems of cylindrical coordinates (R,Θ,Z) and (r,θ,z), which cover the reference

and current configuration, respectively. For both systems, the first coordinate is radial, the second one is circumferential, and the third one is axial.

We assume that the radius of the specimen is preserved, and that only its length varies along the axial direction. Hence, we eliminate any rigid rotation about the principal axis. These restrictions imply that the momentum balance law (2.65a) reduces to a scalar equation in Z, and that the deformation gradient tensor becomes $\boldsymbol{F} = \boldsymbol{e}_r \otimes \boldsymbol{E}^R + \boldsymbol{e}_\theta \otimes \boldsymbol{E}^\Theta + (1 + \frac{\partial u}{\partial Z})\boldsymbol{e}_z \otimes \boldsymbol{E}^Z$, where u is the field of axial displacements. We note that $\{\boldsymbol{E}^R, \boldsymbol{E}^\Theta, \boldsymbol{E}^Z\}$ and $\{\boldsymbol{e}_r, \boldsymbol{e}_\theta, \boldsymbol{e}_z\}$ are the co-vector and vector bases associated with the system of cylindrical coordinates (R, Θ, Z) and (r, θ, z), respectively.

We impose the following boundary conditions on Equations (2.65a)–(2.65h)

$$(-Jp\boldsymbol{g}^{-1}\boldsymbol{F}^{-\mathrm{T}} + \boldsymbol{P}_{\mathrm{sc}}).\boldsymbol{N}_{\mathrm{A}} = \boldsymbol{0}, \qquad \text{on } (\partial\mathscr{B})_{\mathrm{Left}} \text{ and } (\partial\mathscr{B})_{\mathrm{Right}}, \tag{2.71a}$$

$$p = 0, \qquad \text{on } (\partial\mathscr{B})_{\mathrm{Left}} \text{ and } (\partial\mathscr{B})_{\mathrm{Right}}, \tag{2.71b}$$

$$(-\boldsymbol{K}\mathrm{Grad}\, p).\boldsymbol{N}_{\mathrm{C}} = 0, \qquad \text{on } (\partial\mathscr{B})_{\mathrm{C}}, \tag{2.71c}$$

$$(-\rho_{\mathrm{f}}\boldsymbol{D}\mathrm{Grad}\, \omega_{\mathrm{N}}).\boldsymbol{N}_{\mathrm{C}} = 0, \qquad \text{on } (\partial\mathscr{B})_{\mathrm{C}}, \tag{2.71d}$$

$$\omega_{\mathrm{N}} = \omega_{\mathrm{Nenv}}, \qquad \text{on } (\partial\mathscr{B})_{\mathrm{Left}} \text{ and } (\partial\mathscr{B})_{\mathrm{Right}}, \tag{2.71e}$$

$$(\gamma B_\nu \boldsymbol{B}_{\mathrm{p}}\mathrm{Grad}\mathfrak{e}_{\mathrm{p}}).\boldsymbol{N} = 0, \qquad \text{on } \partial\mathscr{B}, \tag{2.71f}$$

where $\partial\mathscr{B} = (\partial\mathscr{B})_{\mathrm{Left}} \cup (\partial\mathscr{B})_{\mathrm{C}} \cup (\partial\mathscr{B})_{\mathrm{Right}}$, $(\partial\mathscr{B})_{\mathrm{C}}$ is the lateral boundary of the cylinder, $(\partial\mathscr{B})_{\mathrm{Left}}$ and $(\partial\mathscr{B})_{\mathrm{Right}}$ are the left and right surface cross-sections at $Z = -L/2$ and $Z = L/2$, respectively, and L is the initial length of the cylinder. Moreover, $\boldsymbol{N}_{\mathrm{A}}$, $\boldsymbol{N}_{\mathrm{C}}$, and $\boldsymbol{N}$ are fields of unit vectors normal to $(\partial\mathscr{B})_{\mathrm{Left}}$ and $(\partial\mathscr{B})_{\mathrm{Right}}$, $(\partial\mathscr{B})_{\mathrm{C}}$, and $\partial\mathscr{B}$, respectively.

Equations (2.71a) and (2.71b) mean that the left and right ends of the cylinder are free boundaries. The relations (2.71c) and (2.71d) are enforced to express that $(\partial\mathscr{B})_{\mathrm{C}}$ is undeformable and impermeable to the fluid and to the nutrients, respectively. Equation (2.71e) is a Dirichlet condition specifying that there always exists a constant availability of nutrients on the boundaries $(\partial\mathscr{B})_{\mathrm{Left}}$ and $(\partial\mathscr{B})_{\mathrm{Right}}$. Finally, the boundary condition (2.71f) is introduced following Anand et al.[14].

To complete the mathematical formulation of the problem, we prescribe the initial conditions,

$$\chi^r(R, \Theta, Z, 0) = R, \tag{2.72a}$$

$$\chi^\vartheta(R, \Theta, Z, 0) = \Theta, \tag{2.72b}$$

$$\chi^z(R, \Theta, Z, 0) = Z, \tag{2.72c}$$

$$p(R, \Theta, Z, 0) = 0, \tag{2.72d}$$

$$\omega_{\mathrm{N}}(R, \Theta, Z, 0) = \omega_{\mathrm{Nenv}}, \tag{2.72e}$$

$$\gamma(R, \Theta, Z, 0) = 1, \tag{2.72f}$$

$$\omega_{\mathrm{p}}(R, \Theta, Z, 0) = 1, \tag{2.72g}$$

$$\varepsilon_{\mathrm{p}}(R,\Theta,Z,0)=0, \tag{2.72h}$$
$$\mathfrak{e}_{\mathrm{p}}(R,\Theta,Z,0)=0, \tag{2.72i}$$

with $R\in[0,R_{\mathrm{b}}]$, $\Theta\in[0,2\pi[$ and $Z\in[-L/2,L/2]$. The conditions (2.72a)–(2.72i) have to be valid in the whole domain $\mathscr{B}$.

The material parameters $k_{0\mathrm{R}}$, m_0, m_1, and $d_{0\mathrm{R}}$, the coefficients ζ_{pn}, ζ_{fp}, ζ_{nf}, and ζ_{Np} as well as the constants ω_{Nenv}, ω_{Ncr}, ω_{N0}, δ_1, δ_2, σ_{th}, and λ_{p} are given in Table 2.1.

In Table 2.1, the length of the cylindric specimen, L, and the radius of its cross section, R_{b}, are chosen within a plausible physical range. However, it is necessary to motivate the choice of the parameters ω_{Nenv}, ω_{Ncr}, and ω_{N0}, which are all taken from Di Stefano et al.[91]. These quantities are adapted from [191], where they were set equal to $\omega_{\mathrm{Nenv}}=7.0\cdot10^{-6}$, $\omega_{\mathrm{Ncr}}=2.0\cdot10^{-6}$, and $\omega_{\mathrm{N0}}=4.2\cdot10^{-6}$, respectively. With the exception of ω_{Ncr}[4], in the work of Mascheroni et al.[191] these values come from experiments performed on tumour spheroids and associated with geometry, size, diffusion length scales and nutrients' characteristic mass fractions that are very different from those considered in our work. Indeed, an essential feature of the benchmark problem investigated by Mascheroni et al. [191] is that, because of the spherical geometry of the tumour, and because of the nutrients being distributed homogeneously on the tumour's surface, the diffusion of the nutrients occurs isotropically, from the boundary to the center of the spheroid, in radial direction. In our problem, instead, the nutrients can diffuse only along the axial direction of the tumour, and they have to travel the length L, which is much larger than the radius, of about 20 μm, of the spheroids considered Mascheroni et al. [191]. Due to these geometric and size aspects, if we used the values of ω_{Nenv}, ω_{Ncr} and ω_{N0} suggested Mascheroni et al., we would generate a situation in which the replenishment of the nutrients "eaten" by the cells would be too slow for the tumour to grow. Indeed, especially in the middle of the tumour, the nutrients' mass fraction would go below the threshold value, ω_{Ncr}, after few hours. Therefore, to avoid a fast inhibition of growth, we have increased the value of ω_{Nenv} of three orders of magnitude in our experiment *in silico*. Note that there is a certain freedom in the choice of ω_{Nenv}, since prescribing its value amounts to preparing the bath of nutrients in which the tumour is immersed. This freedom notwithstanding, the value assigned to ω_{Nenv} should take into account the characteristic length of the tumour —in our case, L— in order to ensure that the effects of growth remain active over a sufficiently long time scale. In principle, ω_{Ncr} and ω_{N0} should be determined experimentally. Still, since we are not aware of any experimental value of ω_{Ncr}, we have calibrated it so that ω_{Ncr} be smaller than ω_{Nenv}, but big enough to

[4]Note that the values attributed to ω_{Ncr} Mascheroni et al.[191] for all the considered studies are never referenced, the only exception being the growth of a tumour spheroid. In this case, however, the reference is a typographical error.

allow for a transition from the stage of tumour growth, for $\omega_{\mathrm{Ncr}} < \omega_{\mathrm{N}} \leq \omega_{\mathrm{Nenv}}$, to the stage of no growth, for $\omega_{\mathrm{N}} \leq \omega_{\mathrm{Ncr}} < \omega_{\mathrm{Nenv}}$. This reasoning has led us to choose ω_{Ncr} three orders of magnitude greater than the value assigned Mascheroni et al. [191]. Finally, the value given to ω_{N0} in our work (see Table 2.1) is two orders of magnitude greater than the one prescribed by Mascheroni et al. [191]. This choice allows us to be consistent with the scale of the nutrients' mass fraction imposed in our work.

2.6 Some computational aspects

The system (2.65a)–(2.65h) features both ordinary differential equations (ODEs) in time, and partial differential equations (PDEs). All the ODEs of our model, including those obtained after that the finite element discretisation of the PDEs is performed, have been discretised adaptively in time, and have been solved by means of a four-step Backward Differentiation Formula (BDF4). This is an implicit linear multistep method, which generalises the implicit Euler method. Since the BDF4 is implicit, it requires in general the solution of nonlinear equations at each time integration step. The BDF4 is available in COMSOL Multiphysics®, which has been used to run our simulations.

The PDEs have been put in weak form and solved by means of Finite Element techniques. In particular, classical methods have been used for (2.65b), (2.65d), and (2.65h), while a "special treatment" has been reserved to the momentum balance law (2.65a), for which the Hu-Washizu method [42] has been employed.

Looking more closely at the PDEs (2.65b), (2.65d), and (2.65h), we notice that (2.65b) is a generalised Poisson equation in the pressure, p, with a time-dependent right-hand-side, $\dot{J}$, which represents the volume change of the solid phase due to the changes in porosity accompanying the flow of the fluid. Equation (2.65d), instead, is a nonlinear diffusion-advection-reaction equation in the mass fraction of the nutrients, ω_{N}, with the nonlinearity being nested in the reaction terms, R_{Np} and R_{s}. Both for (2.65b) and for (2.65d), the Finite Element Method leads to a set of ODEs in which the unknowns are the nodal pressures and the nodal mass fractions of the nutrients, respectively. Finally, Equation (2.65h) is an equation of Helmholtz type and, in this case, the Finite Element method yields a set of algebraic equations in the nodal values of $\mathfrak{e}_{\mathrm{p}}$, which are anyway time-dependent. In the following, we do not fuss over the procedure for obtaining the set of nodal equations associated with (2.65b), (2.65d), and (2.65h), since such procedure is rather standard.

To sketch the formulation of the Hu-Washizu method, we add together the expressions of the stress tensors $\boldsymbol{P}_{\mathrm{f}}$ and $\boldsymbol{P}_{\mathrm{s}}$, and we notice that the weak form of the momentum balance law (2.65a) admits the compact form

$$\int_{\mathscr{B}} (\boldsymbol{P}_{\mathrm{f}} + \boldsymbol{P}_{\mathrm{s}}) : \boldsymbol{g}\,\mathrm{Grad}\,\boldsymbol{U}_{\mathrm{s}} = \int_{\mathscr{B}} \left(-Jp\,\boldsymbol{g}^{-1}\boldsymbol{F}^{-\mathrm{T}} + \boldsymbol{P}_{\mathrm{sc}}\right) : \boldsymbol{g}\,\mathrm{Grad}\,\boldsymbol{U}_{\mathrm{s}} = 0, \qquad (2.73)$$

where $\boldsymbol{U}_{\mathrm{s}}$ is the virtual velocity of the solid, expressed as a function of the points X of $\mathscr{B}$.

One of the main drawbacks of this formulation is that, once a Finite Element scheme is used for solving (2.73), the "limitations" of the interpolations adopted for χ [42], $\boldsymbol{F}$, and $\boldsymbol{F}_{\mathrm{p}}$ are transferred to $\boldsymbol{P}_{\mathrm{sc}}$ through its constitutive representation, $\mathscr{P}_{\mathrm{sc}}(\boldsymbol{F}, \boldsymbol{F}_{\gamma}, \boldsymbol{F}_{\mathrm{p}})$. This ill behaviour persists even increasing the order of the basis functions used for the discretisation of χ, and may lead to a remarkable deterioration of the resolution of $\boldsymbol{P}_{\mathrm{sc}}$, with consequent loss of accuracy of the employed numerical method. A possible way to contain the occurrence of the just depicted numerical phenomenon is supplied by the Hu-Washizu method [42], which we implement for our purposes in its three-field-formulation. Although the Hu-Washizu method is well known in the computational community, we briefly explain here how we adapt it to the case under investigation in this work.

Together with the motion, χ, which is an unknown of the model, we introduce two tensor-valued auxiliary variables, which we regard as additional independent fields of our model: these are an auxiliary "deformation gradient tensor", $\boldsymbol{F}^{\mathrm{HW}}$, and an auxiliary first Piola-Kirchhoff stress tensor, $\boldsymbol{P}_{\mathrm{sc}}^{\mathrm{HW}}$ (note that the superscript "HW" stands for "Hu-Washizu"). Although being independent, $\boldsymbol{F}^{\mathrm{HW}}$ and $\boldsymbol{P}_{\mathrm{sc}}^{\mathrm{HW}}$ must be consistent with the *true* deformation gradient tensor and with the *true* first Piola-Kirchhoff stress tensor, respectively, and are thus bound to satisfy the constraints

$$\boldsymbol{F}^{\mathrm{HW}} = \boldsymbol{F}, \tag{2.74a}$$

$$\boldsymbol{P}_{\mathrm{sc}}^{\mathrm{HW}} = \mathscr{P}_{\mathrm{sc}}(\boldsymbol{F}^{\mathrm{HW}}, \boldsymbol{F}_{\gamma}, \boldsymbol{F}_{\mathrm{p}}). \tag{2.74b}$$

To proceed with the Hu-Washizu method, we rephrase Equations (2.74a) and (2.74b) in weak form. Hence, we write

$$\int_{\mathscr{B}} \left\{ \left[\boldsymbol{F} - \boldsymbol{F}^{\mathrm{HW}}\right] : \boldsymbol{\Pi} + \left[\mathscr{P}_{\mathrm{sc}}(\boldsymbol{F}^{\mathrm{HW}}, \boldsymbol{F}_{\gamma}, \boldsymbol{F}_{\mathrm{p}}) - \boldsymbol{P}_{\mathrm{sc}}^{\mathrm{HW}}\right] : \boldsymbol{\Lambda} \right\} = 0, \tag{2.75}$$

where $\boldsymbol{\Pi}$ and $\boldsymbol{\Lambda}$ denote the virtual variations of $\boldsymbol{P}_{\mathrm{sc}}^{\mathrm{HW}}$ and $\boldsymbol{F}^{\mathrm{HW}}$, respectively, and represent a virtual stress rate and a virtual velocity gradient. Equation (2.75) is now appended to (2.73), which has to be reformulated in terms of the Hu-Washizu auxiliary fields, thereby obtaining

$$\begin{aligned} \int_{\mathscr{B}} \Big\{ &\left[\boldsymbol{P}_{\mathrm{sc}}^{\mathrm{HW}} - (\det \boldsymbol{F}^{\mathrm{HW}}) p \boldsymbol{g}^{-1} (\boldsymbol{F}^{\mathrm{HW}})^{-\mathrm{T}}\right] : \boldsymbol{g} \operatorname{Grad} \boldsymbol{U}_{\mathrm{s}} + \left[\boldsymbol{F} - \boldsymbol{F}^{\mathrm{HW}}\right] : \boldsymbol{\Pi} \\ &+ \left[\mathscr{P}_{\mathrm{sc}}(\boldsymbol{F}^{\mathrm{HW}}, \boldsymbol{F}_{\gamma}, \boldsymbol{F}_{\mathrm{p}}) - \boldsymbol{P}_{\mathrm{sc}}^{\mathrm{HW}}\right] : \boldsymbol{\Lambda} \Big\} = 0. \end{aligned} \tag{2.76}$$

After performing the interpolation of all the fields introduced so far, the algebraic form of (2.76) consists of a block system, in which one block corresponds to the balance of momentum, one block is associated with (2.74a), and one with (2.74b).

2.7 Results

To weigh the effects of the non-local theory of remodelling on the benchmark problem presented in Section 2.5.2, we perform two different simulations: one is done by excluding micro-plasticity, and is thus said to be "standard"; the other one, instead, accounts for micro-plasticity, and refers to the "non-standard" model.

The standard model (ST) is obtained by setting A_ν, B_ν, and Z_ν equal to zero, so that Equation (2.65h) is always satisfied and the evolution law for ε_p only takes into account the first term of the right-hand-side of (2.65f), with $\boldsymbol{\Sigma}_\nu \equiv \boldsymbol{\Sigma}_\nu^{(\mathrm{st})}$. In the non-standard model (NST), the parameters A_ν, B_ν, and Z_ν are different from zero (see Table 2.2), and the full system of equations (2.65a)–(2.65h) has to be solved.

Since, to the best of our knowledge, no measurements for A_ν, B_ν, and Z_ν are available in the scientific literature on soft tissues, we have chosen such parameters after several trials. For this reason, the values used to obtain Figures 2.2–2.5 may be unrealistic for describing a true biological situation. Moreover, we remark that the convergence of the system (2.65a)–(2.65h) was achieved only for $Z_\nu \leq 1$ and $A_\nu > B_\nu$, whereas our computations never converged for $Z_\nu > 1$, regardless of the tested values of A_ν and B_ν. We also emphasise that, for the cases in which the model converged, the results of the simulations featured no remarkable difference.

To report the results of our model, we display the numerical solutions of the displacement, the growth parameter, γ, the mass fraction of the proliferating cells, ω_p, the pressure, p, and the axial component of the effective Cauchy stress tensor, σ_eff^{zz}. We plot all these quantities versus the axial coordinate of the specimen, and at the times $t = 10$ d and $t = 20$ d.

Figure 2.2 shows the displacement of the tumour (left panel) and the growth parameter, γ (right panel). Both quantities are computed only for the case of growth without "plasticity" (remodelling) (NP), i.e., for $\boldsymbol{F}_\mathrm{p} = \boldsymbol{I}$, $\varepsilon_\mathrm{p} = 0$, $\mathfrak{e}_\mathrm{p} = 0$, and for the case in which "plasticity" (remodelling) is active. Moreover, "plasticity" is accounted for as prescribed by the non-standard model (NST). In fact, we could have also used the standard one (ST), but it would have led to imperceptible differences with respect to the non-standard model. As expected, both the displacement and the growth parameter increase as time goes by, but we observe a drastic reduction of their spatiotemporal evolution when remodelling is active. The results presented in Figure 2.2 confirm the ones obtained by Mascheroni et al.[191] and Di Stefano et al. [91], and have been re-computed with the purpose of highlighting the important role that remodelling may play on growth.

To further investigate the possible role of remodelling on growth and, in particular, the switch from the standard to the non-standard approach, we study the evolution of ω_p (Figure 2.3), p (Figure 2.4), and σ_eff^{zz} (Figure 2.5).

Figure 2.3 displays, in the left panel, the progression of the mass fraction of the proliferating cells, ω_p, and, in the right panel, the absolute value of the difference between $\omega_\mathrm{p}^\mathrm{ST}$ and $\omega_\mathrm{p}^\mathrm{NST}$, which denote the mass fractions of the proliferating

cells computed with the standard model (ST) and the non-standard model (NST), respectively. In the left panel, we notice that, at time $t = 10$ d, the differences between $\omega_{\mathrm{p}}^{\mathrm{ST}}$ and $\omega_{\mathrm{p}}^{\mathrm{NST}}$ are irrelevant. However, at $t = 20$ d, a slight, yet appreciable, difference starts to appear. We visualise this difference in the right panel of Figure 2.3. Here, we notice that, due to the Dirichlet boundary condition imposed on ω_{p} at $Z = L/2$, such difference cannot be pronounced for values of the axial coordinate tending to $L/2$. On the other hand, $|\omega_{\mathrm{p}}^{\mathrm{ST}} - \omega_{\mathrm{p}}^{\mathrm{NST}}|$ becomes relatively more visible in the portion of the specimen in which growth is inhibited (see Figure 2.2(right)). This is due to a limited availability of nutrients (data not shown).

In the left panel of Figure 2.4, we show the pressure, p, both for the ST model and for the NST one. For both models, the same behaviour is attained, i.e., the pressure drops from the tumour boundary towards its centre, where it takes negative values. In the right panel of Figure 2.4, we report the absolute value of the difference, at time $t = 20$ d, between p^{ST} and p^{NST}, i.e., the pressures computed with the ST model and the NST model, respectively. The differences between p^{ST} and p^{NST} are relatively small, but visible, in almost all of the half domain and at both times. They are clearly zero at the Dirichlet boundary $Z = L/2$ and, at $t = 20$ d, the maximum of $|p^{\mathrm{ST}} - p^{\mathrm{NST}}|$ is reached at a point between 0.4 cm and 0.5 cm.

Moreover, in Figure 2.5, the axial component of the constitutive part of the Cauchy stress tensor, $\sigma_{\mathrm{sc}}^{zz}$, is shown. Indeed, due to the imposed boundary conditions and the symmetry restrictions of the considered problem, the balance of momentum (2.65a) amounts to requiring $-p+\sigma_{\mathrm{sc}}^{zz} = 0$ everywhere in the specimen. Hence, it holds that $\sigma_{\mathrm{sc}}^{zz} = p$. In addition, the axial component of the stress used to model the mechanotransduction, $\sigma_{\mathrm{eff}}^{zz}$, is different from $\sigma_{\mathrm{sc}}^{zz}$, as it features $\partial \mathfrak{e}_{\mathrm{p}}/\partial Z$ (see Equation (2.70)). However, since this derivative is very small, it occurs that $\sigma_{\mathrm{eff}}^{zz}$ can be safely approximated with $\sigma_{\mathrm{sc}}^{zz}$ and, thus, with p.

A last comment concerns the evolution of $\mathfrak{e}_{\mathrm{p}}$ and ε_{p}. As reported in Figure 2.6, both ε_{p} and $\mathfrak{e}_{\mathrm{p}}$ are increasing functions of time and space. If we focus on ε_{p}, we note that, as time goes by, the remodelling strains augment and accumulate in a neighbourhood of the boundaries of the specimen. This is highlighted by the fact that the slope of the curves corresponding to ε_{p} tends to raise when it approaches the edge. However, as predicted by the theory, $\mathfrak{e}_{\mathrm{p}}$ plays a smoothing role on the remodelling distortions and, in fact, it distributes itself more uniformly along the specimen. A relevant aspect of this result is that, while the curves corresponding to ε_{p} at $t = 10$ d and $t = 20$ d are almost coincident at the centre of the specimen, the curves determining $\mathfrak{e}_{\mathrm{p}}$ are distinguishable from one another.

Table 2.1: Numerical values of the parameters used both for the standard and for the non-standard model.

Parameter	Unit	Value	Equation	Reference
L	[cm]	1.000	—	[91]
R_b	[cm]	$1.000 \cdot 10^{-2}$	—	[91]
k_0R	[mm^4/(N s)]	0.4875	(2.67a)	[149]
m_0	[−]	0.0848	(2.67a)	[149]
m_1	[−]	4.6380	(2.67a)	[149]
d_0R	[m^2/s]	$3.200 \cdot 10^{-9}$	(2.67b)	[149]
σ_th	[Pa]	$1.000 \cdot 10^{-7}$	(2.58)	[130]
λ_p	[m s/kg]	$7.000 \cdot 10^{-7}$	(2.59)	[130]
λ	[Pa]	$1.333 \cdot 10^{4}$	(2.47)	[263]
μ	[Pa]	$1.999 \cdot 10^{4}$	(2.47)	[263]
ω_Ncr	[−]	$1.000 \cdot 10^{-3}$	(2.68a)	[91]
ω_Nenv	[−]	$7.000 \cdot 10^{-3}$	(2.68b)	[91]
ω_N0	[−]	$1.480 \cdot 10^{-4}$	(2.68e)	[91]
δ_1	[−]	$7.138 \cdot 10^{-1}$	(2.68b)	[192]
δ_2	[Pa]	$1.541 \cdot 10^{3}$	(2.68b)	[192]
ζ_pn	[kg/(m^3 s)]	$1.500 \cdot 10^{-3}$	(2.68a)	[62]
ζ_fp	[kg/(m^3 s)]	$1.343 \cdot 10^{-3}$	(2.68b)	[62]
ζ_nf	[kg/(m^3 s)]	$1.150 \cdot 10^{-5}$	(2.68d)	[62]
ζ_Np	[kg/(m^3 s)]	$3.000 \cdot 10^{-4}$	(2.68e)	[57]

Table 2.2: Numerical values of the parameters A_ν, B_ν and Z_ν for the non-standard model.

Parameter	Unit	Value	Equation
A_ν	[Pa]	$1.0 \cdot 10^{-9}$	(2.38c)
B_ν	[Pa m^2]	$1.0 \cdot 10^{-14}$	(2.38d)
Z_ν	[Pa]	$1.0 \cdot 10^{-2}$	(2.65f)

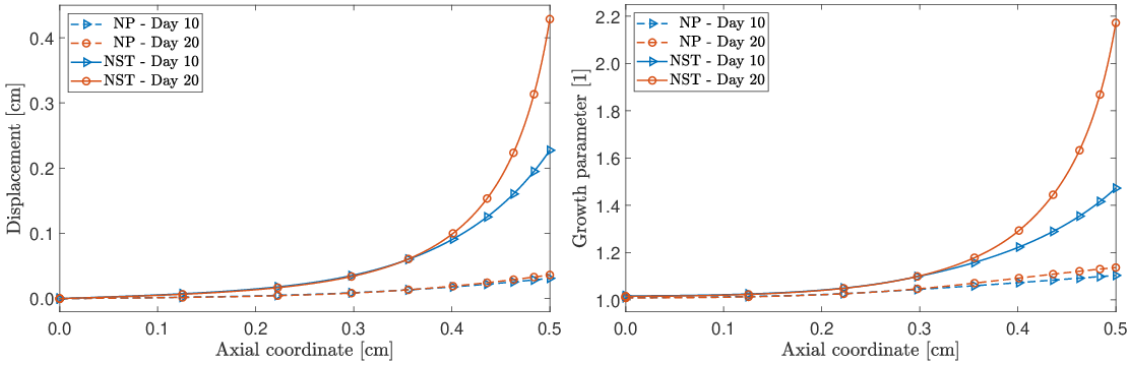

Figure 2.2: *Left panel*: spatial profile of the displacement. *Right panel*: spatial profile of the growth parameter, γ. Since the problem is symmetric, in both panels only the half $[0, L/2]$ of the domain is shown.

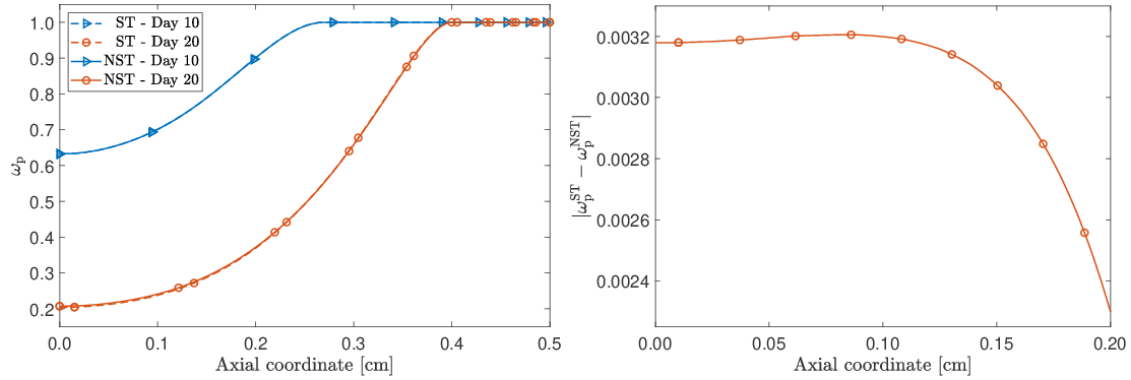

Figure 2.3: *Left panel*: spatial profile of the mass fraction of the proliferating cells, ω_p. Since the problem is symmetric, only the half $[0, L/2]$ of the domain is shown. *Right panel*: spatial profile of the absolute value of the difference between ω_p^{ST} and ω_p^{NST}, i.e., the mass fractions of the proliferating cells computed with the standard model (ST) and the non-standard model (NST), respectively. The picture refers to the portion of the half domain in which $|\omega_p^{ST} - \omega_p^{NST}|$ is greater than, approximatively, $2.25 \cdot 10^{-3}$, and is computed at time $t = 20$ day.

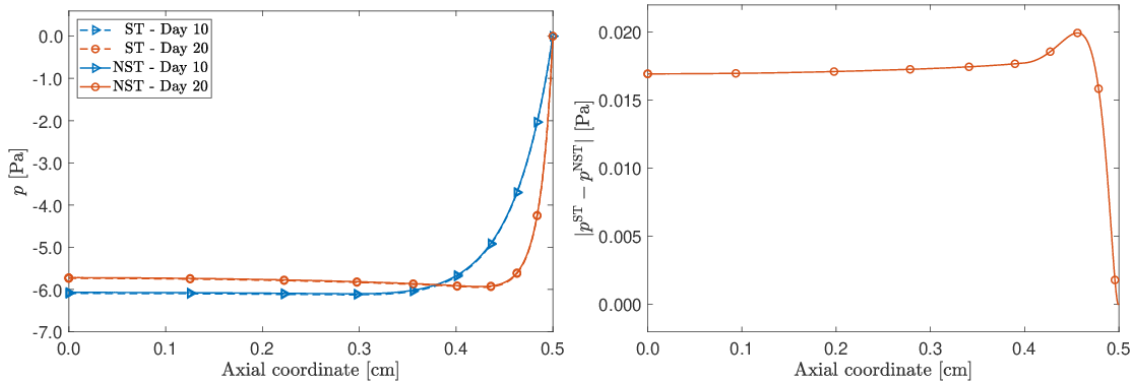

Figure 2.4: *Left panel*: spatial profile of the pressure, p. *Right panel*: spatial profile of the absolute value of the difference between p^{ST} and p^{NST}, which denote the pressure computed with the standard model (ST) and the pressure computed with the non-standard model (NST). The picture is computed at time $t = 20$ day. Since the problem is symmetric, in both panels only the half $[0, L/2]$ of the domain is shown.

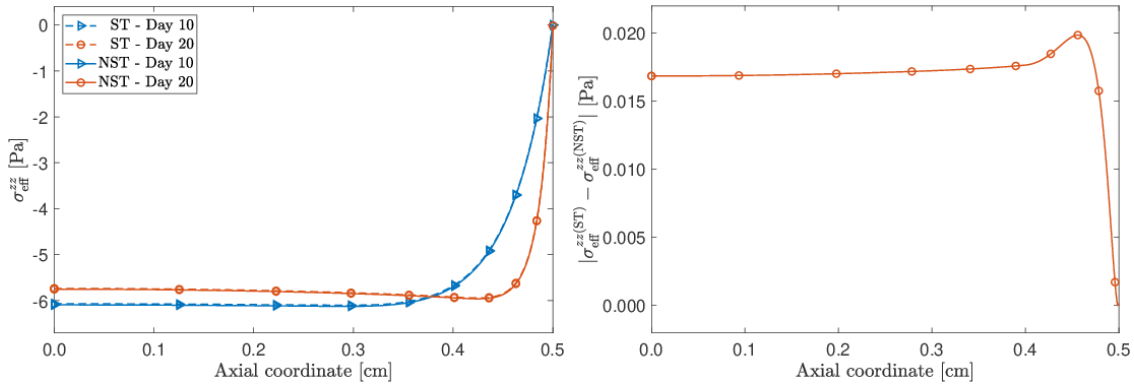

Figure 2.5: *Left panel*: spatial profile of the axial component of the effective Cauchy stress tensor, $\sigma_{\mathrm{eff}}^{zz}$. *Right panel*: spatial profile of the absolute value of the difference between $\sigma_{\mathrm{eff}}^{zz(\mathrm{ST})}$ and $\sigma_{\mathrm{eff}}^{zz(\mathrm{NST})}$, which denote the stress computed with the standard model (ST) and the non-standard model (NST), respectively. The picture is computed at time $t = 20$ day. Since the problem is symmetric, in both panels only the half $[0, L/2]$ of the domain is shown.

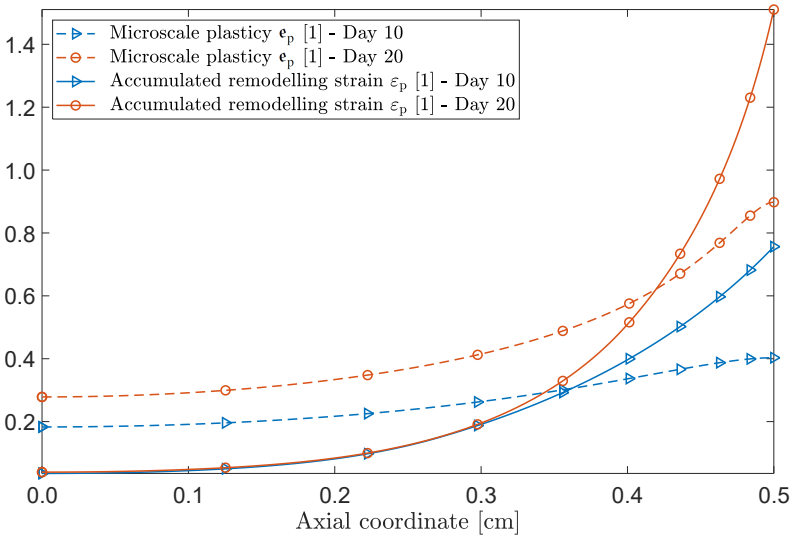

Figure 2.6: Spatial profiles of the accumulated remodelling strain ε_{p} and of the microscale plasticity $\mathfrak{e}_{\mathrm{p}}$. Since the problem is symmetric, only the half $[0, L/2]$ of the domain is shown.

Chapter 3

Influence of non-local diffusion in avascular tumour growth

The work reported in this chapter has been previously published in [235].

3.1 Introduction

For several years now, the scientific literature has experienced an important increase in the mathematical modelling of tumour growth (see e.g. [50, 37, 16, 153, 245, 184, 12, 255, 155, 238, 154] and the references therein). However, there is still the necessity for understanding the connections among the different processes of chemical, biological and/or mechanical nature that take place at different time and length scales and influence the evolution of a tumour.

From the mechanical perspective, the growth of a tumour is closely related to the appearance of transformations of its internal structure that arise in response to mass changes, which may be driven by its chemo-mechanical environment and coexist with the visible deformation of the tumour itself [86, 77, 228]. A relevant aspect of this phenomenology is that the structural transformations are often accompanied by the production of residual stresses [242, 165, 126, 69, 91]. In this respect, we mention the series of experiments conducted by Stylianopoulos et al. [262] on tumour spheroids, which indicate the existence of an incompatible, stress-free state for such systems and, thus, suggest to interpret growth in terms of inelastic distortions in addition to mere changes of shape. This conclusion permits to invoke the Bilby–Kröner–Lee (BKL) multiplicative decomposition of the deformation gradient tensor [201, 126, 246]. As long as volumetric growth is concerned and, as in the case of the present work, no other types of structural transformations are accounted for, the BKL decomposition reduces to decomposing the deformation gradient tensor into two contributions. One is related to the changes of the tissue's internal structure due to the gain or loss of mass, and the other one to distortions

of purely elastic nature (note that, here and in the sequel, we shall use the terms "tumour" and "tissue" interchangeably). We refer to the works [246, 126, 226, 66, 91, 131], and to the references therein, for a more complete discussion on the BKL multiplicative decomposition.

3.1.1 Aim and novelties of our work

In the present work, on the basis of the indications given above, our aim is to highlight and study the influence of the non-local character of diffusion processes that could be acting in an avascular tumour. To accomplish this task, we propose a potentially new constitutive relationship of fractional type for the mass flux vector. Consequently, we refer only to fractional operators in space, so that the model is non-local in space but local in time. In our formulation, the mass flux vector of the chemical species, evaluated at a given spatial point, is put in relation, through an integral operator, to the concentration gradient of that species, evaluated at all other points of the region of space occupied by the tumour. This leads to a generalisation of Fick's law that can be related to Fractional Calculus in a straightforward manner. In particular, this connection will become evident in the specification of the mass flux vector for the study of a benchmark problem (see Section "Definition of the non-locality function").

For our purposes, we adopt part of the modelling assumptions outlined in [191, 91, 131, 221]. Specifically, we study the tumour as a mixture comprising a fluid phase and a solid phase, and we identify its growth with the gain or loss of mass of the solid phase at the expenses or advantage of the fluid one. In particular, the model we employ predicts the gain of mass for a sufficiently high concentration of chemical agents (in fact, nutrients) and the loss of mass when the concentration of these falls below a certain threshold [192, 191]. Moreover, in the case of mass uptake of the solid phase, the model accounts for mechanotransduction [192, 191, 124, 131], thereby allowing a modulation of growth by means of stress [192, 191], whereas both for positive and for negative growth, the onset of structural transformations and their related inelastic distortions are considered. In the remainder of this work, we address only the most pertinent considerations and equations, while we refer the Reader to [191, 91, 221] for further details.

Before going further, we find it convenient to highlight the main novelties of our work, which can be summarised as follows:

1. *Impact of non-local diffusion on tumour growth.* With respect to [191, 91, 131, 221], we study the diffusion of the chemical agents in a growing tumour by hypothesising a non-local constitutive law for the diffusive mass flux vector. This is done with the purpose of weighing how and to which extent the deviation of non-local diffusion from the Fickean one impacts on the main descriptors of the tumour's evolution.

2. *Evolving non-locality driven by the tumour's dynamics.* The model that we are proposing requires to solve a type of non-locality that changes with the dynamics of the tumour through its motion *and* growth. To the best of our knowledge, this is a generalisation of a setting adopted in several papers (see e.g. [82, 151, 252, 174]), where the non-locality is accounted for in advection-diffusion equations without considering the deformation or structural change of the media in which such equations are defined.

3. *Non-locality and non-linearity.* The core of our work is the equation governing the evolution of chemical agents. This is given by an advection-diffusion-reaction equation featuring a fractional diffusive mass flux vector and a non-linear reaction term. We solve this equation *together* with all the other balance laws, expressed by non-linear partial differential equations, that model the tumour and its growth. Therefore, we solve a system of equations in which non-linearity combines with non-locality. To us, this is a novelty because, to the best of our knowledge, papers on Fractional Calculus usually solve one equation in conjunction with a fractional constitutive law. Furthermore, the nature of the problem we are tackling makes it impossible to have recourse to solution techniques based on Fourier and Laplace transforms, which are standard for problems of Fractional Calculus that are linear and/or formulated in unbounded domains. In our case, however, this assumption would be physically unrealistic and we have, thus, to turn to numerical techniques, such as Finite Element (FE) methods.

We point out that the study of fractional diffusion in bounded domains is delicate because of the complexity of the numerics involving operators of fractional type. Nevertheless, in the literature there exist some works dealing with fractional diffusion equations on bounded domains. The majority of these works employ finite-difference Grünwald-Letnikov discretisation schemes (see e.g. [212, 182, 84, 196]), and there also exist studies in which FE methods have been used for solving equations of fractional type [244, 151, 122, 106]. However, to the best of our knowledge, there is still a lack of studies addressing in detail the numerical issues arising in the context of fractional differential equations within a non-linear mechanical framework.

We also mention that, in this work, we suggest a possible way of formulating non-local diffusion on manifolds by adapting the definition of convolution on manifolds given in [253]. Originally, we encountered the necessity of expressing convolution in the non-Euclidean context because we aimed at writing our model in fully covariant formalism as a first step towards non-Euclidean settings. However, we faced some technical difficulties, which made us opt, for the time being, to give just a sketch of the generalisation of non-local diffusion on manifolds. For this reason, we summarised the main steps of our generalisation in Appendix A. Note

that Meerschaert et al. [195] did consider diffusion-like problems on manifolds but within a different framework.

Finally, we would like to point out that, throughout this work, the terminologies "mass fraction" and "concentration" will be often used interchangeably, and the spatial and temporal dependence of the variables are dropped out, unless there is a necessity to account for the non-local character of the problem, where this dependence is explicitly specified.

3.2 Kinematics

Let $\mathscr{S}$ be the three-dimensional Euclidean space, $\mathscr{T}$ an interval of time, and $\mathscr{B} \subset \mathscr{S}$ the reference placement of the mechanical system representing an avascular tumour, in which the tumour may, or may not, be free of stress. In particular, we consider that the tumour is a saturated mixture comprising a solid and a fluid phase. Moreover, the region of $\mathscr{S}$ occupied by the system at time $t \in \mathscr{T}$ is referred to as current configuration and is denoted by $\mathscr{B}_t \equiv \chi(\mathscr{B}, t)$, where $\chi(\cdot, t) : \mathscr{B} \to \mathscr{S}$ describes the motion of the solid phase (for the mixture kinematics, we follow here the same approach as the one adopted in [78]). Then, a point $x \in \mathscr{B}_t$ is given by $x = \chi(X, t)$, with $X \in \mathscr{B}$ and $t \in \mathscr{T}$. By differentiating the motion χ with respect to X, we obtain the deformation gradient tensor, $\boldsymbol{F}$, defined as the tangent map of χ, i.e., $\boldsymbol{F}(\cdot\,, t) \equiv T\chi(\cdot\,, t) : T\mathscr{B} \to T\mathscr{S}$, with $T\mathscr{B} = \sqcup_{X\in\mathscr{B}} T_X\mathscr{B}$ and $T\mathscr{S} = \sqcup_{x\in\mathscr{S}} T_x\mathscr{S}$. Thus, tensor $\boldsymbol{F}(X, t)$ characterises the visible deformations of the system by mapping vectors of the tangent space $T_X\mathscr{B}$ into the tangent space $T_x\mathscr{S}$.

We also introduce the spatial volumetric fractions of the solid and the fluid phases, given by $\varphi_{\mathrm{s}}(x, t)$ and $\varphi_{\mathrm{f}}(x, t)$, respectively. Then, we define the *apparent* mass densities, $\varphi_{\mathrm{s}}(x, t)\varrho_{\mathrm{s}}(x, t)$ and $\varphi_{\mathrm{f}}(x, t)\varrho_{\mathrm{f}}(x, t)$, of the solid and of the fluid, where $\varrho_{\mathrm{s}}(x, t)$ and $\varrho_{\mathrm{f}}(x, t)$ represent the *true* mass densities of the solid and the fluid phase, respectively. We notice that the apparent mass densities express, in each case, the phase mass per unit volume of the mixture as a whole, whereas each true mass density is the inherent density of the corresponding phase. Furthermore, the saturation of the mixture implies that $\varphi_{\mathrm{s}}(x, t) + \varphi_{\mathrm{f}}(x, t) = 1$, for all $x \in \mathscr{B}_t$ and $t \in \mathscr{T}$.

The velocity of the mixture is $\boldsymbol{v}(x, t) := \sum_{\mathrm{k}\in\{\mathrm{s,f}\}} \varphi_{\mathrm{k}}(x, t)\varrho_{\mathrm{k}}(x, t)\boldsymbol{v}_{\mathrm{k}}(x, t)/\varrho(x, t)$, where $\boldsymbol{v}_{\mathrm{s}}(x, t)$ and $\boldsymbol{v}_{\mathrm{f}}(x, t)$ denote the velocities of the solid and the fluid phases, respectively, and $\varrho(x, t) := \sum_{\mathrm{k}\in\{\mathrm{s,f}\}} \varphi_{\mathrm{k}}(x, t)\varrho_{\mathrm{k}}(x, t)$ is the mass density of the mixture as a whole. We notice that, by introducing the solid phase velocity $\boldsymbol{V}_{\mathrm{s}}(X, t) := \dot{\chi}(X, t)$, where the "dot" symbol denotes differentiation with respect to time, the relationship $\boldsymbol{v}_{\mathrm{s}}(x, t) = \boldsymbol{v}_{\mathrm{s}}\left(\chi(X, t), t\right) = \boldsymbol{V}_{\mathrm{s}}(X, t)$ holds true for all $X \in \mathscr{B}$ and $t \in \mathscr{T}$. Furthermore, since the tumour under study is assumed to be a mixture also in $\mathscr{B}$, the solid and the fluid coexist at every point $X \in \mathscr{B}$. This situation implies

that any point x in the fluid phase can be also viewed as the image of X through the motion χ and, consequently, $\boldsymbol{v}_{\mathrm{f}}(x,t) = \boldsymbol{v}_{\mathrm{f}}(\chi(X,t),t) = \boldsymbol{V}_{\mathrm{f}}(X,t)$.

3.2.1 Kinematics of growth

As suggested in several works, see e.g. [114, 262] and references therein, a relevant aspect in the growth of a tumour is the manifestation of irreversible changes of its internal structure. To take this aspect into account, we employ some concepts taken from the theory of inelastic processes. Specifically, for characterising the growth of the tissue under study, we invoke the Bilby-Kröner-Lee (BKL) decomposition of the deformation gradient tensor [201, 66, 246, 242, 126], i.e.,

$$\boldsymbol{F} = \boldsymbol{F}_{\mathrm{e}}\boldsymbol{F}_{\gamma}, \tag{3.1}$$

where the generally non-integrable tensor fields $\boldsymbol{F}_{\mathrm{e}}$ and $\boldsymbol{F}_{\gamma}$ describe the elastic accommodation of the tumour and the inelastic distortions induced by growth, respectively. We denote by $\mathscr{N}_t(X)$ the *natural state* of the body element of the tumour's solid phase associated with X, and we let it represent a stress-free state. We refer to the tensor $\boldsymbol{F}_{\gamma}(X,t) : T_X\mathscr{B} \to \mathscr{N}_t(X)$ as *growth tensor* and we assume that it comprehends the structural transformations undergone by the tumour in the course of its evolution. Then, the accommodating elastic tensor $\boldsymbol{F}_{\mathrm{e}}(X,t)$ maps vectors of $\mathscr{N}_t(X)$ into vectors of $T_x\mathscr{S}$. We refer to the works [246, 126, 226, 66, 91, 131], and references therein, for a more complete discussion on the nature and generalisation of the multiplicative decomposition in Equation (3.1).

In particular, following [191, 91, 131], in the present work we contemplate the case in which the growth tensor is a pure dilatation, that is, we impose $\boldsymbol{F}_{\gamma} = \gamma\boldsymbol{I}$, where $\gamma > 0$ is referred to as *growth parameter* and $\boldsymbol{I}$ is the second-order identity tensor.

3.3 Balance laws

By adopting the modelling assumptions made in [191, 91, 131], we consider that the fluid phase is constituted by chemical agents and "water", with mass fractions c_{a} and c_{w}, respectively, and such that $c_{\mathrm{a}} + c_{\mathrm{w}} = 1$. Furthermore, we hypothesise the solid phase to consist of two type of cells, i.e., the proliferating cells, with mass fraction c_{p}, and the necrotic cells, with mass fraction c_{n}, where $c_{\mathrm{p}} + c_{\mathrm{n}} = 1$.

3.3.1 Mass balance laws

The mass balance laws for the gain and loss of mass of the proliferating and the necrotic cells, and for the mass fraction of the chemical species and the fluid phase

as a whole are

$$\partial_t(\varphi_\mathrm{s}\varrho_\mathrm{s}c_\mathrm{p}) + \mathrm{div}(\varphi_\mathrm{s}\varrho_\mathrm{s}c_\mathrm{p}\boldsymbol{v}_\mathrm{s}) = r_\mathrm{pn} + r_\mathrm{fp}, \tag{3.2a}$$
$$\partial_t(\varphi_\mathrm{s}\varrho_\mathrm{s}c_\mathrm{n}) + \mathrm{div}(\varphi_\mathrm{s}\varrho_\mathrm{s}c_\mathrm{n}\boldsymbol{v}_\mathrm{s}) = r_\mathrm{nf} - r_\mathrm{pn}, \tag{3.2b}$$
$$\partial_t(\varphi_\mathrm{f}\varrho_\mathrm{f}c_\mathrm{a}) + \mathrm{div}(\varphi_\mathrm{f}\varrho_\mathrm{f}c_\mathrm{a}\boldsymbol{v}_\mathrm{f} + \boldsymbol{y}_\alpha) = r_\mathrm{ap}, \tag{3.2c}$$
$$\partial_t(\varphi_\mathrm{f}\varrho_\mathrm{f}) + \mathrm{div}(\varphi_\mathrm{f}\varrho_\mathrm{f}\boldsymbol{v}_\mathrm{f}) = -r_\mathrm{s}, \tag{3.2d}$$

where r_pn, r_fp, r_nf and r_ap denote rates of mass intake and/or reduction [191, 91, 131]. Specifically, they represent the rate at which the proliferating cells turn into necrotic (r_pn), the mass from the fluid phase that promotes the proliferation of cells (r_fp), the necrotic cells that dissolve into the fluid (r_nf), and the chemical agents that are depleted by the proliferating cells (r_ap). Moreover, $r_\mathrm{s} := r_\mathrm{fp} + r_\mathrm{nf}$ is the global source/sink of mass of the solid phase as a whole. Particularly, in writing Equations (3.2a) and (3.2b), we have enforced the consideration that the two cell populations move at the same velocity $\boldsymbol{v}_\mathrm{s}$. In Equation (3.2c), the term $\boldsymbol{y}_\alpha$ corresponds to the mass flux vector of the chemical agents, and since the focus of this work is subordinate to its definition, we prefer to make a deeper analysis of its characterisation and physical meaning in a separate section.

By enforcing that the tissue's cells are mainly composed by water [49, 191, 125], the true mass density of the solid phase, ϱ_s, can be regarded as constant and equal to the true mass density of the fluid phase, ϱ_f, which is set to be equal to the density of water. Thus, by taking into account the saturation constraint and the BKL decomposition in Equation (3.1), Equations (3.2a)–(3.2d), written with respect to the reference configuration, become

$$\dot{\mathfrak{c}}_\mathrm{p} = [R_\mathrm{pn} + R_\mathrm{fp} - R_\mathrm{s}\mathfrak{c}_\mathrm{p}][J_\gamma\Phi_{\mathrm{s}\nu}\varrho_\mathrm{s}]^{-1}, \tag{3.3a}$$
$$\frac{\dot{\gamma}}{\gamma} = [R_\mathrm{fp} + R_\mathrm{nf}][3\varrho_\mathrm{s}\Phi_{\mathrm{s}\nu}J_\gamma]^{-1}, \tag{3.3b}$$
$$\varrho_\mathrm{f}[J - J_\gamma\Phi_{\mathrm{s}\nu}]\dot{\mathfrak{c}}_\mathrm{a} + \varrho_\mathrm{f}\boldsymbol{Q}\,\mathrm{Grad}\,\mathfrak{c}_\mathrm{a} + \mathrm{Div}\boldsymbol{Y}_\alpha = \mathfrak{c}_\mathrm{a}R_\mathrm{s} + R_\mathrm{ap}, \tag{3.3c}$$
$$\mathrm{Div}\boldsymbol{Q} + \dot{J} = 0, \tag{3.3d}$$

where the material filtration velocity $\boldsymbol{Q}$, the material mass flux vector of the chemical agents $\boldsymbol{Y}_\alpha$, the mass fractions $\mathfrak{c}_\mathrm{a}$ and $\mathfrak{c}_\mathrm{p}$, and the material sources/sinks of mass featuring in Equations (3.3a)-(3.3d) are given by

$$\boldsymbol{Q}(X,t) := J(X,t)\boldsymbol{q}(\chi(X,t),t)\boldsymbol{F}^{-\mathrm{T}}(X,t), \tag{3.4a}$$
$$\boldsymbol{Y}_\alpha(X,t) := J(X,t)\boldsymbol{y}_\alpha(\chi(X,t),t)\boldsymbol{F}^{-\mathrm{T}}(X,t), \tag{3.4b}$$
$$\mathfrak{c}_\mathrm{k}(X,t) := c_\mathrm{k}(\chi(X,t),t), \qquad \mathrm{k} \in \{\mathrm{a},\mathrm{p}\} \tag{3.4c}$$
$$R_\beta(X,t) := J(X,t)r_\beta(\chi(X,t),t), \qquad \beta \in \{\mathrm{pn},\mathrm{fp},\mathrm{nf},\mathrm{ap},\mathrm{s}\}, \tag{3.4d}$$

with $\boldsymbol{q} = \varphi_\mathrm{f}[\boldsymbol{v}_\mathrm{f} - \boldsymbol{v}_\mathrm{s}]$. We note that, in writing Equations (3.3a)-(3.3d), the material volumetric fractions $\Phi_\mathrm{s}(X,t) := J(X,t)\varphi_\mathrm{s}(\chi(X,t),t)$ and $\Phi_\mathrm{f}(X,t) :=$

$J(X,t)\varphi_{\mathrm{f}}(\chi(X,t),t)$ have been written as $\Phi_{\mathrm{s}} = J_\gamma \Phi_{\mathrm{s}\nu}$ and $\Phi_{\mathrm{f}} = J - J_\gamma \Phi_{\mathrm{s}\nu}$, where $\Phi_{\mathrm{s}\nu}(X,t) := J_{\mathrm{e}}(X,t)\varphi_{\mathrm{s}}(\chi(X,t),t)$ is the "pull-back" of the solid phase volumetric fraction, φ_{s}, to the natural state [91, 131]. In particular, by imposing that the temporal derivative of J_γ compensates for the mass source r_{s} [102, 9], it can be deduced that the volumetric fraction $\Phi_{\mathrm{s}\nu}$ is independent of time. However, $\Phi_{\mathrm{s}\nu}$ may depend on material points [131]. Furthermore, since it holds true that $J_{\mathrm{e}} = J/J_\gamma$, the volumetric fractions of the solid and the fluid phase can be expressed entirely in terms of the volume ratios J and J_γ, i.e.,

$$\varphi_{\mathrm{s}}(x,t) = \varphi_{\mathrm{s}}(\chi(X,t),t) = \frac{J_\gamma(X,t)\Phi_{\mathrm{s}\nu}(X)}{J(X,t)}, \tag{3.5a}$$

$$\varphi_{\mathrm{f}}(x,t) = 1 - \varphi_{\mathrm{s}}(x,t) = \frac{J(X,t) - J_\gamma(X,t)\Phi_{\mathrm{s}\nu}(X)}{J(X,t)}. \tag{3.5b}$$

3.3.2 Momentum balance laws

In this work, we neglect inertial and body forces, so that the momentum balance laws for the biphasic medium as a whole and for the fluid phase write [141, 129, 221]

$$\operatorname{div}(\boldsymbol{\sigma}_{\mathrm{s}} + \boldsymbol{\sigma}_{\mathrm{f}}) = \mathbf{0}, \tag{3.6a}$$

$$\boldsymbol{q} = -\boldsymbol{k}\,\operatorname{grad} p, \tag{3.6b}$$

where $\boldsymbol{\sigma}_{\mathrm{s}}$ and $\boldsymbol{\sigma}_{\mathrm{f}}$ are the Cauchy stress tensors of the solid and the fluid phase, p is the hydrostatic pressure, Equation (3.6b) expresses Darcy's law [141], and $\boldsymbol{k}$ denotes the *permeability tensor*, which is here taken to be symmetric and positive definite.

Following [141, 39, 128, 91], we assume the fluid phase to be macroscopically inviscid, so that $\boldsymbol{\sigma}_{\mathrm{f}}$ is purely hydrostatic, and we write

$$\boldsymbol{\sigma}_{\mathrm{f}} = -\varphi_{\mathrm{f}} p \boldsymbol{g}^{-1}, \tag{3.7a}$$

$$\boldsymbol{\sigma}_{\mathrm{s}} = -\varphi_{\mathrm{s}} p \boldsymbol{g}^{-1} + \boldsymbol{\sigma}_{\mathrm{sc}}, \tag{3.7b}$$

where $\boldsymbol{\sigma}_{\mathrm{sc}}$ is said to be the constitutive part of $\boldsymbol{\sigma}_{\mathrm{s}}$ and $\boldsymbol{g}^{-1}$ is the inverse of the metric tensor, $\boldsymbol{g}$, associated with $\mathscr{S}$. Then, by substituting Equations (3.7a) and (3.7b) into Equation (3.6a), and performing the backward Piola transformation of Equations (3.6a) and (3.6b), we obtain

$$\operatorname{Div}(-J\mathfrak{p}\mathfrak{g}^{-1}\boldsymbol{F}^{-\mathrm{T}} + \boldsymbol{P}_{\mathrm{sc}}) = \mathbf{0}, \tag{3.8a}$$

$$\boldsymbol{Q} = -\boldsymbol{K}\,\operatorname{Grad}\mathfrak{p}, \tag{3.8b}$$

where we have introduced the notation

$$\mathfrak{p}(X,t) := p(\chi(X,t),t), \tag{3.9a}$$

$$\boldsymbol{K}(X,t) := J(X,t)\boldsymbol{F}^{-1}(\chi(X,t),t)\boldsymbol{k}(\chi(X,t),t)\boldsymbol{F}^{-\mathrm{T}}(X,t), \tag{3.9b}$$

$$\boldsymbol{P}_{\mathrm{sc}}(X,t) := J(X,t)\boldsymbol{\sigma}_{\mathrm{sc}}(\chi(X,t),t)\boldsymbol{F}^{-\mathrm{T}}(X,t), \tag{3.9c}$$

$$\mathfrak{g}(X,t) := \boldsymbol{g}(\chi(X,t)), \tag{3.9d}$$

to denote, respectively, the pressure expressed as a function of time and of the points of $\mathscr{B}$, the material permeability tensor, the constitutive part of the overall first Piola-Kirchhoff stress tensor, and the metric tensor expressed as a function of time and of the points of $\mathscr{B}$. Moreover, Equation (3.8b) represents Darcy's law of filtration, pulled-back to the reference configuration.

3.4 Constitutive laws I: Strain energy density and permeability

Following [191, 91, 131], we hypothesise that the solid phase of the tumour is isotropic and hyperelastic, and introduce the strain energy densities $\mathscr{W}$ and $\mathscr{W}_\nu$, which are written per unit volume of the reference configuration and of the natural state, respectively. To account for the structural changes induced by growth, the strain energy density $\mathscr{W}$ is expressed as a constitutive function, namely $\check{\mathscr{W}}$, depending on $\boldsymbol{F}$, $\boldsymbol{F}_\gamma$ and on material points. Furthermore, we denote by $\check{\mathscr{W}}_\nu$ the constitutive representation of $\mathscr{W}_\nu$, which is supposed here to depend solely on the tensor $\boldsymbol{F}_{\mathrm{e}}$. Therefore, the following relationship holds [102, 73, 91]

$$\check{\mathscr{W}}(\boldsymbol{F}(X,t),\boldsymbol{F}_\gamma(X,t),X) = J_\gamma(X,t)\check{\mathscr{W}}_\nu(\boldsymbol{F}_{\mathrm{e}}(X,t)). \tag{3.10}$$

Within a more general framework, the strain energy density $\check{\mathscr{W}}_\nu$ maintains the explicit dependence on X, and Equation (3.10) does not hold in its present form. This becomes evident when $\check{\mathscr{W}}_\nu$ is parameterised by point-dependent material coefficients or, by expressing $\check{\mathscr{W}}_\nu$ as $\check{\mathscr{W}}_\nu = \Phi_{\mathrm{s}\nu}\varrho_{\mathrm{s}}\check{\Psi}_{\mathrm{s}}$, where $\check{\Psi}_{\mathrm{s}}$ is the solid phase strain energy density per unit mass, when $\Phi_{\mathrm{s}\nu}$ depends on X. However, these circumstances are excluded from the setting of this work, as can be deduced by looking at Table 3.1, in which all the material parameters and $\Phi_{\mathrm{s}\nu}$ are taken as constants.

Hereafter, we adopt a constitutive law of the type proposed in [149] for $\check{\mathscr{W}}_\nu$, i.e.,

$$\check{\mathscr{W}}_\nu(\boldsymbol{F}_{\mathrm{e}}) = \hat{\mathscr{W}}_\nu(\boldsymbol{C}_{\mathrm{e}}) = a_0\big\{\exp(\hat{\Psi}(\boldsymbol{C}_{\mathrm{e}})) - 1\big\}, \tag{3.11a}$$

$$\hat{\Psi}(\boldsymbol{C}_{\mathrm{e}}) = a_1[\hat{I}_1(\boldsymbol{C}_{\mathrm{e}}) - 3] + a_2[\hat{I}_2(\boldsymbol{C}_{\mathrm{e}}) - 3] - a_3\log\big(\hat{I}_3(\boldsymbol{C}_{\mathrm{e}})\big), \tag{3.11b}$$

where $\hat{\mathscr{W}}_\nu$ is the constitutive representation of $\mathscr{W}$ expressed as a function of the elastic, right Cauchy-Green deformation tensor $\boldsymbol{C}_{\mathrm{e}} = \boldsymbol{F}_{\mathrm{e}}^{\mathrm{T}}.\boldsymbol{F}_{\mathrm{e}} = \boldsymbol{F}_\gamma^{-\mathrm{T}}\boldsymbol{C}\boldsymbol{F}_\gamma^{-1}$, $\boldsymbol{C} = \boldsymbol{F}^{\mathrm{T}}.\boldsymbol{F}$ is the "classical", right Cauchy-Green deformation tensor, $\hat{I}_1(\boldsymbol{C}_{\mathrm{e}}) = \mathrm{tr}\,(\boldsymbol{C}_{\mathrm{e}})$, $\hat{I}_2(\boldsymbol{C}_{\mathrm{e}}) = \frac{1}{2}\big\{[\hat{I}_1(\boldsymbol{C}_{\mathrm{e}})]^2 - \mathrm{tr}[(\boldsymbol{C}_{\mathrm{e}})^2]\big\}$, and $\hat{I}_3(\boldsymbol{C}_{\mathrm{e}}) = \det(\boldsymbol{C}_{\mathrm{e}})$ are the principal invariants

of $\boldsymbol{C}_{\mathrm{e}}$, and, as in [149, 269, 91], the parameters a_0, a_1, a_2 and a_3 are expressed in terms of Lamé's parameters λ and μ, i.e.,

$$a_0 = \frac{2\mu+\lambda}{4a_3}, \quad a_1 = a_3\frac{2\mu-\lambda}{2\mu+\lambda}, \quad a_2 = a_3\frac{\lambda}{2\mu+\lambda}, \quad a_3 = a_1 + 2a_2 = 1. \tag{3.12}$$

Then, by using Equations (3.11a) and (3.11b), the constitutive part of the first Piola-Kirchhoff stress tensor reads [91]

$$\boldsymbol{P}_{\mathrm{sc}} = J_\gamma \boldsymbol{F}\boldsymbol{F}_\gamma^{-1}\left(2\frac{\partial\hat{\mathscr{W}}_\nu}{\partial\boldsymbol{C}_{\mathrm{e}}}(\boldsymbol{C}_{\mathrm{e}})\right)\boldsymbol{F}_\gamma^{-\mathrm{T}}. \tag{3.13}$$

Furthermore, we require the permeability tensor to be *"unconditionally isotropic"* [25], i.e., $\boldsymbol{k} = k_0\boldsymbol{g}^{-1}$, so that the material permeability tensor reads

$$\boldsymbol{K} = Jk_0\boldsymbol{C}^{-1}. \tag{3.14}$$

In Equation (3.14), k_0 denotes the *scalar permeability* and is taken here as in [25, 149], i.e.,

$$k_0 = k_{\mathrm{R}}\left[\frac{J - J_\gamma\Phi_{\mathrm{s}\nu}}{J_\gamma\varphi_{\mathrm{fR}}}\right]^{m_0}\exp\left(\frac{m_1}{2}\left[\frac{J^2-J_\gamma^2}{J_\gamma^2}\right]\right), \tag{3.15}$$

where m_0 and m_1 are constant material coefficients, $\varphi_{\mathrm{fR}} := 1 - \Phi_{\mathrm{s}\nu}$ is a reference value of the fluid phase volumetric fraction, and k_{R} is the reference permeability of the medium. In the sequel, both k_{R} and φ_{fR}, and thus $\Phi_{\mathrm{s}\nu}$, are assumed to be constant.

3.5 Constitutive Laws II: Non-Fickean diffusion

As pointed out in the Introduction, our aim is to generalise previous models of tumour growth [191, 91] by using some of the notions and tools offered by the theory of Fractional Calculus [224, 21, 22]. To this end, we introduce a non-Fickean type of diffusion of the chemical agents. Specifically, our purpose is to take into account the non-local behaviour of the gradient of the chemical agents' mass fraction, and study its influence on the growth of an avascular tumour.

3.5.1 Non-Fickean mass flux vector

We propose to express the chemical species' mass flux vector, $\boldsymbol{y}_\alpha$ (see Equation (3.2c)), in terms of a non-local constitutive law of convolution type, in which, in the Euclidean case, the kernel of the convolution integral features a power law in the distance between the points x and $\tilde{x}$ of each pair $(x, \tilde{x})$ of spatial points occupied

by body points. This way, we aim to show how $\boldsymbol{y}_\alpha$, evaluated at x, depends on the gradients of concentration evaluated at all other points $\tilde{x}$, and on the power law chosen for the convolution kernel. To do this, we face two difficulties: the first one is connected to the fact that, since, for the sake of generality, we view the body as a manifold, the concept of convolution has to be suitably generalised; the second one is due to the impossibility of integrating vector fields on manifolds. Whereas the first issue has been investigated in the literature [44, 253, 225], and we refer to the convolution on manifolds put forward in [253], the second issue can be circumvented by re-defining the mass flux vector of the chemical agents in weak form, i.e., for each $t \in \mathscr{T}$, we define $\boldsymbol{y}_\alpha$ through the *duality* product [43]

$$\langle \boldsymbol{y}_\alpha, \operatorname{grad} \check{c} \rangle := -\varrho_{\mathrm{f}} \int_{\mathscr{B}_t} \left\{ \int_{\mathscr{B}_t} [\operatorname{grad} \check{c}(x)]\, \boldsymbol{d}_\alpha(x, \tilde{x}, t) [\operatorname{grad} c_{\mathrm{a}}(\tilde{x}, t)] \mathrm{dv}(\tilde{x}) \right\} \mathrm{dv}(x), \tag{3.16a}$$

$$\boldsymbol{d}_\alpha(x, \tilde{x}, t) := \mathfrak{f}_\alpha(x, \tilde{x})\, \mathfrak{d}_\alpha(x, \tilde{x}, t), \tag{3.16b}$$

for all $\check{c} \in \check{\mathscr{C}} = \{\check{c} \in H^1(\mathscr{B}_t) : \ \check{c} = 0 \text{ on } (\partial\mathscr{B}_t)_{\mathrm{D}}\}$, with $\check{\mathscr{C}}$ being the space of all *virtual variations of the mass fractions*, $(\partial\mathscr{B}_t)_{\mathrm{D}}$ the portion of the boundary of $\mathscr{B}_t$ on which Dirichlet conditions are applied for the mass fraction of the chemical agents, and $H^1(\mathscr{B}_t)$ is the standard Sobolev space of square-integrable functions over $\mathscr{B}_t$ whose weak derivatives up to the order one are square-integrable over $\mathscr{B}_t$ too.

We refer to the second-order tensor $\boldsymbol{d}_\alpha(x, \tilde{x}, t)$ as *non-local diffusivity tensor*, and we express it as the product of the scalar quantity $\mathfrak{f}_\alpha(x, \tilde{x})$ and of the tensor $\mathfrak{d}_\alpha(x, \tilde{x}, t)$. In particular, for a given $x \in \mathscr{B}_t$ and varying $\tilde{x} \in \mathscr{B}_t$, $\mathfrak{f}_\alpha(x, \tilde{x})$, referred to as the *non-locality function*, measures how the intensity of the chemical signal expressed by $\operatorname{grad} c_{\mathrm{a}}(\tilde{x}, t)$ is felt at x. The tensor $\mathfrak{d}_\alpha(x, \tilde{x}, t)$, instead, is denominated *fractional diffusivity tensor*. We emphasise that $\mathfrak{f}_\alpha$ is defined for $x \neq \tilde{x}$ and that, since we are dealing with fractional diffusion, both $\mathfrak{d}_\alpha(x, \tilde{x}, t)$ and $\boldsymbol{d}_\alpha(x, \tilde{x}, t)$ have, in general, physical dimensions different from those of the standard diffusivity tensor, depending on the prescription of $\mathfrak{f}_\alpha$ and $\alpha \in \mathbb{R}^+$.

The way in which $\mathfrak{f}_\alpha(x, \tilde{x})$ is to be understood in the case in which $\mathscr{B}_t$ is viewed as a manifold is reported in Appendix A1. However, from here on, to avoid the technical difficulties of addressing such a general framework, which is out of the scope of this work, we prefer to adopt orthogonal Cartesian coordinates. Then, by regarding $\mathscr{B}_t$ as a flat subset of $\mathscr{S}$ having the same dimensionality as $\mathscr{S}$, $\mathfrak{f}_\alpha(x, \tilde{x})$ can be recast in the form $\mathfrak{f}_\alpha(x, \tilde{x}) = \hat{\mathfrak{f}}_\alpha(x - \tilde{x})$, where $\hat{\mathfrak{f}}_\alpha$ is introduced to re-define $\mathfrak{f}_\alpha$ as a function of the vector $x - \tilde{x}$, i.e., as $\hat{\mathfrak{f}}_\alpha : T_{\tilde{x}}\mathscr{S} \to \mathbb{R}$ (see Appendix A1). Furthermore, we require $\mathfrak{d}_\alpha(x, \tilde{x}, t)$ to be a two-point tensor of the type $\mathfrak{d}_\alpha(x, \tilde{x}, t) = \sum_{a,b=1}^{3} [\mathfrak{d}_\alpha(x, \tilde{x}, t)]^{ab} \boldsymbol{e}_a(x) \otimes \boldsymbol{e}_b(\tilde{x})$, where $\{\boldsymbol{e}_l(x)\}_{l=1}^3$ and $\{\boldsymbol{e}_l(\tilde{x})\}_{l=1}^3$ are the vector bases attached to x and $\tilde{x}$. It is worth noticing that, within a Cartesian setting, and for $x = \tilde{x}$, the tensor $\boldsymbol{e}_a(x) \otimes \boldsymbol{e}_b(\tilde{x}) \equiv \boldsymbol{e}_a(x) \otimes \boldsymbol{e}_b(x)$ is referred to as *"Jacoby*

directional tensor" in [8], where, in a slightly different context, the central Marchaud fractional derivative is extended to the case of two- or three-dimensional problems.

In general, there is no correlation at all between the vector bases $\{\boldsymbol{e}_l(x)\}_{l=1}^3$ and $\{\boldsymbol{e}_l(\tilde{x})\}_{l=1}^3$ and, in fact, each basis can be chosen arbitrarily and independently of the other one. Nevertheless, $\{\boldsymbol{e}_l(\tilde{x})\}_{l=1}^3$ can be enforced to be the result of the parallel transport of $\{\boldsymbol{e}_l(x)\}_{l=1}^3$ along the geodesic connecting x and $\tilde{x}$. In particular, in the Euclidean case, the arch of the geodesic connecting x and $\tilde{x}$ is the segment of the straight line directed from x to $\tilde{x}$ and the parallel transport of $\{\boldsymbol{e}_l(x)\}_{l=1}^3$ along such a line renders $\{\boldsymbol{e}_l(\tilde{x})\}_{l=1}^3$ collinear with $\{\boldsymbol{e}_l(x)\}_{l=1}^3$. Hence, for each $l = 1,2,3$, $\boldsymbol{e}_l(x)$ and $\boldsymbol{e}_l(\tilde{x})$ can be associated with the same direction, hereafter denoted by $\boldsymbol{i}_l$, even though they remain, implicitly, distinct vectors, attached to different spatial points. Within this approach, we hypothesise that $\mathfrak{d}_\alpha(x,\tilde{x},t)$ admits the representation $\mathfrak{d}_\alpha(x,\tilde{x},t) = \sum_{b=1}^3 \mathfrak{d}_\alpha^b(x,\tilde{x},t)\boldsymbol{e}_b(x)\otimes\boldsymbol{e}_b(\tilde{x})$ and, since $\boldsymbol{e}_l(x)$ is collinear with $\boldsymbol{e}_l(\tilde{x})$, this representation of $\mathfrak{d}_\alpha(x,\tilde{x},t)$ mimics the description of an orthotropic tensor function with respect to the set of directions $\{\boldsymbol{i}_1,\boldsymbol{i}_2,\boldsymbol{i}_3\}$. Hence, it is "as if" we had $\mathfrak{d}_\alpha(x,\tilde{x},t) = \sum_{b=1}^3 \mathfrak{d}_\alpha^b(x,\tilde{x},t)\boldsymbol{i}_b\otimes\boldsymbol{i}_b$. Then, by using the definitions in Equation (3.16), we identify the components of the fractional mass flux to be given by the following expression

$$[\boldsymbol{y}_\alpha(x,t)]^b := -\varrho_{\mathrm{f}}\int_{\mathscr{B}_t}\hat{\mathfrak{f}}_\alpha(x-\tilde{x})\mathfrak{d}_\alpha^b(x,\tilde{x},t)\partial_b c_{\mathrm{a}}(\tilde{x},t)\,\mathrm{dv}(\tilde{x}), \tag{3.17}$$

with no sum over $b = 1,2,3$. We call the coefficients $\{\mathfrak{d}_\alpha^b(x,\tilde{x},t)\}_{b=1}^3$ *fractional diffusivities*.

3.5.2 Comparison with other works

Other definitions of fractional mass flux vector can be found that characterise non-Fickean diffusion processes (see e.g. [195, 252] and references therein). For instance, Sapora et al. [252] study a fractional version of Darcy's law in one dimension in which the filtration velocity (also known as "specific mass flux") is taken to be proportional to an integral operator that the Authors refer to as *"Riesz integral"* [252] of pressure (note that the definition of Riesz integral given in [252] differs by a factor $\cos(\beta\pi/2)$, with $\beta\in]0,1[$, from that in [249, 21]). However, when passing to higher dimensionalities, it is necessary to extend the concept of fractional differentiation to other differential operators like the gradient of a scalar function. In this regard, in [97, 1, 267] the fractional gradient of order $\alpha\in\mathbb{R}^+$ of a scalar function is defined as a co-vector, whose components are identified with the fractional partial derivatives, each of which of order α, of the given function. In particular, these fractional partial derivatives are taken in the sense of Riemann-Liouville in [97] and in the sense of Caputo in [267], whereas the Nishimoto fractional derivative [211] is used in [1], for $\alpha\in]0,1]$.

For the purposes of our work, we adopt the definition given in Equation (3.17). This definition presents some fundamental differences with respect to the definition supplied, for instance, in [252]. These differences, however, are not only related to the fact that the physical phenomenon addressed in [252] is distinct from the one we are studying here. Rather, they are intrinsic in the definition of the operator expressing $\boldsymbol{y}_\alpha$, and can be summarised as follows:

- Equation (3.17) is conceived in a three-dimensional setting and, consequently, requires an integration over the whole configuration of the body, $\mathscr{B}_t$, whereas the definition of the mass flux given in [252] features an integration over a bounded interval.

- In our definition, each fractional diffusivity $\mathfrak{d}_\alpha^b(x,\tilde{x},t)$, b = 1,2,3, is part of the integrand of Equation (3.17), and cannot be factorised out of the corresponding integral.

- If, for a given $b_0 \in \{1,2,3\}$, the fractional diffusivity $\mathfrak{d}_\alpha^{b_0}(x,\tilde{x},t)$ could be factorised out of the integral in Equation (3.17) (e.g. by setting $\mathfrak{d}_\alpha^{b_0}(x,\tilde{x},t) \equiv \mathfrak{d}_{0\alpha}$, with $\mathfrak{d}_{0\alpha}$ constant), and if the only nonzero component of $\operatorname{grad} c(\tilde{x},t)$ were $\partial_{b_0} c_\mathrm{a}(\tilde{x},t)$ for all $\tilde{x}$ and t, one would have

$$[\boldsymbol{y}_\alpha(x,t)]^{b_0} = -\varrho_\mathrm{f}\mathfrak{d}_{0\alpha}\int_{\mathscr{B}_t}\hat{\mathfrak{f}}_\alpha(x-\tilde{x})\partial_{b_0}c_\mathrm{a}(\tilde{x},t)\mathrm{dv}(\tilde{x}), \tag{3.18}$$

  where $\hat{\mathfrak{f}}_\alpha(x-\tilde{x})$ is still a function of *all* the components of the vector $x-\tilde{x}$, rather than of its b_0-th component only. This property marks a major difference between our approach and the model developed in [252], and expresses the fact that, even in the presence of a preferred direction (i.e., the one associated with $\partial_{b_0}c_\mathrm{a}$), one should account for the non-locality in all directions.

Before going further, we notice that, if the fractional diffusivities $\{\mathfrak{d}_\alpha^b(x,\tilde{x},t)\}_{b=1}^3$ are all equal to some reference constant value $\mathfrak{d}_{\mathrm{R}\alpha}$ (note that, for simplicity, we call 'fractional diffusivities' the *set of the three principal fractional diffusivities*), the mass flux vector $\boldsymbol{y}_\alpha(x,t)$ can be expressed (in a Cartesian setting) as

$$\boldsymbol{y}_\alpha(x,t) = -\varrho_\mathrm{f}\mathfrak{d}_{\mathrm{R}\alpha}\int_{\mathscr{B}_t}\hat{\mathfrak{f}}_\alpha(x-\tilde{x})\operatorname{grad}c_\mathrm{a}(\tilde{x},t)\mathrm{dv}(\tilde{x}). \tag{3.19}$$

Moreover, for some suitable $\hat{\mathfrak{f}}_\alpha(x-\tilde{x})$, usually written as a power-law that decays in space, the integral on the right-hand-side of Equation (3.19) can be taken as the definition of a *fractional gradient* of c_a of order α, i.e., one can write (in the Cartesian setting)

$$\operatorname{grad}^\alpha c_\mathrm{a}(x,t) := \int_{\mathscr{B}_t}\hat{\mathfrak{f}}_\alpha(x-\tilde{x})\operatorname{grad}c_\mathrm{a}(\tilde{x},t)\mathrm{dv}(\tilde{x}), \tag{3.20a}$$

$$[\mathrm{grad}^{\alpha} c_{\mathrm{a}}(x,t)]_b := \int_{\mathscr{B}_t} \hat{\mathfrak{f}}_{\alpha}(x-\tilde{x})\, \partial_b c_{\mathrm{a}}(\tilde{x},t)\mathrm{dv}(\tilde{x}), \quad b = 1,2,3. \tag{3.20b}$$

Equations (3.20a) and (3.20b) are reminiscent of the definition of fractional gradient of order α supplied in [267]. However, an important difference between that definition and ours is that, in [267], the components of the fractional gradient of c_{a} (i.e., $\{[\mathrm{grad}^{\alpha} c_{\mathrm{a}}(x,t)]_b\}_{b=1}^{3}$ in our notation) are identified with the Caputo derivatives of c_{a} along the principal directions of the vector basis. This, in turn, requires the function $\hat{\mathfrak{f}}_{\alpha}$ of Tarasov [267] to depend, for each Caputo derivative, solely on the b-th component of $x - \tilde{x}$.

3.5.3 Backward Piola transform of the mass flux vector

The backward Piola transformation of Equation (3.16a) is given by

$$\begin{aligned}\langle \boldsymbol{y}_{\alpha}, \mathrm{grad}\check{c}\rangle &= \langle \boldsymbol{Y}_{\alpha}, \mathrm{Grad}\check{\mathfrak{c}}\rangle \\ &= -\varrho_{\mathrm{f}} \int_{\mathscr{B}} \left\{ \int_{\mathscr{B}} [\mathrm{Grad}\check{\mathfrak{c}}(X,t)] \boldsymbol{D}_{\alpha}(X,\tilde{X},t) [\mathrm{Grad}\, \mathfrak{c}_{\mathrm{a}}(\tilde{X},t)] \mathrm{d}V(\tilde{X}) \right\} \mathrm{dV}(X),\end{aligned} \tag{3.21}$$

with $\check{\mathfrak{c}}$ and $\mathfrak{c}_{\mathrm{a}}$ such that $\check{\mathfrak{c}}(X,t) = \check{c}(\chi(X,t))$ and $\mathfrak{c}_{\mathrm{a}}(X,t) = c_{\mathrm{a}}(\chi(X,t),t)$, and we introduced the *material non-local diffusivity tensor*, $\boldsymbol{D}_{\alpha}$, the *material non-locality function*, $\mathfrak{F}_{\alpha}$, and the *material fractional diffusivity tensor*, $\mathfrak{D}_{\alpha}$, as follows

$$\boldsymbol{D}_{\alpha}(X,\tilde{X},t) := J(X,t)\mathfrak{F}_{\alpha}(X,\tilde{X},t)\mathfrak{D}_{\alpha}(X,\tilde{X},t), \tag{3.22a}$$

$$\mathfrak{F}_{\alpha}(X,\tilde{X},t) := \hat{\mathfrak{f}}_{\alpha}\big(\chi(X,t) - \chi(\tilde{X},t)\big), \tag{3.22b}$$

$$\mathfrak{D}_{\alpha}(X,\tilde{X},t) := J(\tilde{X},t)\boldsymbol{F}^{-1}(\chi(X,t),t)\mathfrak{d}_{\alpha}(\chi(X,t),\chi(\tilde{X},t),t)\boldsymbol{F}^{-\mathrm{T}}(\tilde{X},t). \tag{3.22c}$$

More specifically, the components of $\mathfrak{D}_{\alpha}(X,\tilde{X},t)$ and $\boldsymbol{Y}_{\alpha}(X,t)$ are given by

$$[\mathfrak{D}_{\alpha}(X,\tilde{X},t)]^{AB} = J(\tilde{X},t)\sum_{b=1}^{3}[\boldsymbol{F}^{-1}(\chi(X,t),t)]^{A}{}_{b}\, \mathfrak{d}_{\alpha}^{b}(\chi(X,t),\chi(\tilde{X},t),t)\, [\boldsymbol{F}^{-\mathrm{T}}(\tilde{X},t)]_{b}{}^{B}, \tag{3.23a}$$

$$[\boldsymbol{Y}_{\alpha}(X,t)]^{A} = -\varrho_{\mathrm{f}} \int_{\mathscr{B}} J(X,t)\mathfrak{F}_{\alpha}(X,\tilde{X},t) \sum_{B=1}^{3}[\mathfrak{D}_{\alpha}(X,\tilde{X},t)]^{AB}\, \partial_B \mathfrak{c}_{\mathrm{a}}(\tilde{X},t)\, \mathrm{dV}(\tilde{X}). \tag{3.23b}$$

Expression (3.23b) defines the components of the mass flux vector in the material description, whereas $\mathfrak{D}_{\alpha}$ is the material counterpart of the fractional diffusivity tensor $\mathfrak{d}_{\alpha}$.

In the sequel, we assume the spatial fractional diffusivities to be all equal to each other, i.e., $\mathfrak{d}_{\alpha}^{b}(x,\tilde{x},t) = \mathfrak{d}_{\alpha}(x,\tilde{x},t)$, for all $b = 1,2,3$, and that $\mathfrak{d}_{\alpha}(x,\tilde{x},t)$ is

independent of x (more rigorously, we should say that $\mathfrak{d}_\alpha$ can be redefined as a function of time and of the spatial variable with respect to which the integration is made, i.e., $\tilde{x}$). Consequently, with a slight abuse of notation, we simply write $\mathfrak{d}_\alpha(\tilde{x},t)$. Moreover, following [91], we impose that $\mathfrak{d}_\alpha(\tilde{x},t)$ depends on position and time through the volumetric fraction of the fluid phase, thereby setting $\mathfrak{d}_\alpha(\tilde{x},t) = \varphi_{\mathrm{f}}(\tilde{x},t)\mathfrak{d}_{\mathrm{R}\alpha}$, where $\mathfrak{d}_{\mathrm{R}\alpha}$ is a *reference fractional diffusivity*, which is parameterised by α. Since $\varphi_{\mathrm{f}}(\tilde{x},t)$ can be related to the volumetric deformation of the solid phase and to growth through the expression (3.5b), we obtain

$$\mathfrak{d}_\alpha(\chi(\tilde{X},t),t) = \frac{J(\tilde{X},t) - J_\gamma(\tilde{X},t)\Phi_{\mathrm{s}\nu}}{J(\tilde{X},t)}\mathfrak{d}_{\mathrm{R}\alpha}. \tag{3.24}$$

These considerations imply that the components of $\mathfrak{D}_\alpha$ can be written as follows

$$[\mathfrak{D}_\alpha(X,\tilde{X},t)]^{AB} = (J(\tilde{X},t) - J_\gamma(\tilde{X},t)\Phi_{\mathrm{s}\nu})\mathfrak{d}_{\mathrm{R}\alpha}[\boldsymbol{F}^{-1}(\chi(X,t),t)]^A{}_b\,[\boldsymbol{F}^{-\mathrm{T}}(\tilde{X},t)]_b{}^B. \tag{3.25}$$

We notice that the non-local nature of the problem is also reflected in Equation (3.25). Indeed, in a model accounting only for local interactions, the last two terms of Equation (3.25) would give the inverse of the right Cauchy-Green deformation tensor $\boldsymbol{C}$, i.e., $\boldsymbol{C}^{-1} = \boldsymbol{F}^{-1}.\boldsymbol{F}^{-\mathrm{T}}$, since X and $\tilde{X}$ would coincide. Still, this is not true in our case, since the non-locality changes with the dynamics of the tissue. Moreover, even in the case in which all the fractional diffusivities $\{\mathfrak{d}^b_\alpha(x,\tilde{x},t)\}^3_{b=1}$ were independent of x and $\tilde{x}$, their material counterparts $\{[\mathfrak{D}_\alpha(X,\tilde{X},t)]^{AB}\}^3_{A,B=1}$ would still be functions of the points X and $\tilde{X}$ because of the motion, χ.

Remark 6. *Due to the non-local nature of the mass flux vector, its Piola transformation needs to be performed in two steps, i.e., as many as the integrals appearing in Equation* (3.16a)*, or Equation* (3.21)*. In particular, the volume ratio $J(X,t)$ is due to the change of measure of the outermost integral of Equation* (3.21)*, which re-defines the duality product between $\boldsymbol{y}_\alpha$ and* grad$\check{\mathrm{c}}$ *into the duality product between $\boldsymbol{Y}_\alpha$ and* Grad$\check{\mathfrak{c}}$*. In our formalism, this volume ratio is used to define the pull-back of the non-local diffusivity tensor, $\boldsymbol{d}_\alpha$, as prescribed by Equations* (3.22a)–(3.22c)*. Furthermore, the tensor $\boldsymbol{F}^{-1}(\chi(X,t),t)$ featuring in Equation* (3.22c) *stems from the transformation of the gradient of the* virtual concentration*, $\check{c}$, evaluated at x, i.e.,* grad$\check{\mathrm{c}}(\chi(X,t),t)$ = Grad$\check{\mathfrak{c}}(X,t)\boldsymbol{F}^{-1}(\chi(X,t),t)$*, and it contributes, "from the left", to the calculation of the pull-back of the fractional diffusivity tensor. Whereas this first part of the backward Piola transformation of the mass flux vector is standard, the second part of it reveals the non-locality of the constitutive law in Equation* (3.21)*. Indeed, the tensor $\boldsymbol{F}^{-\mathrm{T}}(\tilde{X},t)$ featuring in Equation* (3.22c) *must be evaluated in $\tilde{X}$ because it originates from the transformation of the gradient of the* concentration (not the virtual one)*, which is part of the integrand of the innermost integral, i.e., the one expressing the non-local constitutive law. This tensor*

contributes, "from the right", to determine the pull-back of the fractional diffusivity tensor. Finally, the volume ratio $J(\tilde{X},t)$ is necessary because of the change of measure in the innermost integral of Equation (3.16a) *and is employed to define the pull-back of the fractional diffusivity tensor, $\mathfrak{d}_\alpha$. In conclusion, to determine the pull-back of the mass flux vector, a "double" Piola transformation has to be performed.*

Remark 7. *Looking at the Piola transformation of the mass flux vector, it is worth mentioning that the non-locality of the problem, expressed through $\hat{\mathfrak{f}}_\alpha$ as a function of $(x-\tilde{x})$ in the current configuration, cannot be described in general as a function of $(X-\tilde{X})$ in the reference configuration. Rather, the material non-locality function, $\mathfrak{F}_\alpha$, must be conceived as a function of the three variables X, $\tilde{X}$ and t since, as prescribed by Equation* (3.22b)*, it inherits this dependence from the motion, χ, in a way that, in general, cannot be reduced to a function of time and of the difference $(X-\tilde{X})$. Furthermore, we notice that the non-locality of the problem evolves from the reference to the current configuration. Indeed, two points that are "close" in $\mathscr{B}$ can either be "far away" from each other or become "even closer" in $\mathscr{B}_t$, and vice versa.*

3.6 Model summary and some numerical aspects

In this section, we summarise the equations characterising our mathematical model, specify the expressions for the sinks and sources of mass, and highlight some computational aspects to be taken into account. In the following, we focus on the case in which the considered chemical agents are nutrient substances that are necessary to trigger and maintain the growth of the tumour. Hence, we shall be referring to "nutrients" in lieu of "chemical agents" from here on.

3.6.1 Model equations

Our model is based on the following set of non-linear and coupled equations

$$\dot{\mathfrak{c}}_\mathrm{p} = [R_\mathrm{pn} + R_\mathrm{fp} - R_\mathrm{s}\mathfrak{c}_\mathrm{p}][J_\gamma \Phi_{\mathrm{s}\nu}\varrho_\mathrm{s}]^{-1}, \tag{3.26a}$$

$$\frac{\dot{\gamma}}{\gamma} = [R_\mathrm{fp} + R_\mathrm{nf}][3\varrho_\mathrm{s}\Phi_{\mathrm{s}\nu}J_\gamma]^{-1}, \tag{3.26b}$$

$$\varrho_\mathrm{f}[J - J_\gamma\Phi_{\mathrm{s}\nu}]\dot{\mathfrak{c}}_\mathrm{a} - \varrho_\mathrm{f}[\boldsymbol{K}\,\mathrm{Grad}\mathfrak{p}]\mathrm{Grad}\mathfrak{c}_\mathrm{a} + \mathrm{Div}\boldsymbol{Y}_\alpha = \mathfrak{c}_\mathrm{a}R_\mathrm{s} + R_\mathrm{ap}, \tag{3.26c}$$

$$\dot{J} - \mathrm{Div}(\boldsymbol{K}\,\mathrm{Grad}\mathfrak{p}) = 0, \tag{3.26d}$$

$$\mathrm{Div}(-J\mathfrak{p}\mathfrak{g}^{-1}\boldsymbol{F}^{-\mathrm{T}} + \boldsymbol{P}_\mathrm{sc}) = \boldsymbol{0}, \tag{3.26e}$$

in the $(4+3)$ unknowns $\mathscr{U} := \{\mathfrak{c}_\mathrm{p}, \gamma, \mathfrak{c}_\mathrm{a}, \mathfrak{p}, \{\chi^a\}_{a=1}^3\}$, and with the source and sink terms [191, 91, 192]

$$R_\mathrm{fp} = J\zeta_\mathrm{fp} \left\langle \frac{\mathfrak{c}_\mathrm{a} - \mathfrak{c}_\mathrm{cr}}{\mathfrak{c}_\mathrm{env} - \mathfrak{c}_\mathrm{cr}} \right\rangle_+ \left[1 - \frac{\delta_1 \langle \bar{\sigma} \rangle_+}{\delta_2 + \langle \bar{\sigma} \rangle_+}\right] \underbrace{\frac{J - J_\gamma \Phi_{\mathrm{s}\nu}}{J\varphi_\mathrm{fR}}}_{=\varphi_\mathrm{f}/\varphi_\mathrm{fR}} \underbrace{\frac{J_\gamma \Phi_{\mathrm{s}\nu}}{J}}_{=\varphi_\mathrm{s}} \mathfrak{c}_\mathrm{p}, \tag{3.27a}$$

$$R_\mathrm{nf} = -J\zeta_\mathrm{nf} \frac{J_\gamma \Phi_{\mathrm{s}\nu}}{J}(1 - \mathfrak{c}_\mathrm{p}), \tag{3.27b}$$

$$R_\mathrm{ap} = -J\zeta_\mathrm{ap} \frac{\mathfrak{c}_\mathrm{a}}{\mathfrak{c}_\mathrm{a} + \mathfrak{c}_0} \frac{J_\gamma \Phi_{\mathrm{s}\nu}}{J} \mathfrak{c}_\mathrm{p}, \tag{3.27c}$$

$$R_\mathrm{pn} = -J\zeta_\mathrm{pn} \left\langle 1 - \frac{\mathfrak{c}_\mathrm{a}}{\mathfrak{c}_\mathrm{cr}} \right\rangle_+ \frac{J_\gamma \Phi_{\mathrm{s}\nu}}{J} \mathfrak{c}_\mathrm{p}. \tag{3.27d}$$

In Equations (3.27a)–(3.27c), ζ_fp, ζ_nf, ζ_ap and ζ_pn are constants indicating the characteristic time scales with which the interstitial fluid is absorbed by the proliferating cells, the necrotic cells go into the fluid, nutrients are consumed, and proliferating cells die, respectively. The operator $\langle f \rangle_+ := \max\{0, f\}$ represents Macaulay's brackets, which return the positive part of a function f. Moreover, $\mathfrak{c}_\mathrm{cr}$ is a critical value for the nutrients' mass fraction and $\mathfrak{c}_\mathrm{env}$ refers to the concentration of nutrients present in the surrounding of the tumour. In order for growth to occur, it is necessary that $R_\mathrm{fp} = Jr_\mathrm{fp} > 0$, i.e., it must hold that $\mathfrak{c}_\mathrm{a} > \mathfrak{c}_\mathrm{cr}$, provided $\mathfrak{c}_\mathrm{env} > \mathfrak{c}_\mathrm{cr}$. We also mention that the mass source R_fp features the term in square brackets depending on $\bar{\sigma} := -\frac{1}{3}\mathrm{tr}\boldsymbol{\sigma}$, which is introduced in order to describe the fact that growth can be modulated by mechanical stress, thereby giving rise to a phenomenon known as *mechanotransduction* [192, 191, 124, 131]. Finally, the product of the last three factors in Equation (3.27a) describes the fact that, to allow for the transfer of mass from the fluid to the proliferating cells, there must be a nonzero volumetric fraction of the fluid phase and of the solid phase as well as a nonzero mass fraction of the proliferating cells. Macaulay's brackets in Equation (3.27d) ensure that the proliferating cells become necrotic, i.e., $R_\mathrm{pn} < 0$ when $\mathfrak{c}_\mathrm{a} < \mathfrak{c}_\mathrm{cr}$, and $R_\mathrm{pn} = 0$ otherwise. Equation (3.27b) assumes that R_nf is linear in the volumetric fraction of the solid phase and in the mass fraction of the necrotic cells, i.e., $1 - \mathfrak{c}_\mathrm{p}$, while R_ap establishes that the magnitude with which the nutrients are "eaten" by the proliferating cells depends on the ratio $\mathfrak{c}_\mathrm{a}/\mathfrak{c}_0$, with $\mathfrak{c}_0 \in]0,1]$ being a reference value of the nutrients' concentration that modulates their consumption. We refer the Reader to [192, 191, 91, 131] for further details on these terms, and for their generalisation to include growth-induced structural transformations.

Finally, we recall that the main goal of our model is to quantify the impact of the non-local diffusion of the nutrients, accounted for by $\boldsymbol{Y}_\alpha$, on the overall evolution of the tumour, i.e., on all the unknowns of the model. We note that, apart from the presence of the fractional mass flux vector $\boldsymbol{Y}_\alpha$, our model is the same as the one presented in [191] and extended in [91, 131].

3.6.2 Numerical aspects

The model summarised in Equation (3.26) features ordinary differential equations, partial differential equations and an integro-differential equation of fractional type. Since the model is formulated for a bounded domain and many couplings and nonlinearities are accounted for, the usual techniques adopted in Fractional Calculus for linear problems, such as the Fourier and Laplace transforms, cannot be used. Consequently, we need to resort to numerical techniques. In particular, we solve Equations (3.26a)–(3.26e) by means of a FE scheme that we need to adapt to our purposes in order to take fractional derivatives into account. Here, we do not intend to go into the details of the numerical scheme, which is out of the scope of this work. Nevertheless, we intend to give some insights about the most important computational aspects of our work, while the numerical solutions are obtained by using COMSOL Multiphysics®.

Classical FE techniques [130, 248] have been used for solving numerically Equations (3.26a), (3.26b), (3.26d) and (3.26e), while Equation (3.26c) has required a special care. To this end, we report explicitly only the weak formulation corresponding to it. Before doing this, we denote with $(\partial\mathscr{B})_{\mathrm{D}}$ and $(\partial\mathscr{B})_{\mathrm{N}}$ the Dirichlet and Neumann boundaries of $\mathscr{B}$, respectively, and assume $\partial\mathscr{B} = (\partial\mathscr{B})_{\mathrm{D}} \sqcup (\partial\mathscr{B})_{\mathrm{N}}$. Furthermore, by using the standard formalism for Sobolev spaces [43], and using the space of virtual concentrations, $\check{\mathscr{C}}_{\mathrm{R}} := \{\check{\mathfrak{c}} \in H^1(\mathscr{B}) \text{ s.t. } \check{\mathfrak{c}}|_{(\partial\mathscr{B})_{\mathrm{D}}} = 0\}$, we have that, for all $\check{\mathfrak{c}} \in \check{\mathscr{C}}_{\mathrm{R}}$, the following weak form applies

$$\begin{aligned}&\int_{\mathscr{B}} \{\varrho_{\mathrm{f}}[J - J_\gamma \Phi_{\mathrm{s}\nu}]\dot{\mathfrak{c}}_{\mathrm{a}} - \varrho_{\mathrm{f}}[\boldsymbol{K}\mathrm{Grad}\mathfrak{p}]\mathrm{Grad}\mathfrak{c}_{\mathrm{a}} - \mathfrak{c}_{\mathrm{a}}R_{\mathrm{s}} - R_{\mathrm{ap}}\}\,\check{\mathfrak{c}}\,\mathrm{dV} \\ &\quad - \int_{\mathscr{B}} \boldsymbol{Y}_\alpha \mathrm{Grad}\check{\mathfrak{c}}\,\mathrm{dV} + \int_{(\partial\mathscr{B})_{\mathrm{N}}} \boldsymbol{Y}_\alpha.\boldsymbol{N}\check{\mathfrak{c}}\,\mathrm{dS} = 0,\end{aligned} \tag{3.28}$$

where $\boldsymbol{N}$ is the field of unit vectors normal to $(\partial\mathscr{B})_{\mathrm{N}}$ while $\boldsymbol{Y}_\alpha$ is given in Equation (3.21), so that the second volume integral of Equation (3.28) (without the sign) becomes

$$\begin{aligned}&\int_{\mathscr{B}} \boldsymbol{Y}_\alpha(X,t)\mathrm{Grad}\check{\mathfrak{c}}(X,t)\,\mathrm{dV}(X) \\ &= -\varrho_{\mathrm{f}} \int_{\mathscr{B}} \left\{ \int_{\mathscr{B}} [\mathrm{Grad}\check{\mathfrak{c}}(X,t)]\,\boldsymbol{D}_\alpha(X,\tilde{X},t)[\mathrm{Grad}\mathfrak{c}_{\mathrm{a}}(\tilde{X},t)]\,\mathrm{dV}(\tilde{X}) \right\} \mathrm{dV}(X).\end{aligned} \tag{3.29}$$

After applying a backward Euler scheme for the time derivative, a linearisation procedure, and Galerkin method, Equation (3.28) leads to a system of algebraic equations that, except for a *non-local stiffness matrix*, arising from the double integral in Equation (3.29), is similar to the one obtained in standard FE approaches. From a numerical point of view, the non-local stiffness matrix reflects a long range coupling among the elements in the spatial discretisation. Indeed, it is worth noting that, in the construction of the non-local stiffness matrix, the cross integrations

between the piecewise polynomial *ansatz* functions do not vanish as they would in the case of the stiffness matrix of a standard diffusion problem. That is, even though two discretisation nodes are far away from each other, the entry of the matrix corresponding to these nodes will be non-zero, because of the presence of the non-locality function $\hat{\mathfrak{f}}_\alpha$. This results into stiffness matrices that are denser, the stronger the non-locality is. In fact, this is a typical feature of the numerical study of non-local differential equations based on the use of FE methods (see for instance [117]). Still, as pointed out in [117], standard techniques for the solution of such equations, like Gauss elimination, can be used.

Before closing this section, we would like to remark that, in the simulations carried out in our work, the stiffness matrix associated with Equation (3.29) is symmetric and positive definite.

3.7 Benchmark problem and considerations on the non-locality function

In this section, we specify a benchmark problem in order to simplify and solve the mathematical model given by Equations (3.26a)-(3.26e). To this end, we make use of the problem proposed in [9], and recently investigated in [91, 131] to account for growth-induced inelastic distortions. By doing this, we intend to model the volumetric growth of an avascular tumour in a "jacketed" cylindrical sample (its deformation is restricted to be along the longitudinal axis only), and to investigate, how and to what extent, the non-local diffusivity properties of the nutrients influence the dynamics of the tissue. In the following, we assume that the problem complies with axial symmetry and that it is radially homogeneous regardless of how slender the cylindrical sample is. This will require suitable *a priori* restrictions on all the unknowns of the problem.

3.7.1 Description of the benchmark problem

As in [91, 131], we adopt the cylindrical coordinates (R, Θ, Z) and (r, ϑ, z), associated with the reference and the current configurations of the tumour, respectively. Moreover, we require the motion to satisfy with the conditions

$$\chi^r(R, \Theta, Z, t) = r = R, \tag{3.30a}$$

$$\chi^\vartheta(R, \Theta, Z, t) = \vartheta = \Theta, \tag{3.30b}$$

$$\chi^z(R, \Theta, Z, t) = z = Z + u(Z, t), \tag{3.30c}$$

where u is the unknown axial component of displacement. In this situation, the tumour is allowed to expand itself solely along the axial direction and χ^z is the only unknown component of the motion, χ. Additionally, to comply with the

axial symmetry and with the radial homogeneity of the problem, the pressure $\mathfrak{p}$ is considered to be a function of the axial coordinate and time only. Another restriction pertains to the growth parameter γ, which is also assumed to depend only on Z and t (note that since the growth tensor $\boldsymbol{F}_\gamma = \gamma \boldsymbol{I}$ is spherical, it maintains the symmetries of the problem). Similar requirements also apply for the mass fraction of the proliferating cells, $\mathfrak{c}_\mathrm{p}$, as well as for the mass fraction of the nutrients, $\mathfrak{c}_\mathrm{a}$.

The motion we have assumed implies that the matrix representations of the deformation gradient tensor $\boldsymbol{F}$ and of the right Cauchy-Green deformation tensor $\boldsymbol{C}$ read

$$[\boldsymbol{F}] = \mathrm{diag}\{1,1,1+u'\}, \tag{3.31a}$$
$$[\boldsymbol{C}] = \mathrm{diag}\{1,1,[1+u']^2\}, \tag{3.31b}$$

where u' denotes the derivative of u in the axial direction. Since it holds that $J = \det(\boldsymbol{F}) = 1 + u' > 0$, u' must obey the inequality $u' > -1$.

Additionally, the growth tensor admits the diagonal form

$$[\boldsymbol{F}_\gamma] = \mathrm{diag}\{\gamma,\gamma,\gamma\}, \quad \gamma > 0, \tag{3.32}$$

and, consequently, the elastic right Cauchy-Green deformation tensor $\boldsymbol{C}_\mathrm{e}$ has the representation

$$[\boldsymbol{C}_\mathrm{e}] = \mathrm{diag}\left\{\frac{1}{\gamma^2}, \frac{1}{\gamma^2}, \frac{[1+u']^2}{\gamma^2}\right\}. \tag{3.33}$$

Because of Equations (3.31a), (3.31b), (3.32) and (3.33), of the symmetry properties of the pressure term $-J\mathfrak{p}\mathfrak{g}^{-1}\boldsymbol{F}^{-\mathrm{T}}$, and of the constitutive expression (3.13), the first Piola-Kirchhoff stress tensor $\boldsymbol{P} = -J\mathfrak{p}\mathfrak{g}^{-1}\boldsymbol{F}^{-\mathrm{T}} + \boldsymbol{P}_\mathrm{sc}$ has the diagonal representation

$$[\boldsymbol{P}] = \mathrm{diag}\left\{-J\mathfrak{p} + [\boldsymbol{P}_\mathrm{sc}]^{rR}, -J\mathfrak{p} + [\boldsymbol{P}_\mathrm{sc}]^{\vartheta\Theta}, -\mathfrak{p} + [\boldsymbol{P}_\mathrm{sc}]^{zZ}\right\}, \tag{3.34}$$

where each quantity featuring in each component of $\boldsymbol{P}$ is a function solely of Z and time. Moreover, it applies that $[\boldsymbol{P}_\mathrm{sc}]^{rR} = [\boldsymbol{P}_\mathrm{sc}]^{\vartheta\Theta}$ and, thus, the balance of linear momentum (3.26e) in cylindrical coordinates reduces to

$$\frac{\partial}{\partial Z}\left(-\mathfrak{p} + [\boldsymbol{P}_\mathrm{sc}]^{zZ}\right) = 0. \tag{3.35}$$

This result can be found also in other benchmark problems, such as the confined compression tests of articular cartilage, under symmetry assumptions similar to those made here. Therefore, Equation (3.35) constitutes a simplification obtained by virtue of symmetry and not by invoking the slenderness of the cylinder used in our benchmark (see Table 3.1).

Note also that, according to Equations (3.14) and (3.15), the conditions imposed on the deformation and on the growth tensor are such that k_0 depends, through J and J_γ, only on the axial coordinate and on time. Moreover, the same conclusion can be drawn for the diffusivity $\mathfrak{d}_\alpha$, which, with slight abuse of notation, we express as $\mathfrak{d}_\alpha(Z,t)$ from here on.

By following the same reasoning that has led to Equation (3.35), and noticing that the only non-zero component of the mass flux $\boldsymbol{Q}$ is the axial one, i.e., $\boldsymbol{Q}^Z = -\boldsymbol{K}^{ZZ}\frac{\partial \mathfrak{p}}{\partial Z}$ with $\boldsymbol{K}^{ZZ} = Jk_0[\boldsymbol{C}^{-1}]^{ZZ} = k_0/(1+u')$, the continuity equation (3.26d) becomes

$$\frac{\partial^2 u}{\partial Z\,\partial t} - \frac{\partial}{\partial Z}\left(\frac{k_0}{1+u'}\frac{\partial \mathfrak{p}}{\partial Z}\right) = 0. \tag{3.36}$$

The equations for $\mathfrak{c}_\mathrm{p}$ and γ, that is Equations (3.26a) and (3.26b), are scalar ODEs, and the fact that $\mathfrak{c}_\mathrm{p}$ and γ depend only of Z and t is consistent with the symmetry properties of all the terms featuring in these equations. That said, a remark is in order for Equation (3.26b) to emphasise that the considered benchmark problem remains three-dimensional in spite of the axial symmetry and radial homogeneity that it enjoys. Indeed, looking at the source R_fp in Equation (3.27a), we notice that the mechanotransduction term (i.e., the term between brackets in Equation (3.27a)) features the trace of Cauchy stress tensor, which requires the evaluation of all the stress components, i.e., also of those in the radial and circumferential directions, these being non null because the cylinder is laterally jacketed. Therefore, we conclude that, even though the cylinder used for our benchmark problem is slender, with slenderness ratio $2\cdot 10^{-2}$ (see the geometric data in Table 3.1), the problem itself necessitates to account for all the geometrical dimensions.

The last equation to consider is the balance law for $\mathfrak{c}_\mathrm{a}$ (see Equation (3.26c)) in which the non-standard mass flux $\boldsymbol{Y}_\alpha$ features, at least in principle, all the coordinates (i.e., also the radial and the circumferential coordinates) through the non-locality function $\mathfrak{F}_\alpha(X,\tilde{X},t) = \hat{\mathfrak{f}}_\alpha(\chi(X,t)-\chi(\tilde{X},t))$. To maintain the axial symmetry of the problem and to eliminate the dependence of the nutrients' mass flux on the radial and circumferential coordinates, two paths may be followed. One is discussed in Section "Definition of the non-locality function" and, for consistency with the symmetry requirements introduced so far, it imposes to rephrase the non-locality function as a function of the axial coordinate only. However, another path —valid for the problem at hand— could be to eliminate the dependence of the non-locality function on the radial and circumferential coordinate by taking advantage of the slenderness of the cylinder. To this end, we write the non-locality function as

$$\hat{\mathfrak{f}}_\alpha(x-\tilde{x}) = \mathfrak{f}_{0\alpha}\frac{1}{\|x-\tilde{x}\|^\alpha} = \mathfrak{f}_{0\alpha}\frac{1}{\|(z-\tilde{z})\boldsymbol{e}_z + \boldsymbol{r}_t\|^\alpha}, \tag{3.37}$$

where $\boldsymbol{e}_z$ is the unit vector along which the cylinder's axis is directed, $\mathfrak{f}_{0\alpha}$, with $\alpha\in\,]0{,}1[$, is an α-dependent coefficient to be individuated, and $\boldsymbol{r}_t$ is a vector lying

on the cross-section of the cylinder. Next, we rescale the axial vector $(z-\tilde{z})\boldsymbol{e}_z$ by the undeformed length of the cylinder, i.e., $2L_{\text{in}}$, and the transverse vector $\boldsymbol{r}_t$ by the cylinder diameter prior to deformation, i.e., $2R_{\text{in}}$, so that Equation (3.37) becomes

$$\hat{\mathfrak{f}}_\alpha(x-\tilde{x}) = \mathfrak{f}_{0\alpha}\frac{1}{\|2L_{\text{in}}\boldsymbol{\rho}_a + 2R_{\text{in}}\boldsymbol{\rho}_t\|^\alpha} = \frac{\mathfrak{f}_{0\alpha}}{(2L_{\text{in}})^\alpha}\frac{1}{\|\boldsymbol{\rho}_a + (R_{\text{in}}/L_{\text{in}})\boldsymbol{\rho}_t\|^\alpha}, \tag{3.38}$$

with $\boldsymbol{\rho}_a = (z-\tilde{z})\boldsymbol{e}_z/(2L_{\text{in}})$ and $\boldsymbol{\rho}_t := \boldsymbol{r}_t/(2R_{\text{in}})$. Now, since the slenderness ratio $R_{\text{in}}/L_{\text{in}}$ is $2\cdot 10^{-2}$, we assume, within the first approximation, that the non-locality function can be truncated at the zero-th order in the slenderness ratio, thereby taking the expression

$$\hat{\mathfrak{f}}_\alpha(x-\tilde{x}) \approx \frac{\mathfrak{f}_{0\alpha}}{(2L_{\text{in}})^\alpha}\frac{1}{\|\boldsymbol{\rho}_a\|^\alpha} = \mathfrak{f}_{0\alpha}\frac{1}{\|(z-\tilde{z})\boldsymbol{e}_z\|^\alpha} = \mathfrak{f}_{0\alpha}\frac{1}{|z-\tilde{z}|^\alpha}. \tag{3.39}$$

As discussed below, the coefficient $\mathfrak{f}_{0\alpha}$ acquires the meaning of a normalisation factor.

3.7.2 Initial and boundary conditions

To solve Equations (3.26a)–(3.26e), we impose the same boundary and initial conditions used in [91, 131]. Specifically, at the initial instant of time we consider a reference configuration being characterised by the following relations

$$\chi^r(R,\Theta,Z,0) = R, \quad \chi^\vartheta(R,\Theta,Z,0) = \Theta, \quad \chi^z(R,\Theta,Z,0) = Z, \tag{3.40}$$

where $R \in [0, R_{\text{in}}[$, $\Theta \in [0,2\pi[$ and $Z \in [-L_{\text{in}}, +L_{\text{in}}]$, while R_{in} and $2L_{\text{in}}$ denote the radius and the length of the undeformed specimen. Besides, we enforce that, at $t = 0$, necrotic cells are absent, i.e., $\mathfrak{c}_{\text{p}}(R,\Theta,Z,0) = 1$, the fluid pressure is zero, i.e., $\mathfrak{p}(R,\Theta,Z,0) = 0$, the nutrients' mass fraction equals the environmental one, i.e., $\mathfrak{c}_{\text{a}}(R,\Theta,Z,0) = \mathfrak{c}_{\text{env}} > 0$, and the distribution of the growth parameter is homogeneous and unitary, i.e., $\gamma(R,\Theta,Z,0) = 1$. In addition, we consider the following boundary conditions

$$(-J\mathfrak{p}\mathfrak{g}^{-1}\boldsymbol{F}^{-\text{T}} + \boldsymbol{P}_{\text{sc}}).\boldsymbol{N}_{\text{A}} = \boldsymbol{0}, \qquad \text{on } (\partial\mathscr{B})_{\text{Left}} \text{ and } (\partial\mathscr{B})_{\text{Right}}, \tag{3.41a}$$

$$(-\boldsymbol{K}\text{Grad}\mathfrak{p}).\boldsymbol{N}_{\text{C}} = 0, \qquad \text{on } (\partial\mathscr{B})_{\text{C}}, \tag{3.41b}$$

$$\mathfrak{p} = 0, \qquad \text{on } (\partial\mathscr{B})_{\text{Left}} \text{ and } (\partial\mathscr{B})_{\text{Right}}, \tag{3.41c}$$

$$\mathfrak{c}_{\text{a}} = \mathfrak{c}_{\text{env}}, \qquad \text{on } (\partial\mathscr{B})_{\text{Left}} \text{ and } (\partial\mathscr{B})_{\text{Right}}, \tag{3.41d}$$

$$\boldsymbol{Y}_\alpha.\boldsymbol{N}_{\text{C}} = 0, \qquad \text{on } (\partial\mathscr{B})_{\text{C}}, \tag{3.41e}$$

where $\boldsymbol{N}_{\text{A}}$ and $\boldsymbol{N}_{\text{C}}$ are fields of unit vectors normal to $(\partial\mathscr{B})_{\text{Left}} \cup (\partial\mathscr{B})_{\text{Right}}$ and to $(\partial\mathscr{B})_{\text{C}}$, respectively, and $\partial\mathscr{B} = (\partial\mathscr{B})_{\text{Left}} \cup (\partial\mathscr{B})_{\text{Right}} \cup (\partial\mathscr{B})_{\text{C}}$. Specifically, $(\partial\mathscr{B})_{\text{Left}}$ and $(\partial\mathscr{B})_{\text{Right}}$ are the left and the right surfaces at the extremities of $\mathscr{B}$, and $(\partial\mathscr{B})_{\text{C}}$ is the lateral boundary.

3.7.3 Definition of the non-locality function

A classical approach for defining $\hat{\mathfrak{f}}_\alpha$ is to adopt a power-law that decays in space. To our knowledge, this is customary for problems that are *a priori* formulated as one-dimensional and in which $\hat{\mathfrak{f}}_\alpha(x-\tilde{x})$ is assumed to be proportional to the reciprocal of $|x-\tilde{x}|^\alpha$, with x and $\tilde{x}$ being points of the real line or of an interval of finite length [268, 19, 257, 55, 252]. This choice permits to "import", with slight modifications, the definitions of the fractional derivatives in time (see e.g. [21]) to the fractional differentiation in space. However, in some situations it is necessary to assess an *a priori* relationship between the dimensionality of the problem under study and the non-locality that *must* —or *may*— be resolved, once the dimensionality has been settled. Indeed, in a three-dimensional problem endowed with the symmetry and homogeneity properties we are dealing with, the only non-zero partial derivative of the concentration is the one along the axial direction. In such a situation, the axial mass flux reads

$$[\boldsymbol{y}_\alpha(x,t)]^z = -\varrho_{\mathrm{f}} \int_{\mathscr{B}_t} \hat{\mathfrak{f}}_\alpha(x-\tilde{x})\mathfrak{d}_\alpha(\tilde{z},t)\partial_{\tilde{z}} c_{\mathrm{a}}(\tilde{z},t)\,\mathrm{dv}(\tilde{x}), \tag{3.42}$$

whereas the radial and the circumferential components of the flux are zero. Note that we are using here the customary formalism for cylindrical coordinates, so that $\tilde{x} = (\tilde{r}, \tilde{\vartheta}, \tilde{z})$. As anticipated before, the expression for $[\boldsymbol{y}_\alpha(x,t)]^z$ reminds the definition of fractional gradient given in [267], with the difference that a volume integral is used in (3.42) and that all the components of $x-\tilde{x}$ are considered.

In spite of the fact that the problem is one-dimensional from the point of view of its symmetries, the axial flux is still determined by an integration over the three-dimensional region $\mathscr{B}_t$, and $\hat{\mathfrak{f}}_\alpha(x-\tilde{x})$ describes, as it stands, a non-locality in three dimensions (trivially, because $x-\tilde{x}$ is a vector of a three-dimensional vector space). Therefore, the component of $(x-\tilde{x})$ along the radial or the circumferential direction will influence the axial mass flux, even though the problem was claimed to enjoy axial symmetry and to be independent of the radial coordinate. This result, however, may be physically unsound. Indeed, one would expect non-locality to be coherent with the symmetries of the problem, even though the integral of Equation (3.42) is over the whole configuration $\mathscr{B}_t$, thereby maintaining the physical dimensionality of the problem itself.

To address this issue, we need to take into account how the symmetries of the problem under investigation influence the non-locality in the relationship between $\boldsymbol{y}_\alpha$ and c_{a}. Consequently, the non-locality function $\hat{\mathfrak{f}}_\alpha$ in Equation (3.42) is redefined as

$$\hat{\mathfrak{f}}_\alpha(x-\tilde{x}) := \hat{\mathfrak{h}}_\alpha(z-\tilde{z}) = \frac{1}{\mathcal{N}(\alpha)}\frac{1}{|z-\tilde{z}|^\alpha}, \quad \alpha \in]0,1[\,, \tag{3.43}$$

where $\mathcal{N}(\alpha)$ is a normalisation factor to be determined. From Equations (3.42) and (3.43), we notice that the physical dimensions of the fractional diffusivity, $\mathfrak{d}_\alpha$, are

$L^{1+\alpha}T^{-1}$, where L and T stand for the characteristic "length" and the characteristic "time" of the non-local diffusion process, respectively. Thus, when α tends to 1 (from below), we recover the physical dimensions of the standard diffusivity.

By substituting Equation (3.43) into Equation (3.42), and recalling that $\mathscr{B}_t = \mathscr{C}_\mathrm{R}\times\,]-\ell(t),+\ell(t)[$ (where $\mathscr{C}_\mathrm{R}$ is the cross-section of the cylinder and $2\ell(t)$ is its variable axial length), we obtain the much simpler expression

$$[\boldsymbol{y}_\alpha(x,t)]^z \equiv y^z_\alpha(z,t) = -\frac{\varrho_\mathrm{f}\pi R^2_\mathrm{in}}{\mathcal{N}(\alpha)}\int_{-\ell(t)}^{+\ell(t)}\frac{1}{|z-\tilde{z}|^\alpha}\mathfrak{d}_\alpha(\tilde{z},t)\partial_{\tilde{z}}c_\mathrm{a}(\tilde{z},t)\,\mathrm{d}\tilde{z}. \tag{3.44}$$

For the Equation (3.44) to be physically sound, it has to return the axial component of the standard mass flux vector in the limit $\alpha \to 1^-$. Unfortunately, proving this result for problems defined over bounded domains is not possible without knowing c_a. On the contrary, this difficulty does not arise in problems defined over unbounded domains, because, with the aid of the Fourier transform, it is possible to do the following reasoning:

- Introduce the auxiliary notation $\psi^z_\alpha(\tilde{z},t) := -\varrho_\mathrm{f}\mathfrak{d}_\alpha(\tilde{z},t)\,\partial_z c_\mathrm{a}(\tilde{z},t)$, and assume to prolong $y^z_\alpha(z,t)$ to the whole real line, so that Equation (3.44) becomes

$$\begin{aligned} y^z_\alpha(z,t) &= -\frac{\varrho_\mathrm{f}\pi R^2_\mathrm{in}}{\mathcal{N}(\alpha)}\int_{-\infty}^{+\infty}\frac{1}{|z-\tilde{z}|^\alpha}\mathfrak{d}_\alpha(\tilde{z},t)\partial_{\tilde{z}}c_\mathrm{a}(\tilde{z},t)\,\mathrm{d}\tilde{z} \\ &= \pi R^2_\mathrm{in}\int_{-\infty}^{+\infty}\hat{\mathfrak{h}}_\alpha(z-\tilde{z})\psi^z_\alpha(\tilde{z},t)\mathrm{d}\tilde{z} \\ &= \pi R^2_\mathrm{in}\,[\hat{\mathfrak{h}}_\alpha * \psi^z_\alpha(\,\cdot\,,t)](z), \end{aligned} \tag{3.45}$$

  thereby expressing $y^z_\alpha(z,t)$ as the convolution product between $\hat{\mathfrak{h}}_\alpha$ and $\psi^z_\alpha(\,\cdot\,,t)$.

- Compute the Fourier transform of $y^z_\alpha(z,t)$ as written in Equation (3.45), i.e.,

$$\begin{aligned} \mathscr{F}[y^z_\alpha(\,\cdot\,,t)](\xi) &:= \int_{-\infty}^{+\infty} y^z_\alpha(z,t)\exp(-\mathrm{i}\xi z)\mathrm{d}z \\ &= \pi R^2_\mathrm{in}\mathscr{F}[\hat{\mathfrak{h}}_\alpha](\xi)\mathscr{F}[\psi^z_\alpha(\,\cdot\,,t)](\xi) \\ &= \pi R^2_\mathrm{in}\frac{2\Gamma(1-\alpha)}{\mathcal{N}(\alpha)}\sin\left(\frac{\alpha\pi}{2}\right)|\xi|^{\alpha-1}\mathscr{F}[\psi^z_\alpha(\,\cdot\,,t)](\xi), \end{aligned} \tag{3.46}$$

  where $\xi \in \mathbb{R}\backslash\{0\}$ is the wave number, $\Gamma(\,\cdot\,)$ is the Euler Gamma function and we used the Fourier transform of $\hat{\mathfrak{h}}_\alpha$, i.e.,

$$\mathscr{F}[\hat{\mathfrak{h}}_\alpha](\xi) = \frac{2\Gamma(1-\alpha)}{\mathcal{N}(\alpha)}\sin\left(\frac{\alpha\pi}{2}\right)|\xi|^{\alpha-1}. \tag{3.47}$$

Since $\mathscr{F}[y_\alpha^z(\,\cdot\,,t)](\xi)$ is proportional to the product of $\mathscr{F}[\hat{\mathfrak{h}}_\alpha](\xi)$ and $\mathscr{F}[\psi_\alpha^z(\,\cdot\,,t)](\xi)$, one can identify the non-local contribution of the mass flux with $\mathscr{F}[\mathfrak{h}_\alpha](\xi)$, given in Equation (3.47).

Note that, if $\mathfrak{d}_\alpha(z,t)$ and $c_\mathrm{a}(z,t)$ are both assumed to be even with respect to $z=0$ —an assumption that is consistent with the hypothesis, done later, that the considered problem is symmetric with respect to $z=0$—, $\mathscr{F}[y_\alpha^z(\cdot,t)](\xi)$ can be prolonged to $\xi=0$ and is null for this value. To see this, we first rewrite $\mathscr{F}[\psi_\alpha^z(\cdot,t)](\xi)$ as

$$\mathscr{F}[\psi_\alpha^z(\cdot,t)](\xi) = -\varrho_\mathrm{f}\int_{-\infty}^{+\infty}\mathfrak{d}_\alpha(z,t)\partial_z c_\mathrm{a}(z,t)\exp(-\mathrm{i}\xi z)\mathrm{d}z\,. \tag{3.48}$$

Then, we notice that $\mathscr{F}[\psi_\alpha^z(\,\cdot\,,t)](0)$ is zero, because $\mathfrak{d}_\alpha(z,t)$ is even and $\partial_z c_\mathrm{a}(z,t)$ is odd with respect to $z=0$ for all times. Moreover, because of this result, it also holds that $\lim_{\xi\to 0}|\xi|^{\alpha-1}\mathscr{F}[\psi_\alpha^z(\cdot,t)](\xi)=0$, and, consequently, $\lim_{\xi\to 0}\mathscr{F}[y_\alpha^z(\cdot,t)](\xi)=0$ too.

- Compute the limit of $\mathscr{F}[y_\alpha^z(\,\cdot\,,t)](\xi)$ for $\alpha\to 1^-$, and find $\mathscr{N}(\alpha)$ such that

$$\begin{aligned}\lim_{\alpha\to 1^-}\mathscr{F}[y_\alpha^z(\,\cdot\,,t)](\xi) &= \lim_{\alpha\to 1^-}\mathscr{F}[\psi_\alpha^z(\,\cdot\,,t)](\xi)\\ &= \mathscr{F}[-\varrho_\mathrm{f}\mathfrak{d}_1(\,\cdot\,,t)\,\partial_z c_\mathrm{a}(\,\cdot\,,t)](\xi),\end{aligned} \tag{3.49}$$

with $\mathfrak{d}_1(\tilde{z},t) := \lim_{\alpha\to 1^-}\mathfrak{d}_\alpha(\tilde{z},t)$. We emphasise that this limit is taken uniformly with respect to the pairs $(\tilde{z},t)$ and, in particular, looking at Equation (3.24), it turns out to be uniform with respect to the motion, so that it is intended as

$$\begin{aligned}\lim_{\alpha\to 1^-}\mathfrak{d}_\alpha(\tilde{z},t) = \lim_{\alpha\to 1^-}\mathfrak{d}_\alpha(\chi^z(\tilde{X},t),t) &= \frac{J(\tilde{X},t)-J_\gamma(\tilde{X},t)\Phi_{\mathrm{s}\nu}}{J(\tilde{X},t)}\lim_{\alpha\to 1^-}\mathfrak{d}_{\mathrm{R}\alpha}\\ &= \frac{J(\tilde{X},t)-J_\gamma(\tilde{X},t)\Phi_{\mathrm{s}\nu}}{J(\tilde{X},t)}\mathfrak{d}_{\mathrm{R}1},\end{aligned} \tag{3.50}$$

where, in our model, $\mathfrak{d}_{\mathrm{R}1}$ is a constant having the physical dimensions of a standard diffusivity coefficient. In particular, to meet this requirement, we choose $\mathfrak{d}_{\mathrm{R}\alpha}$ as

$$\mathfrak{d}_{\mathrm{R}\alpha} := d_\mathrm{R}L^{\alpha-1}, \tag{3.51}$$

with d_R being a constant reference value for the standard diffusivity coefficient [25], so that $\mathfrak{d}_{\mathrm{R}1}=d_\mathrm{R}$.

One possible way to comply with Equation (3.49) is that $\mathscr{N}(\alpha)$ satisfies the relation

$$\lim_{\alpha\to 1^-}\frac{2\Gamma(1-\alpha)\pi R_\mathrm{in}^2}{\mathscr{N}(\alpha)} = 1. \tag{3.52}$$

Then, for Equation (3.44) to be (up to the diffusivity $\mathfrak{d}_\alpha$) Caputo's symmetrised fractional derivative of the mass fraction, c_a, which is defined over the interval $]-\ell(t),+\ell(t)[$, we choose the stronger condition

$$\mathcal{N}(\alpha) = 2\Gamma(1-\alpha)\pi R_\mathrm{in}^2, \quad \alpha \in]0{,}1[. \tag{3.53}$$

Clearly, Equation (3.53) represents a "guess", because we are unable to compute directly the normalisation factor for a bounded interval. Nevertheless, plugging Equation (3.53) into Equation (3.44) yields

$$y_\alpha^z(z,t) = -\frac{\varrho_\mathrm{f}}{2\Gamma(1-\alpha)} \int_{-\ell(t)}^{+\ell(t)} \frac{1}{|z-\tilde{z}|^\alpha} \mathfrak{d}_\alpha(\tilde{z},t)\partial_{\tilde{z}} c_\mathrm{a}(\tilde{z},t)\,\mathrm{d}\tilde{z}, \tag{3.54}$$

which, apart from the spatial dependence of the fractional diffusivity $\mathfrak{d}_\alpha(\tilde{z},t)$, coincides with the definition of fractional mass flux in one dimension used by other Authors, see for instance [215, 82] and the references therein. Furthermore, in the case in which the fractional diffusivity can be factorised outside the integral operator, e.g. by setting $\mathfrak{d}_\alpha(\tilde{z},t) = \mathfrak{d}_{0\alpha}$, the axial mass flux becomes proportional to the symmetrised Caputo fractional derivative of order α of c_a [21].

Remark 8 ((On the normalisation factor))**.** *We notice that, apart from the presence of the area of the cylinder's cross-section $|\mathscr{C}_\mathrm{R}| = \pi R_\mathrm{in}^2$, the expression of the normalisation factor $\mathcal{N}(\alpha)$ given in Equation* (3.53) *coincides with the one used in other works (see e.g. [268, 19, 55]). Nevertheless, by looking at Equation* (3.46)*, one can see that other definitions of the normalisation factor can be employed which satisfy the condition of Equation* (3.49)*. Indeed, if the limit in Equation* (3.52) *is rephrased as*

$$\lim_{\alpha\to 1^-} \frac{2\Gamma(1-\alpha)\sin(\alpha\pi/2)\pi R_\mathrm{in}^2}{\hat{\mathcal{N}}(\alpha)} = 1, \tag{3.55}$$

where $\hat{\mathcal{N}}(\alpha)$ is the new normalisation factor sought for, then, upon following the reasoning leading to Equation (3.53)*, one can take $\hat{\mathcal{N}}(\alpha)$ as*

$$\hat{\mathcal{N}}(\alpha) := 2\Gamma(1-\alpha)\sin(\alpha\pi/2)\pi R_\mathrm{in}^2, \tag{3.56}$$

thereby automatically satisfying Equation (3.55)*. Then, by using $\hat{\mathcal{N}}(\alpha)$ in Equation* (3.44) *in lieu of $\mathcal{N}(\alpha)$, the axial mass flux can be written as*

$$\begin{aligned} \hat{y}_\alpha^z(z,t) &= -\frac{\varrho_\mathrm{f}}{2\Gamma(1-\alpha)\sin(\alpha\pi/2)} \int_{-\ell(t)}^{+\ell(t)} \frac{1}{|z-\tilde{z}|^\alpha} \mathfrak{d}_\alpha(\tilde{z},t)\partial_{\tilde{z}} c_\mathrm{a}(\tilde{z},t)\,\mathrm{d}\tilde{z} \\ &= \mathscr{I}^{1-\alpha}_{-\ell(t),+\ell(t)}[-\varrho_\mathrm{f}\mathfrak{d}_\alpha\partial_{\tilde{z}} c_\mathrm{a}](z,t), \end{aligned} \tag{3.57}$$

where $\mathscr{I}^{1-\alpha}_{-\ell(t),+\ell(t)}[-\varrho_{\mathrm{f}}\mathfrak{d}_\alpha\partial_{\tilde{z}}c_{\mathrm{a}}]$ *is the one-dimensional* Riesz potential *of* $-\varrho_{\mathrm{f}}\mathfrak{d}_\alpha\partial_{\tilde{z}}c_{\mathrm{a}}$*, but with integration limits* $\pm\ell(t)$ *instead of* $\pm\infty$ *(see [249] page 223). For this reason, one may refer to Equation* (3.57) *as a "truncated" Riesz potential [87].*

At this point, two comments are in order. First, we note that, for $\alpha \to 1^-$*, both choices of the normalisation factor lead to the same result and, consequently, the mass flux obtained for* $\alpha \to 1^-$ *is the same in both formulations. However, something different occurs for* $\alpha \to 0^+$*. Indeed, by looking at Equation* (3.46)*, if the normalisation factor* $\mathcal{N}(\alpha)$ *is used, we obtain, for* $\xi \neq 0$*, that*

$$\lim_{\alpha\to 0^+} \mathscr{F}[y^z_\alpha(\,\cdot\,,t)](\xi) = 0, \tag{3.58}$$

which suggests that the flux of the species is null for $\alpha \to 0^+$*. On the contrary, if in Equation* (3.46) $\mathcal{N}(\alpha)$ *is replaced with* $\hat{\mathcal{N}}(\alpha)$*, one obtains, for* $\xi \neq 0$*,*

$$\lim_{\alpha\to 0^+} \mathscr{F}[\hat{y}^z_\alpha(\,\cdot\,,t)](\xi) = |\xi|^{-1}\mathscr{F}[-\varrho_{\mathrm{f}}\mathfrak{d}_0(\,\cdot\,,t)\,\partial_z c_{\mathrm{a}}(\,\cdot\,,t)](\xi), \tag{3.59}$$

with $\mathfrak{d}_0 = \lim_{\alpha\to 0^+}\mathfrak{d}_\alpha$*, thereby implying, in general, a non-zero flux. In view of the above results and of the normalisation factor used by other Authors[215, 82, 19, 252], we prefer to employ* $\mathcal{N}(\alpha)$ *as normalisation factor in the remainder of this work. Besides, in this way, the model is able to account for a wider range of diffusion situations, from no diffusion to standard diffusion. Nevertheless, for completeness in our study, in Section "Results and discussion", we provide a comparison between the approach involving* $\mathcal{N}(\alpha)$ *and that involving* $\hat{\mathcal{N}}(\alpha)$*.*

Now, the restrictions imposed on the motion imply that the only component of interest of the deformation gradient tensor is given by $[\boldsymbol{F}(X,t)]^z{}_Z = 1 + u'(Z,t)$. Thus, by taking into account Equation (3.25), the material fractional diffusivity tensor can be rephrased as follows

$$[\mathfrak{D}_\alpha(X,\tilde{X},t)]^{ZZ} = \mathfrak{d}_{\mathrm{R}\alpha}\frac{1+u'(\tilde{Z},t)-J_\gamma(\tilde{Z},t)\Phi_{\mathrm{s}\nu}}{[1+u'(Z,t)][1+u'(\tilde{Z},t)]}, \tag{3.60}$$

whereas the definition (3.43) implies that $\mathfrak{F}_\alpha$, given in Equation (3.22b), can be rephrased as a function of Z, $\tilde{Z}$ and t, i.e.,

$$\mathfrak{F}_\alpha(X,\tilde{X},t) = \mathfrak{H}_\alpha(Z,\tilde{Z},t) = \frac{1}{2\Gamma(1-\alpha)\pi R^2_{\mathrm{in}}}\frac{1}{|Z+u(Z,t)-\tilde{Z}-u(\tilde{Z},t)|^\alpha}, \quad \alpha\in\,]0{,}1[\,. \tag{3.61}$$

Finally, by substituting Equation (3.60) into Equation (3.23b), and taking into account relation (3.22b), the only non-zero component of the material fractional mass flux vector, $\boldsymbol{Y}_\alpha$, is the one along the axial direction, and represents the backward Piola transform of Equation (3.44), i.e.,

$$Y^Z_\alpha(Z,t) = -\frac{\varrho_{\mathrm{f}}}{2\Gamma(1-\alpha)}\int_{-L_{\mathrm{in}}}^{+L_{\mathrm{in}}}\mathfrak{d}_{\mathrm{R}\alpha}\frac{[1+u'(\tilde{Z},t)-J_\gamma(\tilde{Z},t)\Phi_{\mathrm{s}\nu}]}{|Z+u(Z,t)-\tilde{Z}-u(\tilde{Z},t)|^\alpha}\frac{\mathfrak{c}'_{\mathrm{a}}(\tilde{Z},t)}{[1+u'(\tilde{Z},t)]}\,\mathrm{d}\tilde{Z}. \tag{3.62}$$

Looking at Equations (3.61) and (3.62), we remark that, in contrast to what is usually assumed in the "standard" setting of Fractional Calculus, both $\mathfrak{H}_\alpha$ and Y_α^Z depend on the displacement field, rather than depending on the difference between Z and $\tilde{Z}$, only. As anticipated in the Introduction, this result is one of the most relevant novelties of our work, as it prescribes that the non-locality evolves with the change of configuration of the system. Moreover, since in our framework the displacement is driven by growth (even though u and γ are formally independent variables), we conclude that the non-locality of the problem is related also to the variation of the tissue's internal structure, as modelled by γ.

3.8 Results and discussion

In this section, we study the impact of the non-local diffusion of nutrients on the benchmark problem specified above. For this scope, we distinguish between two mathematical models, both characterised by Equations (3.26a)–(3.26e). The first model, referred to as *fractional model*, describes the growth of the considered avascular tumour in the case in which the diffusion of the nutrients is governed by the non-local constitutive law (3.62). The second model, denominated *standard model*, describes the growth of the tumour by employing the same governing equations (3.26a)–(3.26e), with the only difference being that the nutrients' diffusive mass flux vector is expressed by standard Fick's law, i.e.,

$$\boldsymbol{Y}_{\mathrm{std}}(X,t) = -\varrho_{\mathrm{f}}\boldsymbol{D}(X,t)\,\mathrm{Grad}\mathfrak{c}_{\mathrm{a}}(X,t), \tag{3.63}$$

where "std" stands for "standard", and $\boldsymbol{D}$ is the *material diffusivity tensor*, given by [91, 131]

$$\boldsymbol{D}(X,t) = (J(X,t) - J_\gamma(X,t)\Phi_{\mathrm{s}\nu})d_{\mathrm{R}}\boldsymbol{C}^{-1}(X,t). \tag{3.64}$$

We notice that both models, i.e., the fractional and the standard one, share the same set of parameters except for the reference diffusivities $\mathfrak{d}_{\mathrm{R}\alpha}$ and d_{R}. Note also that Equation (3.64) can be obtained from (3.25) by setting $\tilde{X} = X$ and then taking the limit for $\alpha \to 1^-$, i.e., $\lim_{\alpha\to 1^-} \mathfrak{D}_\alpha(X,X,t) = \boldsymbol{D}(X,t)$.

For the purposes of our work, one should not fix $\mathfrak{d}_{\mathrm{R}\alpha}$ independently of d_{R}. Indeed, in order to compare the results of the non-local model with those of the local one, $\mathfrak{d}_{\mathrm{R}\alpha}$ must depend on d_{R} in such a way that it tends to d_{R} in the limit $\alpha \to 1^-$. For this reason, and taking into account that there exist several experimental works in which the standard diffusivity of species in biological tissues has been measured (see e.g. [149, 140]), we use for $\mathfrak{d}_{\mathrm{R}\alpha}$ the definition given in Equation (3.51), and we set $L = 2L_{\mathrm{in}}$. In Table 3.1, we provide the list of all the parameters used in our simulations. We remark that, due to the symmetries of the benchmark problem studied in this work, in the following we report the profile of the main quantities of interest restricted to half of the domain, i.e., $[0, L_{\mathrm{in}}]$.

Table 3.1: List of parameters used in the numerical simulations.

Parameter	Unit	Value	Equation	Reference
L_{in}	cm	0.500	(3.44)	[91]
R_{in}	cm	$1.000 \cdot 10^{-2}$	(3.62)	[91]
λ	Pa	$1.333 \cdot 10^{4}$	(3.12)	[263]
μ	Pa	$1.999 \cdot 10^{4}$	(3.12)	[263]
k_{R}	$\mathrm{m}^2/(\mathrm{Pa\,s})$	$4.875 \cdot 10^{-13}$	(3.15)	[149]
m_0	–	0.0848	(3.15)	[149]
m_1	–	4.638	(3.15)	[149]
d_{R}	m^2/s	$3.200 \cdot 10^{-9}$	(3.51)	[255]
ζ_{fp}	$\mathrm{kg}/(\mathrm{m}^3\,\mathrm{s})$	$1.343 \cdot 10^{-3}$	(3.27a)	[62]
ζ_{nf}	$\mathrm{kg}/(\mathrm{m}^3\,\mathrm{s})$	$1.150 \cdot 10^{-5}$	(3.27b)	[62]
ζ_{cp}	$\mathrm{kg}/(\mathrm{m}^3\,\mathrm{s})$	$3.000 \cdot 10^{-4}$	(3.27c)	[57, 58]
ζ_{pn}	$\mathrm{kg}/(\mathrm{m}^3\,\mathrm{s})$	$1.500 \cdot 10^{-3}$	(3.27d)	[62]
$\mathfrak{c}_{\mathrm{cr}}$	–	$1.000 \cdot 10^{-3}$	(3.27a)	[91]
$\mathfrak{c}_{\mathrm{env}}$	–	$7.000 \cdot 10^{-3}$	(3.27a)	[91]
$\mathfrak{c}_0$	–	$1.000 \cdot 10^{-2}$	(3.27c)	This work
δ_1	–	$7.138 \cdot 10^{-1}$	(3.27a)	[191]
δ_2	Pa	$1.541 \cdot 10^{3}$	(3.27a)	[191]
$\Phi_{\mathrm{s}\nu}$	–	0.8	(3.5a)	[91]
ϱ_{s}	kg/m^3	1000	(3.2)	[91]
ϱ_{f}	kg/m^3	1000	(3.2)	[91]

To start with, in Fig. 3.1, we report the spatial profile of the nutrients' mass fraction $\mathfrak{c}_{\mathrm{a}}(Z,t)$. Specifically, in the left panel of Fig. 3.1, we present the results of our simulations for $\alpha = 0.1$ (dashed line) and $\alpha = 0.9$ (solid line), and for different times. As shown in this plot, the parameter α permits to control how the nutrients diffuse into the tumour from the axial boundaries (i.e., the terminal cross sections $Z = \pm L_{\mathrm{in}}$). In particular, for $\alpha = 0.1$ the diffusion of the nutrients is constrained to the tumour's axial boundary, i.e., close to $Z = \pm L_{\mathrm{in}}$, so that their mass fraction is dramatically reduced in the internal points of the specimen. In such a situation, the proliferating cells consume the nutrients that are already present in the tissue, without the replenishment needed to continue their proliferation. On the contrary, for $\alpha = 0.9$, the nutrients are able to diffuse towards the centre of the tumour, so that their consumption is less localised. For clarity, in the plot we prefer to show only the curves corresponding to $\alpha = 0.1$ and $\alpha = 0.9$. For any other value of $\alpha \in]0.1,0.9[$, the model is able to describe different diffusion profiles ranging between the ones obtained for $\alpha = 0.1$ and for $\alpha = 0.9$. To us, an interesting feature of the curves corresponding to $\alpha = 0.1$ is that, depending on the point Z at which the nutrients' mass fraction is observed, the trend of these curves exhibits a different monotonicity in time. Indeed, the nutrients' mass fraction decreases in

time close to the boundary $Z = L_{\text{in}}$, whereas it increases towards the tumour's centre. Furthermore, in the panel on the right of Fig. 3.1, we compare, for different values of α, the results obtained with the fractional model with those obtained with the standard model at time $t = 20$ d. Specifically, for α close to 0, there is almost no diffusion, while, when α is close to 1, the fractional model conducts to the standard one, as evidenced by our previous calculations (see Equation (3.46)).

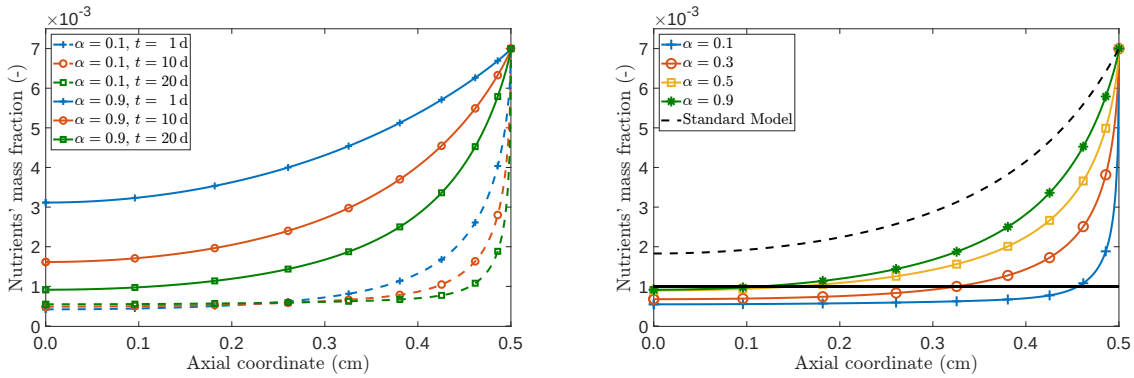

Figure 3.1: Spatial profile of the nutrients' mass fraction $\mathfrak{c}_{\text{a}}(Z,t)$ for different values of α and at different times (panel on the left), and comparison of the results obtained with the fractional and the standard model at time $t = 20\,\text{d}$ (panel on the right).

As shown in Fig. 3.2, the non-local way in which the nutrients diffuse into the tissue affects the manner in which the tumour grows. By increasing α and, thus, enhancing diffusion, one also increases the availability of the nutrients in the tumour, thereby boosting its growth. On the other hand, for $\alpha = 0.1$, the displacement is hindered and its highest values are attained in a neighbourhood of $Z = L_{\text{in}}$. Indeed, this is where the nutrients enter the tumour and their mass fraction still remains high enough to trigger growth, so that the magnitude of the displacement in this region of the tumour is higher than elsewhere. However, moving towards the interior of the tumour, the fact that the nutrients' concentration is below the critical threshold brings growth to a stop, thereby considerably reducing the magnitude of the displacement. This behaviour shows that also the monotonicity in time of the displacement curves depends on the point Z at which they are reckoned. More in detail, the reduction of the displacement in the interior of the tumour may be due to the loss of mass caused by the lack of nutrients, which implies that the proliferating cells start to die, and a region of necrotic cells comes into sight. This behaviour becomes even more evident by looking at the left panel of Fig. 3.3. Moreover, comparing the right panels of Fig. 3.1 and Fig. 3.3, we notice that the part of the domain in which the necrotic cells appear coincides with the one in which the nutrients fall below the critical value $\mathfrak{c}_{\text{cr}}$, represented with the solid horizontal line in the right panel of Fig. 3.1. By referring to Equation (3.27d), when $\mathfrak{c}_{\text{a}} < \mathfrak{c}_{\text{cr}}$, the rate of mass R_{pn} becomes active and, therefore, the proliferating cells change into

necrotic cells.

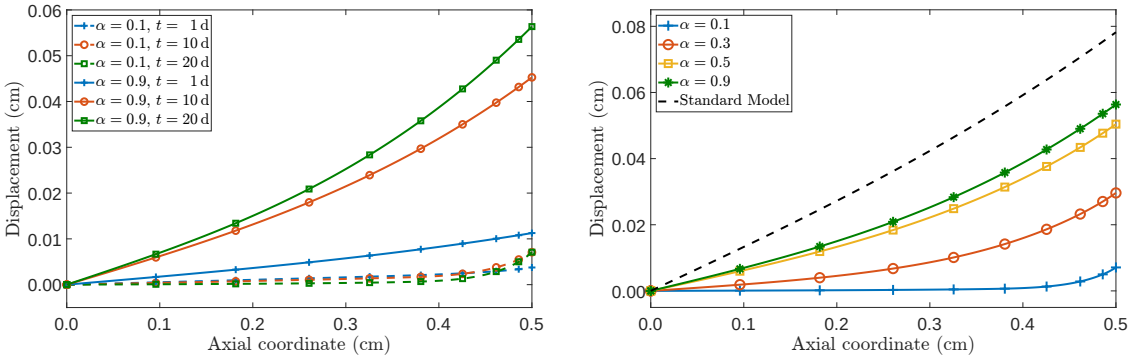

Figure 3.2: Spatial profile of the axial displacement $u(Z,t)$ for different values of α and at different times (panel on the left), and comparison of the results obtained with the fractional and the standard model at time $t = 20\,\mathrm{d}$ (panel on the right).

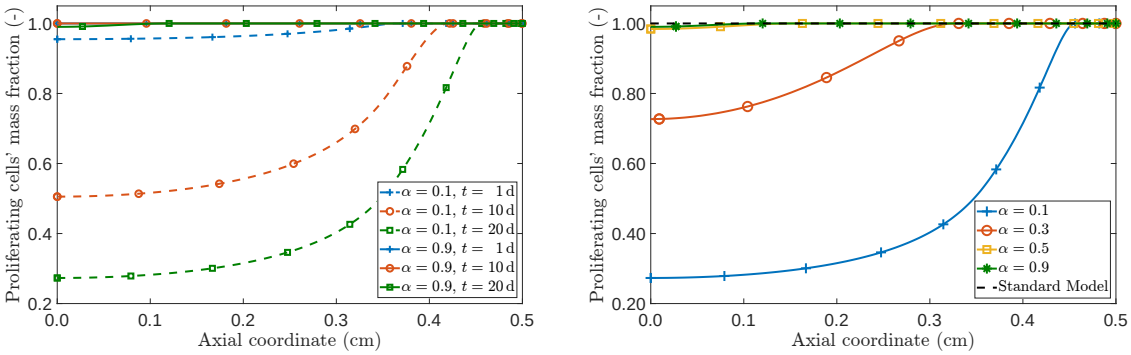

Figure 3.3: Spatial profile of the proliferating cells' mass fraction $\mathfrak{c}_\mathrm{p}(Z,t)$ for different values of α and at different times (panel on the left), and comparison of the results obtained with the fractional and the standard model at time $t = 20\,\mathrm{d}$ (panel on the right).

To continue our analysis, we refer to Fig. 3.4, where we plot the growth parameter γ. By focusing on the panel on the left, we notice, for $\alpha = 0.1$, a localisation of the variation of the growth parameter near the boundary $Z = L_\mathrm{in}$ for increasing time, whereas, for $\alpha = 0.9$, the variation of γ is more uniformly distributed in the whole domain. Besides, for $\alpha = 0.1$, γ is greater than one for all $Z \in [0, L_\mathrm{in}]$ and for all t, even though this is difficult to be observed with the unaided eye. This is because, although for $t \geq 1$ d the mass fraction of the nutrients is above the threshold value $\mathfrak{c}_\mathrm{cr}$ mostly near the boundary (see the left panel of Fig. 3.1), the inner region has undergone a growth process at earlier times. Indeed, since the condition $\mathfrak{c}_\mathrm{a}(Z,0) \equiv \mathfrak{c}_\mathrm{env} > \mathfrak{c}_\mathrm{cr}$ is respected, the mass rate R_fp is greater than zero, and we can conclude that, from the very beginning, the cell proliferation is

promoted until the nutrients' concentration falls below its critical value. Note also that this is accelerated when α is near zero because of the slow pace with which the nutrients are refilled. At this point, the proliferating cells abruptly die, thereby turning into necrotic cells, and go into the fluid (see the definition of R_{nf}), which results in a loss of mass. For $\alpha = 0.9$, instead, it is visible also with the naked eye that γ is greater than unity everywhere in $[0, L_{\text{in}}]$ and for all the considered times. Finally, as noticed for the nutrients' mass fraction and for the displacement, also the monotonicity in time of the trend of the growth parameter depends, for $\alpha = 0.1$, on the point Z at which γ is observed. Indeed, γ is monotonically increasing in time for Z close to $Z = L_{\text{in}}$, and monotonically decreasing for Z "moving" towards the centre of the tumour.

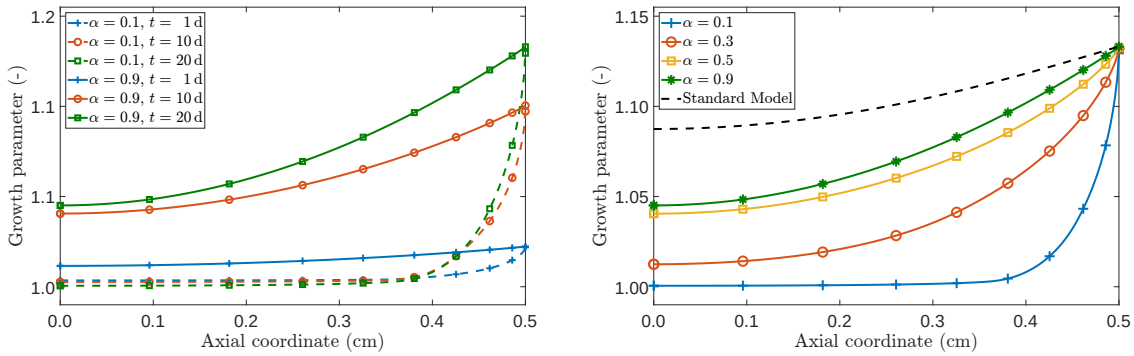

Figure 3.4: Spatial profile of the growth parameter $\gamma(Z, t)$ for different values of α and at different times (panel on the left), and comparison of the results obtained with the fractional and the standard model at time $t = 20\,\text{d}$ (panel on the right).

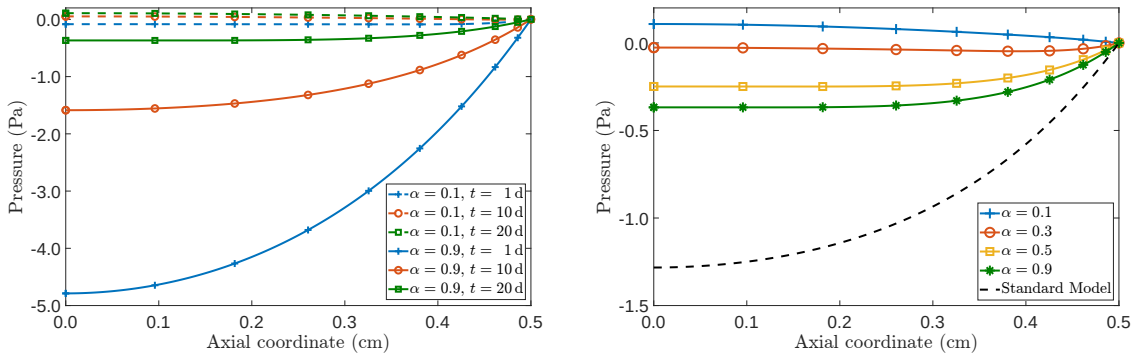

Figure 3.5: Spatial profile of the pressure $\mathfrak{p}(Z, t)$ for different values of α and at different times (panel on the left), and comparison of the results obtained by the fractional and the standard model at time $t = 20\,\text{d}$ (panel on the right).

Now, we report the evolution of the pressure, $\mathfrak{p}$, in Fig. 3.5. For both the standard and the fractional model, when α is close to 1, the pressure of the interstitial

fluid decreases, taking negative values, from the free boundary towards the tumour's centre. However, for α tending towards 0 from above, the pressure in the interior of the tumour tends to become positive. To explain this event, we notice that the proliferating cells absorb fluid from the surrounding environment to fuel their growth, which is possible because the fluid flows towards the tumour's interior. However, due to an over-consumption of nutrients, the level of those drastically decreases in the innermost zone of the tumour. This situation, as evidenced in our simulations (see Fig. 3.4), creates a layer of proliferating cells near the outer surface (i.e., the cross section $Z = L_{\text{in}}$), and a region of necrotic cells at the centre of the tumour. By looking at Equation (3.27b), in this circumstance, the necrotic cells dissolve into the fluid with rate ζ_{nf}, thereby increasing its pressure, which, in turn, generates an outward flux (i.e., a flux in the direction opposite to the fluid flow). This sequence of events, which are consistent with the biological foundations of nutrient diffusion and necrosis in a tumour as explained in [183], arises in the model thanks to the non-local approach presented in this work. That is, the non-locality parameter α is responsible for this picture and, thus, through its inclusion, the fractional model is able to reproduce a scenario that was not initially considered in the model. On the contrary, as the results show, this behaviour would not be observed within a formulation based on standard Fick's law, at least with our model as is.

Finally, as we mentioned before (see Remark 8), for completeness in our discussion, we compare the results corresponding to the adoption of $\mathcal{N}(\alpha)$ versus those obtained with $\hat{\mathcal{N}}(\alpha)$. As shown in Fig. 3.6, top left panel, when the normalisation factor is $\hat{\mathcal{N}}(\alpha)$, we observe, for $\alpha \to 0^+$, a less pronounced decrease of the nutrients' mass fraction. This is compatible with the fact that, even for very small values of α, there is an incoming mass flux of nutrients through the domain's boundaries that reestablishes the nutrients eaten by the cells. This effect, in turn, tends to disappear when the normalisation factor $\mathcal{N}(\alpha)$ is employed since, in that case, the mass flux tends to zero in the limit $\alpha \to 0^+$. Coherently with this observation, we also notice a markedly different behaviour of the growth parameter (see Fig. 3.6, top right panel). Indeed, since the flux of nutrients obtained for $\hat{\mathcal{N}}(\alpha)$ does not vanish for $\alpha \to 0^+$, and a greater amount of nutrients remains available even at time $t = 20$ d, growth can still occur, as is testified by the dotted line marked with "+". Similar comments pertain also to the description of the displacement (see Fig. 3.6, bottom left panel). Indeed, since growth remains active also for small values of α, the displacement also tends to persist even at $t = 20$ d, and remains relatively large in the neighbourhood of the domain's boundaries, where the availability of nutrients is the highest (because of the Dirichlet condition assigned to the nutrients' mass fraction) and growth is present. These differences notwithstanding, it should be emphasised that the qualitative behaviour of the curves describing the nutrients' mass fraction and the growth parameter is the same for both choices of the normalisation factor. On the contrary, the behaviour of the pressure (see Fig. 3.6, bottom right panel) is *both* qualitatively *and* quantitatively different for $\alpha = 0.1$. In fact,

the use of $\hat{\mathcal{N}}(\alpha)$ nullifies the effect visible at $t = 20$ d, for $\alpha = 0.1$ and normalisation factor $\mathcal{N}(\alpha)$, which consisted in the sign change of the pressure. Hence, employing $\hat{\mathcal{N}}(\alpha)$ leaves the pressure negative, thereby triggering no inversion in the flow of the interstitial fluid, which continues to flow from the exterior of the tumour into it.

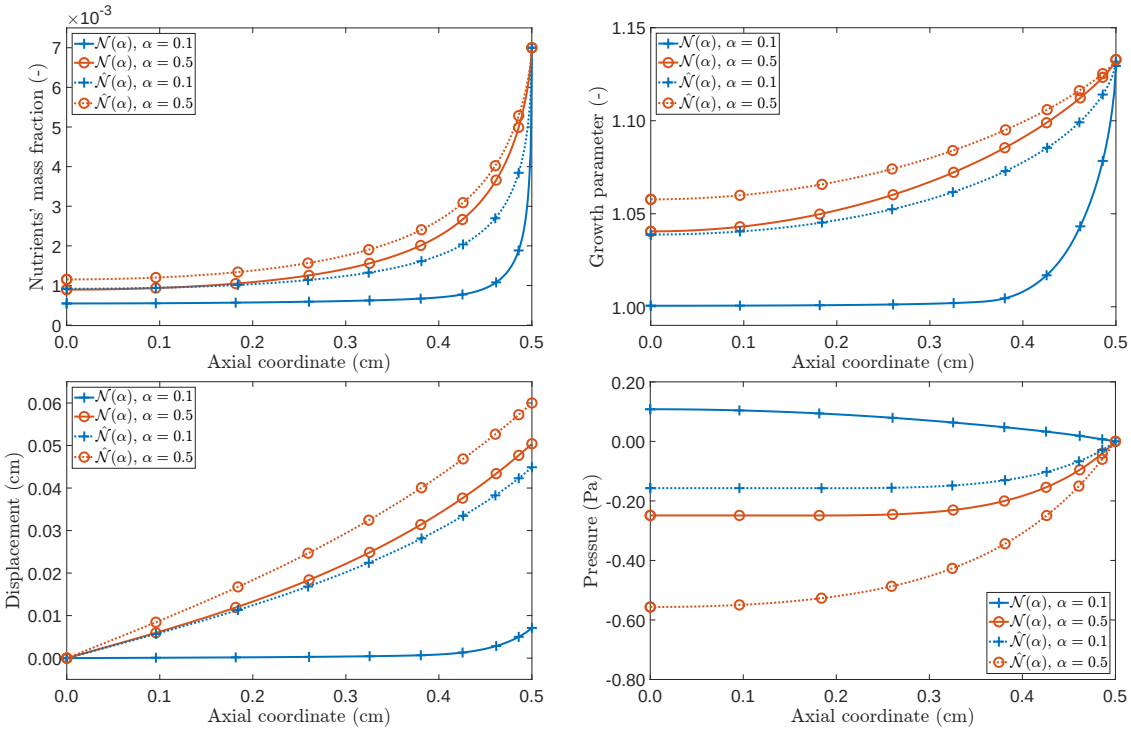

Figure 3.6: Comparison of the spatial profiles of $\mathfrak{c}_{\mathrm{a}}(Z,t)$ (top left), $\gamma(Z,t)$ (top right), $u(Z,t)$ (bottom left) and $\mathfrak{p}(Z,t)$ (bottom right) for the approaches involving $\mathcal{N}(\alpha)$ (solid line) and $\hat{\mathcal{N}}(\alpha)$ (dotted line). In the plots different values of α are used and time is fixed to $t = 20$ d.

Chapter 4

Outlook on further research: non-local diffusion in remodelling anisotropic media

The work reported in this chapter has been previously published in [220]

4.1 Introduction

As already seen in the previous chapters, the growth and remodelling of a biological tissue are often studied from a mechanical point of view and, in such a context, a tissue is modelled as a deformable porous medium hosting, in its pore space, an *interstitial fluid*. Within this approach, the porous medium is usually taken as the representation of a system comprising one or more cell populations, and a fibre network constituting the tissue's extra-cellular matrix (ECM). Although this description could be sometimes too simple, in several cases of biomechanical interest it suffices to give an idea of the environment in which the interstitial fluid flows. Recently, the picture described above has been used in [191, 91].

We remark that, although the evolution of the nutrients is important to understand how growth is set off, we consider here remodelling alone. We do this for the following two reasons. First, the mathematical formulation of remodelling is simpler than the one needed for growth. Indeed, it does not require to introduce sources/sinks of mass, nor does it call for the mass balance laws that describe the dynamics of the tissue's constituents. Second, we are interested here in drawing attention on a possible way in which the structural transformation of a tissue influences the evolution of the nutrients in the interstitial fluid. For our purposes, we consider a transversely isotropic tissue that undergoes remodelling and, by highlighting how the latter contributes to change the tissue's anisotropy, we discuss the influence of remodelling on the nutrients' diffusivity tensor. In addition, we

propose some future developments of the research in this field and, in particular, we point out the extension of the current models to include fractional diffusion in anisotropic media.

Following [232], we report on some aspects of the dynamics of the biphasic system "porous medium–interstitial fluid". To accomplish this task, we invoke the Theory of Mixtures [141, 39], which provides a well-established modelling approach for framing our study. Coherently, the porous medium is described with the classical tools of Continuum Mechanics, appropriately adapted and re-formulated under the light shed by the theory of multiphasic materials. In addition, the interstitial fluid and its interactions with the solid phase are taken care of by having recourse to the standard laws of Fluid Mechanics in porous media.

We emphasise that, the above simplifications notwithstanding, our model can be generalised to include growth and, in fact, this is one of the topics of our current research. However, our scope is to highlight the passive role of the chemical gradient by considering the effect of remodelling on transport properties. In doing this, we regard the fluid constituents as continua, and we focus our study on the relation between remodelling and the diffusion process by which the nutrients are transported throughout the tissue.

4.2 Mass Balance Laws and Dynamics

In our framework, a tissue is viewed as a biphasic medium comprising a solid and a fluid phase. The solid phase consists of cells and collagen fibres, with the latter ones being arranged in a way that renders the tissue transversely isotropic with respect to a given spatial direction. The interstitial fluid is a mixture of chemical substances of various types, among which the most relevant ones for our study are represented by nutrient agents. To focus on the anisotropy of the considered tissue, while keeping our mathematical formulation as simple as possible, in this work we regard the solid phase as a homogenised medium, in which no distinction is made between the dynamics of the cells and that of the fibres. These, in fact, are included with the sole scope of describing the tissue's anisotropy and its evolution in response to deformation *and* remodelling. Clearly, more general models are possible, as is the case in [125, 191, 91], in which, however, the growth is considered and the tissue is regarded as isotropic.

We group the mass balance laws characterising the system under investigation in two sets. The first one refers to the solid phase and can be written as

$$\partial_t(\phi_{\mathrm{s}}\rho_{\mathrm{s}}) + \operatorname{div}(\phi_{\mathrm{s}}\rho_{\mathrm{s}}\mathbf{v}_{\mathrm{s}}) = 0, \tag{4.1}$$

where ϕ_{s} and ρ_{s} are the volumetric fraction and the mass density of the solid phase, and $\mathbf{v}_{\mathrm{s}}$ is its velocity. The second group of mass balance laws pertains to the fluid

phase and to the nutrients dissolved in it (see e.g. [191]), i.e.,

$$\partial_t(\phi_\mathrm{f}\rho_\mathrm{f}) + \mathrm{div}(\phi_\mathrm{f}\rho_\mathrm{f}\mathbf{v}_\mathrm{f}) = 0, \tag{4.2a}$$
$$\partial_t(\phi_\mathrm{f}\rho_\mathrm{f}c_\mathrm{nf}) + \mathrm{div}(\phi_\mathrm{f}\rho_\mathrm{f}c_\mathrm{nf}\mathbf{v}_\mathrm{f}) + \mathrm{div}\,\mathbf{y}_\mathrm{nf} = 0. \tag{4.2b}$$

In (4.2a) and (4.2b), ϕ_f and ρ_f are the volumetric fraction and the mass density of the fluid phase, respectively, $\mathbf{v}_\mathrm{f}$ is the fluid velocity, c_nf is the mass fraction of the nutrients in the fluid phase, and $\mathbf{y}_\mathrm{nf}$ is the mass flux vector of the nutrients, i.e., $\mathbf{y}_\mathrm{nf} = \phi_\mathrm{f}\rho_\mathrm{f}c_\mathrm{nf}\mathbf{u}_\mathrm{nf}$, with $\mathbf{u}_\mathrm{nf}$ being the velocity of the nutrients relative to the centre of mass of the fluid phase. Note that, by enforcing the saturation condition, ϕ_f must comply with the equality $\phi_\mathrm{f} = 1 - \phi_\mathrm{s}$. Furthermore, we assume in the sequel that the mass densities ρ_s and ρ_f are constant, thereby implying that both the solid and the fluid phase are incompressible.

By adhering to the picture put forward in [86, 213], the dynamics of the system discussed so far should be studied at two different, virtually independent levels. One level is associated with the *"visible"* degrees of freedom of the system [86], which correspond to the deformation of the solid phase and to the flow of the interstitial fluid. The other level, instead, is related to the structural transformations undergone by the tissue, and is accounted for by allotting structural degrees of freedom with which suitable kinematic descriptors are associated. A similar framework has been adopted in the majority of previous works of some of us (see e.g. [127, 78] and references therein).

In the limit in which the inertial forces and all the long-range forces (e.g. gravity) are negligible, the "visible" dynamics are represented by the following set of momentum balance laws [141, 129],

$$\mathrm{div}(\boldsymbol{\sigma}_\mathrm{s} + \boldsymbol{\sigma}_\mathrm{f}) = \mathbf{0}, \tag{4.3a}$$
$$\mathrm{div}\,\boldsymbol{\sigma}_\mathrm{f} + p\,\mathbf{g}^{-1}\mathrm{grad}\phi_\mathrm{f} + \boldsymbol{\pi}_\mathrm{f} = \mathbf{0}, \tag{4.3b}$$
$$\tilde{\boldsymbol{\pi}}_\mathrm{nf} - \phi_\mathrm{f}\rho_\mathrm{f}c_\mathrm{nf}\,\mathbf{g}^{-1}\mathrm{grad}\,\tilde{\mu}_\mathrm{nf} = \mathbf{0}. \tag{4.3c}$$

Equation (4.3a) is the momentum balance law of the biphasic medium as a whole, and involves the sum of the Cauchy stress tensors $\boldsymbol{\sigma}_\mathrm{s}$ and $\boldsymbol{\sigma}_\mathrm{f}$ associated with the solid and with the fluid phase, respectively. Equation (4.3b) is the momentum balance law of the fluid: it features the sum of the terms $p\,\mathbf{g}^{-1}\mathrm{grad}\,\phi_\mathrm{f}$ and $\boldsymbol{\pi}_\mathrm{f}$, which represent, respectively, the non-dissipative and the dissipative parts of the linear momentum density exchange rate between the solid and the fluid phase. Here and in the following, $\mathbf{g}$ is the metric tensor field associated with the three-dimensional Euclidean space. We notice that the non-dissipative force density, $p\,\mathbf{g}^{-1}\mathrm{grad}\,\phi_\mathrm{f}$, features the pressure, p. Equation (4.3c) is the momentum balance law of the nutrient substances dissolved in the fluid (details about the procedure for obtaining (4.3c) can be found in [141, 129]): it reduces to the balance between the dissipative force density $\tilde{\boldsymbol{\pi}}_\mathrm{nf}$ and the generalised force $\phi_\mathrm{f}\rho_\mathrm{f}c_\mathrm{nf}\,\mathbf{g}^{-1}\mathrm{grad}\,\tilde{\mu}_\mathrm{nf}$. Here,

$\tilde{\boldsymbol{\pi}}_{\mathrm{nf}}$ describes the dissipative interactions among the nutrients and the fluid itself, while $\tilde{\mu}_{\mathrm{nf}}$ is the chemical potential of the nutrients, μ_{nf}, relative to the chemical potential of water, μ_{wf}, i.e., $\tilde{\mu}_{\mathrm{nf}} := \mu_{\mathrm{nf}} - \mu_{\mathrm{wf}}$.

One can prove that $\boldsymbol{\sigma}_{\mathrm{s}}$ splits additively as $\boldsymbol{\sigma}_{\mathrm{s}} = -\phi_{\mathrm{s}} p\, \mathbf{g}^{-1} + \boldsymbol{\sigma}_{\mathrm{sc}}$ and, under the hypothesis of hyperelastic solid phase, $\boldsymbol{\sigma}_{\mathrm{sc}}$ can be obtained constitutively from a free energy density. Moreover, we assume that $\boldsymbol{\sigma}_{\mathrm{f}}$ reduces to the hydrostatic Cauchy stress tensor $\boldsymbol{\sigma}_{\mathrm{f}} = -\phi_{\mathrm{f}} p\, \mathbf{g}^{-1}$. Before going further, we remark that a similar setting, and identical expressions for $\boldsymbol{\sigma}_{\mathrm{s}}$ and $\boldsymbol{\sigma}_{\mathrm{f}}$ have been used in many previous works of some of us [129, 269, 128, 91, 78], and can be found in many renowned publications of porous media (see e.g. [141, 39]), with or without the hypothesis of incompressibility of the solid and the fluid phase.

By following a standard praxis in porous media mechanics (see e.g. [141, 39]), we express $\boldsymbol{\pi}_{\mathrm{f}}$ and $\tilde{\boldsymbol{\pi}}_{\mathrm{nf}}$ constitutively as linear functions of the fluid filtration velocity, $\mathbf{q} = \phi_{\mathrm{f}}[\mathbf{v}_{\mathrm{f}} - \mathbf{v}_{\mathrm{s}}]$, and of the mass flux vector of the nutrients, $\mathbf{y}_{\mathrm{nf}}$, respectively, i.e.,

$$\boldsymbol{\pi}_{\mathrm{f}} = -\phi_{\mathrm{f}} \mathbf{g}^{-1} \mathbf{k}^{-1} \mathbf{q}, \tag{4.4a}$$

$$\tilde{\boldsymbol{\pi}}_{\mathrm{nf}} = -\phi_{\mathrm{f}} c_{\mathrm{nf}}\, \mathbf{g}^{-1} \boldsymbol{\lambda}_{\mathrm{nf}}^{-1} \mathbf{y}_{\mathrm{nf}}, \tag{4.4b}$$

where $\mathbf{k}$ and $\boldsymbol{\lambda}_{\mathrm{nf}}$ represent, respectively, the permeability tensor of the system and the mobility tensor of the nutrients. We remark that, in the present setting, both tensors are assumed to be invertible, symmetric and positive-definite from the outset. By plugging the relationships $\boldsymbol{\sigma}_{\mathrm{s}} = -\phi_{\mathrm{s}} p \mathbf{g}^{-1} + \boldsymbol{\sigma}_{\mathrm{sc}}$ and $\boldsymbol{\sigma}_{\mathrm{f}} = -\phi_{\mathrm{f}} p\, \mathbf{g}^{-1}$ into (4.3a) and (4.3b), and using the results (4.4a) and (4.4b) in (4.3b) and (4.3c), one obtains

$$\mathrm{div}(-p\, \mathbf{g}^{-1} + \boldsymbol{\sigma}_{\mathrm{sc}}) = \mathbf{0}, \tag{4.5a}$$

$$\mathbf{q} = -\mathbf{k}\, \mathrm{grad} p, \tag{4.5b}$$

$$\mathbf{y}_{\mathrm{nf}} = -\rho_{\mathrm{f}} \boldsymbol{\lambda}_{\mathrm{nf}}\, \mathrm{grad} \tilde{\mu}_{\mathrm{nf}}. \tag{4.5c}$$

We recognise Darcy's law of filtration and Fick's law of diffusion in (4.5b) and (4.5c), respectively.

Following [86], we choose a second order tensor field, denoted by $\mathbf{F}_{\mathrm{p}}$ and referred to as *remodelling tensor*, as kinematic descriptor of the structural changes of the tissue. The remodelling tensor is introduced by having recourse to the Bilby-Kröner-Lee (BKL) decomposition of the deformation gradient tensor of the solid phase, $\mathbf{F}$ (see e.g. [201, 246] for a review). Accordingly, $\mathbf{F}$ is written as $\mathbf{F} = \mathbf{F}_{\mathrm{e}} \mathbf{F}_{\mathrm{p}}$, where $\mathbf{F}_{\mathrm{e}}$ is said to be the *tensor of elastic distortions*. We speak of "distortions" in the sense of Kröner [163], since in general neither $\mathbf{F}_{\mathrm{e}}$ nor $\mathbf{F}_{\mathrm{p}}$ are integrable (this means that there exists no deformation whose gradient is $\mathbf{F}_{\mathrm{e}}$ or $\mathbf{F}_{\mathrm{p}}$). Moreover, we notice that the subscript "g", which usually stands for "growth", is kept here to identify the remodelling tensor. We make this choice to emphasise that, even though no mass sources/sinks are considered here, the remodelling of the considered tissue might be induced by growth.

Given $\mathbf{F}_\mathrm{p}$, we introduce the virtual velocity $\boldsymbol{\mathcal{V}}_\mathrm{g}$ associated with it, i.e., a second-order tensor field representing the virtual rate of change of the remodelling distortions. Then, within a *"theory of grade zero"* [86][1], we introduce generalised forces expending virtual power on $\boldsymbol{\mathcal{V}}_\mathrm{g}$. Such forces may be distinguished in an internal one, $\mathbf{Z}_\mathrm{int}$, and in an external one, $\mathbf{Z}_\mathrm{ext}$, and the Principle of Virtual Powers leads to the local force balance [60, 86]

$$\mathbf{Z}_\mathrm{int} = \mathbf{Z}_\mathrm{ext}, \tag{4.6}$$

holding in the internal points of the reference configuration of the considered tissue, $\mathscr{B}$. We look for constitutive expressions for $\mathbf{Z}_\mathrm{int}$ by exploiting the dissipation inequality for the system under study. Expressed per unit volume of the current configuration of the tissue, the dissipation of the system reads (see e.g. [129])

$$\begin{aligned}\mathfrak{D} &= -\boldsymbol{\pi}_\mathrm{f}.\mathbf{q} - \tilde{\boldsymbol{\pi}}_\mathrm{nf}.\mathbf{u}_\mathrm{nf} + J^{-1}(\boldsymbol{\Sigma}_\mathrm{sc} + \mathbf{Z}_\mathrm{int}) : \bar{\mathbf{L}}_\mathrm{g} \\ &= -\boldsymbol{\pi}_\mathrm{f}.\mathbf{q} - \tilde{\boldsymbol{\pi}}_\mathrm{nf}.\mathbf{u}_\mathrm{nf} + J^{-1}\boldsymbol{\Delta} : \bar{\mathbf{L}}_\mathrm{g} \\ &= -\boldsymbol{\pi}_\mathrm{f}.\mathbf{q} - \tilde{\boldsymbol{\pi}}_\mathrm{nf}.\mathbf{u}_\mathrm{nf} + J^{-1}(\mathrm{dev}\boldsymbol{\Delta}) : \bar{\mathbf{L}}_\mathrm{g} \geq 0, \end{aligned} \tag{4.7a}$$

where $\bar{\mathbf{L}}_\mathrm{g} \equiv \mathbf{F}_\mathrm{p}^{-1}\dot{\mathbf{F}}_\mathrm{g}$ is the rate of distortions due to remodelling, pulled back to the reference configuration, $\boldsymbol{\Sigma}_\mathrm{sc} = J\,\mathbf{F}^\mathrm{T}\boldsymbol{\sigma}_\mathrm{sc}\mathbf{F}^{-\mathrm{T}}$ is said to be the constitutive part of the solid phase Mandel stress tensor, and $\boldsymbol{\Delta} \equiv \boldsymbol{\Sigma}_\mathrm{sc} + \mathbf{Z}_\mathrm{int}$ is the dissipative contribution of $\mathbf{Z}_\mathrm{int}$. Note that $\bar{\mathbf{L}}_\mathrm{g}$ is deviatoric.

The Mandel stress tensor can also be written as $\boldsymbol{\Sigma}_\mathrm{sc} = \mathbf{C}\mathbf{S}_\mathrm{sc}$, where $\mathbf{S}_\mathrm{sc}$ is the constitutive part of the second Piola-Kirchhoff stress tensor of the solid phase and $\mathbf{C} = \mathbf{F}^\mathrm{T}.\mathbf{F} = \mathbf{F}^\mathrm{T}\mathbf{g}\mathbf{F}$ is the right Cauchy-Green deformation tensor. By its own definition, $\boldsymbol{\Sigma}_\mathrm{sc}$ is equipped with the symmetry property $\boldsymbol{\Sigma}_\mathrm{sc}\mathbf{C} = (\boldsymbol{\Sigma}_\mathrm{sc}\mathbf{C})^\mathrm{T} = \mathbf{C}\mathbf{S}_\mathrm{sc}\mathbf{C}$ [101, 194].

Since the definitions given in (4.4a) and (4.4b) satisfy the dissipation inequality (4.7a), we focus on the remodelling part of $\mathfrak{D}$, i.e., $\mathfrak{D}_\mathrm{g} \equiv J^{-1}(\mathrm{dev}\boldsymbol{\Delta}) : \bar{\mathbf{L}}_\mathrm{g} \geq 0$, in order to extract information on $\boldsymbol{\Delta}$. For this purpose, we make here the simplifying assumption of setting $\mathbf{Z}_\mathrm{ext}$ equal to the null tensor (see [60] for a discussion on this issue). Accordingly, the force balance (4.6) implies that $\mathbf{Z}_\mathrm{int}$ is null too, and the dissipative force $\boldsymbol{\Delta}$ coincides with $\boldsymbol{\Sigma}_\mathrm{sc}$, thereby inheriting the same symmetry properties as the Mandel stress tensor, i.e., $\boldsymbol{\Delta}\mathbf{C} = (\boldsymbol{\Delta}\mathbf{C})^\mathrm{T}$ [101, 194]. Therefore, $\mathfrak{D}_\mathrm{g}$ becomes

$$\mathfrak{D}_\mathrm{g} = J^{-1}(\mathrm{dev}\boldsymbol{\Delta}) : \bar{\mathbf{L}}_\mathrm{g} = J^{-1}[(\mathrm{dev}\boldsymbol{\Delta})\mathbf{C}] : \mathrm{sym}(\bar{\mathbf{L}}_\mathrm{g}\mathbf{C}^{-1}) \geq 0, \tag{4.8}$$

and (4.6) can be reformulated as

$$(\mathrm{dev}\boldsymbol{\Delta})\mathbf{C} = (\mathrm{dev}\boldsymbol{\Sigma}_\mathrm{sc})\mathbf{C}. \tag{4.9}$$

[1]This means that $\mathrm{Grad}\,\mathbf{F}_\mathrm{p}$ is not rated among the variables determining the kinematic picture of the theory. Of course, it can be computed *a posteriori*.

If we admit a remodelling of rate-dependent type, we may suggest to express $(\mathrm{dev}\boldsymbol{\Delta})\mathbf{C}$ as a linear constitutive function of $\mathrm{sym}(\bar{\mathbf{L}}_{\mathrm{g}}\mathbf{C}^{-1})$, i.e.,

$$(\mathrm{dev}\boldsymbol{\Delta})\mathbf{C} = \mathbb{K} : \mathrm{sym}(\bar{\mathbf{L}}_{\mathrm{g}}\mathbf{C}^{-1}), \tag{4.10}$$

where $\mathbb{K}$ is a positive-definite fourth-order tensor endowed with both the major and the minor symmetry. Hence, by plugging (4.10) into (4.8), we end up with the following evolution law for $\mathbf{F}_{\mathrm{p}}$:

$$\mathbb{K} : \mathrm{sym}(\mathbf{F}_{\mathrm{p}}^{-1}\dot{\mathbf{F}}_{\mathrm{g}}\mathbf{C}^{-1}) = (\mathrm{dev}\boldsymbol{\Sigma}_{\mathrm{sc}})\mathbf{C}. \tag{4.11}$$

Similar laws can also be found e.g. in [129, 89], with the rate of anelastic distortions expressed as a function of the corresponding measure of stress. A review on the evolution laws for $\mathbf{F}_{\mathrm{p}}$ is given e.g. in [80], whereas some Differential Geometry aspects connected with such laws has been recently provided in [203].

Equations (4.1)–(4.2b), (4.5a)–(4.5c) and (4.11) characterise our mathematical model, which has to be completed by assigning constitutive laws for $\mathbf{k}$, $\boldsymbol{\lambda}_{\mathrm{nf}}$, $\mathbb{K}$, and $\boldsymbol{\sigma}_{\mathrm{sc}}$. We do not focus here on the constitutive representation of $\mathbb{K}$ and $\boldsymbol{\sigma}_{\mathrm{sc}}$, as this is out of the scopes of this chapter. However, we do discuss constitutive laws for $\mathbf{k}$ and $\boldsymbol{\lambda}_{\mathrm{nf}}$. This is, indeed, the subject of the next sections.

4.3 Fick's law and diffusion in anisotropic growing media

When the mass fraction of the nutrient substances dissolved in the interstitial fluid is sufficiently low, the mass flux vector $\mathbf{y}_{\mathrm{nf}}$ can be expressed in terms of Fick's law:

$$\mathbf{y}_{\mathrm{nf}} = -\rho_{\mathrm{f}}\boldsymbol{\lambda}_{\mathrm{nf}}\,\mathrm{grad}\,\tilde{\mu}_{\mathrm{nf}}. \tag{4.12}$$

Equation (4.12) assumes that $\mathbf{y}_{\mathrm{nf}}$ is due to diffusion only, since any dispersive effect of the flow (see e.g. [36, 112] for a review on this issue) is typically neglected for the types of tissues under study.

In general, $\tilde{\mu}_{\mathrm{nf}}$ is expressed as a constitutive function of a list of variables that, beyond c_{nf}, may also contain the deformation. In this work, however, we restrict our study to the case in which $\tilde{\mu}_{\mathrm{nf}}$ is a constitutive function of the sole mass fraction, c_{nf}. Thus, with a slight abuse of notation, we set $\tilde{\mu}_{\mathrm{nf}} = \tilde{\mu}_{\mathrm{nf}}(c_{\mathrm{nf}})$, and we rewrite (4.12) as

$$\mathbf{y}_{\mathrm{nf}} = -\rho_{\mathrm{f}}\boldsymbol{\lambda}_{\mathrm{nf}}\,\mathrm{grad}\,\tilde{\mu}_{\mathrm{nf}} = -\rho_{\mathrm{f}}\boldsymbol{\lambda}_{\mathrm{nf}}\frac{\partial\tilde{\mu}_{\mathrm{nf}}}{\partial c_{\mathrm{nf}}}\,\mathrm{grad}\,c_{\mathrm{nf}}. \tag{4.13}$$

Finally, upon introducing the diffusivity tensor [141, 143],

$$\mathbf{d}_{\mathrm{nf}} := \boldsymbol{\lambda}_{\mathrm{nf}} \frac{\partial \tilde{\mu}_{\mathrm{nf}}}{\partial c_{\mathrm{nf}}}, \tag{4.14}$$

we end up with the well-known expression

$$\mathbf{y}_{\mathrm{nf}} = -\rho_{\mathrm{f}} \mathbf{d}_{\mathrm{nf}} \operatorname{grad} c_{\mathrm{nf}}. \tag{4.15}$$

If, for example, we prescribe $\tilde{\mu}_{\mathrm{nf}}$ (cf. [168], Chapter 6, page 234) as

$$\begin{aligned} \tilde{\mu}_{\mathrm{nf}}(c_{\mathrm{nf}}) =& \frac{RT}{M_{\mathrm{n}}} \log \left(\frac{M_{\mathrm{w}} c_{\mathrm{nf}}}{M_{\mathrm{n}}[1 - c_{\mathrm{nf}}] + M_{\mathrm{w}} c_{\mathrm{nf}}} \right) \\ & - \frac{RT}{M_{\mathrm{w}}} \log \left(\frac{M_{\mathrm{n}}[1 - c_{\mathrm{nf}}]}{M_{\mathrm{n}}[1 - c_{\mathrm{nf}}] + M_{\mathrm{w}} c_{\mathrm{nf}}} \right), \end{aligned} \tag{4.16}$$

where M_{n} and M_{w} are the molar masses of the nutrients and water, respectively, R is the gas constant, and T is the absolute temperature (regarded as a constant in the present framework), we obtain

$$\mathbf{d}_{\mathrm{nf}} = \boldsymbol{\lambda}_{\mathrm{nf}} \frac{\partial \tilde{\mu}_{\mathrm{nf}}}{\partial c_{\mathrm{nf}}} = \boldsymbol{\lambda}_{\mathrm{nf}} \frac{RT/[c_{\mathrm{nf}}(1 - c_{\mathrm{nf}})]}{M_{\mathrm{n}}[1 - c_{\mathrm{nf}}] + M_{\mathrm{w}} c_{\mathrm{nf}}}. \tag{4.17}$$

Since the mobility tensor has to vanish for $c_{\mathrm{nf}} = 0$ and $c_{\mathrm{nf}} = 1$, i.e., in the absence of nutrients and when the nutrients are the only fluid constituent, respectively, one can choose $\boldsymbol{\lambda}_{\mathrm{nf}} = c_{\mathrm{nf}}(1 - c_{\mathrm{nf}}) \boldsymbol{\lambda}^0_{\mathrm{nf}}$, which allows to recast (4.17) in the form

$$\mathbf{d}_{\mathrm{nf}} = \boldsymbol{\lambda}^0_{\mathrm{nf}} \frac{RT}{M_{\mathrm{n}}[1 - c_{\mathrm{nf}}] + M_{\mathrm{w}} c_{\mathrm{nf}}}. \tag{4.18}$$

If the mass fraction c_{nf} is so low that the diffusivity tensor, $\mathbf{d}_{\mathrm{nf}}$, can be taken to be independent of c_{nf}, one can replace (4.18) with

$$\mathbf{d}_{\mathrm{nf}} = \boldsymbol{\lambda}^0_{\mathrm{nf}} \frac{RT}{M_{\mathrm{n}}}. \tag{4.19}$$

This amounts to approximate (4.18) with its zeroth order approximation, obtained for $c_{\mathrm{nf}} = 0$. Since, in the present framework, the term RT/M_{n} features only constants, it can be absorbed in the coefficients defining $\boldsymbol{\lambda}^0_{\mathrm{nf}}$. Hence, the mass flux vector $\mathbf{y}_{\mathrm{nf}}$ is entirely determined by the diffusivity tensor, $\mathbf{d}_{\mathrm{nf}}$, which should be supplied experimentally, and consistently with the theorem of representation for tensor-valued functions (see [25] and references therein).

By adhering to the classification done in [25], which addresses the permeability tensor in fibre-reinforced media undergoing finite deformations, and adapting it to

our study for the case of a transversely isotropic material, we represent $\mathbf{d}_{\mathrm{nf}}$ as (cf. Equation (30) of [25])

$$\begin{aligned}\mathbf{d}_{\mathrm{nf}} &= d_0\,\mathbf{g}^{-1} + d_{1\mathrm{t}}\mathbf{b}_{\mathrm{e}} + 2d_{2\mathrm{t}}\mathbf{b}_{\mathrm{e}}.\mathbf{b}_{\mathrm{e}} \\ &\quad + (d_{1\mathrm{a}} - d_{1\mathrm{t}})\,\mathbf{m}\otimes\mathbf{m} + (d_{2\mathrm{a}} - d_{2\mathrm{t}})\,[(\mathbf{m}\otimes\mathbf{m}).\mathbf{b}_{\mathrm{e}} + \mathbf{b}_{\mathrm{e}}.(\mathbf{m}\otimes\mathbf{m})]\,. \end{aligned} \tag{4.20}$$

Equation (4.20) is the most general representation of a function valued in the space of second-order tensors with transverse isotropy with respect to the direction identified by the spatial vector $\mathbf{m}$. In (4.20), $\mathbf{b}_{\mathrm{e}} := \mathbf{F}_{\mathrm{e}}.\mathbf{F}_{\mathrm{e}}^{\mathrm{T}}$ is the left Cauchy-Green stretch tensor generated by the elastic distortions, and the dot "." is an abbreviation for the metric tensor, $\mathbf{g}$, or for its inverse, $\mathbf{g}^{-1}$, i.e., $\mathbf{b}_{\mathrm{e}}.\mathbf{b}_{\mathrm{e}} \equiv \mathbf{b}_{\mathrm{e}}\mathbf{g}\,\mathbf{b}_{\mathrm{e}}$, and $(\mathbf{m}\otimes\mathbf{m}).\mathbf{b}_{\mathrm{e}} \equiv (\mathbf{m}\otimes\mathbf{m})\mathbf{g}\mathbf{b}_{\mathrm{e}}$. Moreover, the coefficients d_0, $d_{1\mathrm{t}}$, $d_{1\mathrm{a}}$, $d_{2\mathrm{a}}$, and $d_{2\mathrm{t}}$ are scalar functions of the invariants $I_{1\mathrm{e}}$, $I_{2\mathrm{e}}$, $I_{3\mathrm{e}}$, $I_{4\mathrm{e}}$, and $I_{5\mathrm{e}}$, defined as follows

$$I_{1\mathrm{e}} = \mathrm{tr}(\mathbf{b}_{\mathrm{e}}), \tag{4.21a}$$

$$I_{2\mathrm{e}} = \tfrac{1}{2}\left\{I_{1\mathrm{e}}^2 - \mathrm{tr}(\mathbf{b}_{\mathrm{e}}.\mathbf{b}_{\mathrm{e}})\right\}, \tag{4.21b}$$

$$I_{3\mathrm{e}} = \det(\mathbf{b}_{\mathrm{e}}), \tag{4.21c}$$

$$I_{4\mathrm{e}} = [\mathbf{b}_{\mathrm{e}}^{-1} : (\mathbf{m}\otimes\mathbf{m})]^{-1} = \mathbf{C}_{\mathrm{e}} : (\boldsymbol{\nu}\otimes\boldsymbol{\nu}), \tag{4.21d}$$

$$I_{5\mathrm{e}} = \frac{\mathbf{b}_{\mathrm{e}} : (\mathbf{g}\,\overline{\otimes}\,\mathbf{g}) : \mathbf{m}\otimes\mathbf{m}}{\mathbf{b}_{\mathrm{e}}^{-1} : (\mathbf{m}\otimes\mathbf{m})} = \mathbf{C}_{\mathrm{e}}^2 : (\boldsymbol{\nu}\otimes\boldsymbol{\nu}). \tag{4.21e}$$

In (4.21d) and (4.21e), $\boldsymbol{\nu}$ is the unit vector specifying the direction of the fibre in the natural state, and is related to $\mathbf{m}$ through the normalised pull-back and push-forward operations

$$\boldsymbol{\nu} = \frac{\mathbf{F}_{\mathrm{e}}^{-1}\mathbf{m}}{\|\mathbf{F}_{\mathrm{e}}^{-1}\mathbf{m}\|}, \quad \mathbf{m} = \frac{\mathbf{F}_{\mathrm{e}}\boldsymbol{\nu}}{\|\mathbf{F}_{\mathrm{e}}\boldsymbol{\nu}\|}. \tag{4.22}$$

Moreover, in (4.21e), the fourth-order tensor $\mathbf{g}\,\overline{\otimes}\,\mathbf{g}$ is defined as

$$\mathbf{g}\,\overline{\otimes}\,\mathbf{g} := \tfrac{1}{2}[\mathbf{g}\,\underline{\otimes}\,\mathbf{g} + \mathbf{g}\,\overline{\otimes}\,\mathbf{g}], \tag{4.23}$$

and maps symmetric second-order tensors with contravariant components into symmetric second-order tensors with covariant components (see [107]).

Going back to the scalar coefficients of $\mathbf{d}_{\mathrm{nf}}$, we notice that, while d_0 accounts for the purely spherical part of the diffusivity tensor (in the jargon of [25], the term $d_0\mathbf{g}^{-1}$ is said to be *"unconditionally isotropic"*), the sets of coefficients $\{d_{1\mathrm{a}}, d_{2\mathrm{a}}\}$ and $\{d_{1\mathrm{t}}, d_{2\mathrm{t}}\}$ determine the axial and the transversal diffusivities of $\mathbf{d}_{\mathrm{nf}}$, respectively.

A final remark about (4.20) concerns the fact that the elastic Cauchy-Green stretch tensor $\mathbf{b}_{\mathrm{e}}$, rather than $\mathbf{b}$, is employed to construct $\mathbf{d}_{\mathrm{nf}}$: one reason for doing so is that the use of $\mathbf{b}_{\mathrm{e}}$ clearly identifies how the structural reorganisation of the tissue, described by the remodelling tensor $\mathbf{F}_{\mathrm{p}}$, influences the evolution of $\mathbf{d}_{\mathrm{nf}}$. This

becomes evident by performing the backward Piola transformation of $\mathbf{d}_{\mathrm{nf}}$. Indeed, by virtue of the identity $\mathbf{b}_{\mathrm{e}} = \mathbf{F}\mathbf{B}_{\mathrm{g}}\mathbf{F}^{\mathrm{T}}$, with $\mathbf{B}_{\mathrm{g}} := \mathbf{F}_{\mathrm{p}}^{-1}.\mathbf{F}_{\mathrm{p}}^{-\mathrm{T}}$, we obtain

$$\begin{aligned}\mathbf{D}_{\mathrm{nf}} &= J\,\mathbf{F}^{-1}\mathbf{d}_{\mathrm{nf}}\mathbf{F}^{-\mathrm{T}}\\ &= Jd_0\mathbf{C}^{-1} + J\,d_{1\mathrm{t}}\mathbf{B}_{\mathrm{g}} + 2Jd_{2\mathrm{t}}\mathbf{B}_{\mathrm{g}}\mathbf{C}\mathbf{B}_{\mathrm{g}}\\ &+ J\frac{d_{1\mathrm{a}} - d_{1\mathrm{t}}}{I_4}\mathbf{M}\otimes\mathbf{M} + 2J\frac{d_{2\mathrm{a}} - d_{2\mathrm{t}}}{I_4}\mathrm{sym}[\mathbf{B}_{\mathrm{g}}\mathbf{C}(\mathbf{M}\otimes\mathbf{M})],\end{aligned} \tag{4.24}$$

where $I_4 := \mathbf{C} : (\mathbf{M}\otimes\mathbf{M})$ is the fourth invariant of the Cauchy-Green deformation tensor, $\mathbf{C}$, and $\mathbf{M} = \mathbf{F}_{\mathrm{p}}^{-1}\boldsymbol{\nu}/\|\mathbf{F}_{\mathrm{p}}^{-1}\boldsymbol{\nu}\|$ is the normalised pull-back of $\boldsymbol{\nu}$ to the tangent space associated with the medium's reference configuration. From (4.24) it descends that remodelling has a direct impact on the evolution of both the isotropic and the anisotropic part of the diffusion tensor. To complete the picture, we need to prescribe constitutive laws for the diffusivities $\{d_0, d_{1\mathrm{a}}, d_{1\mathrm{t}}, d_{2\mathrm{a}}, d_{2\mathrm{t}}\}$. For this purpose, we follow the suggestions given in [25] for the permeability coefficients, and we adapt them to our framework in order to include remodelling. Hence, we set

$$d_0 = d_{0\nu}\left[\frac{J_{\mathrm{e}} - \Phi_{\mathrm{s}\nu}}{1-\Phi_{\mathrm{s}\nu}}\right]^{\kappa_0}\exp\left(\tfrac{1}{2}m_0[J_{\mathrm{e}}^2 - 1]\right), \tag{4.25a}$$

$$d_{1\mathrm{a}} = \frac{d_{1\mathrm{a}\nu}}{J_{\mathrm{e}}^2}\left[\frac{J_{\mathrm{e}} - \Phi_{\mathrm{s}\nu}}{1-\Phi_{\mathrm{s}\nu}}\right]^{\kappa_{1\mathrm{a}}}\exp\left(\tfrac{1}{2}m_{1\mathrm{a}}[J_{\mathrm{e}}^2 - 1]\right), \tag{4.25b}$$

$$d_{1\mathrm{t}} = \frac{d_{1\mathrm{t}\nu}}{J_{\mathrm{e}}^2}\left[\frac{J_{\mathrm{e}} - \Phi_{\mathrm{s}\nu}}{1-\Phi_{\mathrm{s}\nu}}\right]^{\kappa_{1\mathrm{t}}}\exp\left(\tfrac{1}{2}m_{1\mathrm{t}}[J_{\mathrm{e}}^2 - 1]\right), \tag{4.25c}$$

$$d_{2\mathrm{a}} = \frac{d_{2\mathrm{a}\nu}}{2J_{\mathrm{e}}^4}\left[\frac{J_{\mathrm{e}} - \Phi_{\mathrm{s}\nu}}{1-\Phi_{\mathrm{s}\nu}}\right]^{\kappa_{2\mathrm{a}}}\exp\left(\tfrac{1}{2}m_{2\mathrm{a}}[J_{\mathrm{e}}^2 - 1]\right), \tag{4.25d}$$

$$d_{2\mathrm{t}} = \frac{d_{2\mathrm{t}\nu}}{2J_{\mathrm{e}}^4}\left[\frac{J_{\mathrm{e}} - \Phi_{\mathrm{s}\nu}}{1-\Phi_{\mathrm{s}\nu}}\right]^{\kappa_{2\mathrm{t}}}\exp\left(\tfrac{1}{2}m_{2\mathrm{t}}[J_{\mathrm{e}}^2 - 1]\right), \tag{4.25e}$$

where, as stated above, $\Phi_{\mathrm{s}\nu}$ is the volumetric fraction of the solid phase in the natural state, and the contribution of remodelling is accounted for by the determinant $J_{\mathrm{e}} = J/J_{\mathrm{g}}$, even though we have set $J_{\mathrm{g}} = 1$ in the present study.

According to the definitions (4.25a)–(4.25e), fifteen parameters have to be assigned. These are given by the reference values $d_{0\nu}$, $d_{1\mathrm{a}\nu}$, $d_{1\mathrm{t}\nu}$, $d_{2\mathrm{a}\nu}$, and $d_{2\mathrm{t}\nu}$; the exponents κ_0, $\kappa_{1\mathrm{a}}$, $\kappa_{1\mathrm{t}}$, $\kappa_{2\mathrm{a}}$, and $\kappa_{2\mathrm{t}}$; and the factors m_0, $m_{1\mathrm{a}}$, $m_{1\mathrm{t}}$, $m_{2\mathrm{a}}$, and $m_{2\mathrm{t}}$. For ease of notation, in the sequel these three sets of parameters shall be referred to as d-coefficients, κ-exponents, and m-factors, respectively.

We notice that the d-coefficients must be all non-negative, as they represent the values of the diffusivities in the natural state, i.e., when the condition $J_{\mathrm{e}} = 1$ applies *identically*. This condition, in fact, does not amount, here, to invoke the constraint of isochoric elastic distortions, although such constraint would actually

compel the scalar diffusivities (4.25a)–(4.25e) to be equal to their corresponding reference values, for all admissible $\mathbf{F}_{\mathrm{e}}$.

Since the κ-exponents are generally taken as positive real-valued functions (see e.g. the experimental values presented in [149] for permeability), the fraction

$$\frac{J_{\mathrm{e}} - \Phi_{\mathrm{s}\nu}}{1 - \Phi_{\mathrm{s}\nu}} \tag{4.26}$$

has to be non-negative in order for the scalar diffusivities to be well-defined. If $\Phi_{\mathrm{s}\nu}$ is assumed to be always strictly positive (indeed, the case $\Phi_{\mathrm{s}\nu} = 0$ means that the solid phase is locally absent in the tissue), this condition is met for $\Phi_{\mathrm{s}\nu} < 1$ and, simultaneously, for $\Phi_{\mathrm{s}\nu} \leq J_{\mathrm{e}}$. The first restriction is a natural consequence of the saturation constraint, whereas the second restriction places a lower bound on the elastic distortions: at compression, J_{e} cannot be made arbitrarily small [109].

The permeability tensor, $\mathbf{k}$, is defined analogously to $\mathbf{d}_{\mathrm{nf}}$, and can thus be obtained from (4.20) by replacing the scalar diffusivities d_0, $d_{1\mathrm{a}}$, $d_{1\mathrm{t}}$, $d_{2\mathrm{a}}$, and $d_{2\mathrm{t}}$ with the corresponding scalar permeabilities k_0, $k_{1\mathrm{a}}$, $k_{1\mathrm{t}}$, $k_{2\mathrm{a}}$, and $k_{2\mathrm{t}}$ (see [25]). These, in turn, have the same functional form as the diffusivities given in (4.25a)–(4.25e), and only require the assignment of suitable model parameters of the same type as the d-coefficients, κ-exponents, and m-factors introduced above [25]. The material form of the permeability tensor is determined via the backward Piola transformation of $\mathbf{k}$, i.e., $\mathbf{K} = J\mathbf{F}^{-1}\mathbf{k}\mathbf{F}^{-\mathrm{T}}$, which yields an expression similar to (4.24) for $\mathbf{D}_{\mathrm{nf}}$.

By adapting the results reported in [110, 111] to the diffusivity tensor in (4.24), one may infer that the transversal diffusivities are smaller than the axial ones. This assumption leads to significant simplifications to the expression of $\mathbf{D}_{\mathrm{nf}}$, and, therefore, can be very helpful to reduce the complexity of a mathematical model. However, it leads unavoidably to a weakening of the coupling between diffusion and remodelling, and reduces the role played by remodelling on the evolution of the tissue's anisotropy.

4.4 An Outlook on Some Possible Research Problems

Pulled back to the reference configuration of the tissue, Equation (4.2a) becomes

$$(J - \Phi_{\mathrm{s}\nu})\rho_{\mathrm{f}}\dot{c}_{\mathrm{nf}} + \rho_{\mathrm{f}}(\mathrm{Grad}\, c_{\mathrm{nf}})\mathbf{Q} + \mathrm{Div}\mathbf{Y}_{\mathrm{nf}} = 0, \tag{4.27}$$

where $\dot{c}_{\mathrm{nf}}$ is the material derivative of c_{nf}, evaluated with respect to the solid phase velocity, Grad and Div are the "material" gradient and divergence operators, while $\mathbf{Q} = J\mathbf{F}^{-1}\mathbf{q}$ and $\mathbf{Y}_{\mathrm{nf}} = J\mathbf{F}^{-1}\mathbf{y}_{\mathrm{nf}}$ are the Piola transformed filtration velocity and

nutrient mass flux vector, respectively. In terms of the standard Darcy and Fick's laws, these two quantities read

$$\mathbf{Q} = -\mathbf{K}\mathrm{Grad}\, p, \quad \mathbf{Y}_{\mathrm{nf}} = -\rho_{\mathrm{f}}\mathbf{D}_{\mathrm{nf}}\,\mathrm{Grad} c_{\mathrm{nf}}, \tag{4.28}$$

where $\mathbf{K}$ and $\mathbf{D}_{\mathrm{nf}}$ are defined in Section 4.3 (see, in particular, (4.24) for $\mathbf{D}_{\mathrm{nf}}$).

In this section, we would like to report some generalisations of $(4.28)_2$ to the case of non-Fickean diffusion. Our purpose is to draw attention on diffusion processes that involve the non-local response of $\mathbf{Y}_{\mathrm{nf}}$ to the gradient of the mass fraction $\mathrm{Grad}\, c_{\mathrm{nf}}$, as well as the non-locality of $\mathrm{Grad}\, c_{\mathrm{nf}}$ in terms of orientations. To accomplish this task, we use non-local approaches of fractional type. Before going into the proposed generalisations, we ought to say that, although the literature on Fractional Calculus is very vast and keeps growing (see e.g. [224, 88, 19, 61, 281, 21, 22], and the references therein, to mention just a few), we are not aware, to date, of stringent evidences that call for the necessary fractionalisation of the diffusion processes at the basis of the transport of nutrients in remodelling tissues. Yet, we feel that it could be important to start paving the way towards the inclusion of fractional models into the standard framework of growth and remodelling. Indeed, beyond mere scientific curiosity, there is the interest for understanding how non-local effects influence the overall response of tissues that grow in pathological conditions or for improving our comprehension of the interplay between diffusion and the reorientation of the fibres.

An alternative fractionalisation of diffusion can be obtained by assuming that the mass flux vector of the nutrients is related to the *fractional gradient* of the mass fraction, c_{nf}. Note that, to lighten the notation, in the sequel we drop the subscripts "nf", as it is clear that we are referring to the nutrients in the fluid phase. Hence, by defining the fractional gradient of order $\gamma \in \mathbb{R}$, $0 < \gamma < 1$, of the field c as [195]

$$\mathrm{grad}^{\gamma}_{\mu}\, c(x,t) \equiv \int_{\mathbb{S}^2_x\mathscr{S}} \mathbf{m}[D^{\gamma}_{\mathbf{m}} c(x,t)]\mathrm{d}\mu(\mathbf{m}), \tag{4.29}$$

we require that the mass flux vector of the nutrients in the fluid phase is given by

$$\mathbf{y}^{\gamma}_{\mu} = -\rho_{\mathrm{f}}\bar{\mathbf{d}}\mathrm{grad}^{\gamma}_{\mu}\, c. \tag{4.30}$$

Analogously to what has been said above, $\bar{\mathbf{d}}$ is formally equal to the diffusivity tensor introduced in (4.20), but its physical units have to be adjusted in order to account for the fractional gradient of c.

In (4.29), $\mathbf{m}$ is a unit vector attached to the spatial point $x \in \mathscr{S}$, with $\mathscr{S}$ being the three-dimensional Euclidean space, $\mathbb{S}^2_x\mathscr{S}$ is the set of all the unit vectors emanating from x (it is a vector manifold contained in the tangent space $T_x\mathscr{S}$), $\mu(\,\cdot\,)$ is a *"positive finite measure"* on $\mathbb{S}^2_x\mathscr{S}$ [195], and $D^{\gamma}_{\mathbf{m}} c(x,t)$ is the *fractional directional derivative* of order γ of the field c along the direction $\mathbf{m}$, evaluated at $x \in \mathscr{S}$ and time t. The definition of $D^{\gamma}_{\mathbf{m}} c(x,t)$ is obtained in two steps. First,

we introduce the Fourier transform of c, suitably prolonged over all the three-dimensional Euclidean space, $\mathscr{S}$, i.e.,

$$\hat{c}(\boldsymbol{\xi}, t) = \int_{\mathscr{S}} \mathrm{e}^{-\mathrm{i}\boldsymbol{\xi}[x-x_0]} c(x,t) \mathrm{d}v(x), \tag{4.31}$$

where x_0 is a point of $\mathscr{S}$ chosen as origin. Then, for a given $\mathbf{m} \in \mathbb{S}^2_x\mathscr{S}$, we consider the quantity $[\mathrm{i}\boldsymbol{\xi}\mathbf{m}]^\gamma \hat{c}(\boldsymbol{\xi}, t)$, and we identify $D^\gamma_{\mathbf{m}} c(x,t)$ with the inverse Fourier transform of $[\mathrm{i}\boldsymbol{\xi}\mathbf{m}]^\gamma \hat{c}(\boldsymbol{\xi}, t)$, i.e.,

$$D^\gamma_{\mathbf{m}} c(x,t) = \frac{1}{(2\pi)^3} \int_{\mathscr{K}} \mathrm{e}^{\mathrm{i}\boldsymbol{\xi}[x-x_0]} [\mathrm{i}\boldsymbol{\xi}\mathbf{m}]^\gamma \hat{c}(\boldsymbol{\xi}, t) \mathrm{d}v(\boldsymbol{\xi}), \tag{4.32}$$

where $\mathscr{K}$ is the Fourier space (in fact, isomorphic to $\mathbb{R}^3$).

For our purposes, it suffices to take the measure $\mu(\mathbf{m})$ in such a way that the integral on the right-hand-side of (4.29) can be rewritten as a surface integral, evaluated on the spherical surface enveloping $\mathbb{S}^2_x\mathscr{S}$. Hence, Equation (4.29) becomes

$$\mathrm{grad}^\gamma_\mu \, c(x,t) \equiv \int_0^{2\pi} \int_0^{\pi} \hat{\mathbf{m}}(\vartheta, \varphi) [D^\gamma_{\hat{\mathbf{m}}(\vartheta,\varphi)} c(x,t)] |\sin(\vartheta)| \mathrm{d}\vartheta \mathrm{d}\varphi, \tag{4.33}$$

where $(\vartheta, \varphi) \in [0, \pi] \times [0, 2\pi[$ is a system of spherical coordinates, and $\hat{\mathbf{m}}(\vartheta, \varphi)$ is the parametric representation of $\mathbf{m}$.

Conclusions to Part I

The content reported in this chapter has been previously published in [131, 220, 235].

The scope of this part was to investigate the influence of non-local phenomena on the growth and remodelling of biological tissues, with special focus on the evolution of an avascular tumour tissue.

In particular, in Chapter 2, we study an idealised biological tissue that grows and remodels. As tissue we consider a tumour in avascular stage, and we assume that its remodelling —or structural reorganisation— occurs through a two-scale plasticity-like phenomenon. Following [14], we distinguish a coarse and a fine scale, and we resolve this phenomenon, at the coarse scale, by means of the accumulated remodelling strain, ε_{p}, and, at the fine scale, by means of $\mathfrak{e}_{\mathrm{p}}$. The latter is the representative of the so-called *micro-"plasticity"* and, being related to ε_{p} through a Helmholtz-like equation, it makes ε_{p} non-local [14]. Within this framework, we have set ourselves the scope of evaluating if, how, and to what extent the micro-"plasticity" influences the growth of the tumour. In our approach, such influence can occur both directly and indirectly. The direct way is due to the fact that the *effective* Cauchy stress, $\boldsymbol{\sigma}_{\mathrm{eff}}$, modulates the source of mass R_{fp}, and thus also R_{s}, by giving rise to mechanotransduction. The indirect way, instead, manifests itself through the slight, and to a certain extent visible, changes that the non-local plastic-like distortions induce in some of the physical quantities that characterise the growth of the tumour, as reported in Section 2.7.

It is important to emphasise that the results shown in this work (see Figures 2.2–2.5) are obtained for numerical values of the "non-standard" parameters A_ν, B_ν, and Z_ν (see Table 2.2), which could be far beyond the physical range. Therefore, for the time being, our results aim at being a qualitative contribution to a unified strain-gradient theory of growth and remodelling. However, they are quantitative in evaluating the impact of the considered theory on growth.

We remark that, following an idea put forward by Epstein [98], Di Stefano et al. [91] proposed a model of strain-gradient growth, in which the evolution of γ is governed by a generalised diffusion-reaction equation. Such equation was

obtained by accounting for the growth-induced scalar curvature, ${\kappa_\gamma}^2$, which features the spatial derivatives of γ up to the second order. However, in that model we considered no remodelling. In the present work, instead, we have neglected the role of κ_γ, but we have focussed our attention on strain-gradient remodelling in order to quantify its effect on growth. The role of κ_γ in the current framework can be recovered by simply re-activating $r_{\mathrm{p}\gamma}$ and $r_{\mathrm{n}\gamma}$ in (2.2a) and (2.2b) (see Di Stefano et al.[91] for the definition of these terms as functions of κ_γ).

Apart from the obvious fact that the topics under study necessitate further investigations from our side, two comments are in order: firstly, we have not hypothesised a strain-softening behaviour of the considered material, and no formation of shear bands can be observed that justifies from the outset the use of a strain-gradient regularisation; secondly, the benchmark problem adopted in this work might be inappropriate, since it does not produce the desired/expected localisation of the accumulated plastic strain, ε_{p}, which calls for the employment of a strain-gradient theory. Nevertheless, our model is able to capture the regularising effect that the microscale descriptor $\mathfrak{e}_{\mathrm{p}}$ has on the accumulated remodelling distortions (cf. Figure 2.6).

It is known that the internal structural changes occurring in heterogeneous materials influence their overall macroscopic behaviour. For example, in bones, the change of orientation of the lamellae's collagen fibres modifies the bone's longitudinal effective Young's modulus [270, 240]. In the present work, we attempt to know how, and to what extent, the microscopic plastic-like (remodelling) effects are significant for the macroscopic evolution of the tissue. To the best of our knowledge, there are no experimental studies showing the influence of the microscopic plastic effects on the tissue behaviour. However, one can think of an experiment where, at some level, there can be a relatively strong localisation of the accumulated "plastic" strain, $\mathfrak{e}_{\mathrm{p}}$, because of the presence of constraints (e.g. contact of the tissue with much stiffer materials). In this respect, we hope that our work contributes to understand the interactions between growth and remodelling by merging the theories of multiphasic materials and of strain-gradient plasticity.

To the best of our understanding, another important difference between our work and previous publications (see e.g. [70, 68, 67]) resides in the definition of the internal and external mechanical powers. Indeed, looking for instance at [68], these powers feature only the generalised velocities associated with the "classical" degrees of freedom of a body[3], while the time derivatives of the tensors associated with the

[2]The growth distortions, $\boldsymbol{F}_\gamma = \gamma \boldsymbol{I}$, induce the Riemannian metric tensor $\boldsymbol{C}_\gamma = \gamma^2 \boldsymbol{G}$, which yields Christoffel symbols that allow to determine a Levi-Civita connection with nontrivial fourth-order curvature tensor [190, 126] and, thus, with nontrivial associated Ricci curvature tensor, $\mathfrak{R}_\gamma$. Hence, it is possible to define the scalar curvature as $\kappa_\gamma := \mathfrak{R}_\gamma : \boldsymbol{C}_\gamma^{-1}$ (see [91] for details).

[3]These are the body velocity, $\boldsymbol{V}$, the time derivative of the deformation gradient tensor, $\dot{\boldsymbol{F}}$, and the time derivative of the second gradient of the deformation, i.e., $\overline{\mathrm{Grad}\boldsymbol{F}}$[68].

body's structural changes appear in the study of the dissipation inequality through the derivative of the body's Helmholtz free energy density. In our case, instead, following a philosophy outlined in other papers [133, 60, 86, 135, 14], we introduce the structural kinematic descriptors both constitutively, i.e., as arguments of the solid phase Helmholtz free energy density, and in the formulation of the overall virtual powers of the problem, that is, jointly with the "classical" ones.

In our work, the tensor $\tilde{\boldsymbol{\Sigma}}_\nu$ is entirely determined by mechanical quantities (cf. Equation (2.38a)) and this property is inherited by its associated direction tensor, $\boldsymbol{N}_\nu = \tilde{\boldsymbol{\Sigma}}_\nu / \|\tilde{\boldsymbol{\Sigma}}_\nu\|_{\boldsymbol{\eta}}$. Consequently, the hypothesis of co-directionality of $\tilde{\boldsymbol{D}}_\mathrm{p}$ and $\tilde{\boldsymbol{\Sigma}}_\nu$ implies that the direction of the plastic flow is exclusively dictated by mechanical stress, the latter being augmented by the non-standard contribution $\tilde{\boldsymbol{\Sigma}}_\nu^{(\text{n-st})}$. However, in more general situations, it is possible to define generalised Mandel stress tensors featuring bio-chemical contributions, i.e., depending explicitly on the mass fraction of the nutrients (and on its gradient). In such cases, tensor $\boldsymbol{N}_\nu$ defines the direction of the plastic flow on the basis of chemo-mechanical guidance.

A last comment is on the design of an adequate benchmark problem. Indeed, when Anand et al. [14] developed their theory, they wrote that $\mathfrak{e}_\mathrm{p}$ *"is introduced for the purpose of regularisation of numerical simulations of shear band formation under strain softening conditions"*. To achieve this objective, they called for the concept of micro-scale plasticity, and admitted a physics described by ε_p, $\mathfrak{e}_\mathrm{p}$, and $\mathrm{Grad}\mathfrak{e}_\mathrm{p}$. Then, in order to determine these quantities, they established a thermodynamically consistent framework, rather than simply improving the equations that were problematic from the numerical point of view. In our work, we have extended such thermodynamic set-up to a growth problem, by admitting that its physical meaning goes beyond the necessity of solving numerical issues. Nevertheless, we have seen only a very marginal impact of this modelling choice on our results and we argue that it is of fundamental importance to design benchmark problems capable of capturing the physics behind it. This is part of our ongoing research.

Furthermore, in Chapter 3, we study the influence of a given type of non-local diffusion of nutrients on the growth of an avascular tumour. For this purpose, we generalise Fick's law of diffusion by introducing a non-local constitutive relationship for the mass flux vector that, after some considerations, can be identified with a fractional derivative of the nutrients' mass fraction. We call attention to the fact that, since we are dealing with growth, we need to describe how the non-locality of the prescribed constitutive law evolves with the deformation and the growth-induced inelastic distortions that accompany the evolution of the system under study. This consideration implies that the non-locality of the presumed constitutive response should be subordinate to the motion χ (see Equation (3.22b)) and, thus, that it cannot depend explicitly on the difference $X - \tilde{X}$ between the reference placements of the material points embedded in X and $\tilde{X}$. Furthermore,

we note that, as prescribed by Equation (3.25), the non-local character of the mass flux vector also depends on the structural changes of the tumour through the determinant of $\boldsymbol{F}_\gamma$. To the best of our understanding, the above considerations imply substantial differences between our work and other papers on the subject found in the scientific literature. Moreover, we suggest a formulation of non-local diffusion on manifolds (see Appendix A1).

To investigate the influence of the non-local diffusion of the nutrients on the tumour evolution, we focused on a benchmark problem that allows, due to the enforced symmetries, the reduction of the original three-dimensional framework to a one-dimensional problem. This has an important impact on the selection of the non-locality function, $\hat{\mathfrak{f}}_\alpha$, which has to be able to capture how the geometrical symmetries of the problem affect the description of the non-locality. Particularly, in our analysis, we re-obtained the definition of one-dimensional fractional mass flux proposed in other works [215, 82].

In our work, the numerical solution of the set of equations defining the mathematical model is found by employing the FE method, which has been adapted for the solution of the fractional diffusion equation (3.26c). In particular, the obtained numerical results show that the non-local character of the nutrients' evolution has a considerable repercussion on the growth of the hypothetical tumour under study. Specifically, by varying the parameter $\alpha \in]0,1[$, the model is capable, in the limit cases, of generating situations of no diffusion or of restoring Fick's law. This conclusion evidences the relevance of embracing a fractional framework in our model, since it permits to "control", through the parameter α, the way in which the tumour grows. Finally, we discussed a possible way for defining another normalisation factor, termed $\hat{\mathcal{N}}(\alpha)$, involved in the definition of the mass flux vector, and we provided a comparison between the two approaches.

Certainly, our model can be further generalised and, in the following, we discuss some important issues that should be accounted for in forthcoming works. A first issue arises from the fact that, once the dimensionality and the symmetries of the problem at hand are specified, Equation (3.16) must be adapted accordingly. This implies that the non-locality function and the normalisation factors should be conceived in a symmetry- and dimensional-dependent fashion[4]. To find such relations is part of our ongoing research. Additionally, in our model, the information on the microscopic structure of the tumour is not explicitly taken into account and, thus, its contribution is neglected. As pointed out in the Introduction, the multi-scale and heterogeneous character of the environment in which diffusion takes place is one of the main factors influencing the occurrence of non-Fickean diffusion. Therefore,

[4]Similar problems are subject of investigations conducted by our group in conjunction with our colleague Prof. Dušan Zorica (Mathematical Institute, Serbian Academy of Arts and Sciences, Serbia) and started, from our side, during his visit at the *Politecnico di Torino* (Italy) in January 2020.

the adoption of mathematical techniques, such as the Asymptotic Homogenisation Method [72], could be capable of incorporating these features into a framework of tissue growth [237] and non-local diffusion.

We further remark that an aspect that is not contemplated in the current formulation of the model is that the chemical agents should be both in the fluid phase and in the solid phase, and not only in the fluid phase. One of the main drawbacks of this phenomenological consideration is that it is not possible to link the mass sources to the chemical potentials of the nutrients, nor is it possible to establish a sound and comprehensive thermodynamic framework accounting for interphase mass transfers as non-equilibrium processes. This implies that no information, or only a limited amount of information, can be extracted from the study of the dissipation inequality of the system (and this is not directly due to the fact that growth necessitates the consideration of processes, of cellular or molecular type, that could not be accounted for in the model). Therefore, under the circumstances of the present model, it is not possible to obtain Equation (3.16) from the study of the dissipation inequality, as it would be the case in the classical procedure that leads to Fick's law. In this respect, one of the technical difficulties that arise in our work is that we cannot invert the balance of linear momentum associated with the chemical agents, since the inversion of fractional operators is not always permitted. One possible solution, that seems to be thermodynamically acceptable, is to adopt a procedure similar to the one depicted in [137], that is, to consider the part of the dissipation inequality that is of interest for us, to put it in weak form and to express the flux in terms of a non-local constitutive law depending on the gradient of the chemical potential.

We would like to mention that in recent years Fractional Calculus has demonstrated to be an effective mathematical tool in the description of several phenomena. However, there is still an urgency in incorporating this notion in mathematical models that go beyond the classical ones.

Finally, in Chapter 4, we study how remodelling affects diffusion on a transversely isotropic tissue and propose some future developments of the research in this field.

We notice that the evaluation of the integral on the right-hand-side of (4.33) can be demanding in general, and that suitable numerical algorithms might be needed. A possible approach is the Spherical Design Algorithm [138], which is largely used in determining the overall elastic or flow properties of fibre-reinforced media with statistical distribution of fibres [108, 53].

The parameter γ, featuring in the fractional formula (4.30), can be naturally associated with characteristic length scales that cannot be resolved when standard diffusion is considered. In this respect, it represents an additional source of information on the tissue's material behaviour. A question that, at this stage,

could arise is whether this parameter can be related to the growth and remodelling of the tissue to which it is referred. Assume, indeed, that γ is influenced for instance by the accumulated inelastic strain $\varepsilon_{\mathrm{g}}(X,t) = \sqrt{(2/3)}\int_0^t \|\bar{\mathbf{D}}_{\mathrm{g}}(X,\tau)\|\mathrm{d}\tau$, where $\bar{\mathbf{D}}_{\mathrm{g}} = \mathrm{sym}(\mathbf{G}\bar{\mathbf{L}}_{\mathrm{g}})$ is the symmetric part of $\mathbf{G}\bar{\mathbf{L}}_{\mathrm{g}}$, and $\mathbf{G}$ is the material metric tensor field. Then, a feedback mechanism could be established that connects growth and remodelling with fractional diffusion. We believe that this topic could be of interest for a deeper understanding of these biological phenomena.

Part II

Non-local diffusion in two-scale materials of biological interest

Chapter 5

Non-local diffusion in biological tissues: Motivations for a two-scale study

The work reported in this chapter has been previously published in [140, 241].

Molecular diffusion is the process by which chemical species, e.g., solutes or macromolecules, move from regions of higher concentration to regions of lower concentration. Diffusion plays a vital role in cellular functions, such as protein-protein interactions and metabolism [271]. In porous connective tissues such as ligaments and cartilage, diffusion is one of the primary mechanisms for nutrient transport. For this reason it has been extensively studied in healthy and degraded tissues [188, 47, 275, 276, 171, 172]. Several techniques can be used for measuring self or molecular diffusivity (or diffusion coefficient in the isotropic case) of solutes in biological tissues: fluorescence correlation spectroscopy (c.f., [173]), single-particle tracking (c.f., [230]), and diffusion tensor MRI (c.f., [170, 177]). However, the most common method is Fluorescence Recovery After Photobleaching (FRAP), as it requires less instrumentation than the other approaches (e.g., confocal microscopes), and diffusivity can be directly quantified. In general, in a FRAP experiment, a tissue is stained with fluorescently labelled molecules, and a region of interest (ROI) is photobleached using a high intensity laser beam causing irreversible photochemical bleaching of the ROI. As a result, the fluorescence intensity detected by the microscope drops in the ROI. Due to the Brownian motion, the surrounding labelled molecules will eventually be transported into the ROI, restoring the intensity. By analysing the fluorescence recovery pattern over time, a direct measurement of diffusivity is obtained [30].

One important feature to take into consideration when investigating the motility of chemical species is the complex and heterogeneous environment in which it takes place. In this respect, the spatially heterogeneous and multiscale information that

is often present in biological tissues contributes to additional challenges in the conception of mathematical models. In particular, this multiscale information is often mathematically encoded in terms of non-local operators. For instance, in [63], it is shown that the dynamics of a hierarchical biological system can be represented by a non-local field at each level of organisation. In this study, the Author focused on the nervous system and expressed non-locality in terms of functional interactions. Besides, it shows that local phenomena occurring at a given structural level may not be local at the lower levels.

Usually, local constitutive laws are adopted in the modelling of heterogeneous media (or composite materials), thereby leading, in the majority of cases, to a homogenised local responses. However, in certain circumstances, this has conducted to discrepancies with experimental studies, where non-local constitutive equations may better depict the macroscopic behaviour of composite materials. For instance, according to the experiments performed in [166, 156, 113], the spatial complexity of a medium can impose geometrical constraints on transport processes on several length scales, which can alter the laws of standard diffusion in a non-local fashion, thereby yielding *non-Fickean diffusion* [166, 52, 81]. Furthermore, it is worth noticing that, although the response of the constituents of a composite is often taken to be of local type at the lowest scale, in some cases, non-locality in time or space may arise as a result of homogenisation processes [26, 121, 65], or even by the adoption of standard concepts of solid mechanics [258], without having recourse to homogenisation techniques. On the other hand, as shown in [46], viscoelasticity can be obtained from suitable upscaling of a fluid-structure interaction problem between an elastic medium and a Newtonian fluid.

To the best of our knowledge, there exist few works in which the constitutive laws of the constituents of composite media are assumed to be non-local already at the lower scales [264, 48]. For instance, in [48], the homogenised properties of thermoelastic composites are studied by considering non-local integral operators for the characterisation of the stress-strain constitutive relations. In [48], the Author motivates the need for this constitutive choice by relating it to the complicated internal structure of real materials with length scales ranging over many orders of magnitude, as is the case of hierarchical composite media [158].

Several types of non-locality can be accounted for. For instance, as mentioned in [220], one can introduce higher-order gradients or integro-differential relations in the constitutive laws [164, 104, 136, 18, 88, 17, 33]. Here, continuing the research lines initiated in [220], we exploit Fractional Calculus [56, 224, 21] and the asymptotic homogenisation technique [40, 250, 34, 72] to describe diffusion processes that may deviate from Fick's law because of possible non-local behaviours in space in a two-scale, composite medium. This modelling choice is motivated by the "success" of Fractional Calculus in addressing such phenomena [64, 195, 82, 200] and, in doing this, we have taken inspiration from the works [55, 251, 220].

We mention that the prediction of the overall behaviour of composite materials

in terms of their intrinsic micro-structure and properties of their constituents is the central focus of Homogenisation Theory. Among the different homogenisation techniques used in the modeling of multiscale composites, the scientific literature develops, in general, in two main approaches: the asymptotic homogenisation and the average field theory (see, e.g., the review paper of [150] and the references therein). On one hand, average field techniques [146, 207] aim to find the effective elastic properties that relate the fine-scale strain and stress averages over a representative volume, characterizing, in an ideal form, the heterogeneity of the material. On the other hand, the asymptotic homogenisation technique [34, 40, 72, 250, 27] exploits the scale separation among the characteristic lengths of the local structures and that of the whole material by employing multiple scale expansions of the unknown fields to obtain an effective description of the medium at its coarser scales

Chapter 6

Two-scale, non-local diffusion in homogenised heterogeneous media

The work reported in this chapter has been previously published in [241].

6.1 Introduction

In an effort to understand how and to what extent non-local diffusion may affect the overall evolution of a given chemical substance in a composite medium, we investigate the two-scale, non-local diffusion of a chemical species in a composite medium. For this purpose, we prescribe a two-scale, non-local constitutive law for the mass flux of the considered substance and consider the asymptotic homogenisation technique to determine the effective diffusivity and the macroscopic evolution of the species. In the modelling of multi-scale composites, homogenisation methods permit to decouple the structural characteristic length scales [146, 207, 6, 150, 202, 27], and in particular, the asymptotic homogenisation technique [40, 250, 34, 72] makes use of multiple scale expansions of the unknown fields to obtain an effective description of the medium at its coarser scales.

In particular, we end up with an effective characterisation of the composite that is subjected to the existence of non-local interactions at both the micro- and the macro-scale. Furthermore, we prove that if non-locality is neglected, we recover the classical results of homogenisation theory. As a result, the non-local effects at the micro-scale are *ciphered* in the effective diffusivity while, at the macro-scale, the homogenised problem features an integro-differential equation of fractional type. In particular, in the limit case in which the non-local interactions are neglected, classical results of asymptotic homogenisation theory are re-obtained.

This chapter is organised as follows: in Section 6.2, some aspects of the topology of the composite are discussed, and we introduce the multi-scale governing equations

describing the non-local diffusion of the chemical species. In Section 6.3, we consider the separation of scales between the macro- and the micro-scale, we illustrate the topology of the micro-structure, and discuss some aspects regarding periodicity in a two-scale context. Additionally, we reformulate the original governing equations to account for the two-scale nature of the non-local phenomena. Finally, in Section 6.4, the main mathematical tools of the asymptotic homogenisation technique are introduced, and we derive the effective properties and the homogenised equations for the composite under study.

6.2 Formulation of the problem

6.2.1 Topology of the composite

Let $\mathscr{B} =]0, L[$, with $L > 0$, be an open and bounded set of the one-dimensional Euclidean space, taken as the representation of a heterogeneous cylinder with periodic structure at the micro-scale, in which the heterogeneity is only along the axis of the cylinder. In particular, the open subsets $\mathscr{B}_1 = \cup_{i=0}^{N}]X_{2i}, X_{2i+1}[\subset \mathscr{B}$ and $\mathscr{B}_2 = \cup_{i=0}^{N}]X_{2i+1}, X_{2i+2}[\subset \mathscr{B}$ form the periodic structure of $\mathscr{B}$ and, for every i, each pair of intervals $]X_{2i}, X_{2i+1}[$ and $]X_{2i+1}, X_{2i+2}[$ represents two different constituents of the composite $\mathscr{B}$. Moreover, it holds that $\overline{\mathscr{B}} = \overline{\mathscr{B}}_1 \cup \overline{\mathscr{B}}_2$ and $\overline{\mathscr{B}}_1 \cap \mathscr{B}_2 = \mathscr{B}_1 \cap \overline{\mathscr{B}}_2 = \emptyset$, where the bar symbol indicates the closure of the set. In addition, we use the notation $\mathscr{I}$ to specify the interface separating the constituents $\mathscr{B}_1$ and $\mathscr{B}_2$, namely $\mathscr{I} = \overline{\mathscr{B}}_1 \cap \overline{\mathscr{B}}_2 = \cup_{i=0}^{N} \{X_{2i+1}\}$ (see Figure 6.1).

6.2.2 Diffusion of chemical species

The diffusion of a chemical species in the composite $\mathscr{B}$ is described by

$$\partial_t C(X,t) + \partial_X Q(X,t) = 0, \qquad \text{in } (\mathscr{B} \setminus \mathscr{I}) \times]0, t_\mathrm{f}[, \tag{6.1a}$$

$$[\![C(X_j,t)]\!] = 0, \qquad t \in]0, t_\mathrm{f}[, \tag{6.1b}$$

$$[\![Q(X_j,t)]\!] = 0, \qquad t \in]0, t_\mathrm{f}[, \tag{6.1c}$$

with $\{X_j = X_{2i+1}\}_{i=0}^{N} \subset \mathscr{I}$, together with suitable initial and boundary conditions. Note that for ease of exposition these conditions will be specified later, when the benchmark problems are presented.

Equations (6.1b) and (6.1c) describe the contact on $\mathscr{I}$, which in this case is assumed to be ideal, and the operator $[\![\Phi(X_j,t)]\!]$ denotes the jump of Φ across the interface $\mathscr{I}$, i.e.,

$$[\![\Phi(X_j,t)]\!] := \lim_{X \to X_j^-} \Phi(X,t) - \lim_{X \to X_j^+} \Phi(X,t), \quad X_j \in \mathscr{I}. \tag{6.2}$$

Moreover, Q denotes the mass flux of the chemical species and, as done in [220], we propose to express it in terms of the following non-local constitutive law,

$$Q(X,t) := -\int_{\mathscr{B}} D(X,\tilde{X})\partial_{\tilde{X}} C(\tilde{X},t)\mathrm{d}\tilde{X}, \tag{6.3a}$$

$$D(X,\tilde{X}) := \mathfrak{F}(X-\tilde{X})\mathfrak{D}(X,\tilde{X}), \tag{6.3b}$$

where $D(X,\tilde{X})$ is referred to as *non-local diffusivity*, and is written as the product of the scalar quantity $\mathfrak{F}(X-\tilde{X})$ and the *fractional diffusivity* $\mathfrak{D}(X,\tilde{X})$, both taken to be strictly positive. We emphasise that $\mathfrak{F}$ is defined for $X \neq \tilde{X}$, and that both D and $\mathfrak{D}$ have, in general, physical dimensions different from those of standard diffusivity, depending on the prescription of $\mathfrak{F}$. Additionally, C and Q are continuous in $\mathscr{B}$ which means that they are prolonged at the interfaces.

It is worth noticing that, further generalisations to the study of transport processes, involving for instance Darcy's law, can be found e.g. in [5]. This work, however, pursues goals different from ours, since it considers constitutive laws that relate the time fractional derivative of the mass flux with the time fractional derivative of the classical pressure gradient. On the other hand, a one-dimensional diffusion problem in a bounded homogeneous medium is studied in [252] wherein Darcy's equation is generalised with a fractional integral in space. Furthermore, in the context of hierarchical materials, such as bones and ligaments, a generalised viscoelastic approach has been proposed to describe their rheological properties by using fractional derivatives and integrals [85, 8], while numerical methods has been developed for the case of hereditary-ageing materials in [38]. Additionally, we notice that in [280] the analytical and numerical solution of a generalised heat conduction equation was studied by considering a fractional time derivative instead of the first order partial time derivative of the temperature. Moreover, in [20], the Authors considered a model in which, in addition to the fractional derivative in time, the heat conduction equation in a homogeneous material is extended by replacing the classical gradient of the temperature with its symmetrised Caputo fractional derivative. Finally, we point out that, in the context of viscoleastic composites, the Rabotnov exponential kernel [234], which is employed to construct a type of fractional derivative, have been considered in [243].

6.3 Multi-scale formulation of the problem

6.3.1 Separation of scales

In the characterisation of the two-scale nature of the composite, we assume the existence of two characteristic length scales, associated with the composite as a whole and its internal structure. Specifically, for our purposes, we denote by L_{c} and ℓ the characteristic length scales of the composite medium, and of its

internal structure, respectively. Moreover, we require that the considered length scales are well separated by enforcing that $\ell/L_\mathrm{c} \ll 1$. Therefore, we introduce the dimensionless, smallness parameter ε, referred to as the *scaling parameter*, which is defined as the ratio

$$\varepsilon := \frac{\ell}{L_\mathrm{c}} \ll 1. \tag{6.4}$$

We notice that ε characterises the heterogeneity of the composite, and permits to explicitly specify the two-scale nature of a given physical quantity $\Phi : \mathscr{B}\times[0,t_\mathrm{f}[\to \mathbb{R}$. In fact, following the discussion given in [219, 90], one can take into account the multi-scale character of $\Phi(X,t)$ by rewriting it as $\Phi(X,t) = \check{\Phi}(X,t;\ell,L_\mathrm{c})$. As a particular case of this writing, we can impose that $\check{\Phi}(X,t;\ell,L_\mathrm{c}) = \hat{\Phi}(X/L_\mathrm{c}, X/\ell, t)$, so that the dependence on the characteristic length scales is explicit. In this way, we have that

$$\begin{aligned}\Phi(X,t) = \check{\Phi}(X,t;\ell,L_\mathrm{c}) &= \hat{\Phi}(X/L_\mathrm{c}, X/\ell, t)\\ &= \hat{\Phi}(x,x/\varepsilon,t) = \phi(x,y,t),\end{aligned} \tag{6.5}$$

where the dimensionless variables $x := X/L_\mathrm{c}$ and $y := x/\varepsilon$ are referred to as the *macroscopic*, or *slow*, variable, and the *microscopic*, or *fast*, variable, respectively. Note that, within this non-dimensional setting, $\mathscr{B}$ becomes $\mathscr{X} :=]0, L/L_\mathrm{c}[$ and accordingly, the non-dimensional variables x and y vary in $\mathscr{X}$ and in $\mathscr{X}/\varepsilon =]0, L/\ell[=]0, \frac{1}{\varepsilon}L/L_\mathrm{c}[$, respectively.

As stated in Equation (6.5), one is able to express Φ as a function of two formally independent variables, thereby distinguishing the two scales characterising its nature. This means that for every time t, the newly introduced function ϕ is defined, in general, as $\phi(\cdot,\cdot,t) : \mathscr{D}_x \times \mathscr{D}_y \to \mathbb{R}$, where $\mathscr{D}_x \subseteq \mathscr{X}$ and $\mathscr{D}_y \subseteq \mathscr{X}/\varepsilon$.

Finally, we note that, by using the representation (6.5) and employing the chain rule, we can write

$$\partial_X \Phi(X,t) = \tfrac{1}{L_\mathrm{c}}\left[\partial_x\phi(x,y,t) + \tfrac{1}{\varepsilon}\partial_y\phi(x,y,t)\right]. \tag{6.6}$$

6.3.2 Topology of the micro-structure

At the micro-scale, the *reference*, or *elementary cell*, is the open interval $]0,\ell[$, which in a non-dimensional formalism becomes $\mathscr{Y} =]0{,}1[\subset \mathscr{X}/\varepsilon$. Specifically, we assume $\mathscr{Y}$ to consist of two non-empty, open subsets $\mathscr{Y}_1 =]0, y_\mathrm{I}[$ and $\mathscr{Y}_2 =]y_\mathrm{I}{,}1[$, where $y_\mathrm{I} \in]0{,}1[$ denotes the interface between the intervals $\mathscr{Y}_1$ and $\mathscr{Y}_2$ (see Figure 6.1). Furthermore, we consider that

$$\overline{\mathscr{Y}} = \overline{\mathscr{Y}}_1 \cup \overline{\mathscr{Y}}_2 \quad \text{and} \quad \overline{\mathscr{Y}}_1 \cap \mathscr{Y}_2 = \mathscr{Y}_1 \cap \overline{\mathscr{Y}}_2 = \emptyset. \tag{6.7}$$

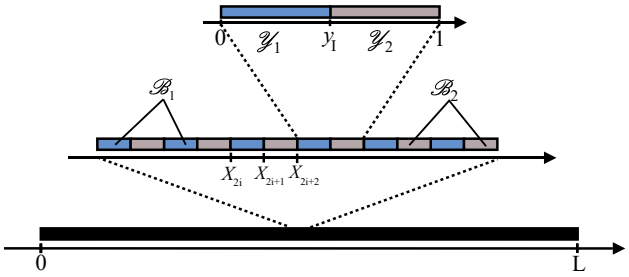

Figure 6.1: Schematic representation of the topology of the composite $\mathscr{B}$ and of its micro-structure.

Here, for the sake of simplicity, we adopt the assumption of *macroscopic uniformity* [148, 217, 218]. This choice allows to choose the elementary cell, $\mathscr{Y}$, independently of the macroscopic variable x, so that $\mathscr{Y}$ is representative of the composite's micro-structure (see Figure 6.1). Moreover, for the type of functions $\phi(\cdot,\cdot,t) : \mathscr{D}_x \times \mathscr{D}_y \to \mathbb{R}$ used in the forthcoming calculations, we assume $\mathscr{Y} \setminus \{y_I\} \subset \mathscr{D}_y$ and the existence of the lateral limits $\lim_{y\to 1^\pm} \phi(x,y,t)$ and $\lim_{y\to 0^+} \phi(x,y,t)$. In the sequel, this property will be used to formalise the periodicity of ϕ with respect to its microscopic variable (this will be referred to as $\mathscr{Y}$-periodicity), especially in the case in which $\mathscr{D}_y$ has the form

$$\mathscr{D}_y = \cup_{p=0}^{N-1} \left(]p, p+y_I[\cup]p+y_I, p+1[\right), \tag{6.8}$$

where N is a sufficiently large natural number. These considerations imply that it is sufficient to reformulate the problem at hand in the reference cell $\mathscr{Y} =]0,1[$, along with the lateral limits outlined above, although for some physical quantities y_I does not belong to the set in which they can be evaluated.

In addition, since $\mathscr{Y}$ is chosen independently of the macroscopic variable x, also the following relation holds

$$\partial_x \left\{ \int_{\mathscr{Y}} \phi(x,y,t) \mathrm{d}y \right\} = \int_{\mathscr{Y}} \partial_x \phi(x,y,t) \mathrm{d}y. \tag{6.9}$$

In general, however, if the hypothesis of macroscopic uniformity is not valid, the topology and geometry of the reference cell, $\mathscr{Y}$, could vary with respect to the macroscopic spatial variable x and, thus, the reference cell should be regarded as a function of x, $\mathscr{Y}(x)$. In this case, Reynolds' transport theorem prescribes to rewrite the derivative of the left-hand-side of Equation (6.9) as

$$\partial_x \left\{ \int_{\mathscr{Y}(x)} \phi(x,y,t) \mathrm{d}y \right\} = \int_{\mathscr{Y}(x)} \partial_x \phi(x,y,t) \mathrm{d}y + \int_{\partial\mathscr{Y}(x)} \phi(x,y,t) w_n(x,y) \mathrm{d}y, \tag{6.10}$$

where $w_n(x,y)$ is the normal "velocity" with which the boundary of the cell varies (see, e.g., [92, 219] and the references therein for more details).

6.3.3 Periodicity

From the point of view of the small characteristic length scale ℓ, the body $\mathscr{B}$ can be approximated as unbounded, so that one can assume $\mathscr{B} = \mathbb{R}$. Within this approximation, a function Φ is said to be ℓ-periodic in the sense that $\Phi(X,t) = \Phi(X + p\ell, t)$, for all $p \in \mathbb{Z}$, provided X and $X + p\ell$ are points in which the function can be evaluated [72].

Within the context of asymptotic homogenisation, one rephrases the periodicity of Φ in terms of the periodicity of the corresponding function ϕ with respect to the microscopic variable y. To this end, and to account for the fact that ϕ may be undefined for some values of y, it is necessary to express the periodicity of ϕ in the weaker sense supplied by

$$\phi(x, y_*^{\pm}, t) = \phi(x, (y_* + 1)^{\pm}, t), \tag{6.11}$$

with $\phi(x, y_*^{\pm}, t) = \lim_{y \to y_*^{\pm}} \phi(x, y, t)$, for all y_* for which both lateral limits exist. This picture is consistent with the case in which $\phi(x, \cdot, t)$ is defined in a set $\mathscr{D}_y$ of the type specified in (6.8) and y_* is either p or $p + y_{\mathrm{I}}$, with $p = 1, \ldots, N-2$. In particular, the case $y_* = p + y_{\mathrm{I}}$ is important for performing the continuous prolongation at the interface of those physical quantities that have to be continuous at this point (for instance, the fluxes).

As anticipated above, the macroscopic uniformity, along with the $\mathscr{Y}$-periodicity of the functions of interest for the problem at hand, enable us to restrict a given physical quantity to a single cell. For this purpose, one may choose the reference cell $\mathscr{Y} =]0,1[$, and take the restriction $\phi(x, \cdot, t)_{|\mathscr{Y}}$. Furthermore, to account for the presence of the interface, which splits the cell in the disjoint union of two materials with different properties, we define $\phi(x, \cdot, t)_{|\mathscr{Y}}$ as the piecewise function

$$\phi(x, y, t)_{|\mathscr{Y}} = \begin{cases} \phi_1(x, y, t) & y \in]0, y_{\mathrm{I}}[\,, \\ \phi_2(x, y, t) & y \in]y_{\mathrm{I}}, 1[\,. \end{cases} \tag{6.12}$$

In particular, to describe the periodicity at $y_* = 0$, we invoke Equation (6.11), so that,

$$\phi(x,0^+,t) = \phi(x,1^+,t). \tag{6.13}$$

Granted this result, we notice that, if ϕ is a function for which the continuity condition at the boundary of the periodic cell must be respected (for example, a concentration or mass flux), we also find

$$\phi_2(x,1^-,t) = \phi_1(x,1^+,t), \tag{6.14}$$

and, thus, because of periodicity,

$$\phi_2(x,1^-,t) = \phi_1(x,0^+,t). \tag{6.15}$$

6.3.4 Multi-scale non-local diffusion

Upon adopting the above considerations, and recalling the identities (6.5) and (6.6), we *rephrase* the original problem (6.1a)-(6.1c) as follows (see Remark 9 for further details),

$$\partial_t c_k(x,y,t) + \left(\partial_x + \tfrac{1}{\varepsilon}\partial_y\right) q_{\alpha,\beta_k}(x,y,t) = 0, \tag{6.16a}$$

$$c_1(x,y_{\mathrm{I}},t) = c_2(x,y_{\mathrm{I}},t), \tag{6.16b}$$

$$q_{\alpha,\beta_1}(x,y_{\mathrm{I}},t) = q_{\alpha,\beta_2}(x,y_{\mathrm{I}},t), \tag{6.16c}$$

with $(x,y,t) \in \mathscr{X} \times \mathscr{Y}_k \times]0,t_{\mathrm{f}}[$, and where the index $k \in \{1,2\}$ indicates in which sub-cell Equation (6.16a) and the quantities c_k and q_{α,β_k} are defined. Particularly, the two-scale, non-local flux q_{α,β_k} is given by

$$q_{\alpha,\beta_k}(x,y,t) := -\int_{\mathscr{X}\times\mathscr{Y}_k} d_{\alpha,\beta_k}(x,\tilde{x},y,\tilde{y}) \left(\partial_{\tilde{x}} + \tfrac{1}{\varepsilon}\partial_{\tilde{y}}\right) c_k(\tilde{x},\tilde{y},t)\mathrm{d}\tilde{x}\mathrm{d}\tilde{y}, \tag{6.17a}$$

$$d_{\alpha,\beta_k}(x,\tilde{x},y,\tilde{y}) := \mathfrak{f}_{\alpha,\beta_k}(x-\tilde{x},y-\tilde{y})\mathfrak{d}_{\alpha,\beta_k}(x,\tilde{x},y,\tilde{y}), \tag{6.17b}$$

where $d_{\alpha,\beta_k}(x,\tilde{x},y,\tilde{y})$ represents a two-scale "version" of the non-local diffusivity coefficient $D(X,\tilde{X})$. More precisely, by using Equation (6.5), we have that $D(X,\tilde{X})$ is replaced by $d_{\alpha,\beta_k}(x,\tilde{x},y,\tilde{y})$, which means that the parameters α and β_k (see below) are already present in $D(X,\tilde{X})$. Analogously, $\mathfrak{f}_{\alpha,\beta_k}(x-\tilde{x},y-\tilde{y})$ and $\mathfrak{d}_{\alpha,\beta_k}(x,\tilde{x},y,\tilde{y})$ replace $\mathfrak{F}(X-\tilde{X})$ and $\mathfrak{D}(X,\tilde{X})$ in the decomposition (6.3b), but describe the non-locality and the fractional diffusivity resolved on the two different scales accounted for in this work. Particularly, $\alpha \in \mathbb{R}^+$ is referred to as the *macro-scale non-locality parameter* and characterises the non-local interactions in the region $\mathscr{X}$. On the other hand, $\beta_k \in \mathbb{R}^+$, with $k = 1,2$, is the *micro-scale non-locality parameter* describing the non-locality within the sub-cell $\mathscr{Y}_k$. Note that q_{α,β_k} absorbs the factor $1/L_{\mathrm{c}}$ that stems from the chain rule (6.6) when one switches to the two-scale representation of the flux.

Remark 9. *The representation of the two-scale, non-local mass flux in Equations* (6.17a) *and* (6.17b) *does not follow directly from* (6.3a)*. This is because the double integral over $\mathscr{X} \times \mathscr{Y}_k$ defining q_{α,β_k} cannot be obtained by only applying the two-scale representation prescribed by* (6.5) *and* (6.6) *to the integrand of* (6.3a)*. Rather, to account for the two-scale resolution of the flux, a further step is needed, which requires to pass from a single integration in the variable $\tilde{X}$ to a double integration in the two auxiliary variables $\tilde{x}$ and $\tilde{y}$. In this respect, it must be clearly stated that the flux q_{α,β_k} is* not *equal to Q, and it is introduced* ad hoc *as a mathematical tool with the purpose of resolving the two-scale dependence of the original flux. Hence, the definition of q_{α,β_k} must be regarded as a* conjecture*, which in the limit $\varepsilon \to 0$, and within the asymptotic homogenisation approach, converges to an* effective *flux that represents the limit of Q (refer to Equation* (6.45b)*). Proving this rigorously*

is part of our current investigations, which involve, among others, the concept of two-scale convergence [210, 72, 272].

We remark that the introduction of the non-local parameters α and β_k follows from the fact that we interpret non-local effects by using the notions of Fractional Calculus [21], in which derivatives and integrals of fractional order are considered. The parameter α accounts for the *intensity* of non-locality at the macro-scale, whereas we have intentionally introduced two different non-locality parameters, β_1 and β_2, at the microscopic level to describe the existence of "long-range" interactions even at the scale of each sub-cell $\mathscr{Y}_k$. This is indeed the essence of the micro-scale non-locality.

We further notice that, if the concentration c_k is dimensionless, the flux q_{α,β_k} must have the physical dimensions of the reciprocal of time, and it follows from Equation (6.17b) that the same must be true for the dimensions of d_{α,β_k}. To guarantee the latter condition, and keeping in mind that $\mathfrak{d}_{\alpha,\beta_k}$ is a (fractional) diffusivity, we take the dimensions of $\mathfrak{d}_{\alpha,\beta_k}$ to be $[\mathfrak{d}_{\alpha,\beta_k}] = \text{length}^{\xi(\alpha,\beta_k)}/\text{time}$, where $\xi(\alpha,\beta_k)$ is a real number expressed as a function of α and β_k, and, consequently, we take $[\mathfrak{f}_{\alpha,\beta_k}] = \text{length}^{-\xi(\alpha,\beta_k)}$. In the local case, the non-locality function may be taken dimensionless, which means that $\xi(\alpha,\beta_k)$ must tend towards zero, and the fractional diffusivity becomes a pure rate, that is $[\mathfrak{d}_{\alpha,\beta_k}] = \text{time}^{-1}$.

In the sequel, we assume that every field is periodic with respect to the micro-scale variable y. Moreover, the spatial fractional diffusivity $\mathfrak{d}_{\alpha,\beta_k}$ is considered to be independent of x, $\tilde{x}$ and y, and with a slight abuse of notation, we simply write $\mathfrak{d}_{\alpha,\beta_k}(\tilde{y})$. This simplification, however, has not major repercussions in the results of the following sections.

6.4 Asymptotic homogenisation approach

In this work, we adopt the asymptotic homogenisation technique and prescribe a formal two-scale expansion for c_k in power series of the smallness parameter $\varepsilon > 0$, namely

$$c_k(x,y,t) = \sum_{n=0}^{+\infty} c_k^{(n)}(x,y,t)\varepsilon^n, \qquad k = 1,2, \tag{6.18}$$

where each $c_k^{(n)}(x,\cdot,t)$, $n = 0,1,2,\ldots$, is assumed to be periodic with respect to y.

Before substituting the formal expansion (6.18) into (6.16a)-(6.16c), we find it convenient to rewrite Equations (6.16a)-(6.16c) as follows

$$\begin{aligned}&\varepsilon^2\partial_t c_k(x,y,t) + \varepsilon^2\partial_x \mathbb{Q}_{\alpha,\beta_k}(x,y,t) + \varepsilon\partial_x \boldsymbol{q}_{\alpha,\beta_k}(x,y,t)\\ &+ \varepsilon\partial_y \mathbb{Q}_{\alpha,\beta_k}(x,y,t) + \partial_y \boldsymbol{q}_{\alpha,\beta_k}(x,y,t) = 0,\end{aligned} \tag{6.19a}$$

$$c_1(x, y_\mathrm{I}, t) = c_2(x, y_\mathrm{I}, t), \tag{6.19b}$$

$$\varepsilon \mathbb{Q}_{\alpha,\beta_1}(x, y_\mathrm{I}, t) + \boldsymbol{q}_{\alpha,\beta_1}(x, y_\mathrm{I}, t) = \varepsilon \mathbb{Q}_{\alpha,\beta_2}(x, y_\mathrm{I}, t) + \boldsymbol{q}_{\alpha,\beta_2}(x, y_\mathrm{I}, t), \tag{6.19c}$$

where the following notation has been adopted

$$\mathbb{Q}_{\alpha,\beta_k}(x, y, t) := -\int_{\mathscr{X}\times\mathscr{Y}_k} \mathfrak{f}_{\alpha,\beta_k}(x-\tilde{x}, y-\tilde{y}) \mathfrak{d}_{\alpha,\beta_k}(\tilde{y}) \partial_{\tilde{x}} c_k(\tilde{x}, \tilde{y}, t) \mathrm{d}\tilde{x}\mathrm{d}\tilde{y}, \tag{6.20a}$$

$$\boldsymbol{q}_{\alpha,\beta_k}(x, y, t) := -\int_{\mathscr{X}\times\mathscr{Y}_k} \mathfrak{f}_{\alpha,\beta_k}(x-\tilde{x}, y-\tilde{y}) \mathfrak{d}_{\alpha,\beta_k}(\tilde{y}) \partial_{\tilde{y}} c_k(\tilde{x}, \tilde{y}, t) \mathrm{d}\tilde{x}\mathrm{d}\tilde{y}. \tag{6.20b}$$

Specifically, in (6.20a) and (6.20b), the uppercase and lowercase symbols $\mathbb{Q}_{\alpha,\beta_k}$ and $\boldsymbol{q}_{\alpha,\beta_k}$ indicate the partial differentiation of c_k inside the integral with respect to $\tilde{x}$ and $\tilde{y}$, respectively. Moreover, it holds that $q_{\alpha,\beta_k} = \mathbb{Q}_{\alpha,\beta_k} + \varepsilon^{-1}\boldsymbol{q}_{\alpha,\beta_k}$.

After substituting (6.18), truncated to the order ε^2, into (6.19a)-(6.19c), (6.20a) and (6.20b), the problem reduces to finding the leading order coefficients $c_k^{(n)}$ of the power series (6.18), which solve the boundary problems resulting from equating all the terms in the same powers of the ε. To this end, it is useful to write explicitly the generic coefficients of the expansion of the fluxes $\boldsymbol{q}_{\alpha,\beta_k}$ and $\mathbb{Q}_{\alpha,\beta_k}$, i.e.,

$$\boldsymbol{q}^{(n)}_{\alpha,\beta_k}(x, y, t) := -\int_{\mathscr{X}\times\mathscr{Y}_k} \mathfrak{f}_{\alpha,\beta_k}(x-\tilde{x}, y-\tilde{y}) \mathfrak{d}_{\alpha,\beta_k}(\tilde{y}) \partial_{\tilde{y}} c^{(n)}_k(\tilde{x}, \tilde{y}, t) \mathrm{d}\tilde{x}\mathrm{d}\tilde{y}, \tag{6.21a}$$

$$\mathbb{Q}^{(n)}_{\alpha,\beta_k}(x, y, t) := -\int_{\mathscr{X}\times\mathscr{Y}_k} \mathfrak{f}_{\alpha,\beta_k}(x-\tilde{x}, y-\tilde{y}) \mathfrak{d}_{\alpha,\beta_k}(\tilde{y}) \partial_{\tilde{x}} c^{(n)}_k(\tilde{x}, \tilde{y}, t) \mathrm{d}\tilde{x}\mathrm{d}\tilde{y}, \tag{6.21b}$$

for $n = 0,1,2,\ldots$, so that, in the limit $\varepsilon \to 0$, $\boldsymbol{q}_{\alpha,\beta_k}$ and $\mathbb{Q}_{\alpha,\beta_k}$ can be approximated by

$$\boldsymbol{q}_{\alpha,\beta_k} = \boldsymbol{q}^{(0)}_{\alpha,\beta_k} + \varepsilon \boldsymbol{q}^{(1)}_{\alpha,\beta_k} + \varepsilon^2 \boldsymbol{q}^{(2)}_{\alpha,\beta_k} + o(\varepsilon^2), \tag{6.22a}$$

$$\mathbb{Q}_{\alpha,\beta_k} = \mathbb{Q}^{(0)}_{\alpha,\beta_k} + \varepsilon \mathbb{Q}^{(1)}_{\alpha,\beta_k} + \varepsilon^2 \mathbb{Q}^{(2)}_{\alpha,\beta_k} + o(\varepsilon^2). \tag{6.22b}$$

Next, the problem (6.16a)-(6.16c), truncated to the order ε^2, splits into three sub-problems, one for each of the considered orders of ε.

In the sequel, to avoid the proliferation of indices, we simplify the notation as follows

$$\boldsymbol{q}^{(n)}_{\alpha,\beta_k} \equiv \boldsymbol{q}^{(n)}_k, \tag{6.23a}$$

$$\mathbb{Q}^{(n)}_{\alpha,\beta_k}(x, y, t) \equiv \mathbb{Q}^{(n)}_k. \tag{6.23b}$$

Analogously, we set $\mathfrak{f}_{\alpha,\beta_k} \equiv \mathfrak{f}_k$ and $\mathfrak{d}_{\alpha,\beta_k} \equiv \mathfrak{d}_k$.

(i) To the order ε^0,

$$\partial_y \boldsymbol{q}_k^{(0)}(x,y,t) = 0, \qquad \text{in } \mathscr{X} \times \mathscr{Y}_k \times]0,t_\mathrm{f}[, \tag{6.24a}$$

$$c_1^{(0)}(x,y_\mathrm{I},t) = c_2^{(0)}(x,y_\mathrm{I},t), \qquad t \in]0,t_\mathrm{f}[, \tag{6.24b}$$

$$\boldsymbol{q}_1^{(0)}(x,y_\mathrm{I},t) = \boldsymbol{q}_2^{(0)}(x,y_\mathrm{I},t), \qquad t \in]0,t_\mathrm{f}[. \tag{6.24c}$$

Equation (6.24a) implies that $\boldsymbol{q}_k^{(0)}$ is independent of the microscopic variable, since its partial derivative with respect to y is zero. One possible way of ensuring this condition could be to drop the dependence of $\mathfrak{f}_k$ on the micro-scale variables. However, this assumption would eliminate the possibility of keeping track of the non-locality at the micro-scale, which is clearly in contrast with our purposes. Instead, to guarantee the fulfilment of Equation (6.24a) and to make sure we remain within a non-local setting, we require $c_k^{(0)}$ to be independent of y. Hence, with a slight abuse of notation, we set

$$c_k^{(0)}(x,y,t) = c_k^{(0)}(x,t), \tag{6.25}$$

thereby satisfying Equations (6.24a)-(6.24c), since $\boldsymbol{q}_k^{(0)} = 0$, without having to rebut the dependence of $\mathfrak{f}_k$ on the micro-scale. The above consideration is a standard result of linear asymptotic homogenisation, whereas it is often assumed for non-linear problems (see e.g. [229, 75, 237]). A direct consequence of (6.25) is that $c_1^{(0)}$ and $c_2^{(0)}$ coincide with each other, so that we can write

$$c^{(0)}(x,t) := c_1^{(0)}(x,t) = c_2^{(0)}(x,t). \tag{6.26}$$

(ii) To the order ε^1

By taking into consideration Equation (6.25), we have that

$$\partial_y \left\{ \boldsymbol{q}_k^{(1)}(x,y,t) + \mathbb{Q}_k^{(0)}(x,y,t) \right\} = 0, \tag{6.27a}$$

$$c_1^{(1)}(x,y_\mathrm{I},t) = c_2^{(1)}(x,y_\mathrm{I},t), \tag{6.27b}$$

$$\boldsymbol{q}_1^{(1)}(x,y_\mathrm{I},t) + \mathbb{Q}_1^{(0)}(x,y_\mathrm{I},t) = \boldsymbol{q}_2^{(1)}(x,y_\mathrm{I},t) + \mathbb{Q}_2^{(0)}(x,y_\mathrm{I},t), \tag{6.27c}$$

with $(x,y,t) \in \mathscr{X} \times \mathscr{Y}_k \times]0,t_\mathrm{f}[$. The structure of (6.27a) implies that, in general, this equation must be solved in the spatial domain $\mathscr{X} \times \mathscr{Y}_k$, which in the context of asymptotic homogenisation means that one needs to consider a problem defined in $\mathscr{Y}_k$ for each $x \in \mathscr{X}$.

Remark 10. *[A comment on the solution to* (6.27a)-(6.27c)*]*
The local counterpart of the problem (6.27a)-(6.27c) *(see [34, 72]) can be obtained by choosing the non-locality function*

$$\mathfrak{f}_k(x-\tilde{x}, y-\tilde{y}) = \delta(x-\tilde{x})\delta(y-\tilde{y}), \tag{6.28}$$

where δ is Dirac's delta. Specifically,

$$-\partial_y\left\{\mathfrak{d}_k(y)\left[\partial_y c_k^{(1)}(x,y,t)+\partial_x c^{(0)}(x,t)\right]\right\}=0, \tag{6.29a}$$

$$c_1^{(1)}(x,y_{\mathrm{I}},t)=c_2^{(1)}(x,y_{\mathrm{I}},t), \tag{6.29b}$$

$$\mathfrak{d}_1(y_{\mathrm{I}})\left[\partial_y c_1^{(1)}(x,y_{\mathrm{I}},t)+\partial_x c^{(0)}(x,t)\right]=\mathfrak{d}_2(y_{\mathrm{I}})\left[\partial_y c_2^{(1)}(x,y_{\mathrm{I}},t)+\partial_x c^{(0)}(x,t)\right], \tag{6.29c}$$

with $(x,y,t)\in\mathscr{X}\times\mathscr{Y}_k\times]0,t_{\mathrm{f}}[$. In Equations (6.29b) *and* (6.29c) *the evaluation in y_{I} of $\mathfrak{d}_k$ and $\partial_y c_k^{(1)}$ are to be understood in the sense of lateral limits $y\to y_{\mathrm{I}}^{\pm}$. In this particular case, the problem* (6.29a)-(6.29c) *admits a unique solution, which is defined up to a function depending solely on time, t, and on the slow variable, x [34, 72]. This unique solution is usually expressed through the* ansatz

$$c_k^{(1)}(x,y,t)=\vartheta_k(x,y,t)\partial_x c^{(0)}(x,t)+\varphi(x,t), \tag{6.30}$$

where ϑ_k is the new unknown of the problem (6.29a)-(6.29c) *and φ is a function of x and t that spans the family of all the solutions [28, 219]. To the best of our knowledge, in the non-local case there is no theorem that guarantees the existence and uniqueness (even in the sense explained above) of the solution. Still, in the absence of a supporting theory, we* guess *that, similarly to the local case, the solution should have the form* (6.30)*, with ϑ_k suitably parametrised by α and β_k.* ■

By substituting (6.30) into (6.27a)-(6.27b), we require the auxiliary functions ϑ_k to satisfy the *non-local cell problem*,

$$\partial_y\left\{\boldsymbol{q}_k^{(1)}(x,y,t)+\mathbb{Q}_k^{(0)}(x,y,t)\right\}=0, \tag{6.31a}$$

$$\vartheta_1(x,y_{\mathrm{I}},t)=\vartheta_2(x,y_{\mathrm{I}},t), \tag{6.31b}$$

$$\boldsymbol{q}_1^{(1)}(x,y_{\mathrm{I}},t)+\mathbb{Q}_1^{(0)}(x,y_{\mathrm{I}},t)=\boldsymbol{q}_2^{(1)}(x,y_{\mathrm{I}},t)+\mathbb{Q}_2^{(0)}(x,y_{\mathrm{I}},t), \tag{6.31c}$$

with $(x,y,t)\in\mathscr{X}\times\mathscr{Y}_k\times]0,t_{\mathrm{f}}[$ and

$$\boldsymbol{q}_k^{(1)}(x,y,t)=-\int_{\mathscr{X}\times\mathscr{Y}_k}\mathfrak{f}_k(x-\tilde{x},y-\tilde{y})\mathfrak{d}_k(\tilde{y})\partial_{\tilde{y}}\vartheta_k(\tilde{x},\tilde{y},t)\partial_{\tilde{x}}c^{(0)}(\tilde{x},t)\mathrm{d}\tilde{x}\mathrm{d}\tilde{y}, \tag{6.32a}$$

$$\mathbb{Q}_k^{(0)}(x,y,t)=-\int_{\mathscr{X}\times\mathscr{Y}_k}\mathfrak{f}_k(x-\tilde{x},y-\tilde{y})\mathfrak{d}_k(\tilde{y})\partial_{\tilde{x}}c^{(0)}(\tilde{x},t)\mathrm{d}\tilde{x}\mathrm{d}\tilde{y}. \tag{6.32b}$$

We notice that the structure of the non-local problem (6.31a)-(6.31c) does not permit, in general, to factorise the macroscopic term $\partial_{\tilde{x}}c^{(0)}(\tilde{x},t)$. This implies that one should account for the macroscopic contributions at the micro-structural level and, thus, for the interchange of information between the two length scales.

(iii) To the order ε^2,

$$\partial_t c^{(0)}(x,y,t) + \partial_x \left\{ \boldsymbol{q}_k^{(1)}(x,y,t) + \mathbb{Q}_k^{(0)}(x,y,t) \right\} + \partial_y \left\{ \boldsymbol{q}_k^{(2)}(x,y,t) + \mathbb{Q}_k^{(1)}(x,y,t) \right\} = 0, \tag{6.33a}$$

$$c_1^{(2)}(x,y_{\mathrm{I}},t) = c_2^{(2)}(x,y_{\mathrm{I}},t), \tag{6.33b}$$

$$\boldsymbol{q}_1^{(2)}(x,y_{\mathrm{I}},t) + \mathbb{Q}_1^{(1)}(x,y_{\mathrm{I}},t) = \boldsymbol{q}_2^{(2)}(x,y_{\mathrm{I}},t) + \mathbb{Q}_2^{(1)}(x,y_{\mathrm{I}},t), \tag{6.33c}$$

with $(x,y,t) \in \mathscr{X} \times \mathscr{Y}_k \times]0,t_{\mathrm{f}}[$.

Before going further in our analysis, we introduce, for a given field ϕ, defined in the cell $\mathscr{Y}$ or in a subset of it having the same measure, the operators

$$\langle \phi \rangle_k(x,t) := \frac{1}{|\mathscr{Y}|} \int_{\mathscr{Y}_k} \phi(x,y,t) \mathrm{d}y, \quad k \in \{1,2\}, \tag{6.34}$$

such that the sum $\langle \phi \rangle_1 + \langle \phi \rangle_2 = \langle \phi \rangle$ is the average of ϕ over the cell $\mathscr{Y}$. Then, by applying these operators to (6.33a), we have

$$\langle \partial_t c^{(0)}(x,t) \rangle_k + \left\langle \partial_x \left\{ \boldsymbol{q}_k^{(1)}(x,y,t) + \mathbb{Q}_k^{(0)}(x,y,t) \right\} \right\rangle_k + \left\langle \partial_y \left\{ \boldsymbol{q}_k^{(2)}(x,y,t) + \mathbb{Q}_k^{(1)}(x,y,t) \right\} \right\rangle_k = 0. \tag{6.35}$$

Because of Equation (6.26), $c^{(0)}$ depends only on x and t and then,

$$\langle \partial_t c^{(0)}(x,t) \rangle_k = \frac{|\mathscr{Y}_k|}{|\mathscr{Y}|} \partial_t c^{(0)}(x,t). \tag{6.36}$$

Moreover, the assumption of macroscopic uniformity (see Section 6.3.2) implies that the differential operator ∂_x and the integral operator $\langle \cdot \rangle_k$ commute, so that, the second term of (6.35) rewrites as,

$$\left\langle \partial_x \left\{ \boldsymbol{q}_k^{(1)}(x,y,t) + \mathbb{Q}_k^{(0)}(x,y,t) \right\} \right\rangle_k = \partial_x \left\langle \boldsymbol{q}_k^{(1)}(x,y,t) + \mathbb{Q}_k^{(0)}(x,y,t) \right\rangle_k. \tag{6.37}$$

Therefore, summing up Equation (6.35) over k and taking into account the relations (6.36) and (6.37), we obtain

$$\partial_t c^{(0)}(x,t) + \partial_x \left\{ \sum_{k=1}^{2} \left\langle \boldsymbol{q}_k^{(1)}(x,y,t) + \mathbb{Q}_k^{(0)}(x,y,t) \right\rangle_k \right\} + \sum_{k=1}^{2} \left\langle \partial_y \left\{ \boldsymbol{q}_k^{(2)}(x,y,t) + \mathbb{Q}_k^{(1)}(x,y,t) \right\} \right\rangle_k = 0. \tag{6.38}$$

We notice that the third term of (6.38) can be computed as

$$\begin{aligned}\sum_{k=1}^{2}\left\langle \partial_y\left\{ \boldsymbol{q}_k^{(2)}(x,y,t)+\mathbb{Q}_k^{(1)}(x,y,t)\right\}\right\rangle_k &= \frac{1}{|\mathscr{Y}|}\sum_{k=1}^{2}\int_{\mathscr{Y}_k}\partial_y\left\{ \boldsymbol{q}_k^{(2)}(x,y,t)+\mathbb{Q}_k^{(1)}(x,y,t)\right\}\mathrm{d}y\\ &= \frac{1}{|\mathscr{Y}|}\Big\{\Big(\boldsymbol{q}_1^{(2)}(x,y_{\mathrm{I}}^-,t)+\mathbb{Q}_1^{(1)}(x,y_{\mathrm{I}}^-,t)\Big)\\ &\quad -\Big(\boldsymbol{q}_1^{(2)}(x,0^+,t)+\mathbb{Q}_1^{(1)}(x,0^+,t)\Big)\\ &\quad +\Big(\boldsymbol{q}_2^{(2)}(x,1^-,t)+\mathbb{Q}_2^{(1)}(x,1^-,t)\Big)\\ &\quad -\Big(\boldsymbol{q}_2^{(2)}(x,y_{\mathrm{I}}^+,t)+\mathbb{Q}_2^{(1)}(x,y_{\mathrm{I}}^+,t)\Big)\Big\}\\ &= 0,\end{aligned}\tag{6.39}$$

where we have employed Gauss' theorem and the continuity of the fluxes at the interface and at the boundaries of the cell. Specifically, because of the continuity of the fluxes at the interface y_{I}, it holds true that

$$\Big(\boldsymbol{q}_1^{(2)}(x,y_{\mathrm{I}}^-,t)+\mathbb{Q}_1^{(1)}(x,y_{\mathrm{I}}^-,t)\Big)-\Big(\boldsymbol{q}_2^{(2)}(x,y_{\mathrm{I}}^+,t)+\mathbb{Q}_2^{(1)}(x,y_{\mathrm{I}}^+,t)\Big)=0,\tag{6.40}$$

which eliminates the first and the fourth summands on the far right-hand-side of Equation (6.39). Moreover, the flux computed at the right boundary of the cell, i.e., $\boldsymbol{q}_2^{(2)}(x,1^-,t)+\mathbb{Q}_2^{(1)}(x,1^-,t)$, must be equal to the flux entering or leaving the neighbouring cell, which can be written as $\boldsymbol{q}_1^{(2)}(x,1^+,t)+\mathbb{Q}_1^{(1)}(x,1^+,t)$. Therefore, by invoking the $\mathscr{Y}$-periodicity of the flux, we can conclude that the second and the third term of Equation (6.39) also cancel themselves, i.e.,

$$\begin{aligned}&\Big(\boldsymbol{q}_2^{(2)}(x,1^-,t)+\mathbb{Q}_2^{(1)}(x,1^-,t)\Big)-\Big(\boldsymbol{q}_1^{(2)}(x,0^+,t)+\mathbb{Q}_1^{(1)}(x,0^+,t)\Big)\\ &=\Big(\boldsymbol{q}_1^{(2)}(x,1^+,t)+\mathbb{Q}_1^{(1)}(x,1^+,t)\Big)-\Big(\boldsymbol{q}_1^{(2)}(x,0^+,t)+\mathbb{Q}_1^{(1)}(x,0^+,t)\Big)\\ &=0.\end{aligned}\tag{6.41}$$

Equations (6.40) and (6.41) explain in detail the reason why Equation (6.39) holds true. Before going further, we emphasise that the considerations done so far hold true also for all the other orders of the asymptotic expansion of the flux, like, for instance, $\boldsymbol{q}_k^{(1)}+\mathbb{Q}_k^{(0)}$.

Then, the substitution of (6.39) into (6.38) yields the homogenised problem for the leading order term $c^{(0)}$, i.e.,

$$\partial_t c^{(0)}(x,t)+\partial_x q^{\mathrm{eff}}(x,t)=0,\tag{6.42}$$

where

$$q^{\mathrm{eff}}(x,t):=-\int_{\mathscr{X}} d^{\mathrm{eff}}(x,\tilde{x},t)\partial_{\tilde{x}}c^{(0)}(\tilde{x},t)\mathrm{d}\tilde{x}\tag{6.43}$$

is referred to as the *non-local effective mass flux*, while d^{eff} is defined through the expression

$$d^{\text{eff}}(x,\tilde{x},t) := \sum_{k=1}^{2} \left\langle \int_{\mathscr{Y}_k} \mathfrak{f}_k(x-\tilde{x},y-\tilde{y})\mathfrak{d}_k(\tilde{y})[1+\partial_{\tilde{y}}\vartheta_k(\tilde{x},\tilde{y},t)]\mathrm{d}\tilde{y} \right\rangle_k$$
$$= \frac{1}{|\mathscr{Y}|}\sum_{k=1}^{2}\int_{\mathscr{Y}_k\times\mathscr{Y}_k} \mathfrak{f}_k(x-\tilde{x},y-\tilde{y})\mathfrak{d}_k(\tilde{y})[1+\partial_{\tilde{y}}\vartheta_k(\tilde{x},\tilde{y},t)]\mathrm{d}\tilde{y}\mathrm{d}y, \quad (6.44)$$

and represents the *non-local effective diffusivity*. We notice that the homogenised equation (6.42) has the same structure as (6.1a), but, in this case, the contributions of the micro-structure are resolved by means of the non-local effective coefficient d^{eff}.

Finally, according to [219, 237] we introduce the notation $\mathscr{X}_{\text{h}}$ to denote the *homogenised version* of the composite medium, and we reformulate the homogenised problem (6.42) and (6.43) as follows

$$\partial_t c^{(0)}(x,t) + \partial_x q^{\text{eff}}(x,t) = 0, \quad \text{in } \mathscr{X}_{\text{h}}\times]0,t_{\text{f}}[, \quad (6.45a)$$

$$q^{\text{eff}}(x,t) = -\int_{\mathscr{X}_{\text{h}}} d^{\text{eff}}(x,\tilde{x},t)\partial_{\tilde{x}}c^{(0)}(\tilde{x},t)\mathrm{d}\tilde{x}, \quad (6.45b)$$

which has to be supplemented with appropriate initial and boundary conditions for the unknown $c^{(0)}$.

Remark 11. *Note that, since $\mathfrak{f}_k$ and $\mathfrak{d}_k$ are short-hand notations for $\mathfrak{f}_{\alpha,\beta_k}$ and $\mathfrak{d}_{\alpha,\beta_k}$, both the non-local effective diffusivity, d^{eff}, and the non-local effective flux, q^{eff}, depend on the collection of all the parameters that describe the non-locality of the problem, i.e., α, β_1 and β_2. Hence, the effective quantities d^{eff} and q^{eff} keep track simultaneously of the non-locality occurring both at the scale of the sub-cells, through β_1 and β_2, and at the scale of the medium, through α. In the following, with the purpose of leaving the notation at a minimum level of complexity, we shall keep the symbols d^{eff} and q^{eff}, although we mean $d^{\text{eff}}_{\alpha,\beta_1,\beta_2}$ and $q^{\text{eff}}_{\alpha,\beta_1,\beta_2}$, respectively.* ■

Remark 12. *It is worth noticing that if the non-locality function is $\mathfrak{f}_k(x-\tilde{x},y-\tilde{y}) = \delta(x-\tilde{x})\delta(y-\tilde{y})$, we end up with classical results of homogenisation theory [34, 72, 219, 239]. That is, by substituting this expression for $\mathfrak{f}_k$ into Equation* (6.31a)*, the cell problem reads*

$$-\,\mathrm{d}_y\left\{\mathfrak{d}_k(y)[1+\mathrm{d}_y\vartheta_k(y)]\right\} = 0, \quad (6.46)$$

where $\mathrm{d}_y\vartheta_k(y)$ denotes the total derivative of ϑ_k. Furthermore, the non-local effective diffusivity, d^{eff}, is

$$d^{\text{eff}}(x,\tilde{x}) = \delta(x-\tilde{x})\sum_{k=1}^{2}\left\langle \mathfrak{d}_k(y)[1+\mathrm{d}_y\vartheta_k(y)]\right\rangle_k$$

$$= \delta(x-\tilde{x})\hat{d}_{\mathrm{st}}^{\mathrm{eff}}, \tag{6.47}$$

with $\hat{d}_{\mathrm{st}}^{\mathrm{eff}}$ *being entirely defined by the sum over* k *in* (6.47)*. In this case,* $\hat{d}_{\mathrm{st}}^{\mathrm{eff}}$ *is a constant coefficient that coincides with the effective diffusivity of a standard diffusion problem in a composite medium [34, 206, 186]. Furthermore, after substitution of* (6.47) *into* (6.45a)*, we obtain the standard homogenised equations*

$$\partial_t c^{(0)}(x,t) + \partial_x q_{\mathrm{st}}^{\mathrm{eff}}(x,t) = 0, \tag{6.48a}$$

$$q_{\mathrm{st}}^{\mathrm{eff}}(x,t) = -\hat{d}_{\mathrm{st}}^{\mathrm{eff}}\partial_x c^{(0)}(x,t), \tag{6.48b}$$

where standard Fick's law is re-obtained for the flux. ■

Remark 13. *We notice that in the present framework, we do not take into account the timescales associated with the problems* (6.24a)*,* (6.27a) *and* (6.33a)*, since we intend to focus on the spatial connections between heterogeneity and non-locality. Nevertheless, one can notice that the characteristic length scales* L_{c} *and* ℓ *associated with the composite medium and with its internal structure, respectively, induce different timescales (see, e.g., [181]). In fact, by virtue of a reference diffusivity* $\mathfrak{d}_{\mathrm{R}}$*, these can be expressed as*

$$\zeta_{\mathrm{c}} = \frac{L_{\mathrm{c}}^2}{\mathfrak{d}_{\mathrm{R}}} \quad \textit{and} \quad \eta_{\mathrm{c}} = \frac{\ell^2}{\mathfrak{d}_{\mathrm{R}}}. \tag{6.49}$$

Since in the sequel we specialise Equation (6.49) *to the case of media with different diffusivities inside the sub-cells* $\mathscr{Y}_1$ *and* $\mathscr{Y}_2$*, we can prescribe* $\mathfrak{d}_{\mathrm{R}} := \min\{\mathfrak{d}_{1\mathrm{R}}, \mathfrak{d}_{2\mathrm{R}}\}$.

By employing (6.49)*, we deduce the following relationship between the characteristic time scales,*

$$\frac{\eta_{\mathrm{c}}}{\zeta_{\mathrm{c}}} = \varepsilon^2 < \varepsilon \ll 1. \tag{6.50}$$

Now, before proceeding further, we mention that in this multi-scale framework, a given physical quantity $\Phi(X,t)$ *can be rewritten as*

$$\Phi(X,t) = \hat{\Phi}(x, x/\varepsilon, \zeta, \zeta/\varepsilon^2) = \phi(x,y,\zeta,\eta), \tag{6.51}$$

with $\zeta := t/\zeta_{\mathrm{c}}$ *and* $\eta := \zeta/\varepsilon^2$ *(compare Equation* (6.51) *with Equation* (6.5) *in which time was not rescaled). Therefore, Equation* (6.16a) *rewrites*

$$\tfrac{1}{\zeta_{\mathrm{c}}}(\partial_\zeta + \tfrac{1}{\varepsilon^2}\partial_\eta)c_k(x,y,\zeta,\eta) + \left(\partial_x + \tfrac{1}{\varepsilon}\partial_y\right) q_{\alpha,\beta_k}(x,y,\zeta,\eta) = 0, \tag{6.52}$$

which, after substituting the two-scale expansion (6.18) *and equating in the same powers of* ε*, up to the order* ε^2*, yields*

$$\varepsilon^0\colon\ \tfrac{1}{\zeta_{\mathrm{c}}}\partial_\eta c_k^{(0)}(x,y,\zeta,\eta) + \partial_y \boldsymbol{q}_k^{(0)}(x,y,\zeta,\eta) = 0, \tag{6.53a}$$

$$\varepsilon^1: \ \tfrac{1}{\zeta_c}\partial_\eta c_k^{(1)}(x,y,\zeta,\eta) + \partial_x \boldsymbol{q}_k^{(0)}(x,y,\zeta,\eta) + \partial_y \left\{ \boldsymbol{q}_k^{(1)}(x,y,\zeta,\eta) + \mathbb{Q}_k^{(0)}(x,y,\zeta,\eta) \right\} = 0, \tag{6.53b}$$

$$\varepsilon^2: \ \tfrac{1}{\zeta_c}\partial_\eta c_k^{(2)}(x,y,\zeta,\eta) + \tfrac{1}{\zeta_c}\partial_\zeta c_k^{(0)}(x,y,\zeta,\eta) + \partial_x \left\{ \boldsymbol{q}_k^{(1)}(x,y,\zeta,\eta) + \mathbb{Q}_k^{(0)}(x,y,\zeta,\eta) \right\} + \partial_y \left\{ \boldsymbol{q}_k^{(2)}(x,y,\zeta,\eta) + \mathbb{Q}_k^{(1)}(x,y,\zeta,\eta) \right\} = 0. \tag{6.53c}$$

As Equations (6.53a)-(6.53c) *prescribe, this approach calls for the solution of diffusion problems at each order of ε. Moreover, the consideration of the separation of the time scales conduces to leading-order problems that are characterised by the presence of the rapid time variable η. The analysis of these equations is part of our current research.*

In the next chapter, we present two simplified benchmark tests in which non-local interactions are considered at the micro-scale or at the macro-scale only to quantify the effects of the non-locality.

Chapter 7

Selected benchmark problems

The work reported in this chapter has been previously published in [241].

7.1 Introduction

Here, we specialise the model presented in Chapter 6 by considering two simplified models in which the non-local effects are only present at the macro-scale or at the micro-scale, and we report some details of the numerical schemes based on FE methods. In both cases, we show that in the limit in which the non-locality parameters β (in the benchmark test I) and α (in the benchmark test II) tend to 1 from below, the fractional cell and homogenised problems lead to the standard ones given in the classical homogenisation literature.

It is worth mentioning that the cell and the homogenised problems obtained in this work feature integro-differential equations of fractional type in bounded domains and, therefore, the classical solution techniques, such as Laplace and Fourier transforms, used in Fractional Calculus are not suitable. Consequently, either do we need to develop dedicated numerical algorithms or we resort to well-established numerical methods, and we adapt them to take into account the presence of fractional differential operators in the considered problems. Here, we follow the second path and, indeed, we write a numerical scheme based on a finite element discretisation of the original integro-differential problems. In doing this, we need to emphasise that, partly because of the very easy geometry of the problems (we deal, in fact, with one-dimensional benchmark studies), and partly because the focus of our work is not on the numerics, the presentation of the FE scheme is very elementary. Indeed, it can be obtained by appropriately rephrasing the one-dimensional formulation of the FE method as presented e.g. in [152]. Moreover, we do not fuss over some technical aspects of the finite element procedures, such as the "element point of view" [152] *et similia*, since our scope is solely meant to highlight how the

symmetrised Caputo fractional derivatives affect the stiffness matrix and the nodal force of the discretisation. Clearly, a more detailed numerical study is required, and this is part of our current investigations. We highlight that previous works in this direction are [244, 151, 106]. In particular, the work we took major inspiration from is [151].

7.2 Considerations on the benchmark problems

In the remainder of this work, the following considerations are adopted.

(i) Fractional diffusivity. We prescribe $\mathfrak{d}_1$ and $\mathfrak{d}_2$ to be constant in $\mathscr{Y}_1$ and $\mathscr{Y}_2$, respectively. Then, by recalling the discussion made in Section 6.3.4, we express each $\mathfrak{d}_k$ as

$$\mathfrak{d}_k = \mathfrak{d}_{k\mathrm{R}} L_{\mathrm{c}}^{-2+\xi(\alpha,\beta_k)}, \quad k = 1,2, \tag{7.1}$$

where $\mathfrak{d}_{k\mathrm{R}}$ is the constant reference diffusivity of $\mathscr{Y}_k$ and it has the dimensions of a standard diffusivity, i.e., length squared over time [220].

(ii) Initial and boundary conditions for the homogenised equation. We enforce an initial spatial distribution for $c^{(0)}$ of the form

$$c^{(0)}(x,0) = c_{\mathrm{in}}(x) := 1 - k \exp\left(-2\frac{(x-x_0)^2}{(r/L_{\mathrm{c}})^2}\right), \tag{7.2}$$

where k, r and x_0 are model parameters.

To contextualise our work, we mention that the initial condition $c_{\mathrm{in}}(x)$ in (7.2) is sometimes employed to simulate the initial concentration of molecules after photobleaching in a *Fluorescence recovery after photobleaching* (FRAP) experiment [31, 220] (see Chapter 5). In this way, following [140], the model is prepared to describe the fluorescence recovery pattern of molecules surrounding a certain region of a tissue (e.g. articular cartilage) after being photobleached, by using a high-intensity laser beam. Here, we do not go into the technical details pertaining to a FRAP experiment, since this is not the focus of our work, and the benchmark proposed hereafter is also markedly different from the one developed in [140]. Thus, we do not claim that our results are meant to simulate a FRAP experiment. Still, since the setting presented in [140] refers to a tissue with hierarchical internal structure, as is the case of articular cartilage, our work might bring some new insight into the interpretation of the experimental results. To this end, we adapt the framework described in [140] to the setting of the homogenised problem (6.45a)-(6.45b) and, specifically, we identify k, r and x_0 with the bleaching depth parameter, the dimension of the bleached area, and the centre of the bleached region, respectively.

We notice that, since this work is framed in a one-dimensional setting, r characterises the measure of a line-segment of $\mathscr{X}_{\mathrm{h}}$, and we choose x_0 as the centre of the macroscopic domain $\mathscr{X}_{\mathrm{h}}$, namely $x_0 = \frac{1}{2}(L/L_{\mathrm{c}})$. In addition, we adapt the boundary conditions given in [140] to the geometry of our problem, and impose Dirichlet boundary conditions for $c^{(0)}$ at $x = 0$ and $x = L/L_{\mathrm{c}}$. Specifically, we set

$$c^{(0)}(0,t) = c_{\mathrm{in}}(0), \tag{7.3a}$$

$$c^{(0)}(L/L_{\mathrm{c}},t) = c_{\mathrm{in}}(L/L_{\mathrm{c}}), \tag{7.3b}$$

which implies

$$c_{\mathrm{in}}(0) = c_{\mathrm{in}}(L/L_{\mathrm{c}}) =: c_{\mathrm{b}}. \tag{7.4}$$

(iii) Parameters. In Table 7.1, we provide the values of the parameters used in our numerical simulations. We notice that the value of r is meant to "cover" 100 reference cells.

Table 7.1: List of parameters used in the numerical simulations.

Parameter	Value	Unit	Equation	Reference
L_{c}	$L = 10$	mm	(6.4)	[91]
ℓ	10^{-2}	mm	(6.4)	This work
$\mathfrak{d}_{1\mathrm{R}}$	$\mathfrak{d}_{2\mathrm{R}}/2$	mm^2/s	(7.1)	This work
$\mathfrak{d}_{2\mathrm{R}}$	3.2×10^{-3}	mm^2/s	(7.1)	[255]
k	0.7	–	(7.2)	[140]
r	1	mm	(7.2)	This work
y_{I}	$\frac{1}{2}$	–	(6.16b)	This work

7.3 Benchmark problem I: Micro-scale non-locality

Let us consider the case in which the non-locality is accounted for only at the micro-scale. This can be achieved by prescribing

$$\mathfrak{f}_k(x-\tilde{x}, y-\tilde{y}) = \delta(x-\tilde{x})\mathfrak{g}_k(y-\tilde{y}), \tag{7.5}$$

that is, we accept the existence of "long-range" interactions in each sub-cell $\mathscr{Y}_k$. Note that we use quotation marks because the concept of long-range interactions has to be understood with respect to each sub-cell, which is microscopic and, in this context, as a synonym of non-locality. We also notice that the index k in $\mathfrak{g}_k$ allows to characterise two different non-local frameworks occurring in each sub-cell $\mathscr{Y}_k$. For instance, as discussed above, we could enforce that the non-local interactions

exist only in one of the two sub-cells, although here we consider non-locality acting in both sub-cells.

Clearly, different forms for $\mathfrak{g}_k$ can be considered, each of which leading to diverse non-local models of diffusion. In this work, we adopt the decaying power-law [215, 19, 55, 252, 220]

$$\mathfrak{g}_k(y-\tilde{y}) := \frac{L_{\mathrm{c}}^{1-\beta_k}}{2\Gamma(1-\beta_k)}\frac{1}{|y-\tilde{y}|^{\beta_k}}, \tag{7.6}$$

where $\Gamma(\cdot)$ denotes the Euler Gamma function and $\beta_k \in]0,1[$. From here on, we set $\beta_1 = \beta_2 = \beta$, thereby obtaining $\mathfrak{g}_1 = \mathfrak{g}_2 = \mathfrak{g}$ and $\mathfrak{f}_1 = \mathfrak{f}_2 = \mathfrak{f}$. We notice that $\mathfrak{g}$ scales multiplicatively with $L_{\mathrm{c}}^{1-\beta}$ because it is expressed as a function of dimensionless variables. Accordingly, the physical dimensions of the fractional diffusivities $\mathfrak{d}_k$ are given by $[\mathfrak{d}_k] = L_{\mathrm{c}}^{-1+\beta}t_{\mathrm{c}}^{-1}$ for each $k = 1,2$. Hence, Equation (7.1) yields

$$\mathfrak{d}_k = \mathfrak{d}_{k\mathrm{R}}L_{\mathrm{c}}^{-2+(-1+\beta)} = \mathfrak{d}_{k\mathrm{R}}L_{\mathrm{c}}^{-3+\beta}. \tag{7.7}$$

7.3.1 The non-local cell problem

By considering Equations (7.5) and (7.6), the non-local cell problem is given by

$$\partial_y\left\{\boldsymbol{q}_k^{(1)}(x,y,t) + \mathbb{Q}_k^{(0)}(x,y,t)\right\} = 0, \tag{7.8a}$$

$$\vartheta_1(x,y_{\mathrm{I}},t) = \vartheta_2(x,y_{\mathrm{I}},t), \tag{7.8b}$$

$$\boldsymbol{q}_1^{(1)}(x,y_{\mathrm{I}},t) + \mathbb{Q}_1^{(0)}(x,y_{\mathrm{I}},t) = \boldsymbol{q}_2^{(1)}(x,y_{\mathrm{I}},t) + \mathbb{Q}_2^{(0)}(x,y_{\mathrm{I}},t), \tag{7.8c}$$

where $(x,y,t) \in \mathscr{X}\times\mathscr{Y}_k\times]0,t_{\mathrm{f}}[$ and

$$\boldsymbol{q}_k^{(1)}(x,y,t) = -\frac{\mathfrak{d}_{k\mathrm{R}}L_{\mathrm{c}}^{-2}\partial_x c^{(0)}(x,t)}{2\Gamma(1-\beta)}\int_{\mathscr{Y}_k}\frac{\partial_{\tilde{y}}\vartheta_k(x,\tilde{y},t)}{|y-\tilde{y}|^{\beta}}\mathrm{d}\tilde{y}, \tag{7.9a}$$

$$\mathbb{Q}_k^{(0)}(x,y,t) = -\frac{\mathfrak{d}_{k\mathrm{R}}L_{\mathrm{c}}^{-2}\partial_x c^{(0)}(x,t)}{2\Gamma(1-\beta)}\int_{\mathscr{Y}_k}\frac{1}{|y-\tilde{y}|^{\beta}}\mathrm{d}\tilde{y}. \tag{7.9b}$$

As shown in (7.9a) and (7.9b), the assumption of non-locality only at the micro-scale permits to factorise $\partial_x c^{(0)}$ from the integrals expressing $\boldsymbol{q}_k^{(1)}$ and $\mathbb{Q}_k^{(0)}$. Consequently, the auxiliary unknowns ϑ_1 and ϑ_2 can be reformulated as functions of y only, and for further use, the following notation is introduced

$$\boldsymbol{q}_k(y) := -\frac{\mathfrak{d}_{k\mathrm{R}}L_{\mathrm{c}}^{-2}}{2\Gamma(1-\beta)}\int_{\mathscr{Y}_k}\frac{\mathrm{d}_{\tilde{y}}\vartheta_k(\tilde{y})}{|y-\tilde{y}|^{\beta}}\mathrm{d}\tilde{y}, \tag{7.10a}$$

$$\mathbb{Q}_k(y) := -\frac{\mathfrak{d}_{k\mathrm{R}}L_{\mathrm{c}}^{-2}}{2\Gamma(1-\beta)}\int_{\mathscr{Y}_k}\frac{1}{|y-\tilde{y}|^{\beta}}\mathrm{d}\tilde{y}. \tag{7.10b}$$

We notice that the quantities $\mathscr{q}_k(y)$ and $\mathbb{Q}_k(y)$ defined in (7.10a) and (7.10b) represent, up to the sign, "dressed" diffusivities rather than fluxes. In fact, we may write

$$\mathscr{q}_k^{(1)}(x,y,t) = \mathscr{q}_k(y)\partial_x c^{(0)}(x,t), \tag{7.11a}$$

$$\mathbb{Q}_k^{(0)}(x,y,t) = \mathbb{Q}_k(y)\partial_x c^{(0)}(x,t). \tag{7.11b}$$

We further mention that, in the proper limit, $\mathscr{q}_k(y)$ and $\mathbb{Q}_k(y)$ return the negative of the standard diffusivities (see Remark 14). Particularly, in Equations (7.10a) and (7.10b), we recognise the symmetrised Caputo fractional derivative of order $\beta \in]0,1[$ [21]. Then, it holds true that

$$\mathscr{q}_k(y) = -\mathfrak{d}_{k\mathrm{R}} L_{\mathrm{c}}^{-2} \mathscr{D}_k^{\beta}[\vartheta_k](y), \tag{7.12a}$$

$$\mathbb{Q}_k(y) = -\mathfrak{d}_{k\mathrm{R}} L_{\mathrm{c}}^{-2} \mathscr{D}_k^{\beta}[\kappa](y), \tag{7.12b}$$

where $\kappa(y) = y$, and

$$\mathscr{D}_k^{\beta}[\phi](y) := \frac{1}{2\Gamma(1-\beta)} \int_{\mathscr{Y}_k} \frac{\mathrm{d}_{\tilde{y}}\phi(\tilde{y})}{|y-\tilde{y}|^{\beta}} \mathrm{d}\tilde{y} \tag{7.13}$$

denotes the symmetrised Caputo fractional derivative of order β of a generic differentiable function ϕ. Furthermore, we notice that $\mathbb{Q}_k(y)$ can be computed explicitly for each $k = 1,2$, and reads

$$\mathbb{Q}_k(y) = -\frac{\mathfrak{d}_{k\mathrm{R}} L_{\mathrm{c}}^{-2}}{2\Gamma(1-\beta)} \mathscr{A}_k(y;\beta), \tag{7.14}$$

where the functions $\mathscr{A}_1$ and $\mathscr{A}_2$ are given by

$$\begin{aligned} \mathscr{A}_1(y;\beta) &= \int_{\mathscr{Y}_1} \frac{1}{|y-\tilde{y}|^{\beta}} \mathrm{d}\tilde{y} = \int_0^{y_{\mathrm{I}}} \frac{1}{|y-\tilde{y}|^{\beta}} \mathrm{d}\tilde{y} \\ &= \frac{y^{1-\beta} + (y_{\mathrm{I}} - y)^{1-\beta}}{1-\beta}, \end{aligned} \tag{7.15a}$$

$$\begin{aligned} \mathscr{A}_2(y;\beta) &= \int_{\mathscr{Y}_2} \frac{1}{|y-\tilde{y}|^{\beta}} \mathrm{d}\tilde{y} = \int_{y_{\mathrm{I}}}^1 \frac{1}{|y-\tilde{y}|^{\beta}} \mathrm{d}\tilde{y} \\ &= \frac{(y - y_{\mathrm{I}})^{1-\beta} + (1-y)^{1-\beta}}{1-\beta}. \end{aligned} \tag{7.15b}$$

Because of these results, the flux (7.11b) admits the explicit expression

$$\mathbb{Q}_k^{(0)}(x,y,t) = -\frac{\mathfrak{d}_{k\mathrm{R}} L_{\mathrm{c}}^{-2}}{2\Gamma(1-\beta)} \mathscr{A}_k(y;\beta)\partial_x c^{(0)}(x,t), \tag{7.16}$$

while, for the time being, no explicit expression can be given to $\boldsymbol{q}_k$, since the functions ϑ_k are still unknowns. Upon recalling the definition (6.12), in which a given function restricted to the elementary cell is assigned in a piecewise manner, the fluxes $\mathbb{Q}_1^{(0)}$ and $\mathbb{Q}_2^{(0)}$ in (65) can be rejoined in a unique flux, whose restriction to $\mathscr{Y}$ is given by

$$\mathbb{Q}^{(0)}(x,y,t)_{|\mathscr{Y}} = \begin{cases} \mathbb{Q}_1^{(0)}(x,y,t) & y \in]0, y_{\mathrm{I}}[\,, \\ \mathbb{Q}_2^{(0)}(x,y,t) & y \in]y_{\mathrm{I}}, 1[\,. \end{cases} \tag{7.17}$$

Now, for the function $\mathbb{Q}^{(0)}$ given in (7.17), we can employ the definition of periodicity specified in (6.13), so that it holds

$$\mathbb{Q}^{(0)}(x,0^+,t) = \mathbb{Q}^{(0)}(x,1^+,t). \tag{7.18}$$

It follows from this result that $\mathbb{Q}^{(0)}$ is $\mathscr{Y}$-periodic and that such periodicity does not depend on the point y_{I} in which the interface is placed within the elementary cell.

By using the above results, the non-local cell problem (7.8a)-(7.8c) can be rewritten as

$$\mathrm{d}_y \boldsymbol{q}_k(y) = -\mathrm{d}_y \mathbb{Q}_k(y), \tag{7.19a}$$

$$\vartheta_1(y_{\mathrm{I}}) = \vartheta_2(y_{\mathrm{I}}), \tag{7.19b}$$

$$\boldsymbol{q}_1(y_{\mathrm{I}}) - \boldsymbol{q}_2(y_{\mathrm{I}}) = \frac{\left[\mathfrak{d}_{1\mathrm{R}} y_{\mathrm{I}}^{1-\beta} - \mathfrak{d}_{2\mathrm{R}}(1-y_{\mathrm{I}})^{1-\beta}\right] L_{\mathrm{c}}^{-2}}{2\Gamma(2-\beta)}, \tag{7.19c}$$

where the right-hand-side of (7.19c) is the result of the difference $\mathbb{Q}_2(y_{\mathrm{I}}) - \mathbb{Q}_1(y_{\mathrm{I}})$. We recall that all the expressions at the interface are to be understood for the values of the limits of the corresponding physical quantities for $y \to y_{\mathrm{I}}^{\pm}$. Indeed, for instance, $\mathbb{Q}_1(y_{\mathrm{I}})$ means, with a slight abuse of notation, $\mathbb{Q}_1(y_{\mathrm{I}}) = \lim_{y \to y_{\mathrm{I}}^-} \mathbb{Q}_1(y)$.

Remark 14. *We notice that for $y \in \mathscr{Y}_k$, it holds*

$$\lim_{\beta \to 1^-} \mathbb{Q}_k(y) = -\lim_{\beta \to 1^-} \frac{\mathfrak{d}_{k\mathrm{R}} L_{\mathrm{c}}^{-2} \mathscr{A}_k(y;\beta)}{2\Gamma(1-\beta)} = -\mathfrak{d}_{k\mathrm{R}} L_{\mathrm{c}}^{-2}, \tag{7.20}$$

while

$$\lim_{\beta \to 1^-} \mathbb{Q}_k(y_{\mathrm{I}}) = -\frac{\mathfrak{d}_{k\mathrm{R}} L_{\mathrm{c}}^{-2}}{2}, \tag{7.21a}$$

$$\lim_{\beta \to 1^-} [\mathbb{Q}_2(y_{\mathrm{I}}) - \mathbb{Q}_1(y_{\mathrm{I}})] = \frac{[\mathfrak{d}_{1\mathrm{R}} - \mathfrak{d}_{2\mathrm{R}}]\, L_{\mathrm{c}}^{-2}}{2}. \tag{7.21b}$$

Then, it follows from Equations (7.20)-(7.21b) *that the convergence of $\mathbb{Q}_k$ for $\beta \to 1^-$ is not uniform in $\overline{\mathscr{Y}}_k$.*

By comparing with classical results of the asymptotic homogenisation technique, the above computations suggest that, for $\beta \to 1^-$, the solution of the non-local cell problem must approach the solution of the classical, local cell problem. We notice that the 2 in the denominator of (7.21b) *does not appear in the formulation of the standard cell problem. Nevertheless, it compensates with the 2 in the denominator of the left-hand-side of* (7.19c)*, hidden in the fractional derivatives defining $\boldsymbol{q}_k$, which can be determined after finding ϑ_k.* ■

7.3.2 The homogenised equation

By taking into account Equations (7.5) and (7.6), the non-local effective coefficient can be rewritten as

$$d^{\,\mathrm{eff}}(x,\tilde{x},t) = \delta(x-\tilde{x}) \sum_{k=1}^{2} \left\langle \frac{\mathfrak{d}_{k\mathrm{R}} L_{\mathrm{c}}^{-2}}{2\Gamma(1-\beta)} \int_{\mathscr{Y}_k} \frac{1+\mathrm{d}_{\tilde{y}}\vartheta_k(\tilde{y})}{|y-\tilde{y}|^{\beta}} \mathrm{d}\tilde{y} \right\rangle_k , \tag{7.22}$$

and, therefore, according to Equation (6.43), the effective flux is given by

$$\begin{aligned} q^{\,\mathrm{eff}}(x,t) &= -\int_{\mathscr{X}_{\mathrm{h}}} d^{\,\mathrm{eff}}(x,\tilde{x},t)\partial_{\tilde{x}} c^{(0)}(\tilde{x},t)\mathrm{d}\tilde{x} \\ &= -\hat{d}^{\,\mathrm{eff}}(\beta)\partial_x c^{(0)}(x,t), \end{aligned} \tag{7.23}$$

where we have set

$$\begin{aligned} \hat{d}^{\,\mathrm{eff}}(\beta) &:= \sum_{k=1}^{2} \left\langle \frac{\mathfrak{d}_{k\mathrm{R}} L_{\mathrm{c}}^{-2}}{2\Gamma(1-\beta)} \int_{\mathscr{Y}_k} \frac{1+\mathrm{d}_{\tilde{y}}\vartheta_k(\tilde{y})}{|y-\tilde{y}|^{\beta}} \mathrm{d}\tilde{y} \right\rangle_k \\ &= \sum_{k=1}^{2} \left\langle \mathfrak{d}_{k\mathrm{R}} L_{\mathrm{c}}^{-2} \left[\frac{\mathscr{A}_k(y;\beta)}{2\Gamma(1-\beta)} + \mathscr{D}_k^{\beta}[\vartheta_k](y) \right] \right\rangle_k . \end{aligned} \tag{7.24}$$

Hence, the effective fractional diffusivity, $\hat{d}^{\,\mathrm{eff}}(\beta)$, can be expressed in terms of the symmetrised Caputo fractional derivative of ϑ_k. We notice that, in this particular case, $\hat{d}^{\,\mathrm{eff}}(\beta)$ does not depend on space and time, while it is parametrised by β. Furthermore, from its mathematical expression it is clear that it ciphers the information on the non-local interactions at the micro-scale.

Remark 15. *The form of the effective fractional diffusivity* (7.24) *recalls the relation obtained in the standard case by means of asymptotic homogenisation [34, 29, 239]. Particularly, by Fubini's theorem and Equation* (7.14)*, $\hat{d}^{\,\mathrm{eff}}(\beta)$ can be equivalently rewritten as*

$$\hat{d}^{\,\mathrm{eff}}(\beta) = \sum_{k=1}^{2} \frac{1}{|\mathscr{Y}|} \int_{\mathscr{Y}_k} \frac{\mathfrak{d}_{k\mathrm{R}} L_{\mathrm{c}}^{-2}}{2\Gamma(1-\beta)} \mathscr{A}_k(\tilde{y};\beta)[1+\mathrm{d}_{\tilde{y}}\vartheta_k(\tilde{y})]\mathrm{d}\tilde{y}$$

$$= -\sum_{k=1}^{2} \frac{1}{|\mathscr{Y}|} \int_{\mathscr{Y}_k} \mathbb{Q}_k(\tilde{y})[1 + \mathrm{d}_{\tilde{y}}\vartheta_k(\tilde{y})]\mathrm{d}\tilde{y}. \tag{7.25}$$

Therefore, taking into account Equation (7.20)*, we obtain that*

$$\lim_{\beta\to 1^-} \hat{d}^{\mathrm{eff}}(\beta) = \sum_{k=1}^{2} \frac{1}{|\mathscr{Y}|} \int_{\mathscr{Y}_k} \mathfrak{d}_{k\mathrm{R}} L_{\mathrm{c}}^{-2} \left[1 + \mathrm{d}_y\vartheta_k(y)\right] \mathrm{d}y, \tag{7.26}$$

which coincides with the effective diffusivity of a standard diffusion problem with unitary reference cell (see e.g. [72]).

Furthermore, since Equations (7.24) *and* (7.25) *provide equivalent writings for* $\hat{d}^{\mathrm{eff}}(\beta)$*, from* (7.26) *it follows that, in the limit* $\beta \to 1^-$*, the symmetrised Caputo fractional derivative of* ϑ_k *converges to the first derivative of* ϑ_k*, namely,*

$$\lim_{\beta\to 1^-} \mathscr{D}_k^{\beta}[\vartheta_k](y) = \mathrm{d}_y\vartheta_k(y), \tag{7.27}$$

and therefore, we can conclude that $\boldsymbol{q}_k^{(1)}$ *(see Equation* (7.11a)*) recovers Fick's law in bounded domains.* ■

Finally, taking into account Equation (7.24) and the initial and boundary conditions (7.2)-(7.4), the homogenised problem reads

$$\partial_t c^{(0)}(x,t) - \hat{d}^{\mathrm{eff}}(\beta)\partial_x^2 c^{(0)}(x,t) = 0, \qquad \text{in } \mathscr{X}_{\mathrm{h}}\times]0,t_{\mathrm{f}}[, \tag{7.28a}$$

$$c^{(0)}(x,0) = c_{\mathrm{in}}(x), \tag{7.28b}$$

$$c^{(0)}(0,t) = c^{(0)}(L/L_{\mathrm{c}},t) = c_{\mathrm{b}}. \tag{7.28c}$$

We notice that, in this simplified case, the non-local cell problem (7.19a)-(7.19c) and the homogenised problem (7.28a)-(7.28c) are not coupled.

7.3.3 Numerical solution

In this section, we solve numerically the mathematical model given by the non-local cell problem (7.19a)-(7.19c) and the homogenised problem (7.28a)-(7.28c). In particular, the homogenised problem is characterised by a partial differential equation, while the non-local cell problem features an integro-differential equation of fractional type.

Before going further, we notice that, in the classical homogenisation literature, the uniqueness of the solution of the cell problem is guaranteed by imposing that $\langle\vartheta_k\rangle_k$ is equal to zero. However, from a computational point of view, a more feasible condition is to fix the value of the auxiliary variables ϑ_k at one point in the cell [222]. Accordingly, here, we impose that ϑ_1 is zero at $y = 0$, and by periodicity ϑ_2 is also zero at $y = 1$.

Now, let us introduce the following spaces of test functions

$$\mathscr{W}_{12} = \left\{ v_1 \in \mathscr{H}^1(\mathscr{Y}_1) : v_1(0) = 0, v_1(y_\mathrm{I}) = v_2(y_\mathrm{I}) \right\}, \tag{7.29a}$$

$$\mathscr{W}_{21} = \left\{ v_2 \in \mathscr{H}^1(\mathscr{Y}_2) : v_2(1) = 0, v_2(y_\mathrm{I}) = v_1(y_\mathrm{I}) \right\}, \tag{7.29b}$$

where $\mathscr{H}^1(\mathscr{Y}_k)$ is the Sobolev space of functions of $L^2(\mathscr{Y}_k)$ with finite $L^2(\mathscr{Y}_k)$-norm of their distributional derivatives up to order one [247]. Then, by multiplying Equation (7.19a) by v_k, integrating over $\mathscr{Y}_k$, and adding over $k = 1,2$, we obtain

$$\begin{aligned} &- \left\{ \sum_{k=1}^{2} \int_{\mathscr{Y}_k} \cancel{q}_k(y) \mathrm{d}_y v_k(y) \mathrm{d}y \right\} + \cancel{q}_1(y) v_1(y) \big|_0^{y_\mathrm{I}} \\ &\quad + \cancel{q}_2(y) v_2(y) \big|_{y_\mathrm{I}}^1 = \left\{ \sum_{k=1}^{2} \int_{\mathscr{Y}_k} \mathbb{Q}_k(y) \mathrm{d}_y v_k(y) \mathrm{d}y \right\} \\ &\quad - \mathbb{Q}_1(y) v_1(y) \big|_0^{y_\mathrm{I}} - \mathbb{Q}_2(y) v_2(y) \big|_{y_\mathrm{I}}^1. \end{aligned} \tag{7.30}$$

Hence, due to the continuity condition at the interface (7.19c), and the restrictions made for v_k, Equation (7.30) reads

$$- \sum_{k=1}^{2} \int_{\mathscr{Y}_k} \cancel{q}_k(y) \mathrm{d}_y v_k(y) \mathrm{d}y = \sum_{k=1}^{2} \int_{\mathscr{Y}_k} \mathbb{Q}_k(y) \mathrm{d}_y v_k(y) \mathrm{d}y. \tag{7.31}$$

Equation (7.31) represents the weak formulation of the non-local cell problem (7.19a)-(7.19c), and is discretised by employing the FE technique. Therefore, we introduce for $\mathscr{Y}_1$ and $\mathscr{Y}_2$, N_1+1 and $(N_2+1)-N_1$ discretisation points, respectively, and the function bases $\{\psi_i^1\}_{i=0}^{N_1}$ and $\{\psi_i^2\}_{i=N_1}^{N_2}$, with $N_1 > 1$ and $N_2 > N_1 + 1$ and, for each $k = 1,2$,

$$\psi_i^k(y_j) = \delta_{ij} = \begin{cases} 1, & i = j, \\ 0, & i \neq j, \end{cases} \tag{7.32}$$

with $y_{N_1} = y_\mathrm{I}$. Then, the test functions v_k are approximated by

$$\check{v}_k(y) = \begin{cases} \sum_{j=1}^{N_1} \upsilon_j^1 \psi_j^1(y), & k = 1, \\ \sum_{s=N_1}^{N_2-1} \upsilon_s^2 \psi_s^2(y), & k = 2, \end{cases} \tag{7.33}$$

where υ_j^k, $k = 1,2$, are non-zero, arbitrary constants. Analogously, the approximated trial functions $\check{\vartheta}_k(y)$ are written as

$$\check{\vartheta}_k(y) = \begin{cases} \sum_{i=1}^{N_1} \omega_i^1 \psi_i^1(y), & k = 1, \\ \sum_{r=N_1}^{N_2-1} \omega_r^2 \psi_r^2(y), & k = 2, \end{cases} \tag{7.34}$$

where ω_i^k are unknown constant coefficients representing the nodal values of $\check{\vartheta}_k$. We notice that, in this particular case, the coefficients ω_i^k do not depend on time, whereas in a more general setting they should be defined as functions of time.

Next, by substituting expressions (7.34) and (7.33) into (7.31), we obtain the following system of equations for ω_i^k,

$$\sum_{j=1}^{N_1}\sum_{i=1}^{N_1} \upsilon_j^1 \left[\mathsf{L}_{ji}^1(\beta)\omega_i^1 + \mathsf{F}_j^1(\beta)\right] + \sum_{s=N_1}^{N_2-1}\sum_{r=_{N_1}}^{N_2-1} \upsilon_s^2 \left[\mathsf{L}_{sr}^2(\beta)\omega_r^2 + \mathsf{F}_s^2(\beta)\right] = 0, \tag{7.35}$$

where

$$\mathsf{L}_{ji}^k(\beta) := \mathfrak{d}_{k\mathrm{R}} L_{\mathrm{c}}^{-2} \int_{\mathscr{Y}_k} \mathrm{d}_y \psi_j^k(y) \mathscr{D}_k^\beta[\psi_i^k](y)\mathrm{d}y, \tag{7.36a}$$

$$\mathsf{F}_j^k(\beta) := \frac{\mathfrak{d}_{k\mathrm{R}} L_{\mathrm{c}}^{-2}}{2\Gamma(1-\beta)} \int_{\mathscr{Y}_k} \mathscr{A}_k(y;\beta)\mathrm{d}_y\psi_j^k(y)\mathrm{d}y, \tag{7.36b}$$

represent, for each $k = 1{,}2$, the components of the *fractional stiffness matrix* of the FE discretisation of the sub-cell $\mathscr{Y}_k$, and of the *nodal fractional force* associated with the j-th node of $\mathscr{Y}_k$, respectively.

Remark 16. *[Density and limit of $\mathsf{L}^k(\beta)$ and $\mathsf{F}^k(\beta)$]*
It is worth noting that, whereas in the standard cell problem the stiffness matrix is tridiagonal for each $k = 1{,}2$, in the present framework it is dense because the cross integrations between the derivatives of the basis functions lead to non-zero components of

$$\begin{aligned}\mathsf{L}_{ji}^k(\beta) &= \mathfrak{d}_{k\mathrm{R}} L_{\mathrm{c}}^{-2} \int_{\mathscr{Y}_k} \mathrm{d}_y \psi_j^k(y) \mathscr{D}_k^\beta[\psi_i^k](y)\mathrm{d}y \\ &= \frac{\mathfrak{d}_{k\mathrm{R}} L_{\mathrm{c}}^{-2}}{2\Gamma(1-\beta)} \int_{\mathscr{Y}_k} \mathrm{d}_y\psi_j^k(y) \left[\int_{\mathscr{Y}_k} \frac{\mathrm{d}_{\tilde{y}}\psi_i^k(\tilde{y})}{|y-\tilde{y}|^\beta}\mathrm{d}\tilde{y}\right]\mathrm{d}y,\end{aligned} \tag{7.37}$$

for each pair of j and i. This is due to the non-locality introduced by the fractional derivatives $\mathscr{D}_k^\beta[\psi_i^k]$, as reported in the far right-hand-side of Equation (7.37). Specifically, even though two discretisation nodes are far away from each other, the entries of the matrix corresponding to those nodes are non-zero. This results in a dense stiffness matrix and, the stronger the non-locality, the denser the matrix will be. Nevertheless, the fractional stiffness matrix will converge to a tridiagonal matrix when $\beta \to 1^-$. Indeed, as discussed in Remark 15, when $\beta \to 1^-$ we obtain

$$\lim_{\beta\to 1^-} \mathsf{L}_{ji}^k(\beta) = \mathfrak{d}_{k\mathrm{R}} L_{\mathrm{c}}^{-2} \int_{\mathscr{Y}_k} \mathrm{d}_y\psi_j^k(y)\mathrm{d}_y\psi_i^k(y)\mathrm{d}y. \tag{7.38}$$

Analogously, from the definition of $\mathsf{F}_j^k(\beta)$, i.e.,

$$\mathsf{F}_j^k(\beta) = \frac{\mathfrak{d}_{k\mathrm{R}} L_{\mathrm{c}}^{-2}}{2\Gamma(1-\beta)} \int_{\mathscr{Y}_k} \mathscr{A}_k(y;\beta)\mathrm{d}_y\psi_j^k(y)\mathrm{d}y$$

$$= \frac{\mathfrak{d}_{k\mathrm{R}} L_{\mathrm{c}}^{-2}}{2\Gamma(1-\beta)} \int_{\mathscr{Y}_k} \left[\int_{\mathscr{Y}_k} \frac{1}{|y-\tilde{y}|^{\beta}} \mathrm{d}\tilde{y} \right] \mathrm{d}_y \psi_j^k(y) \mathrm{d}y, \tag{7.39}$$

we infer that the existence of the non-locality function implies that the entries of $\mathsf{F}_j^k(\beta)$ *are non-zero. Furthermore, recalling that* $\lim_{\beta\to 1^-}[\mathscr{A}_k(y;\beta)/2\Gamma(1-\beta)] = 1$, *for* $y \in \mathscr{Y}_k$, *we have that*

$$\lim_{\beta\to 1^-} \mathsf{F}_j^k(\beta) = \mathfrak{d}_{k\mathrm{R}} L_{\mathrm{c}}^{-2} \int_{\mathscr{Y}_k} \mathrm{d}_y \psi_j^k(y) \mathrm{d}y. \tag{7.40}$$

Equation (7.40) *returns* 0 *for all* $j \neq N_1$ *and* $\mathfrak{d}_{k\mathrm{R}} L_{\mathrm{c}}^{-2}$ *if* $j = N_1$.

To exemplify the limit of the symmetrised Caputo fractional derivative of the bases functions, we report in Figure 7.1 a comparison of the symmetrised Caputo fractional derivative of order $\beta \in]0,1[$ *of the function*

$$\psi(y) = \begin{cases} \dfrac{y-0}{1/2-0}, & 0 \leq y < 1/2, \\ \dfrac{1-y}{1-1/2}, & 1/2 \leq y \leq 1, \end{cases} \tag{7.41}$$

which recalls a Lagrange polynomial of the first order, with the classical first derivative of the same function. ■

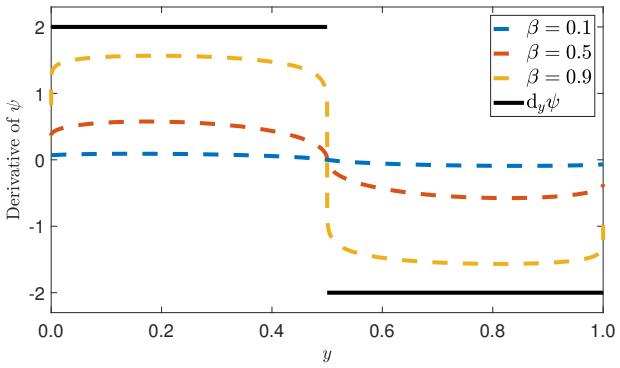

Figure 7.1: Comparison of the symmetrised Caputo fractional derivative of $\psi(y)$, for different values of $\beta \in]0,1[$, with the classical first derivative of $\psi(y)$.

Next, to obtain the algebraic form of the FE procedure, we introduce the notation

$$\{v\} := \{v_1^1, \ldots, v_{N_1-1}^1, v_{N_1}^{\mathrm{I}}, v_{N_1+1}^2, \ldots, v_{N_2-1}^2\}^{\mathrm{T}}, \tag{7.42a}$$

$$\{\omega\} := \{\omega_1^1, \ldots, \omega_{N_1-1}^1, \omega_{N_1}^{\mathrm{I}}, \omega_{N_1+1}^2, \ldots, \omega_{N_2-1}^2\}^{\mathrm{T}}, \tag{7.42b}$$

where $v_{N_1}^{\mathrm{I}} = v_{N_1}^1 = v_{N_1}^2$ and $\omega_{N_1}^{\mathrm{I}} = \omega_{N_1}^1 = \omega_{N_1}^2$ are the nodal values of the virtual concentration and of the unknown concentration at the interface, and we write the

final forms of the fractional stiffness matrix and of the fractional nodal force, as follows

$$[\mathsf{L}] := \begin{cases} [\mathsf{L}^1_{ji}], & j,i = 1,\dots,N_1-1, \\ [\mathsf{L}^1_{jN_1}], & j = 1,\dots,N_1-1, \\ [0], & j = 1,\dots,N_1-1,\ i = N_1+1,\dots,N_2-1, \\ [\mathsf{L}^1_{N_1 i}], & i = 1,\dots,N_1-1, \\ [\mathsf{L}^1_{ji} + \mathsf{L}^2_{sr}], & j,i,s,r = N_1, \\ [\mathsf{L}^2_{N_1 r}], & r = N_1+1,\dots,N_2-1, \\ [0], & s = N_1+1,\dots,N_2-1,\ r = 1,\dots,N_1-1, \\ [\mathsf{L}^2_{sN_1}], & s = N_1+1,\dots,N_2-1, \\ [\mathsf{L}^2_{sr}], & s,r = N_1+2,\dots,N_2-1, \end{cases} \tag{7.43a}$$

$$\{\mathsf{F}\} := \{F^1_1,\dots,F^1_{N_1-1},F^1_{N_1}+F^2_{N_1},F^2_{N_1+1},\dots,F^2_{N_2-1}\}^{\mathrm{T}}. \tag{7.43b}$$

Note that in (7.43a) and (7.43b), we have omitted the dependence on β, although this dependence is understood.

Then, by using the notation introduced in Equations (7.42a)-(7.43b), Equation (7.35) can be rewritten as

$$\{\upsilon\}^{\mathrm{T}}[\mathsf{L}(\beta)]\{\omega\} = -\{\upsilon\}^{\mathrm{T}}\{\mathsf{F}(\beta)\}, \tag{7.44}$$

which leads to the algebraic equation

$$[\mathsf{L}(\beta)]\{\omega\} = -\{\mathsf{F}(\beta)\}. \tag{7.45}$$

On the other hand, by using the expression for $\check{\vartheta}_k$ given in (7.34), the approximation of the effective fractional diffusivity (7.24) can be numerically calculated as

$$\begin{aligned} \hat{d}^{\mathrm{eff}}_{\mathrm{num}}(\beta) := \mathfrak{d}_{1\mathrm{R}} L_{\mathrm{c}}^{-2} \left\langle \frac{\mathscr{A}_1(y;\beta)}{2\Gamma(1-\beta)} + \sum_{i=1}^{N_1} \omega_i^1 \mathscr{D}_1^{\beta}[\psi_i^1](y) \right\rangle_1 \\ + \mathfrak{d}_{2\mathrm{R}} L_{\mathrm{c}}^{-2} \left\langle \frac{\mathscr{A}_2(y;\beta)}{2\Gamma(1-\beta)} + \sum_{r=N_1}^{N_2-1} \omega_r^2 \mathscr{D}_2^{\beta}[\psi_r^2](y) \right\rangle_2, \end{aligned} \tag{7.46}$$

which we call *numerical effective fractional diffusivity*. We provide details about the explicit form of Equations (7.45) and (7.46) in Appendix 8.2.

7.3.4 Results and discussion

In this section, we show the numerical results for the benchmark problem described above, and we discuss the influence of the micro-scale non-local interactions on the homogenised behaviour of the concentration.

To begin with, in Figure 7.2, we report the profile of the solution of the non-local cell problem (7.19a)-(7.19c), i.e., $\check{\vartheta}_k$, and compare it with the solution of the standard, local cell problem. Specifically, the solid lines distinguish the solutions of the non-local cell problem for different values of the non-locality parameter $\beta \in]0,1[$, and the dashed line represents the solution of the standard, local cell problem. In particular, the space discretisation of the computational domain was done by fixing the grid size to $h := y_i - y_{i-1} = 1.3 \times 10^{-3}$ uniformly with respect to i. We notice that the results of the finite element analysis are not affected appreciably by subsequent mesh refinements.

In Figure 7.2, we observe that the spatial distribution of $\check{\vartheta}_k$ varies with β and it converges to the solution of the local cell problem as $\beta \to 1^-$ (dashed line in Figure 7.2). This outcome is coherent with the theoretical results previously obtained in this section. Furthermore, we notice that the non-local solutions fluctuate around the local one, and they intersect each other and the local solution in symmetric points. Nevertheless, the non-local solutions are not symmetric with respect to the line $y = y_{\mathrm{I}}$.

Before going further, few words should be spent about the issue of symmetry. To this end, let us assume just for this discussion that the interface between the sub-cells, y_{I}, is not the midpoint of the cell $\mathscr{Y} =]0,1[$, and let us start with the local case (recovered for $\beta \to 1^-$). In the local case, the solution of the cell problem, here denoted by $\vartheta^{\mathrm{local}}$ and defined as $\vartheta^{\mathrm{local}}(y) = \vartheta_1^{\mathrm{local}}(y)$ for $y \in [0, y_{\mathrm{I}}]$ and $\vartheta^{\mathrm{local}}(y) = \vartheta_2^{\mathrm{local}}(y)$ for $y \in]y_{\mathrm{I}},1]$, is in general *not* symmetric because the diffusivity coefficients are distributed within the cell in a non-symmetric way (clearly, this asymmetry would disappear if the diffusivities were equal to each other). Within the framework studied here, the solution will have, indeed, the shape of a non-symmetric "roof", with an increasing straight line on $[0, y_{\mathrm{I}}]$ and a decreasing straight line on $]y_{\mathrm{I}},1]$, whose slopes have different sign and different absolute value. In other words, the inequality $\mathfrak{d}_{1\mathrm{R}} \neq \mathfrak{d}_{2\mathrm{R}}$ and the position of the interface break the symmetry that the solution would have in the homogeneous case (the solution of the problem at hand would trivially boil down to a constant in the homogeneous case). Symmetry, however, can be partially restored if the interface is assumed to be placed at the midpoint, as is the case in our simulations. This condition, indeed, places a geometric constraint that forces the solution to be symmetric, thereby acquiring the shape of a symmetric "roof", with the slope of the straight line on $[0, y_{\mathrm{I}}]$ being the opposite of the slope of the straight line on $]y_{\mathrm{I}},1]$. This means that we have passed from the continuous symmetry of the homogeneous solution to the discrete symmetry of the heterogeneous solution with interface in the midpoint of the cell.

The picture just described changes considerably when the non-local case is studied. Indeed, for $\beta \in]0,1[$, the fractional derivatives featuring in the non-local cell problem are an additional source of symmetry breaking that, together with the heterogeneity of the diffusivity, make the solution even more non-symmetric. This

remains true even though y_I is the midpoint of the cell. More importantly, since the local solution is symmetric for $y_\mathrm{I} = 1/2$, in spite of the heterogeneity of the diffusivity, this setting singles out the contribution of the fractional derivatives to the symmetry breaking of the problem. We believe that asymmetry of the non-local solution, which decreases in β may be ascribable to an interplay between non-locality and heterogeneity: in the sub-cell in which the medium is more diffusive, the solution is "stiffer" which results into moderate deviations from the standard solution; on the other hand, in the sub-cell in which the diffusivity is smaller, the solution is more "compliant", thereby producing large deviations from the local solution.

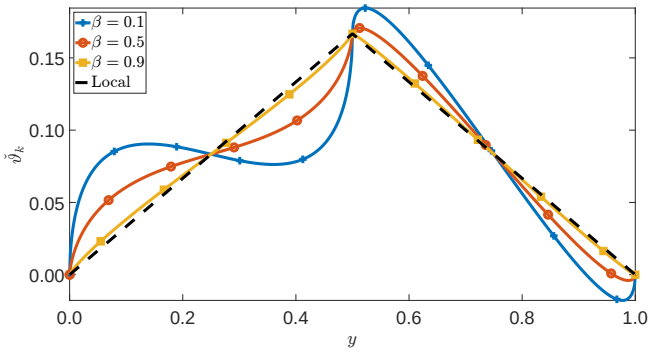

Figure 7.2: Solution of the non-local cell problem and comparison with the solution of the standard cell problem.

Now, once $\check{\vartheta}_k$ is known, we can compute the effective fractional diffusivity $\hat{d}^{\mathrm{eff}}_{\mathrm{num}}$ as prescribed by formula (7.46). Particularly, in Figure 7.3, we plot the values of this homogenised coefficient for varying $\beta \in [0,1]$ and compare them with the classical effective diffusivity, i.e. the one resulting from the local case. Specifically, a closer look at the data reported in Figure 7.3 reveals that, for increasing β, the value of the effective fractional diffusivity resulting from a non-local setting is higher. In particular, as discussed in Remark 15, as β tends to 1 from below, the approximated effective fractional diffusivity converges to the standard effective one given by the local case.

We notice that for $\beta = 0$ the auxiliary problem is ill-posed and, thus, $\check{\vartheta}_k$ cannot be determined. This is also reflected by the fact that the stiffness matrix of the problem, $\mathsf{L}(0)$, becomes singular for $\beta = 0$, and $\check{\vartheta}_k$ becomes non-differentiable at $y = y_\mathrm{I}$ and at the boundaries of the cell. On the other hand, for $\beta > 0$, the gradients of $\check{\vartheta}_k$ exist at these points but their magnitude increases for $\beta \to 0^+$. Nevertheless, it is worth remarking that, for very small values of β, the numerical solution almost does not change. Particularly, the L^∞-norm of the error between the numerical solutions for $\beta = 10^{-8}$ and $\beta = 10^{-3}$ is of the order of 10^{-4}. In addition to these considerations, we would like to point out that neither $\check{\vartheta}_k$ nor its gradient are observable physical quantities. Rather, $\check{\vartheta}_k(y)$ is just an auxiliary quantity for determining the observables $\boldsymbol{q}^{(1)}_k(x,y,t)$, $\boldsymbol{q}_k(y)$, and more importantly,

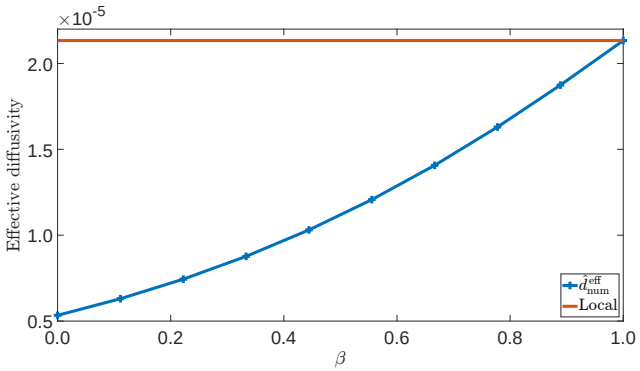

Figure 7.3: Effective fractional diffusivity for ten different values of $\beta \in [0,1]$, and comparison with the standard effective diffusivity resulting from the local counterpart of the cell problem (7.19c)-(7.19a).

the effective fractional diffusivity and the homogenised solution. To this end, we notice that, in fact, $\hat{d}^{\text{eff}}(\beta)$ and $c^{(0)}$ are well behaved for all values of $\beta \in]0,1[$ as shown in Figures 7.3 and 7.4, and also for $\beta = 0$. Specifically, in spite of the technical difficulty for $\beta = 0$, which makes the employment of the FE method impossible, it is still possible to determine the variations

$$\begin{aligned} \vartheta_1(y_{\text{I}}) - \vartheta_1(0) = \vartheta_1(y_{\text{I}}) = -\vartheta_2(1) + \vartheta_2(y_{\text{I}}) = \vartheta_2(y_{\text{I}}) \\ = \frac{\mathfrak{d}_{2\text{R}} - \mathfrak{d}_{1\text{R}}}{2(\mathfrak{d}_{1\text{R}} + \mathfrak{d}_{2\text{R}})}, \end{aligned} \tag{7.47}$$

which return the value of ϑ_k at the interface. This calculation allows us to compute, even in this limit case, the effective diffusivity coefficient $\hat{d}^{\text{eff}}(\beta)$, which, as shown in Equation (7.24), we rephrase as a function of β and, for $\beta = 0$, reads

$$\hat{d}_0^{\text{eff}} = \frac{\mathfrak{d}_{1\text{R}}\mathfrak{d}_{2\text{R}}}{2(\mathfrak{d}_{1\text{R}} + \mathfrak{d}_{2\text{R}})L_{\text{c}}^2}. \tag{7.48}$$

Since, as per Figure 7.3, which is the plot of Equation (7.24), $\hat{d}^{\text{eff}}(\beta)$ is a continuous and monotonically increasing function of $\beta \in [0,1]$, it occurs that the value $\hat{d}_0^{\text{eff}}$ represents the absolute minimum of the effective diffusivity coefficient, i.e., $\hat{d}_0^{\text{eff}} = \min_{\beta\in[0,1]}\{\hat{d}^{\text{eff}}(\beta)\}$, and the absolute maximum is $\hat{d}^{\text{eff}}(1) = \max_{\beta\in[0,1]}\{\hat{d}^{\text{eff}}(\beta)\}$.

The above result describes, for each $\beta \in [0,1]$, the influence of the micro-scale non-locality on the macroscopic distribution of the concentration $c^{(0)}$ (see Figure 7.4). In particular, for β tending towards zero, i.e., for increasing "strength" of the micro-scale non-locality, the macro-scale diffusion of the considered substance is hindered, and $c^{(0)}(x,t)$ consistently tends to vary rather slowly in time. On the contrary, in the limit case $\beta \to 1^-$, $c^{(0)}(x,t)$ varies more rapidly in time, since the diffusion tends to acquire the "classical" behaviour predicted by Fick's law (see

Figure 7.4). In this respect, the consideration of non-local interactions at the micro-scale influences the way in which diffusion takes place in the composite medium. Returning to the FRAP experiment in the context of the benchmark problem, this theoretical behaviour implies that the recovering pattern of chemical species after being photobleached is slower for β near 0, whereas it is faster for β close to 1, thereby simulating a standard diffusion process.

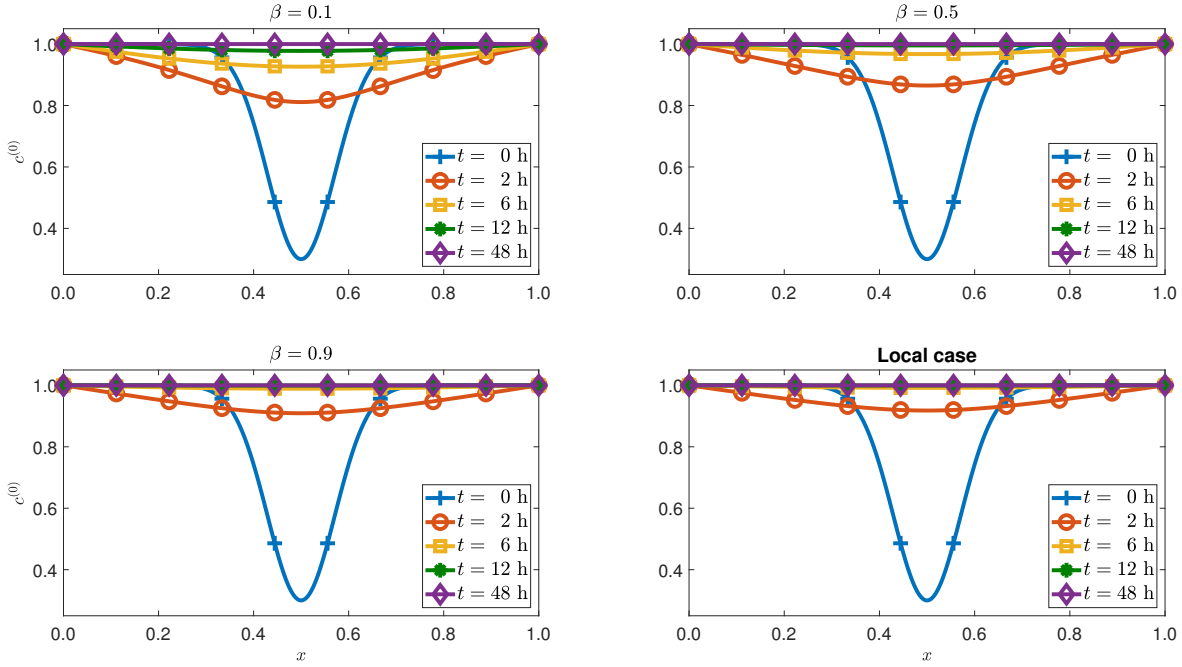

Figure 7.4: Numerical solution of the homogenised equation for different values of β and different times. The diffusion of chemical species is rather slow for $\beta = 0.1$, while it is much faster for $\beta = 0.9$, thereby conducing to the standard diffusion predicted by Fick's law.

7.4 Benchmark problem II: Macro-scale non-locality

In this section, we assume that the non-local interactions are present at the macro-scale only. Thus, by specialising $\mathfrak{f}_{\alpha,\beta_k}$ in (6.17b) to the limit case $\beta_k \to 1^-$, we consider the following form for the non-locality function

$$\mathfrak{f}_\alpha(x - \tilde{x}, y - \tilde{y}) = \mathfrak{h}_\alpha(x - \tilde{x})\delta(y - \tilde{y}). \tag{7.49}$$

Hence, since $\mathfrak{h}_\alpha$ depends only on the difference $x - \tilde{x}$, the non-local character of the diffusion process is accounted for at the macroscopic level only, and similarly

to what was done in the previous section, we write

$$\mathfrak{h}_\alpha(x-\tilde{x}) := \frac{L_\mathrm{c}^{1-\alpha}}{2\Gamma(1-\alpha)}\frac{1}{|x-\tilde{x}|^\alpha}. \tag{7.50}$$

In this particular case, the physical dimensions of the fractional diffusivities $\mathfrak{d}_k$ are $[\mathfrak{d}_k] = L_\mathrm{c}^{-1+\alpha}t_\mathrm{c}^{-1}$ and hence, from (7.1), we have that

$$\mathfrak{d}_k = \mathfrak{d}_{k\mathrm{R}}L_\mathrm{c}^{-3+\alpha}. \tag{7.51}$$

7.4.1 The cell problem

By considering the expressions (7.49)-(7.51), the non-local cell problem (6.31a)-(6.31c) rewrites

$$\partial_y\left\{\boldsymbol{q}_k^{(1)}(x,y,t) + \mathbb{Q}_k^{(0)}(x,y,t)\right\} = 0, \tag{7.52a}$$

$$\vartheta_1(x,y_\mathrm{I},t) = \vartheta_2(x,y_\mathrm{I},t), \tag{7.52b}$$

$$\boldsymbol{q}_1^{(1)}(x,y_\mathrm{I},t) + \mathbb{Q}_1^{(0)}(x,y_\mathrm{I},t) = \boldsymbol{q}_2^{(1)}(x,y_\mathrm{I},t) + \mathbb{Q}_2^{(0)}(x,y_\mathrm{I},t), \tag{7.52c}$$

where $(x,y,t) \in \mathscr{X}\times\mathscr{Y}_k\times]0,t_\mathrm{f}[$ and

$$\boldsymbol{q}_k^{(1)}(x,y,t) = -\frac{\mathfrak{d}_{k\mathrm{R}}L_\mathrm{c}^{-2}}{2\Gamma(1-\alpha)}\int_{\mathscr{X}}\frac{\partial_{\tilde{x}}c^{(0)}(\tilde{x},t)}{|x-\tilde{x}|^\alpha}\partial_y\vartheta_k(\tilde{x},y,t)\mathrm{d}\tilde{x}, \tag{7.53a}$$

$$\begin{aligned}\mathbb{Q}_k^{(0)}(x,y,t) &= -\frac{\mathfrak{d}_{k\mathrm{R}}L_\mathrm{c}^{-2}}{2\Gamma(1-\alpha)}\int_{\mathscr{X}}\frac{\partial_{\tilde{x}}c^{(0)}(\tilde{x},t)}{|x-\tilde{x}|^\alpha}\mathrm{d}\tilde{x}\\ &= -\mathfrak{d}_{k\mathrm{R}}L_\mathrm{c}^{-2}\mathscr{D}^\alpha[c^{(0)}](x,t).\end{aligned} \tag{7.53b}$$

In (7.53b), $\mathscr{D}^\alpha[c^{(0)}]$ represents the symmetrised Caputo fractional derivative of order $\alpha\in]0,1[$ of $c^{(0)}$.

Particularly, the computational complexity of the above cell problem is significantly reduced if the solution ϑ_k is x-constant (which in the present framework also implies that it is constant in time). Then, with a slight abuse of notation we write $\vartheta_k(x,y,t) = \vartheta_k(y)$, and $\boldsymbol{q}_k^{(1)}$ in (7.53a) becomes

$$\begin{aligned}\boldsymbol{q}_k^{(1)}(x,y,t) &= -\mathfrak{d}_{k\mathrm{R}}L_\mathrm{c}^{-2}\mathrm{d}_y\vartheta_k(y)\left[\frac{1}{2\Gamma(1-\alpha)}\int_{\mathscr{X}_\mathrm{h}}\frac{\partial_{\tilde{x}}c^{(0)}(\tilde{x},t)}{|x-\tilde{x}|^\alpha}\mathrm{d}\tilde{x}\right]\\ &= -\mathfrak{d}_{k\mathrm{R}}L_\mathrm{c}^{-2}\mathrm{d}_y\vartheta_k(y)\mathscr{D}^\alpha[c^{(0)}](x,t),\end{aligned} \tag{7.54}$$

while Equation (7.52a) rewrites

$$-\mathrm{d}_y\left\{\mathfrak{d}_{k\mathrm{R}}L_\mathrm{c}^{-2}[1+\mathrm{d}_y\vartheta_k(y)]\right\}\mathscr{D}^\alpha[c^{(0)}](x,t) = 0. \tag{7.55}$$

We notice that $c^{(0)}(x,t) \equiv c^{(0)}(t)$ is the only solution of the equation $\mathscr{D}^{\alpha}[c^{(0)}](x,t) = 0$ [19]. Therefore, by excluding this case, the cell problem can be written in the more standard form

$$-\mathrm{d}_y\left\{\mathfrak{d}_{k\mathrm{R}} L_{\mathrm{c}}^{-2}[1+\mathrm{d}_y\vartheta_k(y)]\right\} = 0, \tag{7.56a}$$

$$\vartheta_1(y_{\mathrm{I}}) = \vartheta_2(y_{\mathrm{I}}), \tag{7.56b}$$

$$-\mathfrak{d}_{1\mathrm{R}} L_{\mathrm{c}}^{-2}\mathrm{d}_y\vartheta_1(y_{\mathrm{I}}) - \mathfrak{d}_{1\mathrm{R}} L_{\mathrm{c}}^{-2} = -\mathfrak{d}_{2\mathrm{R}} L_{\mathrm{c}}^{-2}\mathrm{d}_y\vartheta_2(y_{\mathrm{I}}) - \mathfrak{d}_{2\mathrm{R}} L_{\mathrm{c}}^{-2}. \tag{7.56c}$$

In this specific case, the analytical solution of the cell problem (7.56a)-(7.56c) can be found by using standard techniques for differential equations. However, since our scope is to find the effective coefficient, this is not necessary. Indeed, from (7.56a) we can deduce that

$$\mathfrak{d}_{k\mathrm{R}} L_{\mathrm{c}}^{-2}[1+\mathrm{d}_y\vartheta_k(y)] = a_k, \tag{7.57}$$

where a_k, with $k = 1{,}2$, are two constants to be determined. In particular, substituting (7.57) in (7.56c) yields $a_1 = a_2 \equiv a$, and the constant a can be computed by invoking periodicity and (7.56b). In fact, from (7.57), it follows that

$$\mathrm{d}_y\vartheta_k(y) = \frac{a_k}{\mathfrak{d}_{k\mathrm{R}} L_{\mathrm{c}}^{-2}} - 1, \tag{7.58}$$

and, by applying the operators defined in (6.34) to the last equation, we have

$$0 = \sum_{k=1}^{2} \langle \mathrm{d}_y\vartheta_k \rangle_k = \frac{a}{\mathfrak{d}_{1\mathrm{R}} L_{\mathrm{c}}^{-2}} y_{\mathrm{I}} + \frac{a}{\mathfrak{d}_{2\mathrm{R}} L_{\mathrm{c}}^{-2}}(1-y_{\mathrm{I}}) - 1, \tag{7.59}$$

which implies that

$$a = \frac{\mathfrak{d}_{1\mathrm{R}}\mathfrak{d}_{2\mathrm{R}} L_{\mathrm{c}}^{-2}}{\mathfrak{d}_{2\mathrm{R}} y_{\mathrm{I}} + \mathfrak{d}_{1\mathrm{R}}(1-y_{\mathrm{I}})}. \tag{7.60}$$

Therefore, after substitution of (7.49) and (7.50) into Equation (6.44), and using (7.57) and (7.60), the non-local effective coefficient can be computed as

$$\begin{aligned} d^{\mathrm{eff}}(x,\tilde{x}) &= \frac{1}{2\Gamma(1-\alpha)} \frac{1}{|x-\tilde{x}|^{\alpha}} \sum_{k=1}^{2} \left\langle \mathfrak{d}_{k\mathrm{R}} L_{\mathrm{c}}^{-2}[1+\mathrm{d}_y\vartheta_k(y)] \right\rangle_k \\ &= \frac{\mathfrak{d}_{1\mathrm{R}}\mathfrak{d}_{2\mathrm{R}} L_{\mathrm{c}}^{-2}}{\mathfrak{d}_{2\mathrm{R}} y_{\mathrm{I}} + \mathfrak{d}_{1\mathrm{R}}(1-y_{\mathrm{I}})} \frac{1}{2\Gamma(1-\alpha)} \frac{1}{|x-\tilde{x}|^{\alpha}}. \end{aligned} \tag{7.61}$$

It is worth mentioning that, even though, in this particular formulation, the cell and the homogenised problems have been decoupled, the non-local effective diffusivity (7.61) is still influenced by the non-local interactions occurring at the macroscopic level through the scalar function $|x-\tilde{x}|^{-\alpha}$. Note also that the last two factors of $d^{\mathrm{eff}}(x,\tilde{x})$ in (7.61) are the kernel of the operator defined in (7.50).

7.4.2 The homogenised equation

By using the previous results, the effective non-local mass flux can be recast in the form

$$\begin{aligned} q^{\text{eff}}(x,t) &= -\int_{\mathscr{X}_{\text{h}}} d^{\text{eff}}(x,\tilde{x})\partial_{\tilde{x}}c^{(0)}(\tilde{x},t)\mathrm{d}\tilde{x} \\ &= -\hat{d}_{\text{st}}^{\text{eff}}\frac{1}{2\Gamma(1-\alpha)}\int_{\mathscr{X}_{\text{h}}}\frac{\partial_{\tilde{x}}c^{(0)}(\tilde{x},t)}{|x-\tilde{x}|^{\alpha}}\mathrm{d}\tilde{x} \\ &= -\hat{d}_{\text{st}}^{\text{eff}}\mathscr{D}^{\alpha}[c^{(0)}](x,t), \end{aligned} \tag{7.62}$$

which is thus entirely determined by the symmetrised Caputo fractional derivative of order α of the leading order concentration $c^{(0)}$ and by the effective diffusivity coefficient

$$\hat{d}_{\text{st}}^{\text{eff}} := \frac{\mathfrak{d}_{1\text{R}}\mathfrak{d}_{2\text{R}}L_{\text{c}}^{-2}}{\mathfrak{d}_{2\text{R}}y_{\text{I}}+\mathfrak{d}_{1\text{R}}(1-y_{\text{I}})}. \tag{7.63}$$

We notice that definition (7.63) coincides (not surprisingly) with the constant a defined in Equation (7.60), and with the standard effective diffusivity [34, 72, 219]. Besides, the physical dimensions of $\hat{d}_{\text{st}}^{\text{eff}}$ are those of the reciprocal of time.

Finally, the homogenised equation (6.45a), with the boundary and initial conditions given in (7.2) and (7.4), reduces to

$$\partial_t c^{(0)}(x,t) - \partial_x\left\{\hat{d}_{\text{st}}^{\text{eff}}\mathscr{D}^{\alpha}[c^{(0)}](x,t)\right\} = 0, \tag{7.64a}$$

$$c^{(0)}(x,0) = c_{\text{in}}(x), \tag{7.64b}$$

$$c^{(0)}(0,t) = c^{(0)}(L/L_{\text{c}},t) = c_{\text{b}}. \tag{7.64c}$$

7.4.3 Numerical solution

In this section, we find the numerical solution of the non-local, homogenised problem (7.64a)-(7.64c) by means of FE methods. As we previously mentioned, in this context, the effective diffusivity can be found without recurring to solve the cell problem (compare Equations (7.63) and (7.60)).

To start with, we discretise the time interval $[0,t_{\text{f}}]$ in M subintervals, which we assume of equal amplitude τ. Then, for simplicity of notation, we set $c^{(0)}(x,t_m) = u^m(x)$ and we adopt an implicit Euler scheme for Equation (7.64a) which is thus approximated as

$$u^{m+1}(x) - \tau\hat{d}_{\text{st}}^{\text{eff}}\partial_x\left\{\mathscr{D}^{\alpha}[u^{m+1}](x)\right\} = u^m(x). \tag{7.65}$$

Next, by introducing the space of test functions [247]

$$\mathscr{V} = \{v\in\mathscr{H}^1(\mathscr{X}_{\text{h}}) : v|_{\partial\mathscr{X}_{\text{h}}} = 0\} \equiv \mathscr{H}_0^1(\mathscr{X}_{\text{h}}), \tag{7.66}$$

where $\mathscr{H}^1(\mathscr{X}_\mathrm{h})$ is defined analogously to $\mathscr{H}^1(\mathscr{Y}_k)$, we put Equation (7.65) in weak form. To this end, we multiply Equation (7.65) by the test function $v \in \mathscr{V}$, and after integrating over $\mathscr{X}_\mathrm{h}$, we find

$$\int_{\mathscr{X}_\mathrm{h}} u^{m+1}(x)v(x)\mathrm{d}x + \tau\hat{d}_\mathrm{st}^\mathrm{eff}\int_{\mathscr{X}_\mathrm{h}} \mathscr{D}^\alpha[u^{m+1}](x)\mathrm{d}_x v(x)\mathrm{d}x = \int_{\mathscr{X}_\mathrm{h}} u^m(x)v(x)\mathrm{d}x. \quad (7.67)$$

Next, we discretise the spatial domain $\mathscr{X}_\mathrm{h}$ in N finite elements, and introduce the function basis $\{\psi_i\}_{i=0}^N$, with $\psi_i(x_j) = \delta_{ij}$ and $i, j = 0, \ldots, N$. Then, we approximate $v(x)$, the initial condition $u^0(x)$, and $u^m(x)$, for all m, as

$$\check{v}(x) := \sum_{i=1}^{N-1} \upsilon_i\psi_i(x), \quad (7.68a)$$

$$\check{u}^0(x) := c_\mathrm{b}\psi_0(x) + \sum_{i=1}^{N-1} c_\mathrm{in}(x_i)\psi_i(x) + c_\mathrm{b}\psi_N(x), \quad (7.68b)$$

$$\check{u}^m(x) := c_\mathrm{b}\psi_0(x) + \sum_{i=1}^{N-1} \omega_i^m\psi_i(x) + c_\mathrm{b}\psi_N(x), \quad (7.68c)$$

where ω_i^m, with $m = 1, \ldots, M+1$, are constant coefficients to be determined and $t_{M+1} = t_\mathrm{f}$. Thus, by substituting (7.68a) and (7.68c) into (7.67), and adopting a standard procedure in FE, we find

$$\sum_{j=1}^{N-1}\sum_{i=1}^{N-1} \upsilon_j\left[\mathsf{M}_{ji} + \tau\mathsf{L}_{ji}(\alpha)\right]\omega_i^{m+1} = \sum_{j=1}^{N-1}\sum_{i=1}^{N-1} \upsilon_j\mathsf{M}_{ji}\omega_i^m - \sum_{j=1}^{N-1} \upsilon_j\tau\mathsf{F}_j(\alpha), \quad (7.69)$$

where

$$\mathsf{L}_{ji}(\alpha) := \hat{d}_\mathrm{st}^\mathrm{eff}\int_{\mathscr{X}_\mathrm{h}} \mathrm{d}_x\psi_j(x)\mathscr{D}^\alpha[\psi_i](x)\mathrm{d}x, \quad (7.70a)$$

$$\mathsf{M}_{ji} := \int_{\mathscr{X}_\mathrm{h}} \psi_j(x)\psi_i(x)\mathrm{d}x, \quad (7.70b)$$

$$\mathsf{F}_j(\alpha) := \hat{d}_\mathrm{st}^\mathrm{eff}\int_{\mathscr{X}_\mathrm{h}} \left\{c_\mathrm{b}\mathscr{D}^\alpha[\psi_0](x) + c_\mathrm{b}\mathscr{D}^\alpha[\psi_N](x)\right\}\mathrm{d}_x\psi_j(x)\mathrm{d}x. \quad (7.70c)$$

It is worth to remark that both the stiffness matrix $\mathsf{L}_{ji}(\alpha)$ and the nodal force $\mathsf{F}_j(\alpha)$ depend on the parameter $\alpha \in]0,1[$.

Then, Equation (7.69) can be rewritten as

$$\{\upsilon\}^\mathrm{T}\left([\mathsf{M}] + \tau[\mathsf{L}(\alpha)]\right)\{\omega^{m+1}\} = \{\upsilon\}^\mathrm{T}\left([\mathsf{M}]\{\omega^m\} - \tau\{\mathsf{F}(\alpha)\}\right), \quad (7.71)$$

which, by factorising $\{\upsilon\}^\mathrm{T}$, leads to the linear system

$$\left([\mathsf{M}] + \tau[\mathsf{L}(\alpha)]\right)\{\omega^{m+1}\} = [\mathsf{M}]\{\omega^m\} - \tau\{\mathsf{F}(\alpha)\}. \quad (7.72)$$

Details about the explicit form of Equation (7.72) are provided in Appendix 8.3.

7.4.4 Results and discussion

We notice that, in the present framework, to find the numerical solution of the homogenised problem, we only need to know $\hat{d}_{\mathrm{st}}^{\mathrm{eff}}$ as prescribed by Equation (7.63). Particularly, by using the values reported in Table 7.1, we obtain

$$\hat{d}_{\mathrm{st}}^{\mathrm{eff}} = \frac{\mathfrak{d}_{1\mathrm{R}}\mathfrak{d}_{2\mathrm{R}}L_{\mathrm{c}}^{-2}}{\mathfrak{d}_{2\mathrm{R}}y_{\mathrm{I}} + \mathfrak{d}_{1\mathrm{R}}(1-y_{\mathrm{I}})} = 2.1\bar{3} \times 10^{-5}\,\mathrm{s}^{-1}. \tag{7.73}$$

Then, in Figure 7.5, we show the distribution of $c^{(0)}$ for different values of $\alpha \in]0{,}1[$ and for different instants of time. According to the plots, and similarly to the previous benchmark problem, the variation of the non-locality parameter influences the way in which diffusion takes place, and in which the stationary state is attained. That is, the progression of the solution towards the stationary states for $\alpha = 0.1$ is much slower than in the case determined by $\alpha = 0.9$. In particular, when α approaches 1 from below, the standard diffusion is recovered. We remark that, although we have imposed an initial concentration with very small spatial derivative at the boundary, once time initiates to increase, the tails of the concentration profile tend to raise. This behaviour can be explained by the production of concentration gradients that are needed for the chemical species to diffuse, in this case, towards the centre of the specimen. However, such gradients tend to "turn off" themselves in the course of time since the concentration has to move towards its stationary value.

It is worth noticing that the way in which the non-local interactions are introduced influences the diffusion profile of the chemical species (see Figure 7.6). Indeed, when considering the existence of non-local interactions at the micro-scale, these are ciphered into the effective coefficient $\hat{d}^{\mathrm{eff}}(\beta)$, which is parametrised by β, while the effective mass flux has the classical form given by Fick's law. On the other hand, the consideration of long-range interactions at the macro-scale leads, as prescribed by (7.61), to a non-local effective diffusivity that depends on the spatial points, and thus to a homogenised equation of fractional type for the leading order of concentration. In this case, as shown in Figure 7.6, there is a strong memory of the initial concentration, that is, the fractional operators appearing in Equation (7.64a) help to preserve the information of the initial distribution of chemical species as time passes. This phenomenon is less pronounced when the non-locality is considered only at the micro-scale, and therefore, for $t \leq 6\,\mathrm{h}$ the diffusion near the boundary of the composite is slower. We further notice that, by comparing the curves resulting from the benchmark problem I with the ones from the standard, local framework, the assumption of the non-locality at the micro-scale produces a slower diffusion of the species. Thus, we can conclude that the consideration of non-local effects at the micro-structure impacts the evolution of the concentration at the macro-scale.

Finally, we remark that for $\alpha \to 1^-$ and $\beta \to 1^-$ both benchmark tests restore

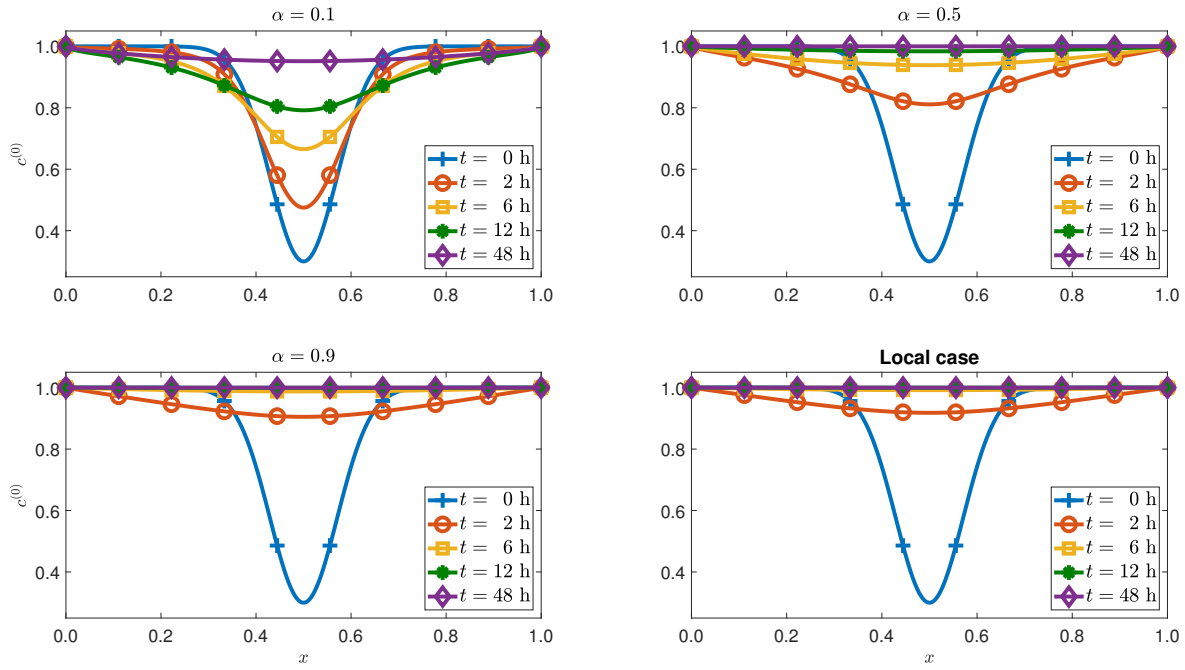

Figure 7.5: Numerical solution of the homogenised equation for different values of α and different times. For $\alpha = 0.1$, there is a strong memory of the initial distribution, whereas for α near 1 the standard diffusion is attained.

the standard diffusion given by Fick's law and, thus, they become indistinguishable in the limit. For this reason, in Figure 7.6, we report only the cases in which there is a strong non-locality, that is when α and β are near zero.

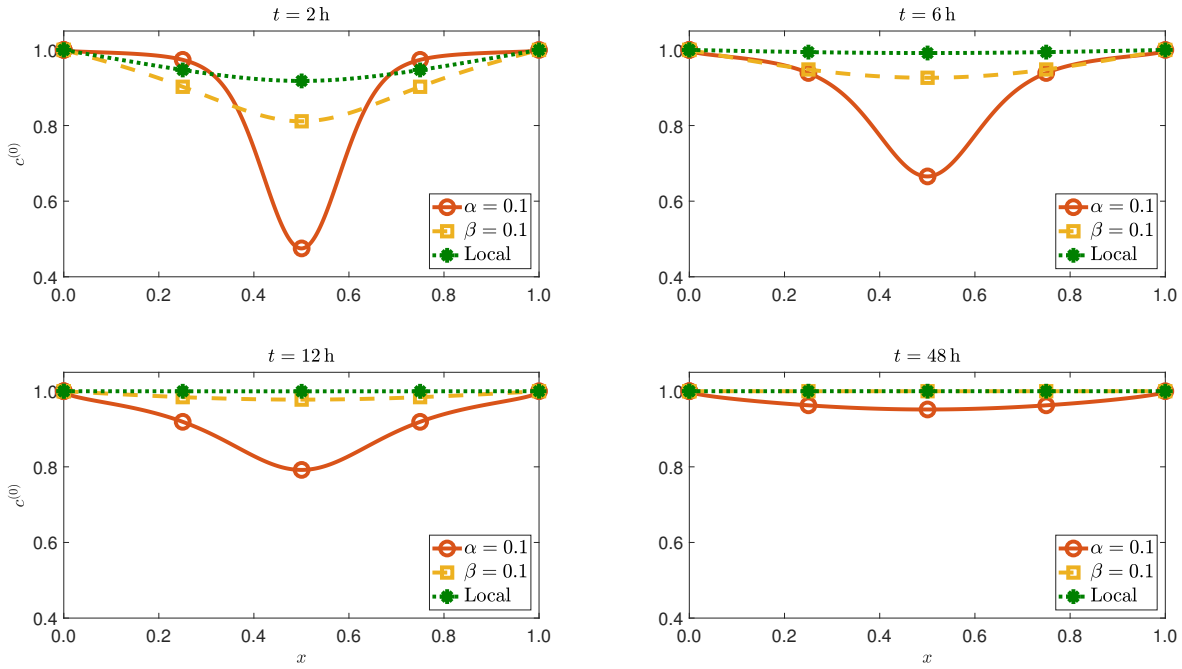

Figure 7.6: Comparison of the numerical solutions resulting from the benchmark problems I and II with the ones from the local framework. The way in which non-locality is introduced influences the diffusion of the chemical species.

Chapter 8

FE discretisation of the non-local cell and homogenised problems

The work reported in this chapter has been previously published in [241].

8.1 Introduction

As remarked in [220], the numerics of fractional diffusion in bounded domains requires special care because of the way in which the integro-differential operators featuring in the constitutive laws are to be handled, e.g., within FE methods. These difficulties increase if the medium in which fractional diffusion takes place is heterogeneous, as is the case in this work. A standard way of addressing numerically fractional differential equations in bounded domains is to have recourse to finite differences, specifically in the form of Grünwald-Letnikov schemes (see, e.g., [182, 196]), although we are aware of works in which FE procedures are adopted [244, 151, 106, 220]. However, this is not done for fractional differential equations in a multi-scale context, at least to our knowledge.

In the case of the benchmark problem I (see Section 7.3), to solve Equations (7.19a)-(7.19c) in a bounded domain, the techniques based on Fourier and Laplace transforms are of little help and, consequently, we solve the non-local cell problem by means of a FE scheme which accounts for fractional derivatives and interface conditions. Since the homogenised problem (7.28a)-(7.28c) involves classical FE techniques, in what follows we report some details concerning the matrices and vectors that arise from the discretisation of the non-local cell problem (7.19a)-(7.19c). Besides, we show how to compute the discretised non-local effective diffusivity defined in (7.24).

On the other hand, here, we also show some specifics in the computation of

the matrices and vectors resulting from the discretisation concerning the benchmark problem II (see Section 7.4). In this particular case, we concentrate on the homogenised equation because it features a derivative of fractional type since the cell problem, described by Equations (7.56a)-(7.56c), takes the form of an ordinary differential equation for which it is possible to find an analytical solution by considering a standard approach.

8.2 Benchmark problem I

Here, we calculate the matrices appearing in Equation (7.45) and the non-local effective diffusivity (7.46). Firstly, we recall that the system (7.45) reads

$$[\mathsf{L}(\beta)]\{\omega\} = -\{\mathsf{F}(\beta)\}, \tag{8.1}$$

with

$$\mathsf{L}^k_{ji}(\beta) = \mathfrak{d}_{k\mathrm{R}} L_{\mathrm{c}}^{-2} \int_{\mathscr{Y}_k} \mathrm{d}_y \psi^k_j(y) \mathscr{D}^\beta_k[\psi^k_i](y) \mathrm{d}y, \tag{8.2a}$$

$$\mathsf{F}^k_j(\beta) = \frac{\mathfrak{d}_{k\mathrm{R}} L_{\mathrm{c}}^{-2}}{2\Gamma(1-\beta)} \int_{\mathscr{Y}_k} \mathscr{A}_k(y;\beta) \mathrm{d}_y \psi^k_j(y) \mathrm{d}y. \tag{8.2b}$$

For the sake of simplicity, let us consider that the basis functions are Lagrange polynomials of the first order,

$$\psi^k_i(y) = \begin{cases} \dfrac{y - y_{i-1}}{y_i - y_{i-1}}, & y_{i-1} \leq y < y_i, \\ \dfrac{y_{i+1} - y}{y_{i+1} - y_i}, & y_i \leq y \leq y_{i+1}, \\ 0, & \text{elsewhere}, \end{cases} \tag{8.3}$$

for $i = 1, \ldots, N_1 - 1$ if $k = 1$, and $i = N_1 + 1, \ldots, N_2 - 1$ for $k = 2$, and at the interface $y_{N_1} = y_{\mathrm{I}}$, we prescribe

$$\psi^1_{N_1}(y) = \begin{cases} \dfrac{y - y_{N_1-1}}{y_{N_1} - y_{N_1-1}}, & y_{N_1-1} \leq y < y_{N_1}, \\ 0, & \text{elsewhere}, \end{cases} \tag{8.4a}$$

$$\psi^2_{N_1}(y) = \begin{cases} \dfrac{y_{N_1+1} - y}{y_{N_1+1} - y_{N_1}}, & y_{N_1} \leq y \leq y_{N_1+1}, \\ 0, & \text{elsewhere}. \end{cases} \tag{8.4b}$$

Then, from the above expressions, the fractional stiffness matrices $\mathsf{L}^k_{ji}(\beta)$ are computed in two steps. First, we calculate the symmetrised Caputo fractional derivatives of (8.3)-(8.4b) and then, we substitute the results into (8.2a) and (8.2b).

However, before doing this, we find it convenient to compute the following integrals,

$$\begin{aligned}\mathscr{C}_{p,q}(y;\beta) &:= (1-\beta)\int_{y_p}^{y_q}\frac{1}{|y-\tilde{y}|^{\beta}}\mathrm{d}\tilde{y}\\ &= |y-y_p|^{1-\beta}\mathrm{sign}(y-y_p)\\ &\quad - |y-y_q|^{1-\beta}\mathrm{sign}(y-y_q),\end{aligned} \tag{8.5a}$$

$$\begin{aligned}\mathscr{H}_{k,l}^{p,q}(\beta) &:= (2-\beta)\int_{y_k}^{y_l}\mathscr{C}_{p,q}(y;\beta)\mathrm{d}y\\ &= |y_q-y_k|^{2-\beta} - |y_q-y_l|^{2-\beta}\\ &\quad + |y_p-y_l|^{2-\beta} - |y_p-y_k|^{2-\beta}.\end{aligned} \tag{8.5b}$$

From here on, for the sake of a lighter notation, we omit the dependence of $\mathscr{H}_{k,l}^{p,q}$ on β. Moreover, we notice that

$$\mathscr{A}_1(y;\beta) = \mathscr{C}_{0,N_1}(y;\beta)/(1-\beta), \tag{8.6a}$$

$$\mathscr{A}_2(y;\beta) = \mathscr{C}_{N_1,N_2}(y;\beta)/(1-\beta). \tag{8.6b}$$

Therefore, by using the definitions for the basis functions ψ_i^k and (8.5a), the symmetrised Caputo fractional derivative of ψ_i^k is given by

$$\mathscr{D}_k^{\beta}[\psi_i^k](y) = \frac{1}{2\Gamma(2-\beta)}\left\{\frac{\mathscr{C}_{i-1,i}(y;\beta)}{y_i-y_{i-1}} - \frac{\mathscr{C}_{i,i+1}(y;\beta)}{y_{i+1}-y_i}\right\}, \tag{8.7}$$

where $i = 1,\ldots,N_1-1$, if $k=1$, and $i = N_1+1,\ldots,N_2-1$, if $k=2$. Besides,

$$\mathscr{D}_1^{\beta}[\psi_{N_1}^1](y) = \frac{1}{2\Gamma(2-\beta)}\frac{\mathscr{C}_{N_1-1,N_1}(y;\beta)}{y_{N_1}-y_{N_1-1}}, \tag{8.8a}$$

$$\mathscr{D}_2^{\beta}[\psi_{N_1}^2](y) = -\frac{1}{2\Gamma(2-\beta)}\frac{\mathscr{C}_{N_1,N_1+1}(y;\beta)}{y_{N_1+1}-y_{N_1}}. \tag{8.8b}$$

We remark that, by taking the limit in expressions (8.7)-(8.8b) for $\beta\to 1^-$, we obtain

$$\begin{aligned}\lim_{\beta\to 1^-}\mathscr{D}_k^{\beta}[\psi_i^k](y) &= \mathrm{d}_y\psi_i^k(y)\\ &= \begin{cases}\frac{1}{y_i-y_{i-1}}, & y_{i-1}<y<y_i,\\ -\frac{1}{y_{i+1}-y_i}, & y_i<y<y_{i+1},\\ 0, & y<y_{i-1}\text{ and }y>y_{i+1},\end{cases}\end{aligned} \tag{8.9}$$

for $y\neq y_i$, $i=1,\ldots,N_1-1,N_1+1,\ldots,N_2$. Moreover, for $y\neq y_{N_1}$,

$$\lim_{\beta\to 1^-}\mathscr{D}_1^{\beta}[\psi_{N_1}^1](y) = \mathrm{d}_y\psi_{N_1}^1(y), \tag{8.10a}$$

$$\lim_{\beta\to 1^-} \mathscr{D}_2^{\beta}[\psi_{N_1}^2](y) = \mathrm{d}_y\psi_{N_1}^2(y). \tag{8.10b}$$

Therefore, the results (8.9)-(8.10b), as previously proved, imply that the symmetrised Caputo fractional derivative of ψ_i^k tends to the first derivative of ψ_i^k for $\beta \to 1^-$.

8.2.1 Computation of L^k

From (8.5b) we have that for $j, i = 1, \ldots, N_1 - 1$, if $k = 1$, and $j, i = N_1 + 1, \ldots, N_2 - 1$, if $k = 2$, the components of the fractional stiffness matrix are

$$\mathsf{L}_{ji}^k(\beta) = \frac{\mathfrak{d}_{k\mathrm{R}} L_{\mathrm{c}}^{-2}}{2\Gamma(3-\beta)} \left\{ \frac{1}{y_i - y_{i-1}} \left(\frac{\mathscr{H}_{i-1,i}^{j-1,j}}{y_j - y_{j-1}} - \frac{\mathscr{H}_{i-1,i}^{j,j+1}}{y_{j+1} - y_j} \right) - \frac{1}{y_{i+1} - y_i} \left(\frac{\mathscr{H}_{i,i+1}^{j-1,j}}{y_j - y_{j-1}} - \frac{\mathscr{H}_{i,i+1}^{j,j+1}}{y_{j+1} - y_j} \right) \right\}. \tag{8.11}$$

Furthermore,

- if $j = 1, \ldots, N_1 - 1$ and $i = N_1$

$$\mathsf{L}_{j\,N_1}^1(\beta) = \frac{\mathfrak{d}_{1\mathrm{R}} L_{\mathrm{c}}^{-2}}{2\Gamma(3-\beta)} \frac{1}{y_{N_1} - y_{N_1-1}} \left(\frac{\mathscr{H}_{N_1-1,N_1}^{j-1,j}}{y_j - y_{j-1}} - \frac{\mathscr{H}_{N_1-1,N_1}^{j,j+1}}{y_{j+1} - y_j} \right), \tag{8.12}$$

- if $j = N_1$ and $i = 1, \ldots, N_1 - 1$

$$\mathsf{L}_{N_1 i}^1(\beta) = \frac{\mathfrak{d}_{1\mathrm{R}} L_{\mathrm{c}}^{-2}}{2\Gamma(3-\beta)} \frac{1}{y_{N_1} - y_{N_1-1}} \left(\frac{\mathscr{H}_{i-1,i}^{N_1-1,N_1}}{y_i - y_{i-1}} - \frac{\mathscr{H}_{i,i+1}^{N_1-1,N_1}}{y_{i+1} - y_i} \right), \tag{8.13}$$

- if $i, j = N_1$

$$\mathsf{L}_{N_1 N_1}^1(\beta) = \frac{\mathfrak{d}_{1\mathrm{R}} L_{\mathrm{c}}^{-2}}{2\Gamma(3-\beta)} \frac{1}{(y_{N_1} - y_{N_1-1})^2} \mathscr{H}_{N_1-1,N_1}^{N_1-1,N_1}, \tag{8.14a}$$

$$\mathsf{L}_{N_1 N_1}^2(\beta) = \frac{\mathfrak{d}_{2\mathrm{R}} L_{\mathrm{c}}^{-2}}{2\Gamma(3-\beta)} \frac{1}{(y_{N_1+1} - y_{N_1})^2} \mathscr{H}_{N_1,N_1+1}^{N_1,N_1+1}, \tag{8.14b}$$

- if $j = N_1$ and $i = N_1 + 1, \ldots, N_2 - 1$

$$\mathsf{L}_{N_1 i}^2(\beta) = -\frac{\mathfrak{d}_{2\mathrm{R}} L_{\mathrm{c}}^{-2}}{2\Gamma(3-\beta)} \frac{1}{y_{N_1+1} - y_{N_1}} \left(\frac{\mathscr{H}_{i-1,i}^{N_1,N_1+1}}{y_i - y_{i-1}} - \frac{\mathscr{H}_{i,i+1}^{N_1,N_1+1}}{y_{i+1} - y_i} \right), \tag{8.15}$$

- if $j = N_1 + 1, \dots, N_2 - 1$ and $i = N_1$

$$\mathsf{L}^2_{j\,N_1}(\beta) = -\frac{\mathfrak{d}_{2\mathrm{R}} L_{\mathrm{c}}^{-2}}{2\Gamma(3-\beta)} \frac{1}{y_{N_1+1} - y_{N_1}} \left(\frac{\mathscr{H}^{j-1,j}_{N_1,N_1+1}}{y_j - y_{j-1}} - \frac{\mathscr{H}^{j,j+1}_{N_1,N_1+1}}{y_{j+1} - y_j} \right). \tag{8.16}$$

By looking at the above expressions, and exploiting the symmetry of $\mathscr{H}^{p,q}_{k,l}$ (here, symmetry means that the subscripts can be exchanged with the superscripts), namely

$$\begin{aligned} \mathscr{H}^{p,q}_{k,l}(\beta) &= |y_q - y_k|^{2-\beta} - |y_q - y_l|^{2-\beta} + |y_p - y_l|^{2-\beta} - |y_p - y_k|^{2-\beta} \\ &= |y_l - y_p|^{2-\beta} - |y_l - y_q|^{2-\beta} + |y_k - y_q|^{2-\beta} - |y_k - y_p|^{2-\beta} \\ &= \mathscr{H}^{k,l}_{p,q}(\beta), \end{aligned} \tag{8.17}$$

it can be proven that the non-local stiffness matrices (one for each subcell) are symmetric as in the standard case, i.e.,

$$\mathsf{L}^k_{ji}(\beta) = \mathsf{L}^k_{ij}(\beta), \quad \forall \beta \in]0,1[. \tag{8.18}$$

8.2.2 Computation of F^k

By recalling the definition of $\mathsf{F}^k(\beta)$ given in (8.2b), and using the expressions (8.6a)-(8.8b), the components of the nodal fractional force are given by

- if $j = 1, \dots, N_1 - 1$

$$\mathsf{F}^1_j(\beta) = \frac{\mathfrak{d}_{1\mathrm{R}} L_{\mathrm{c}}^{-2}}{2\Gamma(3-\beta)} \left(\frac{\mathscr{H}^{0,N_1}_{j-1,j}}{y_j - y_{j-1}} - \frac{\mathscr{H}^{0,N_1}_{j,j+1}}{y_{j+1} - y_j} \right), \tag{8.19}$$

- if $j = N_1$

$$\mathsf{F}^1_{N_1}(\beta) = \frac{\mathfrak{d}_{1\mathrm{R}} L_{\mathrm{c}}^{-2}}{2\Gamma(3-\beta)} \frac{\mathscr{H}^{0,N_1}_{N_1-1,N_1}}{y_{N_1} - y_{N_1-1}}, \tag{8.20a}$$

$$\mathsf{F}^2_{N_1}(\beta) = -\frac{\mathfrak{d}_{2\mathrm{R}} L_{\mathrm{c}}^{-2}}{2\Gamma(3-\beta)} \frac{\mathscr{H}^{N_1,N_2}_{N_1,N_1+1}}{y_{N_1+1} - y_{N_1}}, \tag{8.20b}$$

- if $j = N_1 + 1, \dots, N_2 - 1$

$$\mathsf{F}^2_j(\beta) = \frac{\mathfrak{d}_{2\mathrm{R}} L_{\mathrm{c}}^{-2}}{2\Gamma(3-\beta)} \left(\frac{\mathscr{H}^{N_1,N_2}_{j-1,j}}{y_j - y_{j-1}} - \frac{\mathscr{H}^{N_1,N_2}_{j,j+1}}{y_{j+1} - y_j} \right). \tag{8.21}$$

8.2.3 Numerical approximation of the effective coefficient

By using the definitions introduced in the previous sections, the numerical effective diffusivity $\hat{d}^{\text{eff}}_{\text{num}}$ in Equation (7.46) can be computed as

$$\begin{aligned}\hat{d}^{\text{eff}}_{\text{num}} = \frac{\mathfrak{d}_{1\text{R}} L_{\text{c}}^{-2}}{2\Gamma(3-\beta)} \Bigg\{ \mathscr{H}^{0,N_1}_{0,N_1} + \sum_{i=1}^{N_1-1} \omega^1_i \left(\frac{\mathscr{H}^{i-1,i}_{0,N_1}}{y_i - y_{i-1}} - \frac{\mathscr{H}^{i,i+1}_{0,N_1}}{y_{i+1} - y_i} \right) \\ + \omega^1_{N_1} \frac{\mathscr{H}^{N_1-1,N_1}_{0,N_1}}{y_{N_1} - y_{N_1-1}} \Bigg\} \\ + \frac{\mathfrak{d}_{2\text{R}} L_{\text{c}}^{-2}}{2\Gamma(3-\beta)} \Bigg\{ \mathscr{H}^{N_1,N_2}_{N_1,N_2} - \omega^2_{N_1} \frac{\mathscr{H}^{N_1,N_1+1}_{N_1,N_2}}{y_{N_1+1} - y_{N_1}} \\ + \sum_{r=N_1+1}^{N_2-1} \omega^2_r \left(\frac{\mathscr{H}^{r-1,r}_{N_1,N_2}}{y_r - y_{r-1}} - \frac{\mathscr{H}^{r,r+1}_{N_1,N_2}}{y_{r+1} - y_r} \right) \Bigg\}. \end{aligned} \tag{8.22}$$

We notice that in Equation (8.22), the coefficients ω^k_i are the solutions of the algebraic equation (7.45) and represent the nodal concentrations. Therefore, the effective coefficient can be computed after the non-local cell problem has been solved.

8.3 FE discretisation of the non-local homogenised problem. Benchmark problem II

Analogously to what has been done above, we consider the basis functions to be defined by Lagrange polynomials of the first order, i.e.

$$\psi_0(x) = \begin{cases} \dfrac{x_1 - x}{x_1 - x_0}, & x_0 \le x < x_1, \\ 0, & \text{elsewhere}, \end{cases} \tag{8.23a}$$

$$\psi_i(x) = \begin{cases} \dfrac{x - x_{i-1}}{x_i - x_{i-1}}, & x_{i-1} \le x < x_i, \\ \dfrac{x_{i+1} - x}{x_{i+1} - x_i}, & x_i \le x \le x_{i+1}, \\ 0, & \text{elsewhere}, \end{cases} \quad i = 1, \dots, N-1 \tag{8.23b}$$

$$\psi_N(x) = \begin{cases} \dfrac{x - x_{N-1}}{x_N - x_{N-1}}, & x_{N-1} < x \le x_N, \\ 0, & \text{elsewhere}. \end{cases} \tag{8.23c}$$

Then, by using (8.23b), the mass matrix is given by

$$\mathsf{M}_{ji} = \begin{cases} (x_j - x_{j-1})/6, & i = j-1, \\ (x_{j+1} - x_{j-1})/3, & i = j, \\ (x_{j+1} - x_j)/6, & i = j+1, \\ 0, & \text{otherwise.} \end{cases} \tag{8.24}$$

Now, by recalling the expressions (8.5a) and (8.5b), with a slight abuse of notation, we have that

$$\begin{aligned} \mathscr{C}_{p,q}(x;\alpha) &:= |x - x_p|^{1-\alpha}\text{sign}(x - x_p) \\ &\quad - |x - x_q|^{1-\alpha}\text{sign}(x - x_q), \end{aligned} \tag{8.25a}$$

$$\begin{aligned} \mathscr{H}^{p,q}_{k,l}(\alpha) &:= |x_q - x_k|^{2-\alpha} - |x_q - x_l|^{2-\alpha} \\ &\quad + |x_p - x_l|^{2-\alpha} - |x_p - x_k|^{2-\alpha}, \end{aligned} \tag{8.25b}$$

where x replaces y, and the parameter α replaces β. In the following discussion, we omit the dependence of $\mathscr{H}^{p,q}_{k,l}$ on α.

Thus, by using expressions (8.25a) and (8.25b), and the symmetrised Caputo derivative of order α of ψ_i, $i = 1, \ldots, N$, i.e.

$$\mathscr{D}^{\alpha}[\psi_i](x) = \frac{1}{2\Gamma(2-\alpha)} \left\{ \frac{\mathscr{C}_{i-1,i}(x;\alpha)}{x_i - x_{i-1}} - \frac{\mathscr{C}_{i,i+1}(x;\alpha)}{x_{i+1} - x_i} \right\}, \tag{8.26}$$

the fractional stiffness matrix $\mathsf{L}(\alpha)$ can be computed as follows

$$\begin{aligned} \mathsf{L}_{ji}(\alpha) = \frac{\hat{d}^{\text{eff}}_{\text{st}}}{2\Gamma(3-\alpha)} \Bigg\{ & \frac{1}{x_i - x_{i-1}} \left(\frac{\mathscr{H}^{j-1,j}_{i-1,i}}{x_j - x_{j-1}} - \frac{\mathscr{H}^{j,j+1}_{i-1,i}}{x_{j+1} - x_j} \right) \\ & - \frac{1}{x_{i+1} - x_i} \left(\frac{\mathscr{H}^{j-1,j}_{i,i+1}}{x_j - x_{j-1}} - \frac{\mathscr{H}^{j,j+1}_{i,i+1}}{x_{j+1} - x_j} \right) \Bigg\}. \end{aligned} \tag{8.27}$$

Moreover, by taking into account that

$$\mathscr{D}^{\alpha}[\psi_0](x) = -\frac{1}{2\Gamma(2-\alpha)} \frac{1}{x_1 - x_0} \mathscr{C}_{0,1}(x;\alpha), \tag{8.28a}$$

$$\mathscr{D}^{\alpha}[\psi_N](x) = \frac{1}{2\Gamma(2-\alpha)} \frac{1}{x_N - x_{N-1}} \mathscr{C}_{N-1,N}(x;\alpha), \tag{8.28b}$$

the elements of the fractional nodal force $\mathsf{F}(\alpha)$ are given by

$$\mathsf{F}_j(\alpha) = \frac{\hat{d}^{\text{eff}}_{\text{st}}}{2\Gamma(3-\alpha)} \left\{ -\frac{c_{\text{b}}}{x_1 - x_0} \left(\frac{\mathscr{H}^{0,1}_{j-1,j}}{x_j - x_{j-1}} - \frac{\mathscr{H}^{0,1}_{j,j+1}}{x_{j+1} - x_j} \right) \right.$$

$$+\frac{c_{\mathrm{b}}}{x_N - x_{N-1}}\left(\frac{\mathscr{H}^{N-1,N}_{j-1,j}}{x_j - x_{j-1}} - \frac{\mathscr{H}^{N-1,N}_{j,j+1}}{x_{j+1} - x_j}\right)\Bigg\}. \tag{8.29}$$

As previously discussed, also in this case both the fractional stiffness matrix and the fractional nodal force tend to their classical counterparts when $\alpha \to 1^-$.

Conclusions to Part II

The content reported in this chapter has been previously published in [241].

In this second part of the Thesis, we study the two-scale, non-local diffusion of a chemical species in a composite medium. This is addressed by prescribing a two-scale constitutive law of fractional type for the mass flux of the chemical species and, with the aid of the asymptotic homogenisation technique, we obtain an effective characterisation of the composite, which is subjected to the existence of non-local interactions at both length scales. As a result, the non-local effects at the micro-scale are *ciphered* in the effective diffusivity while, at the macro-scale, the homogenised problem features an integro-differential equation. In particular, we show that we can obtain classical results of homogenisation theory if the non-locality assumption is ignored.

In Chapter 6, we establish a combined framework in which some constitutive laws involving fractional derivatives are studied in conjunction with asymptotic homogenisation, in order to solve problems characterised by non-local diffusion at different scales. Furthermore, we note that even though we adopted a formalism that can be easily adapted to a two- or three-dimensional context, we prefer, for the time being, to contextualise our mathematical model in a one-dimensional framework. It is worth mentioning that although we focus our attention on the connections between spatial environment and non-locality, we present some discussions towards the addition of the time scales induced by the characteristic length scales in our model.

Furthermore, in Chapter 7, we employ asymptotic homogenisation to determine the effective diffusivity coefficient of the considered medium. Our computations predict that, at the macro-scale, the attainment of the stationary state of the diffusion process is appreciably hindered by the non-local interactions accounted for by the operators of fractional differentiation that define the diffusion fluxes. This retardation manifests itself for decreasing values of a real parameter (the fractional order of differentiation) that defines the strength of such non-local interactions, at the micro- and at the macro-scale.

It is important to emphasise that the way in which the non-local interactions influence the macroscopic behaviour of the system depends on the scale at which these interactions are introduced. When the non-local interactions are considered at the micro-scale, they emerge also at the macro-scale through the effective fractional diffusivity $\hat{d}^{\text{eff}}(\beta)$ and by slowing down the diffusion. However, the effect of the non-local interactions is more evident when those are accounted for at the macro-scale, and occurs through a deceleration of the diffusion process that is stronger than in the previous case. Hence, the information enclosed in the initial distribution of the concentration is kept for a "longer" time.

As we stated before, we conceived a model in one dimension. Clearly, this model can be generalised to higher dimensions. However, there are some issues that must be tackled. One of them is that the non-locality function and the normalisation factors should be conceived in a symmetry- and dimension-dependent way. Moreover, a more detailed numerical study would be required. These issues are part of our current research.

Finally, in Chapter 8, we address the FE discretisation of benchmark problems that include the non-local nature of the mass flux and the role of the heterogeneous structure of the medium under study. We remark that the presentation of the FE scheme presented in this work is very elementary and can be obtained by appropriately rephrasing the one-dimensional formulation of the FE method as presented e.g. in [152]. Nevertheless, the simplicity of the numerics allows us to discuss some of the specific properties of the algebraic equations resulting from the discretisation process. In particular, in the benchmark problems, the presence of the symmetrised Caputo fractional derivative results in fractional stiffness matrices and fractional nodal forces. More specifically, we prove that the fractional stiffness matrices are symmetric and, although they are dense because of the presence of the fractional derivatives, in the limits $\alpha \to 1^-$ and $\beta \to 1^-$ they become the standard stiffness matrices of tridiagonal form. The numerical simulations are in harmony with these theoretical predictions.

Part III

Non-locality in the electrophysiology of nerve cells

Chapter 9

Electrophysiology of nerve cells: The Poisson–Nernst–Planck model

The work reported in this chapter is taken from [236][1].

9.1 Introduction

A neuron is a cell within the nervous system distinguished by its function of transmitting information to other nerve cells. A neuron consists of three main parts: the *soma* (or cell body), the *dendrites* and the *axon*. The function of the dendrites is to carry information received from other neurons to the soma, where this information is contained, and then transmitted through the axon to other cells. So, the dendrites act as the "input" part of the neuron, whereas the axon acts as the "output" part.

The soma is the largest volumetric part of the cell body. On the other hand, the dendrites form a dense chain of branches and the axon is the longest branch ending with a number of terminals that are connected to the dendrites of other neurons [256]. A membrane separates the interior of the cell to the external aqueous environment having very different compositions. At the interior of the cell chloride (Cl^-) and sodium (Na^+) ions have lower concentrations than at the outside, while the concentration of potassium (K^+) ions is larger at the exterior of the cell with respect to its interior [256]. One of the roles of the membrane is to handle the movement of ions in the direction of the concentration gradient between the intracellular

[1]The work [236] is also used in the MSc thesis of Mr. Vito Napoli. The Author of this PhD thesis was co-advisor of that MSc thesis.

and extracellular space through ion channels. This movement determines what is known as the *membrane potential*, denoted by V. This is an electro-chemical signal given by the difference in electrical potential between the internal and external part of the cell membrane.

The membrane potential of a non-excited nerve cell at rest is called the *resting potential*. That is the resting potential is the baseline state of the membrane potential. On the other hand, the terminology *action potential* is used to describe the membrane potential of an excited nerve cell during the transmission of a nerve impulse. In particular, the action potential is evoked when a sufficiently large depolarisation (the interior voltage becomes less negative) happens because of the activation of certain voltage-gated ion channels allowing the exchange of ions across the membrane [256].

As pointed out in [187, 180] several neuropathological incidents occur in the membrane structure and/or are a consequence of membrane dysfunctioning. Abnormalities in the membrane potential induced, e.g. by improper levels of ions concentrations, affect the neurophysiological function of the brain and stimulates conduction, which is at the base of various diseases, such as epilepsy [7]. Therefore, the mathematical modelling of the concentration dynamics in brain tissues, as well as their effect on the membrane potential is fundamental in the understanding of neurodegeneration and neuroprotection.

In this chapter, we revisit some of the more salient aspects of the model presented in [96], which we slightly modify according to our needs. In doing so, to highlight the differences in our approach, we compare the model in [96] with some other models available in the literature of the sector, such as, for example, those discussed in [261, 279, 277, 278].

9.2 Integral and local form of Maxwell's equations

We start by outlining Maxwell's equations retrieved in the form they take in the matter [169, 193, 208, 167, 103], and under the hypothesis that the material is at rest in the chosen reference system. In the most general formulation, but restricted to the problem under consideration, Maxwell's equations in their *integral form* are given by

$$\int_{\partial\Sigma} \boldsymbol{E}\cdot\boldsymbol{\tau}\,\mathrm{ds} = -\frac{\mathrm{d}}{\mathrm{d}t}\int_{\Sigma}\boldsymbol{B}\cdot\boldsymbol{n}\,\mathrm{da}, \tag{9.1a}$$

$$\int_{\partial\Omega} \boldsymbol{B}\cdot\boldsymbol{n}\,\mathrm{da} = 0, \tag{9.1b}$$

$$\int_{\partial\Sigma} \boldsymbol{H}\cdot\boldsymbol{\tau}\,\mathrm{ds} = \int_{\Sigma}\boldsymbol{J}\cdot\boldsymbol{n}\,\mathrm{da} + \frac{\mathrm{d}}{\mathrm{d}t}\int_{\Sigma}\boldsymbol{D}\cdot\boldsymbol{n}\,\mathrm{da}, \tag{9.1c}$$

$$\int_{\partial\Omega} \boldsymbol{D}\cdot\boldsymbol{n}\,\mathrm{da} = \int_{\Omega} \varrho_{\mathrm{f}}\,\mathrm{dv}, \tag{9.1d}$$

where $\boldsymbol{E}$ and $\boldsymbol{B}$ represent the electric and the magnetic induction fields, respectively. Moreover, $\boldsymbol{H}$ is the magnetic field, $\boldsymbol{J}$ is the current density, $\boldsymbol{D}$ is the electric induction field, and ϱ_{f} is the the volumetric density of the free charges. In the framework of this work, it is assumed that the current density $\boldsymbol{J}$ is constituted by a term generated because of the relative motion of the electric charges with respect to the motion of the considered medium and by any conduction and/or imposed current densities.

In equations (9.1a)–(9.1d), the open and connected set Ω represents the fixed region of space contained in the considered body and whose boundary is given by the closed surface $\partial\Omega$. Additionally, Σ denotes an open surface, also fixed and contained in the body under study, and whose boundary is represented by the closed and regular curve $\partial\Sigma$. The symbol $\boldsymbol{\tau}$ is used to denote the vector field tangent to the curve $\partial\Sigma$, while $\boldsymbol{n}$ is the vector field normal to a given surface, which, in our context, can be Σ or $\partial\Omega$. Finally, "ds", "da" and "dv" are, respectively, the "classic" line, area and volume measures (e.g. Riemann or Lebesgue).

Since we are considering that Σ is a fixed surface in space, Reynolds' theorem for surfaces allows us to conclude that the time rate of change of the magnetic and electric induction terms in Equations (9.1a) and (9.1c) can be written as

$$\frac{\mathrm{d}}{\mathrm{d}t}\int_{\Sigma} \boldsymbol{B}\cdot\boldsymbol{n}\,\mathrm{da} = \int_{\Sigma} \partial_t\boldsymbol{B}\cdot\boldsymbol{n}\,\mathrm{da}, \tag{9.2a}$$

$$\frac{\mathrm{d}}{\mathrm{d}t}\int_{\Sigma} \boldsymbol{D}\cdot\boldsymbol{n}\,\mathrm{da} = \int_{\Sigma} \partial_t\boldsymbol{D}\cdot\boldsymbol{n}\,\mathrm{da}. \tag{9.2b}$$

We remark that if Σ is a surface changing with time, the above expressions have to be accordingly rewritten with the help of Reynolds' transport theorem (refer to, e.g. [59]).

Substituting the results (9.2a) and (9.2b) in Equations (9.1a) and (9.1c), and considering Stokes' theorem for the integrals on $\partial\Sigma$ and Gauss's theorem for the integrals on $\partial\Omega$ in Equations (9.1b) e (9.1d), we obtain

$$\int_{\Sigma} (\mathrm{curl}\boldsymbol{E})\cdot\boldsymbol{n}\,\mathrm{da} = -\int_{\Sigma} \partial_t\boldsymbol{B}\cdot\boldsymbol{n}\,\mathrm{da}, \tag{9.3a}$$

$$\int_{\Omega} \mathrm{div}\boldsymbol{B}\,\mathrm{dv} = 0, \tag{9.3b}$$

$$\int_{\Sigma} (\mathrm{curl}\boldsymbol{H})\cdot\boldsymbol{n}\,\mathrm{da} = \int_{\Sigma} \boldsymbol{J}\cdot\boldsymbol{n}\,\mathrm{da} + \int_{\Sigma} \partial_t\boldsymbol{D}\cdot\boldsymbol{n}\,\mathrm{da}, \tag{9.3c}$$

$$\int_{\Omega} \mathrm{div}\boldsymbol{D}\,\mathrm{dv} = \int_{\Omega} \varrho_{\mathrm{f}}\,\mathrm{dv}. \tag{9.3d}$$

Finally, the localisation of Equations (9.3a)–(9.3d), leads to the local form of Maxwell's equations, namely

$$\mathrm{curl}\boldsymbol{E} = -\partial_t \boldsymbol{B}, \tag{9.4a}$$
$$\mathrm{div}\boldsymbol{B} = 0, \tag{9.4b}$$
$$\mathrm{curl}\boldsymbol{H} = \boldsymbol{J} + \partial_t \boldsymbol{D}, \tag{9.4c}$$
$$\mathrm{div}\boldsymbol{D} = \varrho_{\mathrm{f}}. \tag{9.4d}$$

9.3 Maxwell's equations in the electrodynamics of nerve cells

The electrodynamics of nerve cells is usually studied by considering that the magnetic induction field, $\boldsymbol{B}$, varies slowly over time, so that the partial derivative $\partial_t \boldsymbol{B}$ can be neglected in (9.4a) [96, 277]. Consequently, Maxwell's equations reduce to

$$\mathrm{curl}\boldsymbol{E} = 0, \tag{9.5a}$$
$$\mathrm{div}\boldsymbol{B} = 0, \tag{9.5b}$$
$$\mathrm{curl}\boldsymbol{H} = \boldsymbol{J} + \partial_t \boldsymbol{D}, \tag{9.5c}$$
$$\mathrm{div}\boldsymbol{D} = \varrho_{\mathrm{f}}. \tag{9.5d}$$

All the quantities involved in (9.5a)–(9.5d) are referred to a generic region $\mathscr{R} \subset \mathscr{S}$ of the three-dimensional Euclidean space, $\mathscr{S}$, identifiable either with the intra-cellular space or with the extra-cellular space of the nerve cell, indicated, respectively, with $\Omega^{(\mathrm{i})}$ and $\Omega^{(\mathrm{e})}$. Here and in the following, $\mathscr{R}$ is a connected open subset of $\mathscr{S}$. In this context, when specifying whether a given physical quantity f, which can be a scalar, vector or tensor quantity, is defined in $\Omega^{(\mathrm{i})}$ or in $\Omega^{(\mathrm{e})}$, we will adopt the notation $f^{(\mathrm{i})} := f_{|\Omega^{(\mathrm{i})}}$ or $f^{(\mathrm{e})} := f_{|\Omega^{(\mathrm{e})}}$. In this section, however, to streamline the presentation of the results, we omit to explicitly write to which portion of space the fields considered are restricted. Furthermore, we assume that all the fields considered are of class C^2 in the region of space in which they are defined or restricted.

Equation (9.5a) implies that the electric field $\boldsymbol{E}$ can be expressed as

$$\boldsymbol{E} = -\mathrm{grad}\,\phi, \tag{9.6}$$

where ϕ is referred to as the *scalar potential* (see, for instance [167]). Moreover, because of the form of the system (9.5a)–(9.5d), the electric induction field, $\boldsymbol{D}$, still appears coupled with the magnetic field, $\boldsymbol{H}$. However, this coupling can be eliminated by combining Equation (9.5c) with (9.5d) such that we obtain the equation of conservation of free electric charges. For this purpose, we apply the divergence

operator to Equation (9.5c) and consider the vector identity $\operatorname{div}(\operatorname{curl}\boldsymbol{H}) = 0$ and the property

$$\operatorname{div}\partial_t \boldsymbol{D} = \partial_t \operatorname{div}\boldsymbol{D} = \partial_t \varrho_{\mathrm{f}}. \tag{9.7}$$

Then, by decoupling the condition on $\boldsymbol{B}$ of solenoid field, i.e. $\operatorname{div}\boldsymbol{B} = 0$, from the remaining three Maxwell's equations, we obtain that

$$\boldsymbol{E} = -\operatorname{grad}\phi, \tag{9.8a}$$
$$0 = \operatorname{div}\boldsymbol{J} + \partial_t \varrho_{\mathrm{f}}, \tag{9.8b}$$
$$\operatorname{div}\boldsymbol{D} = \varrho_{\mathrm{f}}. \tag{9.8c}$$

9.4 The Poisson–Nernst–Planck (PNP) model

Following [96], in the next sessions, we discuss some of the main considerations that lead to the Poisson–Nernst–Planck (PNP) model.

9.4.1 Ion concentration dynamics

We denote by c_k, with $k = 1,2,\ldots,N$, the molar concentrations of the k-th ionic species. Then, the density of free charges is considered to be given by the expression [96]

$$\varrho_{\mathrm{f}} := \sum_{k=1}^{N} F z_k c_k, \tag{9.9}$$

where F is Faraday constant and $z_k \in \mathbb{Z}$ is the valence of the k-th ionic species.

The current density, $\boldsymbol{J}$, is defined through the sum of the current density of the k-th ionic species, $\boldsymbol{J}_k$, weighted by the respective valences of the ionic species [96]. That is,

$$\boldsymbol{J} := \sum_{k=1}^{N} F z_k \boldsymbol{J}_k. \tag{9.10}$$

In particular, the current density of the k-th ionic species is supposed to be additively split in a diffusive and an electric part so that [96]

$$\begin{aligned} \boldsymbol{J}_k &:= -D_k \operatorname{grad} c_k + \frac{F z_k D_k}{RT} c_k \boldsymbol{E} \\ &= -D_k \operatorname{grad} c_k - \frac{F z_k D_k}{RT} c_k \operatorname{grad}\phi, \end{aligned} \tag{9.11}$$

with R being the gas constant, T the absolute temperature, and D_k the molecular diffusion coefficient of the k-th ionic species [96]. Particularly, it is assumed that the temperature T is constant in time and space, and that each D_k, $k = 1,2,\ldots,N$, is scalar function, since the materials contained in $\mathscr{R}$ are considered isotropic with respect to the phenomenon of molecular diffusion. The combination of Equations (9.10) and (9.11) yields

$$\boldsymbol{J} = -\sum_{k=1}^{N} F z_k D_k \operatorname{grad} c_k - \sigma \operatorname{grad} \phi, \tag{9.12}$$

where σ is the conductivity of the medium [261] and is given by

$$\sigma := \sum_{k=1}^{N} \frac{(F z_k)^2 D_k}{RT} c_k. \tag{9.13}$$

We notice that the form of $\boldsymbol{J}$ given in (9.12) deviates from Ohm's law because it includes the influence of the ionic species on the total current density.

Now, we turn our attention to the third Maxwell equation given by (9.8b) in its simplified form. This expression represents the local form of the law of conservation of the total density and it will be used in the model as a balance law. Furthermore, each ionic species must obey its own balance law and, therefore, in the absence of sources and sinks of electric charge, we can write [96]

$$\partial_t c_k + \operatorname{div} \boldsymbol{J}_k = 0, \qquad k = 1,\ldots,N, \tag{9.14}$$

where $\boldsymbol{J}_k$ is specified in (9.11).

The total number of ionic concentrations $c_1,\ldots,c_N$ are constrained by the *electroneutrality* condition which implies that the production or removal of negative and positive charges happen at equal rates. In our framework, this condition is equivalent to requiring that the total current, $\boldsymbol{J}$, be solenoidal [23, 96], namely

$$\operatorname{div} \boldsymbol{J} \equiv \operatorname{div} \left(\sum_{k=1}^{N} F z_k \boldsymbol{J}_k \right) = 0. \tag{9.15}$$

Equation (9.15) establishes the new form of the balance equation given in (9.8b). Therefore, the fields involved in (9.15), i.e. the concentrations $c_1,\ldots,c_N$ and the scalar potential ϕ, must be such that the total current density $\boldsymbol{J}$ is solenoidal. We notice that, according to (9.8b), the electroneutrality condition implies that $\partial_t \varrho_{\mathrm{f}} = 0$ and, consequently, the total density of free charges is time-independent. This property, however, does not allow us to conclude that the ionic concentrations of the single species, that is $c_1,\ldots,c_N$, are constant functions of time. In fact, by virtue of (9.9), only the combination $\varrho_{\mathrm{f}} = \sum_{k=1}^{N} F z_k c_k$ will be time-independent.

Taking into account the above considerations, we have that

$$\operatorname{div}\boldsymbol{J} = 0, \tag{9.16a}$$

$$\partial_t c_k + \operatorname{div}\boldsymbol{J}_k = 0, \tag{9.16b}$$

or equivalently,

$$0 = \operatorname{div}\left[\sum_{k=1}^{N} F z_k \left(-D_k \operatorname{grad} c_k - \frac{F z_k D_k}{RT} c_k \operatorname{grad}\phi\right)\right], \tag{9.17a}$$

$$0 = \partial_t c_k + \operatorname{div}\left[-D_k \operatorname{grad} c_k - \frac{F z_k D_k}{RT} c_k \operatorname{grad}\phi\right], \qquad k = 1, \ldots, N. \tag{9.17b}$$

In (9.17a) and (9.17b), the unknowns are given by the scalar potential, ϕ, and by the ionic concentrations, $c_1, \ldots, c_N$.

Following the ideas put forward in [96] and assuming that the electric induction field, $\boldsymbol{D}$ depends linearly on the electric field $\boldsymbol{E}$, we write

$$\boldsymbol{D} = \varepsilon_0 \varepsilon_r \boldsymbol{E} = -\varepsilon_0 \varepsilon_r \operatorname{grad}\phi, \tag{9.18}$$

where ε_0 and ε_r are, respectively, the dielectric constant in the vacuum and the relative permittivity of the region that the material occupies. Therefore, known ϕ, it is possible to go back to the electric field, $\boldsymbol{E}$, and the density of free charges, ϱ_{f}, through the relations

$$\boldsymbol{E} = -\operatorname{grad}\phi, \tag{9.19a}$$

$$\varrho_{\mathrm{f}} = \operatorname{div}\boldsymbol{D} = \operatorname{div}\left(\varepsilon_0 \varepsilon_r \boldsymbol{E}\right) = -\operatorname{div}\left(\varepsilon_0 \varepsilon_r \operatorname{grad}\phi\right). \tag{9.19b}$$

9.4.2 Governing equations in the intracellular and extracellular space

We observe that each of the Equations (9.17a)–(9.19b) must be particularised to $\Omega^{(\mathrm{i})}$ and to $\Omega^{(\mathrm{e})}$. This means that each term, be it an unknown field or a material parameter, acquires a "label", which specifies whether the term itself is defined in $\Omega^{(\mathrm{i})}$ or in $\Omega^{(\mathrm{e})}$. Thus, we will set $\phi^{(\mathrm{e})}$ and $\phi^{(\mathrm{i})}$ depending on whether the scalar potential is restricted to $\Omega^{(\mathrm{e})}$ or $\Omega^{(\mathrm{i})}$. Similarly, we will write $c_k^{(\mathrm{e})}$ and $c_k^{(\mathrm{i})}$ for ion concentrations, and $D_k^{(\mathrm{e})}$ and $D_k^{(\mathrm{i})}$ for the molecular diffusion coefficients. Therefore, we can write [96]:

In $\Omega^{(\mathrm{i})}$:

$$\operatorname{div}\left[\sum_{k=1}^{N} F z_k \left(-D_k^{(\mathrm{i})} \operatorname{grad} c_k^{(\mathrm{i})} - \frac{F z_k D_k^{(\mathrm{i})}}{RT} c_k^{(\mathrm{i})} \operatorname{grad}\phi^{(\mathrm{i})}\right)\right] = 0, \tag{9.20a}$$

$$\partial_t c_k^{(\mathrm{i})} + \operatorname{div}\left[-D_k^{(\mathrm{i})} \operatorname{grad} c_k^{(\mathrm{i})} - \frac{F z_k D_k^{(\mathrm{i})}}{RT} c_k^{(\mathrm{i})} \operatorname{grad} \phi^{(\mathrm{i})}\right] = 0, \quad k = 1, \ldots, N. \tag{9.20b}$$

In $\Omega^{(\mathrm{e})}$:

$$\operatorname{div}\left[\sum_{k=1}^{N} F z_k \left(-D_k^{(\mathrm{e})} \operatorname{grad} c_k^{(\mathrm{e})} - \frac{F z_k D_k^{(\mathrm{e})}}{RT} c_k^{(\mathrm{e})} \operatorname{grad} \phi^{(\mathrm{e})}\right)\right] = 0, \tag{9.21a}$$

$$\partial_t c_k^{(\mathrm{e})} + \operatorname{div}\left[-D_k^{(\mathrm{e})} \operatorname{grad} c_k^{(\mathrm{e})} - \frac{F z_k D_k^{(\mathrm{e})}}{RT} c_k^{(\mathrm{e})} \operatorname{grad} \phi^{(\mathrm{e})}\right] = 0, \quad k = 1, \ldots, N. \tag{9.21b}$$

Thus, each equation of the system (9.17a)–(9.19b) splits into two equations, coupled through the interface $\mathscr{M}$, which denotes the cell membrane and forms both the boundary of $\Omega^{(\mathrm{i})}$ and the inner boundary of $\Omega^{(\mathrm{e})}$ (see Figure 9.1). We denote by $\partial\Omega^{(\mathrm{i})}$ the boundary of $\Omega^{(\mathrm{i})}$, and the boundary of $\Omega^{(\mathrm{e})}$ is represented in the form $\partial\Omega^{(\mathrm{e})} = \partial\Omega^{(\mathrm{e,i})} \sqcup \partial\Omega^{(\mathrm{e,e})}$, where $\partial\Omega^{(\mathrm{e,e})}$ and $\partial\Omega^{(\mathrm{e,i})}$ are, respectively, the outer and the inner boundaries of $\Omega^{(\mathrm{e})}$. Therefore, we have $\mathscr{M} \equiv \partial\Omega^{(\mathrm{i})} \equiv \partial\Omega^{(\mathrm{e,i})}$. Based on these geometric properties, we emphasize that for the model to be well-posed, we must impose appropriate conditions on $\mathscr{M}$ and $\partial\Omega^{(\mathrm{e,e})}$.

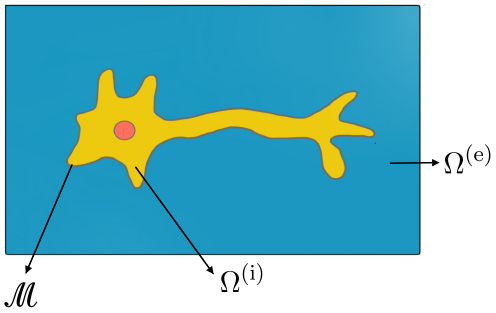

Figure 9.1: Schematic of a neuron. In our framework $\Omega^{(\mathrm{i})}$ denotes the intracellular space, $\Omega^{(\mathrm{e})}$ is the extracellular space and $\mathscr{M}$ defines the interface between $\Omega^{(\mathrm{i})}$ and $\Omega^{(\mathrm{e})}$.

9.4.3 Interface conditions between the scalar potentials

The potentials $\phi^{(\mathrm{i})}$ and $\phi^{(\mathrm{e})}$, in general, *cannot be "collected" with continuity* on $\mathscr{M}$, from which it follows that $\phi^{(\mathrm{i})}_{|\mathscr{M}}(x,t) \neq \phi^{(\mathrm{e})}_{|\mathscr{M}}(x,t)$. From a physical point of view, this is due to the fact that the cell membrane, here described by the surface $\mathscr{M}$, is the site where electrochemical phenomena occur, the most relevant of which are due to the accumulation of electrical charges on its two faces. As we mentioned above, these charge accumulations generate the scalar potential difference at the

two faces of the membrane (i.e. the membrane potential) [256, 96, 261, 278, 95, 147]

$$V := \phi^{(\mathrm{i})}_{|\mathscr{M}} - \phi^{(\mathrm{e})}_{|\mathscr{M}}, \tag{9.22}$$

which, in turn, produces both capacitive and conductive electric currents through the membrane.

The definition (9.22) can be employed as a Dirichlet condition for $\phi^{(\mathrm{i})}$ on $\mathscr{M}$, thus providing [96]

$$\phi^{(\mathrm{i})}_{|\mathscr{M}} = \phi^{(\mathrm{e})}_{|\mathscr{M}} + V \tag{9.23}$$

as the first boundary condition for Equation (9.20a). Given the geometry of the problem, Equation (9.23) constitutes an inner-boundary condition also for $\phi^{(\mathrm{e})}$, although for the latter field it is necessary to provide conditions also on the outer boundary of $\Omega^{(\mathrm{e})}$.

Since $\mathscr{M}$ constitutes an inner boundary for $\Omega^{(\mathrm{i})}$ (and, more precisely, a discontinuity surface), a further condition on $\mathscr{M}$ is needed for $\phi^{(\mathrm{i})}$. The latter is provided by the physical condition of continuity of the normal component to $\mathscr{M}$ of the total electric current density. As in [96], we therefore consider that

$$\boldsymbol{J}^{(\mathrm{i})} \cdot \boldsymbol{n}^{(\mathrm{ie})} = -\boldsymbol{J}^{(\mathrm{e})} \cdot \boldsymbol{n}^{(\mathrm{ei})}, \qquad \text{on } \mathscr{M}, \tag{9.24}$$

where $\boldsymbol{n}^{(\mathrm{ie})}$ and $\boldsymbol{n}^{(\mathrm{ei})}$ are the unit normal vectors to $\mathscr{M}$ from $\Omega^{(\mathrm{i})}$ to $\Omega^{(\mathrm{e})}$ and from $\Omega^{(\mathrm{e})}$ to $\Omega^{(\mathrm{i})}$. Furthermore, $\boldsymbol{J}^{(\mathrm{i})}$ and $\boldsymbol{J}^{(\mathrm{e})}$ are the current densities defined, respectively, in $\Omega^{(\mathrm{i})}$ and in $\Omega^{(\mathrm{e})}$, i.e.

$$\boldsymbol{J}^{(\mathrm{i})} := \sum_{k=1}^{N} F z_k \left(-D_k^{(\mathrm{i})} \operatorname{grad} c_k^{(\mathrm{i})} - \frac{F z_k D_k^{(\mathrm{i})}}{RT} c_k^{(\mathrm{i})} \operatorname{grad} \phi^{(\mathrm{i})} \right), \tag{9.25a}$$

$$\boldsymbol{J}^{(\mathrm{e})} := \sum_{k=1}^{N} F z_k \left(-D_k^{(\mathrm{e})} \operatorname{grad} c_k^{(\mathrm{e})} - \frac{F z_k D_k^{(\mathrm{e})}}{RT} c_k^{(\mathrm{e})} \operatorname{grad} \phi^{(\mathrm{e})} \right). \tag{9.25b}$$

Each member of Equation (9.24) must, at the same time, equal the total current density that crosses the membrane in the direction normal to it. Therefore, if we denote by I the transmembrane current density, it is possible to write [96]

$$\boldsymbol{J}^{(\mathrm{i})} \cdot \boldsymbol{n}^{(\mathrm{ie})} = I, \qquad \text{on } \mathscr{M}, \tag{9.26a}$$

$$-\boldsymbol{J}^{(\mathrm{e})} \cdot \boldsymbol{n}^{(\mathrm{ei})} = I, \qquad \text{on } \mathscr{M}. \tag{9.26b}$$

Note that Equations (9.26a) and (9.26b) become inhomogeneous Neumann conditions for $\phi^{(\mathrm{i})}$ and for $\phi^{(\mathrm{e})}$, i.e.

$$-\sum_{k=1}^{N} \frac{(F z_k)^2 D_k^{(\mathrm{i})}}{RT} c_k \frac{\partial \phi^{(\mathrm{i})}}{\partial \boldsymbol{n}^{(\mathrm{ie})}} = I + \sum_{k=1}^{N} F z_k D_k^{(\mathrm{i})} \frac{\partial c_k^{(\mathrm{i})}}{\partial \boldsymbol{n}^{(\mathrm{ie})}}, \qquad \text{on } \mathscr{M}, \tag{9.27a}$$

$$\sum_{k=1}^{N} \frac{(Fz_k)^2 D_k^{(\mathrm{e})}}{RT} c_k \frac{\partial \phi^{(\mathrm{e})}}{\partial \boldsymbol{n}^{(\mathrm{ei})}} = I - \sum_{k=1}^{N} F z_k D_k^{(\mathrm{e})} \frac{\partial c_k^{(\mathrm{e})}}{\partial \boldsymbol{n}^{(\mathrm{ei})}}, \qquad \text{on } \mathscr{M}. \tag{9.27b}$$

9.4.4 Constitutive relations of the membrane current: The Hodgkin & Huxley model

According to the physics of the membrane [256, 96, 279, 261, 278, 277, 95, 147], the current I consists of a capacitive term, several conductive terms —due to the conductivity of transmembrane ion channels—, and possible other contributions of synaptic or electrical stimuli. Specifically, we consider that [96, 277, 278, 261, 279]

$$I = I^{(\mathrm{cap})} + I^{(\mathrm{ionic})}. \tag{9.28}$$

Capacitive current: The capacitive term of the total current I can be written as (see, e.g. [96, 147, 95, 256])

$$I^{(\mathrm{cap})} = C\,\partial_t \Big(\phi^{(\mathrm{i})}_{|\mathscr{M}} - \phi^{(\mathrm{e})}_{|\mathscr{M}} \Big) \equiv C\,\partial_t V, \tag{9.29}$$

where C is the membrane capacitance.

Ionic currents: The total conductive contribution, associated with the ionic currents flowing through the membrane, is given by [256, 261, 96]

$$I^{(\mathrm{ionic})} = \sum_{k=1}^{N} I_k^{(\mathrm{ionic})}, \tag{9.30}$$

with $I_k^{(\mathrm{ionic})}$ denoting the transmembrane current density produced by the passage of the k-th ionic species through $\mathscr{M}$. In particular, for each $k = 1, \ldots, N$, the total ion current of the k-th species is given by [96, 279, 278, 277]

$$I_k^{(\mathrm{ionic})} = I_k^{(\mathrm{pass})} + I_k^{(\mathrm{HH})} + I_k^{(\mathrm{syn})}, \tag{9.31}$$

where $I_k^{(\mathrm{pass})}$ is called the *passive current*, $I_k^{(\mathrm{HH})}$ is the *Hodgkin & Huxley* ion current and $I_k^{(\mathrm{syn})}$ denotes the *synaptic current density*. We notice that in the classical model of the Hodgkin & Huxley axon, only three ionic species are considered, identified with sodium, potassium and chlorine. We therefore assume $N = 3$ and, by convention, assign $k = 1$ to the sodium, $k = 2$ to the potassium and $k = 3$ to the chlorine species. In doing so, and for consistency with the Hodgkin & Huxley model, we impose [96]

$$I_k^{(\mathrm{syn})} = 0, \qquad \text{for } k \in \{2,3\}, \tag{9.32a}$$

$$I_3^{(\mathrm{HH})} = 0. \tag{9.32b}$$

We notice that each $I_k^{(\mathrm{ionic})}$ is expressed as a function of the potential difference V through constitutive laws [256, 96, 147].

In particular, the explicit expressions of $I_k^{(\mathrm{pass})}$ for the considered ionic species [96, 279, 261, 278, 277, 256, 147] are

$$I_1^{(\mathrm{pass})} = G_1^{(\mathrm{pass})}[V - E_1], \tag{9.33a}$$
$$I_2^{(\mathrm{pass})} = G_2^{(\mathrm{pass})}[V - E_2], \tag{9.33b}$$
$$I_3^{(\mathrm{pass})} = G_3^{(\mathrm{pass})}[V - E_3], \tag{9.33c}$$

where $G_1^{(\mathrm{pass})}$, $G_2^{(\mathrm{pass})}$ and $G_3^{(\mathrm{pass})}$ are the membrane conductances of the passive model. Note that each of these conductances is constant and the corresponding reference value is chosen as in [256, 96]. Moreover, in (9.33a)–(9.33c), the Nernst potentials, E_k, are given by (see e.g., [256, 96, 95, 147])

$$E_k = \mathscr{E}_k \circ (c_{k|\mathscr{M}}^{(\mathrm{e})}, c_{k|\mathscr{M}}^{(\mathrm{i})}) = \frac{RT}{z_k F}\, \log\left(\frac{c_{k|\mathscr{M}}^{(\mathrm{e})}}{c_{k|\mathscr{M}}^{(\mathrm{i})}}\right), \qquad k = 1, \ldots, 3. \tag{9.34}$$

Equivalently, the expressions for I_k^{HH} are given by [256, 96, 147]

$$I_1^{(\mathrm{HH})} = G_1^{(\mathrm{HH})}[V - E_1], \tag{9.35a}$$
$$I_2^{(\mathrm{HH})} = G_2^{(\mathrm{HH})}[V - E_2], \tag{9.35b}$$
$$I_3^{(\mathrm{HH})} = G_3^{(\mathrm{HH})}[V - E_3]. \tag{9.35c}$$

In this case, the conductances of individual ionic species vary both explicitly in time and in response to the instantaneous value of the membrane potential. In particular, the way in which these dependencies are described defines the type of axon studied. In the Hodgkin & Huxley model, $G_3^{(\mathrm{HH})}$ is set equal to zero, while $G_1^{(\mathrm{HH})}$ and $G_2^{(\mathrm{HH})}$ are expressed by functions dependent both explicitly on time and on the membrane potential through three *gating variables*, denoted by m, n and h. The latter are auxiliary functions, obtained as solutions of the decoupled system of ordinary differential equations [96, 256, 147]

$$\partial_t m = \alpha_m - [\alpha_m + \beta_m]m, \tag{9.36a}$$
$$\partial_t h = \alpha_h - [\alpha_h + \beta_h]h, \tag{9.36b}$$
$$\partial_t n = \alpha_n - [\alpha_n + \beta_n]n, \tag{9.36c}$$

where α_m, β_m, α_h, β_h, α_n and β_n are phenomenological functions of the membrane potential V which, in the Hodgkin & Huxley model, are given by [256, 147]

$$\alpha_m(x,t) = \hat{\alpha}_m(V(x,t)) = 0.1\, \frac{25 - V(x,t)}{\exp([25 - V(x,t)]/25) - 1}, \tag{9.37a}$$

$$\alpha_h(x,t) = \hat{\alpha}_h(V(x,t)) = 0.07\ \exp(-V(x,t)/20)\,, \tag{9.37b}$$

$$\alpha_n(x,t) = \hat{\alpha}_n(V(x,t)) = 0.01\ \frac{10 - V(x,t)}{\exp([10 - V(x,t)]/10) - 1}, \tag{9.37c}$$

$$\beta_m(x,t) = \hat{\beta}_m(V(x,t)) = 4\ \exp(-V(x,t)/18)\,, \tag{9.37d}$$

$$\beta_h(x,t) = \hat{\beta}_h(V(x,t)) = \frac{1}{\exp[(30 - V(x,t)]/10) + 1}, \tag{9.37e}$$

$$\beta_n(x,t) = \hat{\beta}_n(V(x,t)) = 0.125\ \exp(-V(x,t)/80)\,. \tag{9.37f}$$

Note that each of the functions defined in (9.37a)–(9.37f) is dimensionally homogeneous to the reciprocal of the characteristic time –dependent on V– of the corresponding *gating* variable. For example, $\alpha_m + \beta_m$ is the reciprocal of the characteristic time of m. Moreover, each of the numerical coefficients in Equations (9.37a)–(9.37f) possesses physical dimensions such that the expression in which it appears makes sense. For example, with reference to (9.37a), the numerical coefficient "25" has dimensions $[25] = \mathrm{V}$, while the coefficient "0.1" has dimensions $[0.1] = (\mathrm{V}\cdot\mathrm{s})^{-1}$.

From the knowledge of the *gating* variables, it is possible to determine, by means of the Hodgkin & Huxley model, the conductances $G_1^{(\mathrm{HH})}$ and $G_2^{(\mathrm{HH})}$, which are then given by [96, 256, 147]

$$G_1^{(\mathrm{HH})}(x,t) = \overline{g}_1[m(V(x,t),t)]^3 h(V(x,t),t), \tag{9.38a}$$

$$G_2^{(\mathrm{HH})}(x,t) = \overline{g}_2[n(V(x,t),t)]^4. \tag{9.38b}$$

The expressions (9.38a) and (9.38b) are derived from the fact that each of the *gating* variables represents the dynamics of a gate present in a channel, which is selective to the passage of a given ion [147]. In the specific case of sodium, with conductance $G_1^{(\mathrm{HH})}$, there are three gates of type "m" and one gate of type "h" [147], corresponding, respectively, to the exponents 3 and 1 in (9.38a). Each of these types of gates refers to a given protein complex which, by remodelling, allows the passage of sodium [147]. Similarly, in the case of potassium, there are four "n" gates, i.e. of another type of protein complex which, as the potential V changes, becomes permeable or impermeable to this ion. For a more in-depth discussion of the *gating* variables we refer to the works [96, 277, 278, 261, 279, 256]. Here, we merely point out that the Equations (9.36a)-(9.36c) are to be considered an integral part of the model.

Finally, the term $I_k^{(\mathrm{syn})}$ refers to the synapses that the cell forms with other surrounding neurons. In particular, for the sodium, we write [96]

$$I_1^{(\mathrm{syn})}(x,t) = \mathcal{J}_1^{(\mathrm{syn})}(V(x,t), c_{1|\mathcal{M}}^{(\mathrm{i})}(x,t), c_{1|\mathcal{M}}^{(\mathrm{e})}(x,t), x, t)$$

$$=G_1^{(\mathrm{syn})} H(x) \exp\left(-\frac{t-t_0}{\alpha}\right) [V(x,t) - E_1(c^{(\mathrm{i})}_{1|\mathscr{M}}(x,t), c^{(\mathrm{e})}_{1|\mathscr{M}}(x,t))], \quad (9.39)$$

where t_0 is the initial time instant of observation of the system; $G_1^{(\mathrm{syn})}$ is the synaptic conductance; H is the characteristic function of the considered synaptic domain (this function specifies the region of the membrane where such currents actually take place); α is the time constant of synaptic excitation; and E_1 is sodium's Nernst potential, which is assigned in terms of a constitutive function of the ratio of the sodium concentration at the membrane from the "inner side" of the cell to that from the "outer side" as defined in (9.34).

Putting together the results reported in this Section, we conclude that I must be determined through the equation [96, 277, 278, 261, 279]

$$I = C\,\partial_t V + \sum_{k=1}^{N} I_k^{(\mathrm{ionic})}. \quad (9.40)$$

9.4.5 Interface conditions for the ionic concentrations

A condition on $\mathscr{M}$ concerning the k-th ionic species is obtained by requiring that $\boldsymbol{J}_k^{(\mathrm{i})} \cdot \boldsymbol{n}^{(\mathrm{ie})}$ and $\boldsymbol{J}_k^{(\mathrm{e})} \cdot \boldsymbol{n}^{(\mathrm{ei})}$, rather than being equal to each other, are equal to densities of membrane currents associated with the ionic species under consideration. Denoting such current densities by $I_k^{(\mathrm{i})}$ and $I_k^{(\mathrm{e})}$, we assume that [96]

$$\boldsymbol{J}_k^{(\mathrm{i})} \cdot \boldsymbol{n}^{(\mathrm{ie})} = I_k^{(\mathrm{i})}, \quad (9.41a)$$

$$-\boldsymbol{J}_k^{(\mathrm{e})} \cdot \boldsymbol{n}^{(\mathrm{ei})} = I_k^{(\mathrm{e})}. \quad (9.41b)$$

We notice that the introduction of $I_k^{(\mathrm{i})}$ and $I_k^{(\mathrm{e})}$, with $k = 1, \ldots, N$, introduces $2N$ new unknowns into the model. For the problem at hand, they can be constitutively specified as (see [96])

$$I_k^{(\mathrm{i})} = \frac{1}{F z_k} \left\{ I_k^{(\mathrm{ionic})} + \alpha_k^{(\mathrm{i})} \left[I - I^{(\mathrm{ionic})} \right] \right\}, \quad (9.42a)$$

$$I_k^{(\mathrm{e})} = \frac{1}{F z_k} \left\{ I_k^{(\mathrm{ionic})} + \alpha_k^{(\mathrm{e})} \left[I - I^{(\mathrm{ionic})} \right] \right\}, \quad (9.42b)$$

where $\alpha_k^{(\mathrm{i})}, \alpha_k^{(\mathrm{e})} \in]0,1[$ are partition coefficients that measure the proportion of membrane capacitive current that contributes to the normal flows $\boldsymbol{J}_k^{(\mathrm{i})} \cdot \boldsymbol{n}^{(\mathrm{ie})}$ and $\boldsymbol{J}_k^{(\mathrm{e})} \cdot \boldsymbol{n}^{(\mathrm{ei})}$, according to (9.41a) and (9.41b). Following [96], we write

$$\alpha_k^{(\mathrm{i})} = \frac{D_k^{(\mathrm{i})} z_k^2 c_k^{(\mathrm{i})}}{\sum_{j=1}^{N} D_j^{(\mathrm{i})} z_j^2 c_j^{(\mathrm{i})}}, \quad (9.43a)$$

$$\alpha_k^{(\mathrm{e})} = \frac{D_k^{(\mathrm{e})} z_k^2 c_k^{(\mathrm{e})}}{\sum_{j=1}^{N} D_j^{(\mathrm{e})} z_j^2 c_j^{(\mathrm{e})}}. \quad (9.43b)$$

9.4.6 Further conditions on the model unknowns

Following [96], we assume that the outer boundary of $\Omega^{(\mathrm{e})}$, i.e. $\partial\Omega^{(\mathrm{e,e})}$, is impermeable to the passage of the ionic species considered in model and, therefore, that the normal component to $\partial\Omega^{(\mathrm{e,e})}$ of each current density $\boldsymbol{J}_k^{(\mathrm{e})}$ is zero. Therefore, [96]

$$\boldsymbol{J}_k^{(\mathrm{e})} \cdot \boldsymbol{n}^{(\mathrm{ee})} = 0, \quad \text{on } \partial\Omega^{(\mathrm{e,e})}, \quad \forall\, k = 1, \ldots, N. \tag{9.44}$$

Considering the definition (9.11), Equation (9.44) constitutes a Robin condition for each concentration $c_k^{(\mathrm{e})}$ on $\partial\Omega^{(\mathrm{e,e})}$. Furthermore, from Equation (9.44) it follows directly that the normal component of the total current density, $\boldsymbol{J}^{(\mathrm{e})}$, must be zero (see [96]), i.e.

$$\boldsymbol{J}^{(\mathrm{e})} \cdot \boldsymbol{n}^{(\mathrm{ee})} = \left(\sum_{k=1}^{N} F z_k \boldsymbol{J}_k^{(\mathrm{e})} \right) \cdot \boldsymbol{n}^{(\mathrm{ee})} = 0, \quad \text{on } \partial\Omega^{(\mathrm{e,e})}. \tag{9.45}$$

Equation (9.45) constitutes an inhomogeneous Neumann condition on $\phi^{(\mathrm{e})}$.

It is also necessary to provide conditions on $\phi^{(\mathrm{e})}$. In particular, we set [96]

$$\langle \phi^{(\mathrm{e})} \rangle_{\Omega^{(\mathrm{e})}} := \frac{1}{|\Omega^{(\mathrm{e})}|} \int_{\Omega^{(\mathrm{e})}} \phi^{(\mathrm{e})} = 0, \tag{9.46}$$

according to which $\phi^{(\mathrm{e})}$ must have zero mean on $\Omega^{(\mathrm{e})}$. This constraint is necessary for the well-posedness of the boundary problem, although it is not the only possible option. In fact, it eliminates the indeterminacy on the solution of the considered problem, due to the fact that, for the typology of the model equations, and for the Neumann condition (9.45), if a given field $\phi^{(\mathrm{e})}$ is a solution, so will be $\phi^{(\mathrm{e})} + \phi_0$, with ϕ_0 an arbitrary constant. Alternatively, it is possible to impose a Dirichlet condition for $\phi^{(\mathrm{e})}$ on $\partial\Omega^{(\mathrm{e,e})}$, e.g.

$$\phi^{(\mathrm{e})}_{|\partial\Omega^{(\mathrm{e,e})}} = \phi_{\mathrm{b}}, \tag{9.47}$$

so that, by varying ϕ_{b}, it is possible to perform a parametric study of the model. This option, however, makes the problem more "rigid", since it prescribes that $\phi^{(\mathrm{e})}$ takes on $\partial\Omega^{(\mathrm{e,e})}$ fixed known values. On the other hand, the condition $\langle \phi^{(\mathrm{e})} \rangle_{\Omega^{(\mathrm{e})}} = 0$ leaves to $\phi^{(\mathrm{e})}$ the possibility of self-adjustment, implying also an alternation of sign compatible with the physics of the problem.

9.4.7 Membrane variables

Based on the above discussions, we note that it is possible to proceed by choosing as membrane variables either the potential difference V and the transmembrane

current density I or only one of them. In the first case, we speak of *mixed reformulation* and, by virtue of the similarity of the latter with Hu-Washizu's method [42], we will call it *formulation according to Hu-Washizu*. In the following, we will focus on this computational choice.

We take both V and I as model unknowns for the membrane, and express constitutively the current densities $I_k^{(\mathrm{ionic})}$ and the partition coefficients $\alpha_k^{(\mathrm{i})}$ and $\alpha_k^{(\mathrm{e})}$, for $k = 1, \dots, N$, so that the current densities $I_k^{(\mathrm{i})}$ and $I_k^{(\mathrm{e})}$ are also assigned by constitutive laws. More specifically, we have that:

(i) From the definition (9.39) of the synaptic current, we infer that the constitutive form of this current can be assigned as

$$I_1^{(\mathrm{syn})} = \mathcal{J}_1^{(\mathrm{syn})} \circ (V, c_{1|\mathcal{M}}^{(\mathrm{i})}, c_{1|\mathcal{M}}^{(\mathrm{e})}, \kappa_{\mathrm{S}}, \kappa_{\mathrm{T}}), \tag{9.48}$$

where $\kappa_{\mathrm{S}} : \mathcal{S} \times \mathcal{T} \to \mathcal{S}$ and $\kappa_{\mathrm{T}} : \mathcal{S} \times \mathcal{T}$ are two auxiliary functions, such that $\kappa_{\mathrm{S}}(x,t) = x$ and $\kappa_{\mathrm{T}}(x,t) = t$, $\mathcal{S}$ being the three-dimensional Euclidean space and $\mathcal{T}$ a time interval, and where $c_1^{(\mathrm{i})}$ and $c_1^{(\mathrm{e})}$ are, respectively, the sodium concentrations in $\Omega^{(\mathrm{i})}$ and in $\Omega^{(\mathrm{e})}$. Employing this result, and considering Equation (9.31) together with the explicit functional laws (9.33a)–(9.35c) of the passive axon and Hodgkin & Huxley [147, 256, 261, 96], the constitutive expression of the k-th total ion current is given by

$$I_k^{(\mathrm{ionic})} := \mathcal{J}_k^{(\mathrm{ionic})} \circ (V, c_{k|\mathcal{M}}^{(\mathrm{i})}, c_{k|\mathcal{M}}^{(\mathrm{e})}, \kappa_{\mathrm{S}}, \kappa_{\mathrm{T}}), \qquad k = 1, \dots, N. \tag{9.49}$$

(ii) Since the writing $I^{(\mathrm{ionic})} = \sum_{k=1}^{N} I_k^{(\mathrm{ionic})}$ holds, Equation (9.49) allows us to conclude that the total ionic current density admits constitutive expression of the type

$$I^{(\mathrm{ionic})} := \mathcal{J}^{(\mathrm{ionic})} \circ (V, \mathscr{C}_{|\mathcal{M}}^{(\mathrm{i})}, \mathscr{C}_{|\mathcal{M}}^{(\mathrm{e})}, \kappa_{\mathrm{S}}, \kappa_{\mathrm{T}}), \tag{9.50}$$

where we have used the notation

$$\mathscr{C}^{(\mathrm{i})} := (c_1^{(\mathrm{i})}, \dots, c_N^{(\mathrm{i})}), \tag{9.51a}$$

$$\mathscr{C}^{(\mathrm{e})} := (c_1^{(\mathrm{e})}, \dots, c_N^{(\mathrm{e})}). \tag{9.51b}$$

(iii) According to the definitions (9.43a) and (9.43b), the partition coefficients $\alpha_k^{(\mathrm{i})}$ and $\alpha_k^{(\mathrm{e})}$ can be rewritten as constitutive functions, respectively, of the ion concentrations $\mathscr{C}_{|\mathcal{M}}^{(\mathrm{i})}$ and $\mathscr{C}_{\mathcal{M}}^{(\mathrm{e})}$. Therefore,

$$\alpha_k^{(\mathrm{i})} := \hat{\alpha}_k^{(\mathrm{i})} \circ \mathscr{C}_{|\mathcal{M}}^{(\mathrm{i})}, \tag{9.52a}$$

$$\alpha_k^{(\mathrm{e})} := \hat{\alpha}_k^{(\mathrm{e})} \circ \mathscr{C}_{|\mathcal{M}}^{(\mathrm{e})}. \tag{9.52b}$$

(iv) On the basis of the definitions (9.49), (9.52a) and (9.52b) and recalling that V and I are independent variables of the model, we conclude that $I_k^{(\mathrm{i})}$ and $I_k^{(\mathrm{e})}$ (refer to (9.42a) e (9.42b)) can be expressed through the constitutive laws

$$I_k^{(\mathrm{i})} = \mathscr{I}_k^{(\mathrm{i})} \circ (V, I, \mathscr{C}_{|\mathscr{M}}^{(\mathrm{i})}, \mathscr{C}_{|\mathscr{M}}^{(\mathrm{e})}, \kappa_{\mathrm{S}}, \kappa_{\mathrm{T}}), \qquad k = 1, \ldots, N, \tag{9.53a}$$

$$I_k^{(\mathrm{e})} = \mathscr{I}_k^{(\mathrm{e})} \circ (V, I, \mathscr{C}_{|\mathscr{M}}^{(\mathrm{i})}, \mathscr{C}_{|\mathscr{M}}^{(\mathrm{e})}, \kappa_{\mathrm{S}}, \kappa_{\mathrm{T}}), \qquad k = 1, \ldots, N. \tag{9.53b}$$

9.4.8 Summary of the PNP model

In summary, the model equations are given by: (i) the electroneutrality conditions (9.20a) and (9.21a), written for $\Omega^{(\mathrm{i})}$ and for $\Omega^{(\mathrm{e})}$; (ii) the $2N$ balance equations for the ionic species (9.20b) and (9.21b), one for each $k = 1, \ldots, N$ and written for $\Omega^{(\mathrm{i})}$ and for $\Omega^{(\mathrm{e})}$; (iii) the relation (9.22), which binds V to the potentials at the membrane, i.e. $\phi_{|\mathscr{M}}^{(\mathrm{i})}$ and $\phi_{|\mathscr{M}}^{(\mathrm{e})}$; (iv) Equations (9.26a) and (9.26b), which express both the continuity of the total current densities normal to the membrane and the way that each binds to the transmembrane current density I; (v) the equation for the membrane, given by (9.40), which binds together I to V. Below, we summarise these equations [96]

$$\operatorname{div}\left[-\sum_{k=1}^{N} F z_k D_k^{(\mathrm{i})} \operatorname{grad} c_k^{(\mathrm{i})} - \left(\sum_{k=1}^{N} \frac{(F z_k)^2 D_k^{(\mathrm{i})}}{RT} c_k^{(\mathrm{i})}\right) \operatorname{grad} \phi^{(\mathrm{i})}\right] = 0, \quad \text{in } \Omega^{(\mathrm{i})}, \tag{9.54a}$$

$$\operatorname{div}\left[-\sum_{k=1}^{N} F z_k D_k^{(\mathrm{e})} \operatorname{grad} c_k^{(\mathrm{e})} - \left(\sum_{k=1}^{N} \frac{(F z_k)^2 D_k^{(\mathrm{e})}}{RT} c_k^{(\mathrm{e})}\right) \operatorname{grad} \phi^{(\mathrm{e})}\right] = 0, \quad \text{in } \Omega^{(\mathrm{e})}, \tag{9.54b}$$

$$\phi^{(\mathrm{i})}(x,t) = \phi^{(\mathrm{e})}(x,t) + V(x,t), \qquad \text{on } \mathscr{M}, \tag{9.54c}$$

$$\boldsymbol{J}^{(\mathrm{i})} \cdot \boldsymbol{n}^{(\mathrm{ie})} = I, \qquad \text{on } \mathscr{M}, \tag{9.54d}$$

$$\boldsymbol{J}^{(\mathrm{e})} \cdot \boldsymbol{n}^{(\mathrm{ei})} = -I, \qquad \text{on } \mathscr{M}, \tag{9.54e}$$

$$\boldsymbol{J}^{(\mathrm{e})} \cdot \boldsymbol{n}^{(\mathrm{ee})} = 0, \qquad \text{on } \partial\Omega^{(\mathrm{e,e})}, \tag{9.54f}$$

$$\langle \phi^{(\mathrm{e})} \rangle_{\Omega^{(\mathrm{e})}} = 0, \qquad \text{in } \Omega^{(\mathrm{e})}, \tag{9.54g}$$

$$\partial_t c_k^{(\mathrm{i})} + \operatorname{div}\left[-D_k^{(\mathrm{i})} \operatorname{grad} c_k^{(\mathrm{i})} - \frac{F z_k D_k^{(\mathrm{i})}}{RT} c_k^{(\mathrm{i})} \operatorname{grad} \phi^{(\mathrm{i})}\right] = 0, \qquad \text{in } \Omega^{(\mathrm{i})}, \tag{9.54h}$$

$$\partial_t c_k^{(\mathrm{e})} + \operatorname{div}\left[-D_k^{(\mathrm{e})} \operatorname{grad} c_k^{(\mathrm{e})} - \frac{F z_k D_k^{(\mathrm{e})}}{RT} c_k^{(\mathrm{e})} \operatorname{grad} \phi^{(\mathrm{e})}\right] = 0, \qquad \text{in } \Omega^{(\mathrm{e})}, \tag{9.54i}$$

$$\boldsymbol{J}_k^{(\mathrm{i})} \cdot \boldsymbol{n}^{(\mathrm{ie})} = \frac{1}{F z_k}\left\{I_k^{(\mathrm{ionic})} + \alpha_k^{(\mathrm{i})}\left[I - I^{(\mathrm{ionic})}\right]\right\} \equiv I_k^{(\mathrm{i})}, \qquad \text{on } \mathscr{M}, \tag{9.54j}$$

$$\boldsymbol{J}_k^{(\mathrm{e})} \cdot \boldsymbol{n}^{(\mathrm{ei})} = -\frac{1}{F z_k}\left\{I_k^{(\mathrm{ionic})} + \alpha_k^{(\mathrm{e})}\left[I - I^{(\mathrm{ionic})}\right]\right\} \equiv I_k^{(\mathrm{e})}, \qquad \text{on } \mathscr{M}, \tag{9.54k}$$

$$\boldsymbol{J}_k^{(\mathrm{e})} \cdot \boldsymbol{n}^{(\mathrm{ee})} = 0, \qquad \text{on } \partial\Omega^{(\mathrm{e,e})}, \tag{9.54l}$$

$$I = C\,\partial_t V + \sum_{k=1}^{N} I_k^{(\mathrm{ionic})}, \qquad \text{on } \mathscr{M}, \tag{9.54m}$$

where $I_k^{(\text{ionic})}$, $\alpha_k^{(\text{i})}$, $\alpha_k^{(\text{e})}$, and $I^{(\text{ionic})}$ are to be understood constitutively defined, as stated in the previous sections. Finally, the model must be completed by assigning appropriate initial conditions.

9.5 Weak form of the model equations

In this section, we put in weak form the Equations (9.54a)–(9.54m). For this purpose, we introduce the test functions

- $u^{(\text{i})}$ and $u^{(\text{e})}$, associated, respectively, to $\phi^{(\text{i})}$ and $\phi^{(\text{e})}$;
- $\omega_k^{(\text{i})}$ and $\omega_k^{(\text{e})}$, associated, respectively, to $c_k^{(\text{i})}$ and $c_k^{(\text{e})}$, for each $k = 1, \dots, N$;
- Θ, associated to V;
- Y, associated with I.

Each test function belongs to an appropriate functional space, which will be discussed when we address the more technical issues related to the Finite Element procedure. For the moment, we focus only on the fact that, having required $\phi^{(\text{e})}$ to have zero mean on $\Omega^{(\text{e})}$, the test function $u^{(\text{e})}$ must also share the same property. It, therefore, cannot be completely arbitrary and must be compatible with the constraint $\langle u^{(\text{e})} \rangle_{\Omega^{(\text{e})}} = 0$. Note that, in the following, we will take the implicit notation $\boldsymbol{J}^{(\text{i})}$, $\boldsymbol{J}^{(\text{e})}$, $\boldsymbol{J}_k^{(\text{i})}$ and $\boldsymbol{J}_k^{(\text{e})}$ for the current densities given in square brackets in Equations (9.54a), (9.54b), (9.54h) and (9.54i), as well as for the scalar current densities $I_k^{(\text{ionic})}$ and $I^{(\text{ionic})}$ and for the coefficients $\alpha_k^{(\text{i})}$ and $\alpha_k^{(\text{e})}$. However, we specify that each of the quantities listed is a "functional" of the unknowns of the model given by

$$\boldsymbol{J}^{(\text{i})} := \boldsymbol{\mathcal{J}}^{(\text{i})} \circ (\mathscr{C}^{(\text{i})}, \phi^{(\text{i})}), \tag{9.55a}$$

$$\boldsymbol{J}^{(\text{e})} := \boldsymbol{\mathcal{J}}^{(\text{e})} \circ (\mathscr{C}^{(\text{e})}, \phi^{(\text{e})}), \tag{9.55b}$$

$$\boldsymbol{J}_k^{(\text{i})} := \boldsymbol{\mathcal{J}}_k^{(\text{i})} \circ (c_k^{(\text{i})}, \phi^{(\text{i})}), \qquad k = 1, \dots, N, \tag{9.55c}$$

$$\boldsymbol{J}_k^{(\text{e})} := \boldsymbol{\mathcal{J}}_k^{(\text{e})} \circ (c_k^{(\text{e})}, \phi^{(\text{e})}), \qquad k = 1, \dots, N, \tag{9.55d}$$

$$I_k^{(\text{ionic})} := \mathcal{J}_k^{(\text{ionic})} \circ (V, c_{k|\mathcal{M}}^{(\text{i})}, c_{k|\mathcal{M}}^{(\text{e})}, \kappa_{\text{S}}, \kappa_{\text{T}}), \qquad k = 1, \dots, N, \tag{9.55e}$$

$$I^{(\text{ionic})} := \mathcal{J}^{(\text{ionic})} \circ (V, \mathscr{C}_{|\mathcal{M}}^{(\text{i})}, \mathscr{C}_{|\mathcal{M}}^{(\text{e})}, \kappa_{\text{S}}, \kappa_{\text{T}}), \tag{9.55f}$$

$$\alpha_k^{(\text{i})} := \hat{\alpha}_k^{(\text{i})} \circ \mathscr{C}_{|\mathcal{M}}^{(\text{i})}, \qquad k = 1, \dots, N, \tag{9.55g}$$

$$\alpha_k^{(\text{e})} := \hat{\alpha}_k^{(\text{e})} \circ \mathscr{C}_{|\mathcal{M}}^{(\text{e})}, \qquad k = 1, \dots, N, \tag{9.55h}$$

$$I_k^{(\text{i})} = \mathcal{J}_k^{(\text{i})} \circ (V, I, \mathscr{C}_{|\mathcal{M}}^{(\text{i})}, \mathscr{C}_{|\mathcal{M}}^{(\text{e})}, \kappa_{\text{S}}, \kappa_{\text{T}}), \qquad k = 1, \dots, N, \tag{9.55i}$$

$$I_k^{(\text{e})} = \mathcal{J}_k^{(\text{e})} \circ (V, I, \mathscr{C}_{|\mathcal{M}}^{(\text{i})}, \mathscr{C}_{|\mathcal{M}}^{(\text{e})}, \kappa_{\text{S}}, \kappa_{\text{T}}), \qquad k = 1, \dots, N. \tag{9.55j}$$

9.5.1 Weak form of the equations for the scalar potentials

We start with Equation (9.54a) for the scalar potential $\phi^{(\mathrm{i})}$, which is not subjected to constrains, and multiply it by the test function $u^{(\mathrm{i})}$, so that

$$u^{(\mathrm{i})}\mathrm{div}[\boldsymbol{\mathcal{J}}^{(\mathrm{i})} \circ (\mathscr{C}^{(\mathrm{i})}, \phi^{(\mathrm{i})})] = 0. \tag{9.56}$$

Thus, by using Leibniz's rule of the derivative of a product, integrating the result over the region $\Omega^{(\mathrm{i})}$, employing Gauss's Theorem and the boundary condition (9.54d), the weak form of (9.54a) is

$$\int_{\mathscr{M}} u^{(\mathrm{i})} \underbrace{[\boldsymbol{\mathcal{J}}^{(\mathrm{i})} \circ (\mathscr{C}^{(\mathrm{i})}, \phi^{(\mathrm{i})})] \cdot \boldsymbol{n}^{(\mathrm{ie})}}_{=I} - \int_{\Omega^{(\mathrm{i})}} [\boldsymbol{\mathcal{J}}^{(\mathrm{i})} \circ (\mathscr{C}^{(\mathrm{i})}, \phi^{(\mathrm{i})})]\mathrm{grad}u^{(\mathrm{i})} = 0. \tag{9.57}$$

We now turn to Equation (9.54b) for the scalar potential $\phi^{(\mathrm{e})}$. In this case, we multiply Equation (9.54b) by the test function $u^{(\mathrm{e})}$ such that $\langle u^{(\mathrm{e})}\rangle_{\Omega^{(\mathrm{e})}} = 0$. To account for this restriction, we follow the same procedure as described for $\phi^{(\mathrm{i})}$ and which led to (9.57) but, this time, we add to the result the term $\Lambda^{(\mathrm{e})}\langle u^{(\mathrm{e})}\rangle_{\Omega^{(\mathrm{e})}}$, where $\Lambda^{(\mathrm{e})}$ is an unknown *Lagrange multiplier*. Therefore, by also employing Equations (9.54e) and (9.54f), we get

$$\begin{aligned}\int_{\mathscr{M}} u^{(\mathrm{e})} \underbrace{[\boldsymbol{\mathcal{J}}^{(\mathrm{e})} \circ (\mathscr{C}^{(\mathrm{e})}, \phi^{(\mathrm{e})})] \cdot \boldsymbol{n}^{(\mathrm{ei})}}_{=-I} + \int_{\partial\Omega^{(\mathrm{e,e})}} u^{(\mathrm{e})} \underbrace{[\boldsymbol{\mathcal{J}}^{(\mathrm{e})} \circ (\mathscr{C}^{(\mathrm{e})}, \phi^{(\mathrm{e})})] \cdot \boldsymbol{n}^{(\mathrm{ee})}}_{=0} \\ - \int_{\Omega^{(\mathrm{e})}} [\boldsymbol{\mathcal{J}}^{(\mathrm{e})} \circ (\mathscr{C}^{(\mathrm{e})}, \phi^{(\mathrm{e})})]\mathrm{grad}u^{(\mathrm{e})} + \lambda^{(\mathrm{e})} \int_{\Omega^{(\mathrm{e})}} u^{(\mathrm{e})} = 0,\end{aligned} \tag{9.58}$$

where

$$\lambda^{(\mathrm{e})} := \frac{\Lambda^{(\mathrm{e})}}{|\Omega^{(\mathrm{e})}|}, \tag{9.59}$$

identifies the "rescaled" Lagrange multiplier $\lambda^{(\mathrm{e})}$ as the new unknown of the problem. We observe that, since $\lambda^{(\mathrm{e})}$ is *dual* to the integral $\int_{\Omega^{(\mathrm{e})}} \phi^{(\mathrm{e})}$, it is a function of time constant in space.

In summary, the weak forms for the equations determining the scalar potentials $\phi^{(\mathrm{i})}$ and $\phi^{(\mathrm{e})}$ are given by

$$- \int_{\Omega^{(\mathrm{i})}} [\boldsymbol{\mathcal{J}}^{(\mathrm{i})} \circ (\mathscr{C}^{(\mathrm{i})}, \phi^{(\mathrm{i})})]\mathrm{grad}u^{(\mathrm{i})} + \int_{\mathscr{M}} u^{(\mathrm{i})} I = 0, \tag{9.60a}$$

$$- \int_{\Omega^{(\mathrm{e})}} [\boldsymbol{\mathcal{J}}^{(\mathrm{e})} \circ (\mathscr{C}^{(\mathrm{e})}, \phi^{(\mathrm{e})})]\mathrm{grad}u^{(\mathrm{e})} - \int_{\mathscr{M}} u^{(\mathrm{e})} I \; + \; \lambda^{(\mathrm{e})} \int_{\Omega^{(\mathrm{e})}} u^{(\mathrm{e})} = 0. \tag{9.60b}$$

9.5.2 Weak form of the equations for the concentrations

For each $k = 1, \dots, N$, we multiply Equations (9.54h) and (9.54i) by the test concentrations $\omega_k^{(\mathrm{i})}$ and $\omega_k^{(\mathrm{e})}$, respectively. Furthermore, by using Leibniz's rule; integrating the resulting expressions over $\Omega_k^{(\mathrm{i})}$ and $\Omega_k^{(\mathrm{e})}$; invoking Gauss's theorem; and employing the boundary conditions (9.54j), (9.54k) and (9.54l), we obtain, for all $k = 1, \dots, N$,

$$\int_{\Omega^{(\mathrm{i})}} \omega_k^{(\mathrm{i})} \partial_t c_k^{(\mathrm{i})} - \int_{\Omega^{(\mathrm{i})}} [\boldsymbol{\mathcal{J}}_k^{(\mathrm{i})} \circ (c_k^{(\mathrm{i})}, \phi^{(\mathrm{i})})] \mathrm{grad}\, \omega_k^{(\mathrm{i})} + \int_{\mathscr{M}} \omega_k^{(\mathrm{i})} [\mathcal{J}_k^{(\mathrm{i})} \circ (V, I, \mathscr{C}_{|\mathscr{M}}^{(\mathrm{i})}, \mathscr{C}_{|\mathscr{M}}^{(\mathrm{e})}, \kappa_{\mathrm{S}}, \kappa_{\mathrm{T}})] = 0, \tag{9.61a}$$

$$\int_{\Omega^{(\mathrm{e})}} \omega_k^{(\mathrm{e})} \partial_t c_k^{(\mathrm{e})} - \int_{\Omega^{(\mathrm{e})}} [\boldsymbol{\mathcal{J}}_k^{(\mathrm{e})} \circ (c_k^{(\mathrm{e})}, \phi^{(\mathrm{e})})] \mathrm{grad}\, \omega_k^{(\mathrm{e})} + \int_{\mathscr{M}} \omega_k^{(\mathrm{e})} [\mathcal{J}_k^{(\mathrm{e})} \circ (V, I, \mathscr{C}_{|\mathscr{M}}^{(\mathrm{i})}, \mathscr{C}_{|\mathscr{M}}^{(\mathrm{e})}, \kappa_{\mathrm{S}}, \kappa_{\mathrm{T}})] = 0. \tag{9.61b}$$

9.5.3 Weak form of the equations in the membrane

The membrane potential, V, binds the extensions of $\phi^{(\mathrm{i})}$ and $\phi^{(\mathrm{e})}$ to the membrane, which we denoted by $\phi_{|\mathscr{M}}^{(\mathrm{i})}$ and $\phi_{|\mathscr{M}}^{(\mathrm{e})}$, as prescribed by Equation (9.54c). The latter is an algebraic equation and, as such, does not, in principle, need to be put into weak form. However, for the sake of uniformity, it is convenient to perform this step. We multiply, therefore, Equation (9.54c) by the test function Y, which represents a *virtual variation of current*, and integrate the result on the membrane, obtaining

$$\int_{\mathscr{M}} [\phi^{(\mathrm{i})} - \phi^{(\mathrm{e})}] Y - \int_{\mathscr{M}} V Y = 0. \tag{9.62}$$

9.5.4 Weak form of the equation for the membrane current density

The weak form of Equation (9.54m) is obtained by multiplying (9.54m) by the test function *Theta*, which is defined exclusively on $\mathscr{M}$ and represents a *virtual variation of membrane potential*. Thus, by integrating the result on $\mathscr{M}$, we obtain

$$\int_{\mathscr{M}} \Theta I = \int_{\mathscr{M}} \Theta\, C\, \partial_t V + \int_{\mathscr{M}} \sum_{k=1}^{N} \Theta [\mathcal{J}_k^{(\mathrm{ionic})} \circ (V, c_{k|\mathscr{M}}^{(\mathrm{i})}, c_{k|\mathscr{M}}^{(\mathrm{e})}, \kappa_{\mathrm{S}}, \kappa_{\mathrm{T}})]. \tag{9.63}$$

9.5.5 The null mean condition

Finally, we account for the null mean condition for $\phi^{(\mathrm{e})}$ by multiplying the constraint $\langle\phi^{(\mathrm{e})}\rangle_{\Omega^{(\mathrm{e})}}$ by a constant $\bar{\ell}^{(\mathrm{e})}$, which represents the virtual variation of the Lagrange multiplier $\Lambda^{(\mathrm{e})}$. We obtain, therefore,

$$\bar{\ell}^{(\mathrm{e})}\langle\phi^{(\mathrm{e})}\rangle_{\Omega^{(\mathrm{e})}} = \ell^{(\mathrm{e})}\int_{\Omega^{(\mathrm{e})}}\phi^{(\mathrm{e})} = 0, \qquad \ell^{(\mathrm{e})} := \frac{\bar{\ell}^{(\mathrm{e})}}{|\Omega^{(\mathrm{e})}|}, \tag{9.64}$$

with $\ell^{(\mathrm{e})}$ being the virtual variation of $\lambda^{(\mathrm{e})}$.

9.5.6 Summary of equations in weak form

The model equations, written in weak form, are given by the following $5+2N$ integral equations

$$-\int_{\Omega^{(\mathrm{i})}}[\boldsymbol{\mathcal{J}}^{(\mathrm{i})}\circ(\mathscr{C}^{(\mathrm{i})},\phi^{(\mathrm{i})})]\mathrm{grad}u^{(\mathrm{i})} + \int_{\mathscr{M}}u^{(\mathrm{i})}I = 0, \tag{9.65a}$$

$$-\int_{\Omega^{(\mathrm{e})}}[\boldsymbol{\mathcal{J}}^{(\mathrm{e})}\circ(\mathscr{C}^{(\mathrm{e})},\phi^{(\mathrm{e})})]\mathrm{grad}u^{(\mathrm{e})} - \int_{\mathscr{M}}u^{(\mathrm{e})}I \;+\; \lambda^{(\mathrm{e})}\int_{\Omega^{(\mathrm{e})}}u^{(\mathrm{e})} = 0, \tag{9.65b}$$

$$\int_{\mathscr{M}}[\phi^{(\mathrm{i})}-\phi^{(\mathrm{e})}]Y - \int_{\mathscr{M}}VY = 0, \tag{9.65c}$$

$$-\int_{\mathscr{M}}\Theta I + \int_{\mathscr{M}}\Theta\, C\,\partial_t V + \int_{\mathscr{M}}\sum_{k=1}^{N}\Theta[\mathcal{I}_k^{(\mathrm{ionic})}\circ(V,c_{k|\mathscr{M}}^{(\mathrm{i})},c_{k|\mathscr{M}}^{(\mathrm{e})},\kappa_{\mathrm{S}},\kappa_{\mathrm{T}})] = 0, \tag{9.65d}$$

$$\ell^{(\mathrm{e})}\int_{\Omega^{(\mathrm{e})}}\phi^{(\mathrm{e})} = 0, \tag{9.65e}$$

$$\begin{aligned}&\int_{\Omega^{(\mathrm{i})}}\omega_k^{(\mathrm{i})}\partial_t c_k^{(\mathrm{i})} - \int_{\Omega^{(\mathrm{i})}}[\boldsymbol{\mathcal{J}}_k^{(\mathrm{i})}\circ(c_k^{(\mathrm{i})},\phi^{(\mathrm{i})})]\mathrm{grad}\,\omega_k^{(\mathrm{i})}\\ &+\int_{\mathscr{M}}\omega_k^{(\mathrm{i})}[\mathcal{I}_k^{(\mathrm{i})}\circ(V,I,\mathscr{C}_{|\mathscr{M}}^{(\mathrm{i})},\mathscr{C}_{|\mathscr{M}}^{(\mathrm{e})},\kappa_{\mathrm{S}},\kappa_{\mathrm{T}})] = 0,\end{aligned} \tag{9.65f}$$

$$\begin{aligned}&\int_{\Omega^{(\mathrm{e})}}\omega_k^{(\mathrm{e})}\partial_t c_k^{(\mathrm{e})} - \int_{\Omega^{(\mathrm{e})}}[\boldsymbol{\mathcal{J}}_k^{(\mathrm{e})}\circ(c_k^{(\mathrm{e})},\phi^{(\mathrm{e})})]\mathrm{grad}\,\omega_k^{(\mathrm{e})}\\ &+\int_{\mathscr{M}}\omega_k^{(\mathrm{e})}[\mathcal{I}_k^{(\mathrm{e})}\circ(V,I,\mathscr{C}_{|\mathscr{M}}^{(\mathrm{i})},\mathscr{C}_{|\mathscr{M}}^{(\mathrm{e})},\kappa_{\mathrm{S}},\kappa_{\mathrm{T}})] = 0,\end{aligned} \tag{9.65g}$$

in the $5+2N$ unknowns grouped in the following set

$$\mathscr{U} := \{\phi^{(\mathrm{i})},\phi^{(\mathrm{e})},V,I,\lambda^{(\mathrm{e})},c_1^{(\mathrm{i})},\ldots,c_N^{(\mathrm{i})},c_1^{(\mathrm{e})},\ldots,c_N^{(\mathrm{e})}\}. \tag{9.66}$$

Remark 17 (Non-linearities and couplings in the model)**.** *Equations* (9.60a)–(9.63) *constitute a non-linear and strongly coupled system. In particular, the non-linearity depends on the law by which the constitutive expressions of the coefficients* $\hat{\alpha}_k^{(\mathrm{i})}$ *and*

$\hat{\alpha}_k^{(\mathrm{e})}$ *depend on the concentrations, and the law by which the constitutive expressions of the membrane ionic currents* $\mathcal{J}_k^{(\mathrm{ionic})}$ *and* $\mathcal{J}^{(\mathrm{ionic})}$ *depend on the potential difference* V *on* $\mathscr{M}$ *as well as on the ratio of the ionic concentrations on either side of* $\mathscr{M}$*. On the other hand, the strong coupling between the equations depends on the interface conditions on the current densities, which cause* I *and* V *to appear in both the equations for the evolution of the ion concentrations and those for the scalar potentials in the regions* $\Omega^{(\mathrm{i})}$ *and* $\Omega^{(\mathrm{e})}$ *as well as in the equation linking* I *to* V *on* $\mathscr{M}$*.*

Remark 18 (Simplified version of the model)**.** *We note that the model equations and the corresponding unknowns are listed in such a way that the subsystem* (9.65a)–(9.65e)*, in the* 5 *unknowns* $\phi^{(\mathrm{i})}$*,* $\phi^{(\mathrm{e})}$*,* V*,* I*,* $\lambda^{(\mathrm{e})}$*, can be "extracted" from the system* (9.65a)–(9.65g)*. The system* (9.65a)–(9.65e) *can be seen as a simplified version of the full model in which the concentrations are considered known. The study of this simplified model is instructive to understand the mathematical structure of the problem under consideration, especially from the point of view of the Finite Element implementation. In fact, the presence of the Lagrange multiplier* $\lambda^{(\mathrm{e})}$ *leads to a matrix with a zero on the main diagonal, which is typical of constrained problems.*

9.6 Benchmark problem in a simplified geometry

In this section, we report some numerical results of the PNP model using the commercial software COMSOL Multiphysics®. Following [96], we consider the two-dimensional domain shown in Fig. 9.2. Specifically, we define Ω as the union of two sets representing the intra-cellular space $\Omega^{(\mathrm{i})}$ and the extra-cellular space $\Omega^{(\mathrm{e})}$ communicating through the membrane $\mathscr{M}$. In particular, the intra-cellular domain is defined as the rectangle $\Omega^{(\mathrm{i})} = [6\cdot10^{-6}\,\mathrm{m},\, 5.6\cdot10^{-5}\,\mathrm{m}]\times[2.8\cdot10^{-5}\mathrm{m},\, 3.4\cdot 10^{-5}\mathrm{m}]$. On the other hand, the extra-cellular domain is specified by the domain $\Omega^{(\mathrm{e})} = [0\,\mathrm{m},\, 6\cdot10^{-5},\mathrm{m}]\times[0\mathrm{m},\, 6\cdot10^{-5}\mathrm{m}]\setminus\Omega^{(\mathrm{i})}$. The size of Ω has been chosen so that the solution, being strongly variable in the immediate vicinity of the cell membrane, is not affected by the null flux condition imposed on $\partial\Omega^{(\mathrm{ee})}$. With such an arrangement, the cell membrane is given by the edge of the innermost rectangle, i.e. $\mathscr{M}\equiv\partial\Omega^{(\mathrm{i})}$.

We mention that, in [96], the numerical simulations were conducted by activating, time by time, the different terms of the ionic current presented in Section 9.4.4. Here, we simulate the system in the time interval $\mathcal{T} = [0\,\mathrm{ms},\, 100\,\mathrm{ms}]$ with a synaptic stimulus generated by a train of pulses centred at the instants 0 ms, 30 ms and 60 ms with the synaptic current defined in (9.39). That is, in our simulations

$$I_1^{(\mathrm{syn})} = \sum_{i=1}^{3} \chi_{[t_i,100\,\mathrm{ms}]} G_1^{(\mathrm{syn})} H \exp\left(-\frac{t-t_i}{\alpha}\right)[V - E_1(c_{1|\mathscr{M}}^{(\mathrm{i})}, c_{1|\mathscr{M}}^{(\mathrm{e})})], \tag{9.67}$$

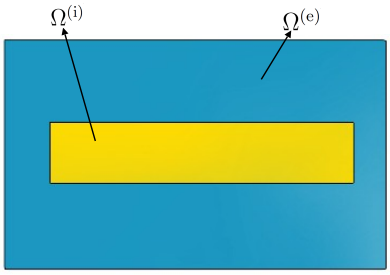

Figure 9.2: Computational domain used in the computational simulations.

where $\chi_{[t_i,100\,\mathrm{ms}]}(t) = 1$ if $t \in [t_i,100\,\mathrm{ms}]$ and $\chi_{[t_i,100\,\mathrm{ms}]}(t) = 0$, otherwise. The synaptic current is only activated on the "left part" of the cell via the characteristic function $H_{[5\cdot10^{-6},10^{-5}]\times[0,6\cdot10^{-5}]}(x,y)$. The values of the parameters chosen to carry out the simulations are given in Table 9.1.

We start our analysis by activating only the passive ionic current terms, so that

$$\begin{aligned} I = I^{(\mathrm{cap})} + I^{(\mathrm{ionic})} &= C\partial_t V + \sum_{k=1}^{3} I_k^{(\mathrm{pass})} + I_1^{(\mathrm{syn})} \\ &= C\partial_t V + \sum_{k=1}^{3} G_k^{(\mathrm{pass})}(V - E_k) + I_1^{(\mathrm{syn})}, \end{aligned} \tag{9.68}$$

where the Nernst potentials, E_k, were introduced in (9.34) and the synaptic current for the sodium, $I_1^{(\mathrm{syn})}$, is given in (9.67). In Figure 9.3 (left panel), we show the membrane potential of the PNP model for the case of a passive membrane. In this case, it is observed that the membrane potential, starting from an initial value of $-65\,\mathrm{mV}$ peaks at about $-30\,\mathrm{mV}$ with each stimulus of the synaptic current. After the realisation of this peak, the potential shows the attainment of a steady state (about $-45\,\mathrm{mV}$) which is perturbed only when a new stimulus occurs. In this case, because the model is linear, the hyper-polarisation process does not occur. That is, the membrane potential does not become more negative (i.e. less than $-65\,\mathrm{mV}$). So, in this situation, action potentials are inhibited.

A different situation can be observed when we include the Hodgkin & Huxley current in the model. In such a case, we have that

$$\begin{aligned} I &= I^{(\mathrm{cap})} + I^{(\mathrm{ionic})} \\ &= C\partial_t V + \sum_{k=1}^{3} I_k^{(\mathrm{pass})} + \sum_{k=1}^{2} I_k^{(\mathrm{HH})} + I_1^{(\mathrm{syn})} \\ &= C\partial_t V + \sum_{k=1}^{3} G_k^{(\mathrm{pass})}(V - E_k) + \sum_{k=1}^{2} G_k^{(\mathrm{HH})}(V - E_k) + I_1^{(\mathrm{syn})}, \end{aligned} \tag{9.69}$$

Table 9.1: List of parameters used in the numerical simulations [96].

Description	Symbol	Value
Faraday constant	F	$9.648 \cdot 10^6\,\mathrm{C/mol}$
Absolute temperature	T	$300\,\mathrm{K}$
Gas constant	R	$8.31\,\mathrm{J/(mol\,K)}$
Membrane capacitance	C	$0.01\,\mathrm{F/m}$
Sodium diffusion coefficient	$D_1^{(\mathrm{i})} \equiv D_1^{(\mathrm{e})}$	$1.33 \cdot 10^{-9}\,\mathrm{m^2/s}$
Potassium diffusion coefficient	$D_2^{(\mathrm{i})} \equiv D_2^{(\mathrm{e})}$	$1.96 \cdot 10^{-9}\,\mathrm{m^2/s}$
Chloride diffusion coefficient	$D_3^{(\mathrm{i})} \equiv D_3^{(\mathrm{e})}$	$2.03 \cdot 10^{-9}\,\mathrm{m^2/s}$
Initial intracellular sodium concentration	$c_{1_0}^{(\mathrm{i})}$	$12\,\mathrm{mM}$
Initial extracellular sodium concentration	$c_{1_0}^{(\mathrm{e})}$	$100\,\mathrm{mM}$
Initial intracellular potassium concentration	$c_{2_0}^{(\mathrm{i})}$	$125\,\mathrm{mM}$
Initial extracellular potassium concentration	$c_{2_0}^{(\mathrm{e})}$	$4\,\mathrm{mM}$
Initial intracellular chloride concentration	$c_{3_0}^{(\mathrm{i})}$	$137\,\mathrm{mM}$
Initial extracellular chloride concentration	$c_{3_0}^{(\mathrm{e})}$	$104\,\mathrm{mM}$
Passive conductivity of sodium	$G_1^{(\mathrm{pass})}$	$2.0\,\mathrm{S/m^2}$
Passive conductivity of potassium	$G_2^{(\mathrm{pass})}$	$8.0\,\mathrm{S/m^2}$
Passive conductivity of chloride	$G_3^{(\mathrm{pass})}$	$0\,\mathrm{S/m^2}$
Conductivity of sodium	$\overline{g}_1$	$1200\,\mathrm{S/m^2}$
Passive conductivity of potassium	$\overline{g}_2$	$360\,\mathrm{S/m^2}$
Passive conductivity of chloride	$\overline{g}_3$	$0.3\,\mathrm{S/m^2}$

where $G_k^{(\mathrm{HH})}$, with $k = 1,2$, are expressed as functions of the gating variables m, h and n as described in (9.38a) and (9.38b). In this situation, as shown in Figure 9.3 (right panel), starting from an initial condition of 65 mV, the membrane potential shows the realisation of three peaks, each corresponding to a stimulus from the synaptic current. In this context, the process of hyper-polarisation that the cell undergoes after the peak potential is realised. That is, the membrane potential reaches values lower than the resting potential of the cell, $V_R = -65\,\mathrm{mV}$.

Of particular interest is the evolution of the concentration of the ions contributing to the conduction of the membrane potential (in our framework, sodium, potassium and chlorine). In particular, in Figure 9.4, we show the evolution of the sodium in the extracellular space for the case in which all currents are active at two different instants of time coinciding with the activation of the synaptic current,

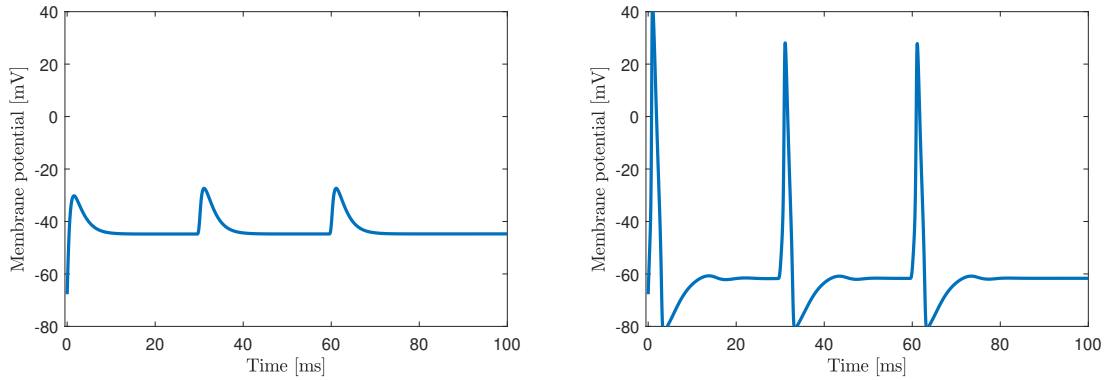

Figure 9.3: (Left) Membrane potential in a passive membrane. (Right) Membrane potential with Hodgkin & Huxley membrane model.

namely $t = 30\,[\text{ms}]$ (left panel) and $t = 60\,[\text{ms}]$ (right panel). The study of the variation of the ionic concentration in $\Omega^{(\text{i})}$ and in $\Omega^{(\text{e})}$, shows how, given stimulation in the synaptic zone, the membrane potential propagates along the length of the cell reaching the opposite end. In this case, it is observed that the concentration differs from the initial value only in the vicinity of the cell membrane. In particular, the value of the membrane potential at locations where the cell is not stimulated by the synapse can be used to study the response of synaptic buttons to the electrical potential for neurotransmitter release [159].

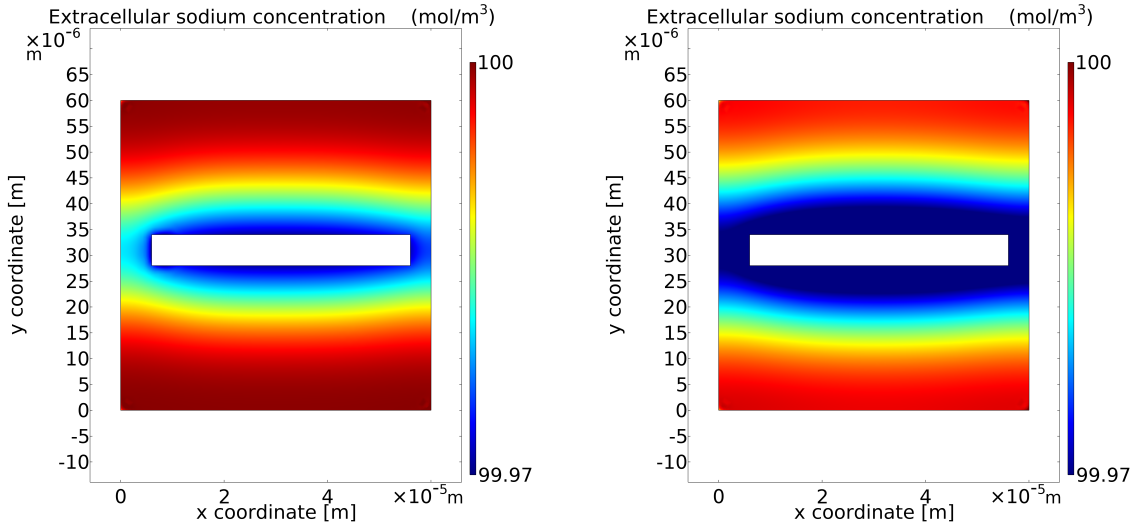

Figure 9.4: Extracellular sodium concentration in the surroundings of a cell membrane at $t = 30\,[\text{ms}]$ (left panel) and $t = 60\,[\text{ms}]$ (right panel)

Chapter 10

The fractal PNP model

The work reported in this chapter is taken from [236][1].

10.1 Introduction

According to [259], the complex branching pattern of neuron dendrites can be described by means of a fractal dimension, which reflects the fractal-like geometry of neurons. Knowing how neurons connect to each other and how this distribution influences the propagation of electrochemical signals is fundamental in the understanding of neuropathological diseases [259].

In the last decades, there has been a growing interest in using the mathematical tools offered by the theory of fractional calculus for the description of fractal media [56, 54, 214, 266]. For instance, in [266], Maxwell's Equations are presented in the case of a medium with fractal geometry. In this context, fractal current densities are introduced through the definition of appropriate transition functions from the fractal to the "classical" measure [266]. By virtue of the presence of such functions, Tarasov [266] speaks of "fractional currents". Here, taking inspiration in [266], we reformulate the PNP model introduced in Chapter 9 in a fractal context, i.e. by assuming that the current densities $\boldsymbol{J}_k^{(\mathrm{i})}$ and $\boldsymbol{J}_k^{(\mathrm{e})}$, with $k = 1, \ldots, N$, are expressed in terms of constitutive laws of fractal type.

10.1.1 Brief on fractal integration

In order to carry out the fractal formulation of Maxwell's Equations, we start by reviewing the introduction of the fractal measure for volume, surface and line

[1]The work [236] is also used in the MSc thesis of Mr. Vito Napoli. The Author of this PhD thesis was co-advisor of that MSc thesis.

integrals, according to Tarasov's [266].

Fractal measure for volume integrals

Let us consider the region of space $\Omega \subset \mathscr{S}$, where $\mathscr{S}$ is the three-dimensional Euclidean space, and let us denote by $\mu_3(\Omega) \geq 0$ the Lebesgue measure of Ω, which can be identified with the integral

$$\mu_3(\Omega) = \int_\Omega \mathrm{dv} \equiv \mathrm{Vol}(\Omega), \tag{10.1}$$

with dv denoting the classical Lebesgue volume measure. Introducing the real number $P_3 \in]2,3[$, referred to as *fractal dimension*, we call *fractal measure* of Ω, the positive real number defined by

$$\mu_{P_3}(\Omega) := \int_\Omega \mathfrak{f}_{P_3}(x)\mathrm{dv}(x) \geq 0, \tag{10.2}$$

where $\mathfrak{f}_{P_3} : \Omega \to \mathbb{R}$ is a transition function linking the classical Lebesgue measure to the fractal measure. In [266], $\mathfrak{f}_{P_3}$ is given by

$$\mathfrak{f}_{P_3}(x) := 2^{3-P_3}\frac{\Gamma(3/2)}{\Gamma(P_3/2)}\frac{1}{\|x - x_0\|^{3-P_3}}, \tag{10.3}$$

with x_0 being a fixed point (coincident, for example, with the origin of the reference system in consideration), and Γ is the Gamma function. In particular, by defining the measure

$$\mathrm{dv}_{P_3}(x) := \mathfrak{f}_{P_3}(x)\mathrm{dv}(x), \tag{10.4}$$

we can rewrite Equation (10.2) in the compact form [266]

$$\mu_{P_3}(\Omega) = \int_\Omega \mathrm{dv}_{P_3}(x). \tag{10.5}$$

Note that, in (10.3), P_3 plays the role of a parameter and, as P_3 varies in $]2,3[$, it is possible to vary the fractal measure of Ω, $\mu_{P_3}(\Omega)$, with continuity.

Remark 19 (Fractal volume measure in volume integrals)**.** *The second member of Equation* (9.1d) *determines the total free electric charge in* Ω*, i.e.*

$$Q_{\mathrm{f},3}(\varrho_\mathrm{f}, \Omega; t) := \int_\Omega \varrho_\mathrm{f}(x,t)\,\mathrm{dv}(x), \tag{10.6}$$

calculated with respect to the classical Lebesgue measure in Ω*. The subscript "3" in "*$Q_{\mathrm{f},3}(\varrho_\mathrm{f}, \Omega; t)$*" indicates that the integral in Equation* (10.6) *is performed in the*

three-dimensional region Ω. This charge is itself a measure (with sign), generally time-varying, and whose numerical value, at a given instant of time t and for Ω fixed, depends on the measure with respect to which it is integrated in Ω. Using the definition in (10.4)*, we define the* fractal total charge*, by replacing the measure* $\mathrm{dv}(x)$ *with the fractal measure* $\mathrm{dv}_{P_3}(x)$*, i.e. by writing*

$$\begin{aligned} Q_{\mathrm{f},P_3}(\varrho_{\mathrm{f}},\Omega;t) &:= \int_\Omega \varrho_{\mathrm{f}}(x,t)\,\mathrm{dv}_{P_3}(x) \\ &= \int_\Omega \varrho_{\mathrm{f}}(x,t)\mathfrak{f}_{P_3}(x)\mathrm{dv}(x) \\ &= \int_\Omega [\mathfrak{f}_{P_3}(x)\varrho_{\mathrm{f}}(x,t)]\mathrm{dv}(x) \\ &= Q_{\mathrm{f},3}(\varrho_{\mathrm{f},P_3},\Omega;t), \end{aligned} \tag{10.7}$$

where we have introduced the fractal total free charge density

$$\varrho_{\mathrm{f},P_3}(x,t) := \mathfrak{f}_{P_3}(x)\varrho_{\mathrm{f}}(x,t). \tag{10.8}$$

This result indicates that the total fractal charge calculated with respect to the density ϱ_{f}, i.e. $Q_{\mathrm{f},P_3}(\rho_{\mathrm{f}},\Omega,t)$, is equal to the total classical charge calculated with respect to the fractal density ϱ_{f,P_3}, namely $Q_{\mathrm{f},3}(\varrho_{\mathrm{f},P_3},\Omega;t)$.

Fractal measure for surface integrals

Let us consider a fixed surface, denoted by $\mathscr{A}$, which can be either open or closed, and let $\mu_2(\mathscr{A}) \geq 0$ be the measure of $\mathscr{A}$, i.e.

$$\mu_2(\mathscr{A}) = \int_{\mathscr{A}} \mathrm{da}. \tag{10.9}$$

Following, with slight modifications, Tarasov's notation [266], we consider the *fractal dimension* $P_2 \in]P_3-1,2[$, and define the *fractal measure of* $\mathscr{A}$ by the expression

$$\mu_{P_2}(\mathscr{A}) := \int_{\mathscr{A}} \mathfrak{f}_{P_2}(x)\mathrm{da}(x) \geq 0, \tag{10.10}$$

where, analogously to the above discussions, $\mathfrak{f}_{P_2} : \mathscr{A} \to \mathbb{R}$ is the transition function from the classical surface measure to the fractal surface measure. As in [266], we write

$$\mathfrak{f}_{P_2}(x) := 2^{2-P_2}\frac{1}{\Gamma(P_2/2)}\frac{1}{\|x-x_0\|^{2-P_2}}, \tag{10.11}$$

and, by introducing the measure

$$\mathrm{da}_{P_2}(x) := \mathfrak{f}_{P_2}(x)\mathrm{da}(x), \tag{10.12}$$

4654 we rewrite Equation (10.10) in the compact form

$$\mu_{P_2}(\mathscr{A}) = \int_{\mathscr{A}} \mathrm{da}_{P_2}(x). \tag{10.13}$$

4655 **Remark 20** (Fractal surface measure in flux integrals)**.** *In the "classical" Maxwell*
4656 *equations (see Equations* (9.1a)–(9.1d)*), one often encounters integrals of the type*

$$\Phi_2(\boldsymbol{Y}, \mathscr{A}; t) = \int_{\mathscr{A}} \boldsymbol{Y}(x,t) \cdot \boldsymbol{n}(x)\, \mathrm{da}(x), \tag{10.14}$$

4657 *where the surface $\mathscr{A}$ can represent either the open surface Σ or the closed surface*
4658 *$\partial\Omega$. In the above expression, $\boldsymbol{Y}(\,\cdot\,,t)$, at each time t, is a generic field of pseudo-*
4659 *vectors on $\mathscr{A}$, which can represent $\boldsymbol{B}(\,\cdot\,,t)$, $\partial_t\boldsymbol{B}(\,\cdot\,,t)$, $\boldsymbol{J}(\,\cdot\,,t)$, $\boldsymbol{D}(\,\cdot\,,t)$ or $\partial_t\boldsymbol{D}(\,\cdot\,,t)$*
4660 *(refer to Chapter 9). Furthermore, $\Phi_2(\boldsymbol{Y}, \mathscr{A}; t)$ is the flow of $\boldsymbol{Y}(\,\cdot\,,t)$ through $\mathscr{A}$*
4661 *at time t. Note that the subscript "2" in $\Phi_2(\boldsymbol{Y}, \mathscr{A}; t)$ reminds us that the flow is*
4662 *referred to a surface of dimension 2. So, we generalise the expression* (10.14) *as*
4663 *[266]*

$$\begin{aligned}
\Phi_{P_2}(\boldsymbol{Y}, \mathscr{A}; t) &= \int_{\mathscr{A}} \boldsymbol{Y}(x,t) \cdot \boldsymbol{n}(x)\, \mathrm{da}_{P_2}(x) \\
&= \int_{\mathscr{A}} [\boldsymbol{Y}(x,t) \cdot \boldsymbol{n}(x)]\, \mathfrak{f}_{P_2}(x) \mathrm{da}(x) \\
&= \int_{\mathscr{A}} [\mathfrak{f}_{P_2}(x) \boldsymbol{Y}(x,t)] \cdot \boldsymbol{n}(x) \mathrm{da}(x) \\
&= \Phi_2(\boldsymbol{Y}_{P_2}, \mathscr{A}; t),
\end{aligned} \tag{10.15}$$

4664 *where we have introduced the* fractal pseudo-vector field

$$\boldsymbol{Y}_{P_2}(x,t) := \mathfrak{f}_{P_2}(x) \boldsymbol{Y}(x,t) \equiv \hat{\boldsymbol{Y}}_{P_2}(x,t;\mathfrak{f}_{P_2}), \tag{10.16}$$

4665 *whose definition depends on the transition function $\mathfrak{f}_{P_2}$. Note that the identity*

$$\Phi_{P_2}(\boldsymbol{Y}, \mathscr{A}; t) = \Phi_2(\boldsymbol{Y}_{P_2}, \mathscr{A}; t), \tag{10.17}$$

4666 *for which it is possible to redefine the fractal flux of the "classical" field $\boldsymbol{Y}$ as the*
4667 *"classical" flux of the fractal flow $\boldsymbol{Y}_{P_2}$.*

4668 **Fractal measure for line integrals**

4669

4670 Let us consider a regular curve, $\mathscr{C}$, which can be either closed or open, and let
4671 us call by $\mu_1(\mathscr{C}) \geq 0$ the measure of $\mathscr{C}$, i.e. its length

$$\mu_1(\mathscr{C}) = \int_{\mathscr{C}} \mathrm{ds}, \tag{10.18}$$

where s represents the curvilinear abscissa of the curve itself. As above, we introduce the *fractal dimension* $P_1 \in]P_2 - 1,1[$, to redefine the fractal measure of $\mathscr{C}$ as

$$\mu_{P_1}(\mathscr{C}) = \int_{\mathscr{C}} \mathfrak{f}_{P_1}(x)\mathrm{ds}(x) \geq 0, \tag{10.19}$$

where $\mathfrak{f}_{P_1} : \mathscr{C} \to \mathbb{R}$ is the transition function connecting the classical line measure to the fractal measure. In [266], $\mathfrak{f}_{P_1}$ is defined as

$$\mathfrak{f}_{P_1}(x) := 2^{1-P_1}\frac{\Gamma(1/2)}{\Gamma(P_1/2)}\frac{1}{\|x - x_0\|^{1-P_1}}. \tag{10.20}$$

As in the three-dimensional and two-dimensional case, we can define the new fractal measure

$$\mathrm{ds}_{P_1}(x) := \mathfrak{f}_{P_1}(x)\mathrm{ds}(x), \tag{10.21}$$

so that Equation (10.19) takes the compact form [266]

$$\mu_{P_1}(\mathscr{C}) = \int_{\mathscr{C}} \mathrm{ds}_{P_1}(x). \tag{10.22}$$

Remark 21 (Fractal line measure in line integrals)**.** *The fractal measure for line integrals can be used to compute integrals of the type*

$$U(\boldsymbol{T}, \mathscr{C}; t) := \int_{\mathscr{C}} \boldsymbol{T}(x,t) \cdot \boldsymbol{\tau}(x)\mathrm{ds}(x), \tag{10.23}$$

which appear in Maxwell's Equations, where $\mathscr{C}$ represents a closed path, $\boldsymbol{\tau}$ is the field of tangent vectors to $\mathscr{C}$ and $\boldsymbol{T}(\cdot\,, t)$ is a generic field of co-vectors on $\mathscr{C}$, which can be interpreted either by $\boldsymbol{E}(\cdot\,, t)$ or by $\boldsymbol{H}(\cdot\,, t)$. To generalise the expression (10.23) *to the fractal measure given in* (10.22)*, we write [266]*

$$\begin{aligned} U_{P_1}(\boldsymbol{T}, \mathscr{C}; t) &= \int_{\mathscr{C}} \boldsymbol{T}(x,t) \cdot \boldsymbol{\tau}(x)\, \mathrm{ds}_{P_1}(x) \\ &= \int_{\mathscr{A}} [\boldsymbol{T}(x,t) \cdot \boldsymbol{\tau}(x)]\, \mathfrak{f}_{P_1}(x)\mathrm{ds}(x) \\ &= \int_{\mathscr{A}} [\mathfrak{f}_{P_1}(x)\boldsymbol{T}(x,t)] \cdot \boldsymbol{\tau}(x)\mathrm{ds}(x) \\ &= U(\boldsymbol{T}_{P_1}, \mathscr{C}; t), \end{aligned} \tag{10.24}$$

where we have introduced the fractal co-vector field

$$\boldsymbol{T}_{P_1}(x,t) := \mathfrak{f}_{P_1}(x)\boldsymbol{T}(x,t) \equiv \hat{\boldsymbol{T}}_{P_1}(x,t;\mathfrak{f}_{P_1}), \tag{10.25}$$

whose definition depends on the transition function $\mathfrak{f}_{P_1}$.

10.2 Fractal Maxwell equations

In order to introduce the fractal measure in Maxwell's Equations, we start from their writing in integral form. In particular, following the ideas in [266], we write

$$\int_{\partial\Sigma}[\mathfrak{f}_{P_1}(x)\boldsymbol{E}(x,t)]\cdot\boldsymbol{\tau}(x)\mathrm{ds}(x)=-\frac{\mathrm{d}}{\mathrm{d}t}\int_{\Sigma}[\mathfrak{f}_{P_2}(x)\boldsymbol{B}(x,t)]\cdot\boldsymbol{n}(x)\mathrm{da}(x), \tag{10.26a}$$

$$\int_{\partial\Omega}[\mathfrak{f}_{P_2}(x)\boldsymbol{B}(x,t)]\cdot\boldsymbol{n}(x)\mathrm{da}(x)=0, \tag{10.26b}$$

$$\begin{aligned}\int_{\partial\Sigma}[\mathfrak{f}_{P_1}(x)\boldsymbol{H}(x,t)]\cdot\boldsymbol{\tau}(x)]\mathrm{ds}(x)=&\int_{\Sigma}[\mathfrak{f}_{P_2}(x)\boldsymbol{J}(x,t)]\cdot\boldsymbol{n}(x)\mathrm{da}(x)\\&+\frac{\mathrm{d}}{\mathrm{d}t}\int_{\Sigma}[\mathfrak{f}_{P_2}(x)\boldsymbol{D}(x,t)]\cdot\boldsymbol{n}(x)\mathrm{da}(x),\end{aligned} \tag{10.26c}$$

$$\int_{\partial\Omega}[\mathfrak{f}_{P_2}(x)\boldsymbol{D}(x,t)]\cdot\boldsymbol{n}(x)\mathrm{da}(x)=\int_{\Omega}[\mathfrak{f}_{P_3}(x)\varrho_{\mathrm{f}}(x,t)]\mathrm{dv}(x), \tag{10.26d}$$

in which the region of space Ω, the surfaces $\partial\Omega$ and Σ, and the closed curve $\partial\Sigma$ are the same as those introduced in the "classical" Maxwell equations (9.1a)–(9.1d)[2]. Thus, localising (10.26a)–(10.26d), we obtain the local form of Maxwell equations, namely

$$\mathrm{curl}[\mathfrak{f}_{P_1}\boldsymbol{E}]=-\mathfrak{f}_{P_2}\partial_t\boldsymbol{B}, \tag{10.27a}$$

$$\mathrm{div}[\mathfrak{f}_{P_2}\boldsymbol{B}]=0, \tag{10.27b}$$

$$\mathrm{curl}[\mathfrak{f}_{P_1}\boldsymbol{H}]=\mathfrak{f}_{P_2}\boldsymbol{J}+\mathfrak{f}_{P_2}\partial_t\boldsymbol{D}, \tag{10.27c}$$

$$\mathrm{div}[\mathfrak{f}_{P_2}\boldsymbol{D}]=\mathfrak{f}_{P_3}\varrho_{\mathrm{f}}. \tag{10.27d}$$

We observe that, from now on, we neglect the term $\partial_t\boldsymbol{B}$, exactly as we did in Chapter 9. Therefore, Equation (10.27a) becomes

$$\mathrm{curl}[\mathfrak{f}_{P_1}\boldsymbol{E}]=\boldsymbol{0}, \tag{10.28}$$

from which we can deduce the existence of a generalised potential, that we also indicate with ϕ, so that

$$\mathfrak{f}_{P_1}\boldsymbol{E}=-\mathrm{grad}\,\phi\quad\text{and}\quad\boldsymbol{E}=-\frac{1}{\mathfrak{f}_{P_1}}\mathrm{grad}\,\phi. \tag{10.29}$$

Now, considering the divergence in Equation (10.27c), we obtain

$$0=\mathrm{div}[\mathfrak{f}_{P_2}\boldsymbol{J}]+\mathrm{div}[\mathfrak{f}_{P_2}\partial_t\boldsymbol{D}], \tag{10.30}$$

[2]Note that, given a generic function $g:\Sigma\times\mathcal{T}\to\mathbb{R}$, such that $(x,t)\mapsto g(x,t)$, we are employing the slight abuse of notation $\frac{\mathrm{d}}{\mathrm{d}t}\int_{\Sigma}g(x,t)\mathrm{da}(x)\equiv\left[\frac{\mathrm{d}}{\mathrm{d}t}\int_{\Sigma}g(x,\cdot,)\mathrm{da}(x)\right](t)$.

and, taking into account that $\mathfrak{f}_{P_2}$ does not explicitly depend on time, we can write

$$0 = \operatorname{div}[\mathfrak{f}_{P_2}\boldsymbol{J}] + \partial_t \operatorname{div}[\mathfrak{f}_{P_2}\boldsymbol{D}]. \tag{10.31}$$

So, by substituting (10.27d) in the second term of the right-hand side of (10.31), we obtain

$$0 = \operatorname{div}[\mathfrak{f}_{P_2}\boldsymbol{J}] + \partial_t[\mathfrak{f}_{P_3}\varrho_{\mathrm{f}}]. \tag{10.32}$$

Here, we also consider the electroneutrality condition [96], which, in the present framework reads

$$\operatorname{div}[\mathfrak{f}_{P_2}\boldsymbol{J}] = 0. \tag{10.33}$$

We notice that this constraint requires the fractal current, $\mathfrak{f}_{P_2}\boldsymbol{J}$, to be solenoidal, rather than $\boldsymbol{J}$, as in the classical model studied in the previous chapter.

10.3 The fractal PNP model

In this section, we specialise the results obtained in Chapter 9 for the geometry specified therein. For this purpose, we consider that $\Omega \equiv \Omega^{(\mathrm{i})}$ for the internal region of the cell, and $\Omega \equiv \Omega^{(\mathrm{e})}$ for the external space. Moreover, as in Chapter 9, we denote by $\mathscr{M}$ the surface dividing $\Omega^{(\mathrm{i})}$ and $\Omega^{(\mathrm{e})}$. Consequently, the electroneutrality condition (10.33) must be written as

$$\operatorname{div}[\mathfrak{f}^{(\mathrm{i})}_{P_2}\boldsymbol{J}^{(\mathrm{i})}] = 0, \qquad \text{in } \Omega^{(\mathrm{i})}, \tag{10.34a}$$

$$\operatorname{div}[\mathfrak{f}^{(\mathrm{e})}_{P_2}\boldsymbol{J}^{(\mathrm{e})}] = 0, \qquad \text{in } \Omega^{(\mathrm{e})}. \tag{10.34b}$$

Together with the currents $\boldsymbol{J}^{(\mathrm{i})}$ e $\boldsymbol{J}^{(\mathrm{e})}$, it is necessary to introduce the potentials $\phi^{(\mathrm{i})}$ and $\phi^{(\mathrm{e})}$, defined, respectively, in $\Omega^{(\mathrm{i})}$ and $\Omega^{(\mathrm{e})}$, and such that, in general, we have that $\phi^{(\mathrm{e})}_{|\mathscr{M}} \neq \phi^{(\mathrm{i})}_{|\mathscr{M}}$. Therefore, also in this fractal case, we define the difference between the potentials on the membrane $\mathscr{M}$ as

$$V(x,t) := \phi^{(\mathrm{i})}(x,t) - \phi^{(\mathrm{e})}(x,t), \quad \text{for all } x \in \mathscr{M} \text{ and } t \in \mathscr{T}, \tag{10.35}$$

and, as in the standard case, we call V membrane potential.

In order to study the transport of ionic species in the context of the fractal model, it is necessary to study the fractal form of the mass balance laws. In particular, we need to determine the fractal expressions of the electric currents $\boldsymbol{J}^{(\mathrm{i})}_k$ and $\boldsymbol{J}^{(\mathrm{e})}_k$, with $k = 1, \ldots, N$, due to the motion of each ionic species. This implies that we need to find Fick's law in fractal form for each species, which, at the same time, requires to study the dissipation of the system under investigation. Before

going further, we consider that the equation for the membrane current (9.54m) remains unchanged also in the fractal case. Thus, we write

$$I = C\,\partial_t V + \sum_{k=1}^{N} I_k^{(\text{ionic})}, \tag{10.36}$$

where the different terms involved in the above equation have been introduced in Chapter 9.

We mention that, to close the model, we still need to introduce the corresponding boundary conditions, an initial condition for the membrane potential, and the constitutive laws for the ionic currents (for instance, by considering the Hodgkin & Huxley model [147]).

With reference to the k-th ionic species, without specifying whether we refer to $\Omega^{(\text{i})}$ or $\Omega^{(\text{e})}$, we recall that, in the non-fractal case, the current density, which we here simply denote by $\boldsymbol{J}_k$, is given by the expression

$$\boldsymbol{J}_k = -D_k \text{grad}\, c_k - \frac{F z_k D_k}{RT} c_k \text{grad}\, \phi, \tag{10.37}$$

where the physical units of $\boldsymbol{J}_k$ are $[\boldsymbol{J}_k] = \text{mol}/(\text{m}^2 \cdot \text{s})$. Moreover,

$$[D_k] = \frac{\text{m}^2}{\text{s}}, \quad [c_k] = \frac{\text{mol}}{\text{m}^3}, \quad [F] = \frac{\text{C}}{\text{mol}}, \quad [R] = \frac{\text{J}}{\text{mol} \cdot \text{K}}, \tag{10.38a}$$

$$[z_k] = 1, \quad [\phi] = V = \frac{\text{N} \cdot \text{m}}{\text{C}}, \quad \text{and} \quad [T] = K \tag{10.38b}$$

10.3.1 Balance equations in fractal form

In order to determine the fractal expressions for the ionic currents $\boldsymbol{J}_k^{(\text{i})}$ and $\boldsymbol{J}_k^{(\text{e})}$ and for the total currents $\boldsymbol{J}^{(\text{i})}$ and $\boldsymbol{J}^{(\text{e})}$, we investigate the mass balance equations and the dissipation of the system under study. For this purpose, we follow the approach presented in [142, 39, 129, 236][3] and adapt the main results in [142, 39, 129] to the fractal case we are considering here for the case of a monophasic mixture with $N+1$ constituents. Particularly, the first N constituents are considered to be the ionic species, while the $N+1$ constituent is the fluid in which we found these species.

We remark that a more systematic approach to the problem under consideration should take into account the "mechanical" balance laws together with Maxwell's equations. Indeed, the electric field, beyond influencing the motion of the charges through Fick's law, acts on the mechanics of the system by redefining its stress

[3]The work [236] is also used in the MSc thesis of Mr. Vito Napoli. The Author of this PhD thesis was co-advisor of that MSc thesis.

tensor through Maxwell's tensor. Yet, since at this stage we concentrate solely on the main aspects of transport, and thus on the determination of its current, we coherently consider the stress tensor of purely mechanical nature.

Before going further, we write below a list of the symbols we will work with in the following sections [129].

- ρ_i, with $i = 1, \dots, N+1$, is the volumetric mass density of the i-th constituent of the mixture and $\rho := \sum_{i=1}^{N+1} \rho_i$ is the volumetric mass density of the mixture.

- $q_i := \rho_i/\rho$, with $i = 1, \dots, N+1$, is the mass fraction of the i-th constituent, so that ρ_i can be computed as $\rho_i = \rho q_i$. The mass fractions are not all linearly independent since, by definition, it holds $\sum_{i=1}^{N+1} q_i = 1$.

- $M_{\mathrm{m}i}$, with $i = 1, \dots, N+1$, is the molar mass of the i-th constituent. In particular, $\rho_i = \rho q_i = M_{\mathrm{m}i} c_i$, where c_i is the molar concentration, with physical unit $[c_i] = \mathrm{mol} \cdot \mathrm{m}^{-3}$.

- $\boldsymbol{v}_i$, with $i = 1, \dots, N+1$, is the velocity of the i-th constituent.

- $\boldsymbol{v} := \sum_{i=1}^{N+1} q_i \boldsymbol{v}_i$ is the velocity of the mixture's centre of mass.

- $\boldsymbol{w}_i := \boldsymbol{v}_i - \boldsymbol{v}$, with $i = 1, \dots, N+1$, is the velocity of the i-th constituent relative to the velocity of the centre of mass of the mixture. By construction, the relative velocity $\boldsymbol{w}_1, \dots, \boldsymbol{w}_{N+1}$ must be compatible with the constraint $\sum_{i=1}^{N+1} q_i \boldsymbol{w}_i = \boldsymbol{0}$.

- $\boldsymbol{m}_i$, with $i = 1, \dots, N+1$, is the internal volumetric force density due to the interchange of momentum between the i-th constituent and all the other constituents of the mixture. Since the mixture is *closed in terms of momentum* [142, 39, 236][4], the force densities $\boldsymbol{m}_1, \dots, \boldsymbol{m}_{N+1}$ must satisfy the constraints

$$\sum_{i=1}^{N+1} \boldsymbol{m}_i = \boldsymbol{0}. \tag{10.39}$$

- $\boldsymbol{t}_i$, with $i = 1, \dots, N+1$, is the Cauchy stress tensor relative to the i-th constituent of the mixture.

- $\boldsymbol{f}_i$, with $i = 1, \dots, N+1$, is the external volumetric force density acting on the i-th constituent of the mixture. Such force density (in the sequel referred to as "force") is identified with the *Lorentz force*.

[4]The work [236] is also used in the MSc thesis of Mr. Vito Napoli. The Author of this PhD thesis was co-advisor of that MSc thesis.

10.3.2 Mass and momentum balance equations

Let us consider a mixture with $N+1$ constituents occupying a region $\mathscr{R}$ of the three-dimensional Euclidean space, $\mathscr{S}$, having boundary $\partial\mathscr{R}$. This region can denote, here, both the internal space and the space inside the cell.

Mass balance laws

We write the mass balance equation of the mixture in global form as

$$\frac{\mathrm{d}}{\mathrm{d}t}\int_{\mathscr{P}} \rho \,\mathrm{dv} = 0, \tag{10.40}$$

where $\mathscr{P}$ is an element of the set of parts of $\mathscr{R}$ and where the contribution of sink and source terms has been neglected. This equation, which is written for a region with a standard Riemann or Lebesgue measure, can be rewritten by virtue of Gauss's and Reynolds' transport theorems as

$$\int_{\mathscr{P}} \partial_t \rho \,\mathrm{dv} + \int_{\partial\mathscr{P}} \rho \boldsymbol{v}\cdot\boldsymbol{n} \,\mathrm{da} = 0. \tag{10.41}$$

If we consider the region $\mathscr{P}$ endowed with fractal measure, Equation (10.41) can be written, using the transition functions $\mathfrak{f}_{P_3}$ and $\mathfrak{f}_{P_2}$, as

$$\int_{\mathscr{P}} \partial_t(\mathfrak{f}_{P_3}\rho) \,\mathrm{dv} + \int_{\partial\mathscr{P}} [\mathfrak{f}_{P_2}\rho \boldsymbol{v}\cdot\boldsymbol{n}] \,\mathrm{da} = 0, \tag{10.42}$$

which following the usual localisation procedures takes the local form

$$\partial_t(\mathfrak{f}_{P_3}\rho) + \mathrm{div}(\mathfrak{f}_{P_2}\rho\boldsymbol{v}) = 0. \tag{10.43}$$

On the other hand, the integral form of the mass balance equation for the i-th constituent of the mixture can be written, in the case of a standard Riemann or Lebesgue measurement, as

$$\frac{\mathrm{d}}{\mathrm{d}t}\int_{\mathscr{P}} \rho q_i \,\mathrm{dv} + \int_{\partial\mathscr{P}} \rho q_i \boldsymbol{w}_i\cdot\boldsymbol{n} \,\mathrm{da} = 0, \qquad i = 1,\ldots,N+1, \tag{10.44}$$

where q_i denotes the mass fraction of the i-th constituent and $\boldsymbol{w}_i := \boldsymbol{v}_i - \boldsymbol{v}$ is the velocity of the i-th constituent relative to the velocity of the centre of mass of the mixture. We note that, also in this case, we have neglected the contribution of sink and source terms for the i-th constituent. In particular, if the region $\mathscr{P}$ is endowed with the fractal volume measure dv_{P_3} and its boundary with the fractal surface measure da_{P_2}, Equation (10.44) takes the form

$$\frac{\mathrm{d}}{\mathrm{d}t}\int_{\mathscr{P}} \rho q_i \,\mathrm{dv}_{P_3} + \int_{\partial\mathscr{P}} \rho q_i \boldsymbol{w}_i\cdot\boldsymbol{n} \,\mathrm{da}_{P_2} = 0, \qquad i = 1,\ldots,N+1, \tag{10.45}$$

which can be rewritten by virtue of the definitions (10.4) and (10.12) as

$$\frac{\mathrm{d}}{\mathrm{d}t}\int_{\mathscr{P}} \rho q_i \mathfrak{f}_{P_3}\,\mathrm{dv} + \int_{\partial\mathscr{P}} \rho q_i \boldsymbol{w}_i\cdot\boldsymbol{n}\mathfrak{f}_{P_2}\,\mathrm{da} = 0, \qquad i = 1,\ldots,N+1. \tag{10.46}$$

Following usual localisation procedures, by virtue of Gauss's theorem, we arrive at the local form of the mass balance equation for the i-th constituent in the form

$$\partial_t(\mathfrak{f}_{P_3}\rho q_i) + \mathrm{div}(\rho q_i \mathfrak{f}_{P_2}\boldsymbol{w}_i) = 0, \qquad i = 1,\ldots,N+1. \tag{10.47}$$

Momentum balance

We write the linear momentum balance law for a mixture with $N+1$ components as

$$\int_{\partial\mathscr{P}} \boldsymbol{t}\boldsymbol{n}\,\mathrm{da} + \int_{\mathscr{P}} \boldsymbol{f}\,\mathrm{dv} = \boldsymbol{0}, \tag{10.48}$$

where $\boldsymbol{t}$ denotes the Cauchy stress tensor of the mixture as a whole and $\boldsymbol{f}$ denotes the volumetric density of external force, which, here, can represent the Lorentz force. We note that the inertial terms have been neglected in (10.48). Equivalently to what has been done for the mass balance equation, if the region $\mathscr{P}$ is provided with a fractal volumetric measure dv_{P_3} and its boundary, $\partial\mathscr{P}$, is endowed with a fractal surface measure da_{P_2}, we write Equation (10.48) as

$$\int_{\partial\mathscr{P}} \boldsymbol{t}\,\boldsymbol{n}\,\mathrm{da}_{P_2} + \int_{\mathscr{P}} \boldsymbol{f}\,\mathrm{dv}_{P_3} = \boldsymbol{0}, \tag{10.49}$$

which, by virtue of the expressions of the transition functions to the fractal measure (10.3) and (10.11), becomes

$$\int_{\partial\mathscr{P}} [\mathfrak{f}_{P_2}\boldsymbol{t}]\boldsymbol{n}\,\mathrm{da} + \int_{\mathscr{P}} \mathfrak{f}_{P_3}\boldsymbol{f}\,\mathrm{dv} = \boldsymbol{0}. \tag{10.50}$$

So, the local form of (10.50) is given by

$$\mathrm{div}[\mathfrak{f}_{P_2}\boldsymbol{t}] + \mathfrak{f}_{P_3}\boldsymbol{f}\,\mathrm{dv} = 0. \tag{10.51}$$

On the other hand, by neglecting inertia terms, we write the integral form of the linear momentum balance equation for the i-th constituent of the mixture as

$$\int_{\partial\mathscr{P}} [\mathfrak{f}_{P_2}\boldsymbol{t}_i]\boldsymbol{n}\,\mathrm{da} + \int_{\mathscr{P}} \mathfrak{f}_{P_3}[\boldsymbol{m}_i + \boldsymbol{f}_i]\,\mathrm{dv} = \boldsymbol{0}, \qquad i = 1,\ldots,N+1, \tag{10.52}$$

where we are considering the region $\mathscr{P}$ to be equipped with fractal volume and surface measures. We note that, in this case, the momentum balance relative to the i-th constituent predicts a volumetric internal force density, $\boldsymbol{m}_i$, due to the impulse exchanges between the i-th constituent and all other constituents in the mixture. In particular, localising Equation (10.52), we obtain

$$\mathrm{div}(\mathfrak{f}_{P_2}\boldsymbol{t}_i) + \mathfrak{f}_{P_3}[\boldsymbol{m}_i + \boldsymbol{f}_i] = \boldsymbol{0}, \quad i = 1,\ldots,N+1. \tag{10.53}$$

Remark 22. *We remark that, by summing the* (10.53) *over* $i = 1, \dots, N+1$ *and using the property* (10.39)*, we obtain that*

$$\sum_{i=1}^{N+1} \mathfrak{f}_{P_3}[\boldsymbol{f}_i + \boldsymbol{m}_i] + \sum_{i=1}^{N+1} \operatorname{div}(\mathfrak{f}_{P_2}\boldsymbol{t}_i) = \boldsymbol{0}. \tag{10.54}$$

Furthermore, recalling the constraint on volume fractions, namely

$$\sum_{i=1}^{N+1} q_i = 1 \Rightarrow -\sum_{i=1}^{N} \frac{q_i}{q_{N+1}} = 1, \tag{10.55}$$

Equation (10.54) *can be rewritten as*

$$\begin{aligned}&\sum_{i=1}^{N} \mathfrak{f}_{P_3}\left[\boldsymbol{f}_i - \tfrac{q_i}{q_{N+1}}\boldsymbol{f}_{N+1}\right] + \sum_{i=1}^{N}\left[\operatorname{div}(\mathfrak{f}_{P_2}\boldsymbol{t}_i) - \tfrac{q_i}{q_{N+1}}\operatorname{div}(\mathfrak{f}_{P_2}\boldsymbol{t}_{N+1})\right]\\ &+ \sum_{i=1}^{N} \mathfrak{f}_{P_3}\left(\boldsymbol{m}_i - \tfrac{q_i}{q_{N+1}}\boldsymbol{m}_{N+1}\right) = \boldsymbol{0}.\end{aligned} \tag{10.56}$$

Equation (10.56) *represents the linear momentum balance law written in relative terms.*

10.3.3 Fractal dissipation

Here, we aim of providing a thermodynamically admissible expression of the fractal current density by studying the dissipation in the light of the fractal theory presented in [266]. To this end, by adapting the approach presented in [39], we write the dissipation of the system on the portion $\mathscr{P}$ of $\mathscr{R}$ endowed with fractal volume and surface measures (10.4) and (10.12), so that

$$\begin{aligned}\int_{\mathscr{P}} \mathfrak{f}_{P_3}\,\mathfrak{D}\,\mathrm{dv} = &-\frac{\mathrm{d}}{\mathrm{dt}}\int_{\mathscr{P}} \mathfrak{f}_{P_3}\,\rho\,\psi\,\mathrm{dv} + \int_{\mathscr{P}} \sum_{i=1}^{N+1} \mathfrak{f}_{P_3}\,\boldsymbol{f}_i\cdot\boldsymbol{w}_i\,\mathrm{dv}\\ &+ \int_{\partial\mathscr{P}} \sum_{i=1}^{N+1} \mathfrak{f}_{P_2}\,(\boldsymbol{t}_i\boldsymbol{n})\cdot\boldsymbol{w}_i\,\mathrm{da} - \int_{\partial\mathscr{P}} \sum_{i=1}^{N+1} \mathfrak{f}_{P_2}\,\rho q_i\psi_i\boldsymbol{w}_i\cdot\boldsymbol{n}\,\mathrm{da} \geq 0,\end{aligned} \tag{10.57}$$

where $\psi := \sum_{k=1}^{N+1} q_k\psi_k$ and ψ_k, for each $k = 1, \dots, N$, denotes the Helmholtz free energy density per unit mass of the k-th species. Thus, Equation (10.57) can be rewritten as

$$\int_{\mathscr{P}} \mathfrak{f}_{P_3}\,\mathfrak{D}\,\mathrm{dv} = -\int_{\mathscr{P}} \mathfrak{f}_{P_3}\rho\,\partial_t\psi\,\mathrm{dv} + \int_{\mathscr{P}} \sum_{i=1}^{N+1} \mathfrak{f}_{P_3}\boldsymbol{f}_i\cdot\boldsymbol{w}_i\,\mathrm{dv}$$

$$+\int_{\mathscr{P}}\sum_{i=1}^{N+1}\left[\operatorname{div}\left(\mathfrak{f}_{P_2}\boldsymbol{t}_i\right)\cdot\boldsymbol{w}_i+\mathfrak{f}_{P_2}\boldsymbol{t}_i:\operatorname{grad}\boldsymbol{w}_i\right]\mathrm{dv}$$
$$-\int_{\mathscr{P}}\sum_{i=1}^{N+1}\left[\operatorname{grad}(\mathfrak{f}_{P_2}\rho q_i\psi_i)\cdot\boldsymbol{w}_i+\mathfrak{f}_{P_2}\rho q_i\psi_i\boldsymbol{I}:\operatorname{grad}\boldsymbol{w}_i\right]\mathrm{dv}\geq 0, \tag{10.58}$$

where we have used Gauss's theorem and the tensorial identity $\operatorname{div}(\mathfrak{f}_{P_2}\boldsymbol{t}_i\boldsymbol{w}_i)=\operatorname{div}(\mathfrak{f}_{P_2}\boldsymbol{t}_i)\cdot\boldsymbol{w}_i+\mathfrak{f}_{P_2}\boldsymbol{t}_i:\operatorname{grad}\boldsymbol{w}_i$. Furthermore, by virtue of momentum balance equation for the mixture given in (10.54), (10.58) takes the equivalent form

$$\int_{\mathscr{P}}\mathfrak{f}_{P_3}\mathscr{D}\,\mathrm{dv}=-\int_{\mathscr{P}}\mathfrak{f}_{P_3}\rho\,\partial_t\psi\,\mathrm{dv}+\int_{\mathscr{P}}\sum_{i=1}^{N+1}\left[\mathfrak{f}_{P_2}\boldsymbol{t}_i-\mathfrak{f}_{P_2}\rho q_i\psi_i\boldsymbol{I}\right]:\operatorname{grad}\boldsymbol{w}_i\mathrm{dv}$$
$$-\int_{\mathscr{P}}\sum_{i=1}^{N+1}\left[\operatorname{grad}(\mathfrak{f}_{P_2}\rho q_i\psi_i)+\mathfrak{f}_{P_3}\boldsymbol{m}_i\right]\cdot\boldsymbol{w}_i\,\mathrm{dv}\geq 0. \tag{10.59}$$

In particular, considering the constraint on the relative velocities, i.e.

$$\boldsymbol{w}_{N+1}=-\sum_{i=1}^{N}\tfrac{q_i}{q_{N+1}}\boldsymbol{w}_i, \tag{10.60}$$

and working on the second addend of Equation (10.59), we can write

$$\begin{aligned}\int_{\mathscr{P}}\sum_{i=1}^{N+1}\mathbb{Q}_i:\operatorname{grad}\boldsymbol{w}_i\mathrm{dv}=&\int_{\mathscr{P}}\sum_{i=1}^{N}\mathbb{Q}_i:\operatorname{grad}\boldsymbol{w}_i\mathrm{dv}+\int_{\mathscr{P}}\mathbb{Q}_{N+1}:\left(-\sum_{i=1}^{N}\tfrac{q_i}{q_{N+1}}\operatorname{grad}\boldsymbol{w}_i\right)\mathrm{dv}\\&-\int_{\mathscr{P}}\mathbb{Q}_{N+1}\operatorname{grad}\left(\tfrac{q_i}{q_{N+1}}\right)\cdot\boldsymbol{w}_i\mathrm{dv}\\=&\int_{\mathscr{P}}\sum_{i=1}^{N}\left(\mathbb{Q}_i-\tfrac{q_i}{q_{N+1}}\mathbb{Q}_{N+1}\right):\operatorname{grad}\boldsymbol{w}_i\mathrm{dv}\\&-\int_{\mathscr{P}}\mathbb{Q}_{N+1}\operatorname{grad}\left(\tfrac{q_i}{q_{N+1}}\right)\cdot\boldsymbol{w}_i\mathrm{dv},\end{aligned} \tag{10.61}$$

where we have defined the quantity $\mathbb{Q}_i:=[\mathfrak{f}_{P_2}\boldsymbol{t}_i-\mathfrak{f}_{P_2}\rho q_i\psi_i\boldsymbol{I}]$. In a similar way, by defining $\boldsymbol{p}_i:=[\operatorname{grad}(\mathfrak{f}_{P_2}\rho q_i\psi_i)+\mathfrak{f}_{P_3}\boldsymbol{m}_i]$, the third addend in (10.59) is rewritten as

$$\begin{aligned}-\int_{\mathscr{P}}\sum_{i=1}^{N+1}\boldsymbol{p}_i\cdot\boldsymbol{w}_i\,\mathrm{dv}=&-\int_{\mathscr{P}}\sum_{i=1}^{N}\boldsymbol{p}_i\cdot\boldsymbol{w}_i\,\mathrm{dv}+\boldsymbol{p}_{N+1}\cdot\left(-\sum_{i=1}^{N}\tfrac{q_i}{q_{N+1}}\boldsymbol{w}_i\right)\\=&-\int_{\mathscr{P}}\sum_{i=1}^{N}\left(\boldsymbol{p}_i-\tfrac{q_i}{q_{N+1}}\boldsymbol{p}_{N+1}\right)\cdot\boldsymbol{w}_i\,\mathrm{dv}.\end{aligned} \tag{10.62}$$

Thus, combining the results obtained in (10.61) and (10.62), Equation (10.59) can be equivalently rewritten as

$$\begin{aligned}\int_{\mathscr{P}} \mathfrak{f}_{P_3}\,\mathfrak{D}\,\mathrm{dv} = &-\int_{\mathscr{P}} \mathfrak{f}_{P_3}\rho\,\partial_t\psi\,\mathrm{dv}\\ &+\int_{\mathscr{P}}\sum_{i=1}^{N}\left[\mathfrak{f}_{P_2}\left(\boldsymbol{t}_i-\tfrac{q_i}{q_{N+1}}\boldsymbol{t}_{N+1}\right)-\mathfrak{f}_{P_2}\rho\left(q_i\psi_i-\tfrac{q_i}{q_{N+1}}q_{N+1}\psi_{N+1}\right)\boldsymbol{I}\right]:\mathrm{grad}\,\boldsymbol{w}_i\mathrm{dv}\\ &-\int_{\mathscr{P}}\sum_{i=1}^{N}\left[\mathfrak{f}_{P_2}\boldsymbol{t}_{N+1}-\mathfrak{f}_{P_2}\rho q_{N+1}\psi_{N+1}\right]\mathrm{grad}\left(\tfrac{q_i}{q_{N+1}}\right)\cdot\boldsymbol{w}_i\mathrm{dv}\\ &-\int_{\mathscr{P}}\sum_{i=1}^{N}\left\{\mathrm{grad}\left(\mathfrak{f}_{P_2}\rho q_i\psi_i\right)-\tfrac{q_i}{q_{N+1}}\mathrm{grad}\left(\mathfrak{f}_{P_2}\rho q_{N+1}\psi_{N+1}\right)\right\}\cdot\boldsymbol{w}_i\\ &-\int_{\mathscr{P}}\sum_{i=1}^{N}\left\{\mathfrak{f}_{P_3}\left(\boldsymbol{m}_i-\tfrac{q_i}{q_{N+1}}\boldsymbol{m}_{N+1}\right)\right\}\cdot\boldsymbol{w}_i\,\mathrm{dv}\geq 0,\end{aligned}\tag{10.63}$$

or by reorganising the terms as

$$\begin{aligned}\int_{\mathscr{P}} \mathfrak{f}_{P_3}\,\mathfrak{D}\,\mathrm{dv} = &-\int_{\mathscr{P}} \mathfrak{f}_{P_3}\rho\,\partial_t\psi\,\mathrm{dv}\\ &+\int_{\mathscr{P}}\sum_{i=1}^{N}\left[\mathfrak{f}_{P_2}\left(\boldsymbol{t}_i-\tfrac{q_i}{q_{N+1}}\boldsymbol{t}_{N+1}\right)-\mathfrak{f}_{P_2}\rho q_i\left(\psi_i-\psi_{N+1}\right)\boldsymbol{I}\right]:\mathrm{grad}\,\boldsymbol{w}_i\mathrm{dv}\\ &-\int_{\mathscr{P}}\sum_{i=1}^{N}\mathfrak{f}_{P_2}\boldsymbol{t}_{N+1}\mathrm{grad}\left(\tfrac{q_i}{q_{N+1}}\right)\cdot\boldsymbol{w}_i\mathrm{dv}\\ &-\int_{\mathscr{P}}\sum_{i=1}^{N}\mathrm{grad}\left(\mathfrak{f}_{P_2}\rho q_i\left[\psi_i-\psi_{N+1}\right]\right)\cdot\boldsymbol{w}_i\mathrm{dv}\\ &-\int_{\mathscr{P}}\sum_{i=1}^{N}\mathfrak{f}_{P_3}\left[\boldsymbol{m}_i-\tfrac{q_i}{q_{N+1}}\boldsymbol{m}_{N+1}\right]\cdot\boldsymbol{w}_i\,\mathrm{dv}\geq 0.\end{aligned}\tag{10.64}$$

Furthermore, by assigning a constitutive relation for ψ of the type

$$\psi=\hat{\psi}\circ(q_1,\ldots,q_N),\tag{10.65}$$

we have that

$$\mathrm{grad}\,\psi=\sum_{i=1}^{N}\left(\tfrac{\partial\hat{\psi}}{\partial q_i}\circ(q_1,\ldots,q_N)\right)\,\mathrm{grad}\,q_i.\tag{10.66}$$

Therefore, by virtue of the (10.65) and (10.66), and assuming the mixture velocity $\boldsymbol{v}$ to be null, it is possible to rewrite the first addend of (10.64) as

$$-\int_{\mathscr{P}}\mathfrak{f}_{P_3}\rho\,\partial_t\psi\,\mathrm{dv}=-\int_{\mathscr{P}}\sum_{i=1}^{N}\mathfrak{f}_{P_3}\rho\,\left(\tfrac{\partial\hat{\psi}}{\partial q_k}\circ(q_1,\ldots,q_N)\right)\partial_t q_i\mathrm{dv}$$

$$
\begin{aligned}
&= \int_{\mathscr{P}} \sum_{i=1}^{N} \left(\tfrac{\partial \hat{\psi}}{\partial q_i} \circ (q_1, \dots, q_N) \right) \mathfrak{f}_{P_2} \rho q_i \boldsymbol{I} : \mathrm{grad} \boldsymbol{w}_i \mathrm{dv} \\
&\quad + \int_{\mathscr{P}} \sum_{i=1}^{N} \left(\tfrac{\partial \hat{\psi}}{\partial q_i} \circ (q_1, \dots, q_N) \right) \mathrm{grad} \left(\mathfrak{f}_{P_2} \rho q_i \right) \cdot \boldsymbol{w}_i \mathrm{dv}, \qquad (10.67)
\end{aligned}
$$

where we have used the local mass balance equations of the first N constituents. Therefore, the substitution of (10.67) into the (10.64) leads to

$$
\begin{aligned}
\int_{\mathscr{P}} \mathfrak{f}_{P_3} \mathfrak{D} \, \mathrm{dv} = & \int_{\mathscr{P}} \sum_{i=1}^{N} \left[\mathfrak{f}_{P_2} \rho q_i \left(\tfrac{\partial \hat{\psi}}{\partial q_i} \circ (q_1, \dots, q_N) \right) \right] \boldsymbol{I} : \mathrm{grad} \boldsymbol{w}_i \mathrm{dv} \\
& + \int_{\mathscr{P}} \sum_{i=1}^{N} \left[\mathfrak{f}_{P_2} \left(\boldsymbol{t}_i - \tfrac{q_i}{q_{N+1}} \boldsymbol{t}_{N+1} \right) - \mathfrak{f}_{P_2} \rho q_i \left(\psi_i - \psi_{N+1} \right) \boldsymbol{I} \right] : \mathrm{grad} \, \boldsymbol{w}_i \mathrm{dv} \\
& + \int_{\mathscr{P}} \sum_{i=1}^{N} \left(\tfrac{\partial \hat{\psi}}{\partial q_i} \circ (q_1, \dots, q_N) \right) \mathrm{grad} \left(\mathfrak{f}_{P_2} \rho q_i \right) \cdot \boldsymbol{w}_i \mathrm{dv} \\
& - \int_{\mathscr{P}} \sum_{i=1}^{N} \mathfrak{f}_{P_2} \boldsymbol{t}_{N+1} \mathrm{grad} \left(\tfrac{q_i}{q_{N+1}} \right) \cdot \boldsymbol{w}_i \mathrm{dv} \\
& - \int_{\mathscr{P}} \sum_{i=1}^{N} \mathrm{grad} \left(\mathfrak{f}_{P_2} \rho q_i \left[\psi_i - \psi_{N+1} \right] \right) \cdot \boldsymbol{w}_i \mathrm{dv} \\
& - \int_{\mathscr{P}} \sum_{i=1}^{N} \mathfrak{f}_{P_3} \left[\boldsymbol{m}_i - \tfrac{q_i}{q_{N+1}} \boldsymbol{m}_{N+1} \right] \cdot \boldsymbol{w}_i \, \mathrm{dv} \geq 0. \qquad (10.68)
\end{aligned}
$$

By merging the first two terms of (10.68) under the same integral sign, the new integrand function has the form

$$
\mathfrak{f}_{P_2} \rho q_i \left[- \left(\psi_i \boldsymbol{I} - \tfrac{\boldsymbol{t}_i}{\rho q_i} \right) + \left(\psi_{N+1} \boldsymbol{I} - \tfrac{\boldsymbol{t}_{N+1}}{\rho q_{N+1}} \right) + \left(\tfrac{\partial \hat{\psi}}{\partial q_i} \circ (\dots) \right) \boldsymbol{I} \right] : \mathrm{grad} \, \boldsymbol{w}_i, \qquad (10.69)
$$

where, in order not to make the notation more cumbersome, we have chosen to use $(\dots)$ to indicate the list of volume fractions $(q_1, \dots, q_N)$.

Now, following the approach discussed in [39, 236][5], the Cauchy stress tensors, $\boldsymbol{t}_i$, can be written as $\boldsymbol{t}_i := -p_i \boldsymbol{t}_i$, where p_i denotes the *partial pressure* of the i-th constituent, so Equation (10.69) can be rewritten as

$$
\mathfrak{f}_{P_2} \rho q_i \left[- \left(\psi_i + \tfrac{p_i}{\rho q_i} \right) + \left(\psi_{N+1} + \tfrac{p_{N+1}}{\rho q_{N+1}} \right) + \left(\tfrac{\partial \hat{\psi}}{\partial q_i} \circ (\dots) \right) \right] \boldsymbol{I} : \mathrm{grad} \, \boldsymbol{w}_i, \qquad (10.70)
$$

[5]The work [236] is also used in the MSc thesis of Mr. Vito Napoli. The Author of this PhD thesis was co-advisor of that MSc thesis.

in which we recognise the expression of the *chemical potential* $\mu_i := \psi_i + \frac{p_i}{\rho q_i}$ relative to the i-th constituent. Particularly, by defining the relative chemical potential as $\tilde{mi}u_i = \mu_i - \mu_{N+1}$, we get the most compact writing

$$\mathfrak{f}_{P_2}\rho q_i \left[-\tilde{\mu}_i + \left(\frac{\partial\hat{\psi}}{\partial q_i} \circ (\dots)\right)\right] \operatorname{div} \boldsymbol{w}_i, \tag{10.71}$$

which, when substituted in the (10.68), returns

$$\begin{aligned}\int_{\mathscr{P}} \mathfrak{f}_{P_3}\, \mathscr{D}\, \mathrm{dv} = &\int_{\mathscr{P}} \sum_{i=1}^{N} \mathfrak{f}_{P_2}\rho q_i \left[-\tilde{\mu}_i + \left(\frac{\partial\hat{\psi}}{\partial q_i} \circ (\dots)\right)\right] \operatorname{div} \boldsymbol{w}_i \mathrm{dv} \\ &+ \int_{\mathscr{P}} \sum_{i=1}^{N} \left(\frac{\partial\hat{\psi}}{\partial q_i} \circ (\dots)\right) \operatorname{grad}\left(\mathfrak{f}_{P_2}\rho q_i\right) \cdot \boldsymbol{w}_i \mathrm{dv} \\ &- \int_{\mathscr{P}} \sum_{i=1}^{N} \mathfrak{f}_{P_2}\boldsymbol{t}_{N+1} \operatorname{grad}\left(\frac{q_i}{q_{N+1}}\right) \cdot \boldsymbol{w}_i \mathrm{dv} \\ &- \int_{\mathscr{P}} \sum_{i=1}^{N} \operatorname{grad}\left(\mathfrak{f}_{P_2}\rho q_i \left[\psi_i - \psi_{N+1}\right]\right) \cdot \boldsymbol{w}_i \mathrm{dv} \\ &- \int_{\mathscr{P}} \sum_{i=1}^{N} \mathfrak{f}_{P_3} \left[\boldsymbol{m}_i - \tfrac{q_i}{q_{N+1}}\boldsymbol{m}_{N+1}\right] \cdot \boldsymbol{w}_i \,\mathrm{dv} \geq 0. \end{aligned} \tag{10.72}$$

Equivalently, operating on the remaining terms of (10.72), we obtain the integrand function

$$\begin{aligned}\sum_{i=1}^{N} \Big[&\left(\frac{\partial\hat{\psi}}{\partial q_i} \circ (\dots)\right) \operatorname{grad}\left(\mathfrak{f}_{P_2}\rho q_i\right) - \mathfrak{f}_{P_2}\boldsymbol{t}_{N+1} \operatorname{grad}\left(\frac{q_i}{q_{N+1}}\right) - \operatorname{grad}\left(\mathfrak{f}_{P_2}\rho q_i \left[\psi_i - \psi_{N+1}\right]\right) \\ &- \mathfrak{f}_{P_3} \left(\boldsymbol{m}_i - \tfrac{q_i}{q_{N+1}}\boldsymbol{m}_{N+1}\right)\Big] \cdot \boldsymbol{w}_i, \end{aligned} \tag{10.73}$$

which, by applying Leibniz's rule, we rewrite as

$$\begin{aligned}\sum_{i=1}^{N} \Big[&-\mathfrak{f}_{P_2}\rho q_i \operatorname{grad}\left(\frac{\partial\hat{\psi}}{\partial q_i} \circ (\dots)\right) - \mathfrak{f}_{P_2}\boldsymbol{t}_{N+1} \operatorname{grad}\left(\frac{q_i}{q_{N+1}}\right) - \mathfrak{f}_{P_3} \left(\boldsymbol{m}_i - \tfrac{q_i}{q_{N+1}}\boldsymbol{m}_{N+1}\right) \\ &- \operatorname{grad}\left(\mathfrak{f}_{P_2}\rho q_i \left[\psi_i - \psi_{N+1}\right] - \mathfrak{f}_{P_2}\rho q_i \left(\frac{\partial\hat{\psi}}{\partial q_i} \circ (\dots)\right)\right)\Big] \cdot \boldsymbol{w}_i. \end{aligned} \tag{10.74}$$

From the expression given in (10.74), we obtain the following new form of the fractal dissipation

$$\int_{\mathscr{P}} \mathfrak{f}_{P_3}\, \mathscr{D}\, \mathrm{dv} = \int_{\mathscr{P}} \sum_{i=1}^{N} \mathfrak{f}_{P_2}\rho q_i \left[-\tilde{\mu}_i + \left(\frac{\partial\hat{\psi}}{\partial q_i} \circ (\dots)\right)\right] \operatorname{div} \boldsymbol{w}_i \mathrm{dv}$$

$$
\begin{aligned}
&- \int_{\mathscr{P}} \sum_{i=1}^{N} \Big[\mathfrak{f}_{P_2} \rho q_i \mathrm{grad} \left(\tfrac{\partial \hat{\psi}}{\partial q_i} \circ (\dots) \right) + \mathfrak{f}_{P_2} \boldsymbol{t}_{N+1} \mathrm{grad} \left(\tfrac{q_i}{q_{N+1}} \right) \\
&\qquad + \mathfrak{f}_{P_3} \left(\boldsymbol{m}_i - \tfrac{q_i}{q_{N+1}} \boldsymbol{m}_{N+1} \right) \\
&\qquad + \mathrm{grad} \left(\mathfrak{f}_{P_2} \rho q_i \left[\psi_i - \psi_{N+1} \right] \right) \\
&\qquad - \mathrm{grad} \left(\mathfrak{f}_{P_2} \rho q_i \left(\tfrac{\partial \hat{\psi}}{\partial q_i} \circ (\dots) \right) \right) \Big] \cdot \boldsymbol{w}_i \mathrm{dv} \geq 0. \qquad (10.75)
\end{aligned}
$$

At this point, we proceed by considering the mass balance equation for the mixture in global form as a constraint, and study the constrained dissipation by introducing the Lagrange multiplier ζ [39]. Therefore, we write

$$
\begin{aligned}
\int_{\mathscr{P}} \mathfrak{f}_{P_3} \mathscr{D} \, \mathrm{dv} = &\int_{\mathscr{P}} \sum_{i=1}^{N} \mathfrak{f}_{P_2} \rho q_i \left[-\tilde{\mu}_i + \left(\tfrac{\partial \hat{\psi}}{\partial q_i} \circ (\dots) \right) - \tfrac{\zeta}{\rho} \left(\tfrac{\partial \hat{\rho}}{\partial q_i} \circ (\dots) \right) \right] \mathrm{div} \, \boldsymbol{w}_i \mathrm{dv} \\
&- \int_{\mathscr{P}} \sum_{i=1}^{N} \Big\{ \mathfrak{f}_{P_2} \rho q_i \mathrm{grad} \left(\tfrac{\partial \hat{\psi}}{\partial q_i} \circ (\dots) \right) + \mathfrak{f}_{P_2} \boldsymbol{t}_{N+1} \mathrm{grad} \left(\tfrac{q_i}{q_{N+1}} \right) \\
&\qquad + \mathfrak{f}_{P_3} \left[\boldsymbol{m}_i - \tfrac{q_i}{q_{N+1}} \boldsymbol{m}_{N+1} \right] \\
&\qquad + \mathrm{grad} \left[\mathfrak{f}_{P_2} \rho q_i \left(\left[\psi_i - \psi_{N+1} \right] - \left(\tfrac{\partial \hat{\psi}}{\partial q_i} \circ (\dots) \right) \right) \right] \\
&\qquad + \tfrac{\zeta}{\rho} \left(\tfrac{\partial \hat{\rho}}{\partial q_i} \circ (\dots) \right) \mathrm{grad} (\mathfrak{f}_{P_2} \rho q_i) \Big\} \cdot \boldsymbol{w}_i \mathrm{dv} \geq 0, \qquad (10.76)
\end{aligned}
$$

in which we have introduced the constitutive dependency $\rho = \hat{\rho} \circ (q_1, \dots, q_N)$. Following [39], we write the Lagrange multiplier in the form $\zeta := p/\rho$ and, then, returning to the dissipation, with a slight abuse of notation we obtain

$$
\begin{aligned}
\int_{\mathscr{P}} \mathfrak{f}_{P_3} \mathscr{D} \, \mathrm{dv} = &\int_{\mathscr{P}} \sum_{i=1}^{N} \mathfrak{f}_{P_2} \rho q_i \left[-\tilde{\mu}_i + \tfrac{\partial}{\partial q_i} \left(\hat{\psi} + \tfrac{p}{\hat{\rho}} \right) \right] \mathrm{div} \, \boldsymbol{w}_i \mathrm{dv} \\
&- \int_{\mathscr{P}} \sum_{i=1}^{N} \Big\{ \mathfrak{f}_{P_2} \rho q_i \mathrm{grad} \left[\tfrac{\partial}{\partial q_i} \left(\hat{\psi} + \tfrac{p}{\hat{\rho}} \right) \right] + \mathfrak{f}_{P_2} \boldsymbol{t}_{N+1} \mathrm{grad} \left(\tfrac{q_i}{q_{N+1}} \right) \\
&\qquad + \mathrm{grad} \left[\mathfrak{f}_{P_2} \rho q_i \left(\left[\psi_i - \psi_{N+1} \right] - \tfrac{\partial}{\partial q_i} \left(\hat{\psi} + \tfrac{p}{\hat{\rho}} \right) \right) \right] \\
&\qquad + \mathfrak{f}_{P_3} \left[\boldsymbol{m}_i - \tfrac{q_i}{q_{N+1}} \boldsymbol{m}_{N+1} \right] \Big\} \cdot \boldsymbol{w}_i \mathrm{dv} \geq 0. \qquad (10.77)
\end{aligned}
$$

As done in [39], we provide the expression of the Gibbs free energy as

$$
\hat{\mathscr{G}} = \hat{\psi} + \frac{p}{\hat{\rho}}, \qquad (10.78)
$$

which permits to write the i-th relative chemical potential as

$$
\tilde{\mu}_i = \frac{\partial \hat{\mathscr{G}}}{\partial q_i} = \frac{\partial}{\partial q_i} \left[\hat{\psi} + \frac{p}{\hat{\rho}} \right]. \qquad (10.79)
$$

If we use (10.79) in Equation (10.77), we obtain that

$$\begin{aligned}\int_{\mathscr{P}} \mathfrak{f}_{P_3}\,\mathscr{D}\,\mathrm{dv} = -\int_{\mathscr{P}} \sum_{i=1}^{N} \Big\{ &\mathfrak{f}_{P_2}\rho q_i \mathrm{grad}\,\tilde{\mu}_i + \mathfrak{f}_{P_2}\boldsymbol{t}_{N+1}\mathrm{grad}\left(\tfrac{q_i}{q_{N+1}}\right) \\ &+ \mathrm{grad}\left[\mathfrak{f}_{P_2}\rho q_i\left([\psi_i - \psi_{N+1}] - \tilde{\mu}_i\right)\right] \\ &+ \mathfrak{f}_{P_3}\left[\boldsymbol{m}_i - \tfrac{q_i}{q_{N+1}}\boldsymbol{m}_{N+1}\right]\Big\}\cdot \boldsymbol{w}_i \mathrm{dv} \geq 0. \end{aligned} \tag{10.80}$$

So, if we introduce the notation

$$\begin{aligned}\mathfrak{f}_{P_3}\mathfrak{m}_{\mathrm{d}i} := \; &\mathfrak{f}_{P_2}\rho q_i \mathrm{grad}\,\tilde{\mu}_i + \mathfrak{f}_{P_2}\boldsymbol{t}_{N+1}\mathrm{grad}\left(\tfrac{q_i}{q_{N+1}}\right) \\ &+ \mathrm{grad}\left[\mathfrak{f}_{P_2}\rho q_i\left([\psi_i - \psi_{N+1}] - \tilde{\mu}_i\right)\right] \\ &+ \mathfrak{f}_{P_3}\left[\boldsymbol{m}_i - \tfrac{q_i}{q_{N+1}}\boldsymbol{m}_{N+1}\right]. \end{aligned} \tag{10.81}$$

where $\mathfrak{m}_{\mathrm{d}i}$ denotes a dissipative volumetric density force relative to the i-th constituent, the dissipation can be written as

$$\int_{\mathscr{P}} \mathfrak{f}_{P_3}\,\mathscr{D}\,\mathrm{dv} = -\int_{\mathscr{P}} \sum_{i=1}^{N} \mathfrak{f}_{P_3}\mathfrak{m}_{\mathrm{d}i}\cdot\boldsymbol{w}_i \mathrm{dv}. \tag{10.82}$$

Moreover, in view of (10.81), it is possible to rewrite the i-th relative momentum balance equation as

$$\begin{aligned}&\mathfrak{f}_{P_3}\left(\boldsymbol{f}_i - \tfrac{q_i}{q_{N+1}}\boldsymbol{f}_{N+1}\right) + \mathrm{div}\,\left(\mathfrak{f}_{P_2}\boldsymbol{t}_i - \tfrac{q_i}{q_{N+1}}\mathfrak{f}_{P_2}\boldsymbol{t}_{N+1}\right) \\ &+ \mathfrak{f}_{P_3}\mathfrak{m}_{\mathrm{d}i} + \mathrm{grad}\left[\mathfrak{f}_{P_2}\rho q_i\left(\tilde{\mu}_i - (\psi_i - \psi_{N+1})\right)\right] - \mathfrak{f}_{P_2}\rho q_i\,\mathrm{grad}\tilde{\mu}_i = \boldsymbol{0}, \end{aligned} \tag{10.83}$$

which in the light of the definition of the relative chemical potential $\tilde{\mu}_i$ and the Cauchy stress tensor $\boldsymbol{t}_i$ becomes

$$\mathfrak{f}_{P_3}\left(\boldsymbol{f}_i - \tfrac{q_i}{q_{N+1}}\boldsymbol{f}_{N+1}\right) + \mathfrak{f}_{P_3}\mathfrak{m}_{\mathrm{d}i} - \mathfrak{f}_{P_2}\rho q_i\,\mathrm{grad}\tilde{\mu}_i = \boldsymbol{0}. \tag{10.84}$$

Finally, by writing the volumetric density of dissipative force as

$$\mathfrak{m}_{\mathrm{d}i} = -M_i^{-1}\boldsymbol{w}_i, \tag{10.85}$$

it is possible to give the expression of the i-th relative velocity, i.e.

$$\boldsymbol{w}_i = -M_i\left[\frac{\mathfrak{f}_{P_2}}{\mathfrak{f}_{P_3}}\rho q_i\,\mathrm{grad}\tilde{\mu}_i - \left(\boldsymbol{f}_i - \tfrac{q_i}{q_{N+1}}\boldsymbol{f}_{N+1}\right)\right], \tag{10.86}$$

where, we denote the motility of the i-th constituent with M_i. By means of the (10.86), we define the i-th flux as

$$\boldsymbol{J}_i = \frac{\rho q_i}{\mathrm{M}_{\mathrm{m}i}}\boldsymbol{w}_i, \tag{10.87}$$

having physical units $[\boldsymbol{J}_i] = \mathrm{mol}/(\mathrm{m}^2 \cdot \mathrm{s})$. From Equation (10.87) we obtain an explicit expression of the fractal current density which, by means on the considerations made for the Lorentz force, leads to the fractal current density of the PNP-fractal model, namely

$$\boldsymbol{J}_i := -\frac{1}{\mathrm{M}_{\mathrm{m}i}}\left[\rho q_i M_i \frac{\mathfrak{f}_{P_2}}{\mathfrak{f}_{P_3}} \rho q_i \,\mathrm{grad}\tilde{\mu}_i - \rho q_i M_i \left(\boldsymbol{f}_i - \tfrac{q_i}{q_{N+1}}\boldsymbol{f}_{N+1}\right)\right]. \tag{10.88}$$

10.3.4 The fractal flux

In this section, we write an expression for the current density by making explicit the various components as a function of the variables of the fractal PNP Model. For this purpose, we assign an expression for the volumetric force density $\boldsymbol{f}_i$ related to the i-th constituent. Since the only non-negligible volumetric force in the problem under consideration is electric, we identify with $\boldsymbol{f}_i$ the constitutive expression of the Lorentz force, i.e.

$$\boldsymbol{f}_i := F z_i c_i \boldsymbol{E} = -F z_i c_i \mathrm{grad}\,\phi. \tag{10.89}$$

We note that the $(N+1)$-th constituent, i.e. water, has zero valence z_{N+1}, so it is possible to write the (10.88) as

$$\boldsymbol{J}_i = -\left[\frac{\rho q_i}{\mathrm{M}_{\mathrm{m}i}}\frac{\mathfrak{f}_{P_2}}{\mathfrak{f}_{P_3}} M_i \rho q_i \,\mathrm{grad}\tilde{\mu}_i - \frac{\rho q_i}{\mathrm{M}_{\mathrm{m}i}} M_i \boldsymbol{f}_i\right]. \tag{10.90}$$

Defining the volumetric mobility as $\mathsf{M}_i := \rho q_i M_i$ and noting that

$$\mathrm{M}_{\mathrm{m}i} c_i = \rho q_i, \tag{10.91}$$

we write Equation (10.90) as

$$\boldsymbol{J}_i = -\left[\frac{\mathfrak{f}_{P_2}}{\mathfrak{f}_{P_3}} \mathsf{M}_i c_i \,\mathrm{grad}\tilde{\mu}_i - \frac{\mathsf{M}_i}{\mathrm{M}_{\mathrm{m}i}}\boldsymbol{f}_i\right]. \tag{10.92}$$

Given the constitutive dependence of the relative chemical potential on the volume fractions $(q_1, \ldots, q_N)$, it is possible to write

$$\mathrm{grad}\,\tilde{\mu}_i = \left(\frac{\partial \check{\tilde{\mu}}_i}{\partial q_i} \circ (q_1, \ldots, q_N)\right) \mathrm{grad}\, q_i, \tag{10.93}$$

which leads to

$$\boldsymbol{J}_i = -\left[\frac{\mathfrak{f}_{P_2}}{\mathfrak{f}_{P_3}} \mathsf{M}_i c_i \left(\frac{\partial \check{\tilde{\mu}}_i}{\partial q_i} \circ (q_1, \ldots, q_N)\right) \mathrm{grad}\, q_i - \frac{\mathsf{M}_i}{\mathrm{M}_{\mathrm{m}i}}\boldsymbol{f}_i\right]. \tag{10.94}$$

Using the relation (10.91) in (10.94), and prescribing an appropriate functional relation for $\check{\tilde{\mu}}_i$, we obtain

$$\boldsymbol{J}_i = -\left[\frac{\mathfrak{f}_{P_2}}{\mathfrak{f}_{P_3}} D_i \mathrm{grad}\, c_i + D_i \frac{F z_i}{RT} \mathrm{grad}\phi\right]. \tag{10.95}$$

Making the assumption that the concentration fields are assigned and constant, we write, by means of the (10.95), the total current density as

$$\boldsymbol{J} = \sum_{i=1}^{N} F z_i \boldsymbol{J}_i = -\sigma \mathrm{grad}\phi, \tag{10.96}$$

where we have defined the conductivity σ as [261]

$$\sigma = \sum_{i=1}^{N} D_i \frac{F^2 z_i^2}{RT} c_i. \tag{10.97}$$

Note that the conductivity in (10.97) also depends on the fractality of the geometry via the definition of the diffusivity tensor D_i related to the i-th constituent. Equation (10.96), when specialised to the domains $\Omega^{(\mathrm{i})}$ and $\Omega^{(\mathrm{e})}$ gives the current density of the fractal PNP Model.

10.3.5 The fractal PNP model

In summary, the equations defining the fractal PNP model are given by: (i) the electroneutrality conditions (10.34a) and (10.34b), written for $\Omega^{(\mathrm{i})}$ and for $\Omega^{(\mathrm{e})}$; ; (ii) the $2N$ fractal balance equations for the ionic species, one for each $k = 1, \ldots, N$ and written for $\Omega^{(\mathrm{i})}$ and for $\Omega^{(\mathrm{e})}$; (iii) the relation (9.22), which binds V to the potentials at the membrane, i.e. $\phi^{(\mathrm{i})}_{|\mathscr{M}}$ and $\phi^{(\mathrm{e})}_{|\mathscr{M}}$; (iv) the equations expressing both the continuity of the total current densities normal to the membrane and the way that each binds to the transmembrane current density I; (v) the equation for the membrane which binds together I to V; and (vi) the null average condition for $\phi^{(\mathrm{e})}$ and the boundary condition at $\partial\Omega^{(\mathrm{e,e})}$. Specifically,

$$\mathrm{div}\left[-\frac{(\mathfrak{f}_{P_2})^2}{\mathfrak{f}_{P_3}} \sum_{k=1}^{N} F z_k D_k^{(\mathrm{i})} \mathrm{grad}\, c_k^{(\mathrm{i})} - \mathfrak{f}_{P_2} \sigma^{(i)} \mathrm{grad}\, \phi^{(\mathrm{i})}\right] = 0, \qquad \text{in } \Omega^{(\mathrm{i})}, \tag{10.98a}$$

$$\mathrm{div}\left[-\frac{(\mathfrak{f}_{P_2})^2}{\mathfrak{f}_{P_3}} \sum_{k=1}^{N} F z_k D_k^{(\mathrm{e})} \mathrm{grad}\, c_k^{(\mathrm{e})} - \mathfrak{f}_{P_2} \sigma^{(e)} \mathrm{grad}\, \phi^{(\mathrm{e})}\right] = 0, \qquad \text{in } \Omega^{(\mathrm{e})}, \tag{10.98b}$$

$$\partial_t(\mathfrak{f}_{P_3} c_k^{(\mathrm{i})}) + \mathrm{div}\left[-\frac{(\mathfrak{f}_{P_2})^2}{\mathfrak{f}_{P_3}} D_k^{(\mathrm{i})} \mathrm{grad}\, c_k^{(\mathrm{i})} - \mathfrak{f}_{P_2} \frac{F z_k D_k^{(\mathrm{i})}}{RT} c_k^{(\mathrm{i})} \mathrm{grad}\, \phi^{(\mathrm{i})}\right] = 0, \qquad \text{in } \Omega^{(\mathrm{i})}, \tag{10.98c}$$

$$\partial_t(\mathfrak{f}_{P_3} c_k^{(\mathrm{e})}) + \operatorname{div}\left[-\frac{(\mathfrak{f}_{P_2})^2}{\mathfrak{f}_{P_3}} D_k^{(\mathrm{e})} \operatorname{grad} c_k^{(\mathrm{e})} - \mathfrak{f}_{P_2} \frac{F z_k D_k^{(\mathrm{e})}}{RT} c_k^{(\mathrm{e})} \operatorname{grad} \phi^{(\mathrm{e})}\right] = 0, \quad \text{in } \Omega^{(\mathrm{e})}, \tag{10.98d}$$

$$\phi^{(\mathrm{i})}(x,t) = \phi^{(\mathrm{e})}(x,t) + V(x,t), \qquad \text{on } \mathscr{M}, \tag{10.98e}$$

$$\boldsymbol{J}^{(\mathrm{i})} \cdot \boldsymbol{n}^{(\mathrm{ie})} = I, \qquad \text{on } \mathscr{M}, \tag{10.98f}$$

$$\boldsymbol{J}^{(\mathrm{e})} \cdot \boldsymbol{n}^{(\mathrm{ei})} = -I, \qquad \text{on } \mathscr{M}, \tag{10.98g}$$

$$\boldsymbol{J}_k^{(\mathrm{i})} \cdot \boldsymbol{n}^{(\mathrm{ie})} = I_k^{(\mathrm{i})}, \qquad \text{on } \mathscr{M}, \tag{10.98h}$$

$$\boldsymbol{J}_k^{(\mathrm{e})} \cdot \boldsymbol{n}^{(\mathrm{ei})} = I_k^{(\mathrm{e})}, \qquad \text{on } \mathscr{M}, \tag{10.98i}$$

$$I = C\,\partial_t V + \sum_{k=1}^{N} I_k^{(\mathrm{ionic})}, \qquad \text{on } \mathscr{M}, \tag{10.98j}$$

$$\int_{\Omega^{(\mathrm{e})}} \phi^{(\mathrm{e})} \mathfrak{f}_{P_3} \mathrm{dv} = 0, \qquad \text{in } \Omega^{(\mathrm{e})}, \tag{10.98k}$$

$$\boldsymbol{J}_k^{(\mathrm{e})} \cdot \boldsymbol{n}^{(\mathrm{ee})} = 0, \qquad \text{on } \partial\Omega^{(\mathrm{e,e})}. \tag{10.98l}$$

where $I_k^{(\mathrm{ionic})}$, $\alpha_k^{(\mathrm{i})}$, $\alpha_k^{(\mathrm{e})}$, and $I^{(\mathrm{ionic})}$ are to be understood constitutively defined, as stated in the previous chapter. Finally, the model must be completed by assigning appropriate initial conditions.

Conclusions to Part III

The content reported in this chapter is taken from [236][6].

This part constitutes a starting point of a research project concerning the mathematical and computational modelling of problems in neurobiology.

Following [96], in Chapter 9, we start by considering the Poisson–Nernst–Planck (PNP) model, but adapted to our context with slight modifications. The main scope of this chapter is to construct a benchmark model from which we can start adding additional hypothesis and that serves us as a foundation in the development of computational simulations. In doing this, we start by considering Maxwell's equations for the derivation of the mathematical model and we adopt standard modelling assumptions found in the scientific literature [261, 279, 277, 278]. Particularly, we pay special attention to the description of the weak formulation of the model, which is essential for the development of the numerical simulations. Finally, following [96], we present some numerical results to describe the electrophysiology of a single neuron in the case of a simplified geometry.

In Chapter 10, we reformulate the PNP model presented in Chapter 9 using the ideas and definitions introduced in [266]. For this purpose, we reinterpret Maxwell's equations in a fractal context by making use of the fractal measures presented in [266], which involve the definition of transition functions from the standard measure to the fractal measure [266]. A particularly delicate and crucial aspect in this fractal framework is the definition of the fractal current density, which is obtained through a detailed study of the dissipation of the system following the ideas proposed in [141, 39, 129]. Therefore, the proposed fractal PNP Model is derived by following the investigation of the mass and momentum balance equations, together with the dissipation principle, for the the case of a mixture by adapting the approach presented in [141, 39, 129] to the fractal framework under consideration.

[6]The work [236] is also used in the MSc thesis of Mr. Vito Napoli. The Author of this PhD thesis was co-advisor of that MSc thesis.

Among the further developments of the investigation presented in this part, we mention the need of the conception of computational simulations to describe the electrophysiology of neurons. However, this constitutes a demanding and challenging task because, for instance, of the complexities in describing the computational domain. Even though the design of such numerical simulations are out of the scope of the Thesis, this is part of our current and future research.

Appendix A

Some aspects of non-locality on manifolds

In the following, we propose a possible way for the formulation of non-local diffusion on manifolds. For this purpose, let us recall that the fractional mass flux vector $\boldsymbol{y}_\alpha$ is defined through the duality product

$$\langle \boldsymbol{y}_\alpha, \operatorname{grad} \check{c} \rangle := -\varrho_{\mathrm{f}} \int_{\mathscr{B}_t} \left\{ \int_{\mathscr{B}_t} [\operatorname{grad} \check{c}(x)]\, \boldsymbol{d}_\alpha(x, \tilde{x}, t) [\operatorname{grad} c_{\mathrm{a}}(\tilde{x}, t)] \mathrm{dv}(\tilde{x}) \right\} \mathrm{dv}(x), \tag{A.1a}$$

$$\boldsymbol{d}_\alpha(x, \tilde{x}, t) := \mathfrak{f}_\alpha(x, \tilde{x})\, \mathfrak{d}_\alpha(x, \tilde{x}, t), \tag{A.1b}$$

where the non-locality function is given by the following relationship

$$\mathfrak{f}_\alpha(x, \tilde{x}) := \mathfrak{f}_\alpha^{(0)}\left(x_0, \mathcal{T}_x^{x_0}(\tilde{x})\right). \tag{A.2}$$

In Equation (A.2), the notation $\mathcal{T}_x^{x_0} := \exp_{x_0} \circ (\mathcal{P}_{x_0}^x)^{-1} \circ \exp_x^{-1}$ is used, and the following operators are introduced:

- Let $T_{x,\delta}\mathscr{B}_t$ be the subset of the tangent space $T_x\mathscr{B}_t$ defined by

$$T_{x,\delta}\mathscr{B}_t := \{ \boldsymbol{v}_x \in T_x\mathscr{B}_t \,|\, \langle \boldsymbol{v}_x, \boldsymbol{v}_x \rangle_{\boldsymbol{g}} \leq \delta, \text{ with } \delta > 0 \}, \tag{A.3}$$

  and let $\mathscr{U}_t(x, \delta) := \{ \tilde{x} \in \mathscr{B}_t | \operatorname{dist}_{\mathscr{B}_t}(x, \tilde{x}) \leq \delta \}$ be a closed neighbourhood of x having radius δ, with $\operatorname{dist}_{\mathscr{B}_t} : \mathscr{B}_t \times \mathscr{B}_t \to \mathbb{R}_0^+$ denoting the *distance function*[1] on $\mathscr{B}_t$ [253]. The operator

$$\exp_x : T_{x,\delta}\mathscr{B}_t \to \mathscr{U}_t(x, \delta), \tag{A.4}$$

[1] Given the geodesic from x to $\tilde{x}$, and denoting by $\eta : [0,1] \to \mathscr{B}_t$ its parameterisation, so that $x = \eta(0)$ and $\tilde{x} = \eta(1)$, we set $\operatorname{dist}_{\mathscr{B}_t}(x, \tilde{x}) := \int_0^1 \|\eta'(\sigma)\| \mathrm{d}\sigma$.

referred to as *exponential map*, is injective and associates each element of $T_{x,\delta}\mathscr{B}_t$ with the point $\tilde{x} = \exp_x(\boldsymbol{v}_x) \in \mathscr{U}_t(x,\delta)$, which is the projection of $\boldsymbol{v}_x$ onto $\mathscr{U}_t(x,\delta)$. Note that the result of this operation generalises the concept of translation to the case of a manifold. To construct $\exp_x(\boldsymbol{v}_x)$, we take $\boldsymbol{v}_x \in T_{x,\delta}\mathscr{B}_t$ and consider the unique solution to the geodesic equation (see e.g. [189]), parameterised by $\eta : [0,1] \to \mathscr{U}_t(x,\delta)$, and in harmony with the "initial" conditions $\eta(0) = x$ and $\eta'(0) = \boldsymbol{v}_x$. Then, we identify $\exp_x(\boldsymbol{v}_x)$ with $\eta(1)$, i.e., $\exp_x(\boldsymbol{v}_x) = \eta(1) \equiv \tilde{x}$.

By construction, the exponential map is invertible and its inverse, i.e., $\exp_x^{-1} : \mathscr{U}_t(x,\delta) \to T_{x,\delta}\mathscr{B}_t$, returns a unique tangent vector of $T_{x,\delta}\mathscr{B}_t$ for each point of $\mathscr{U}_t(x,\delta)$. Therefore, by taking $\tilde{x} \in \mathscr{U}_t(x,\delta)$, with $\tilde{x} = \eta(1)$, it holds that $\exp_x^{-1}(\eta(1)) = \eta'(0)$.

- Let us consider two points of the manifold, e.g. $x_0, x \in \mathscr{B}_t$, and let $\zeta : [0,s] \to \mathscr{B}_t$, with $\zeta(0) = x_0$ and $\zeta(s) = x$, be the parameterisation of the geodesic connecting x_0 to x. Moreover, let us take the sets of tangent vectors $T_{x_0,\delta}\mathscr{B}_t$ and $T_{x,\delta}\mathscr{B}_t$, with $\delta > 0$. Then, to transport parallely the elements of $T_{x_0,\delta}\mathscr{B}_t$ into $T_{x,\delta}\mathscr{B}_t$ along the geodesic parameterised by ζ, we define the shifter operator

$$\mathscr{P}_{x_0}^{x} : T_{x_0,\delta}\mathscr{B}_t \to T_{x,\delta}\mathscr{B}_t, \quad \boldsymbol{v}_{x_0} \mapsto \mathscr{P}_{x_0}^{x}\boldsymbol{v}_{x_0} = \boldsymbol{v}_x. \tag{A.5}$$

  Clearly, $\mathscr{P}_{x_0}^{x}$ is invertible and its inverse reads $(\mathscr{P}_{x_0}^{x})^{-1} = \mathscr{P}_{x}^{x_0} : T_{x,\delta}\mathscr{B}_t \to T_{x_0,\delta}\mathscr{B}_t$. In addition, $\mathscr{P}_{x_0}^{x_0}$ is the identity operator from $T_{x_0,\delta}\mathscr{B}_t$ into itself.

- To represent $\mathfrak{f}_\alpha(x,\tilde{x})$ properly, we explain in detail our understanding of the procedure sketched in [253]. For this purpose, we start recalling that $\mathfrak{f}_\alpha(x,\tilde{x})$ measures how, at time t, the value of $\mathrm{grad} c_{\mathrm{a}}(\tilde{x},t)$ is "felt" at x, for all pairs of points $x, \tilde{x} \in \mathscr{B}_t$, such that $\tilde{x} \in \mathscr{U}_t(x,\delta)$, with $\delta > 0$. This influence has to be described in a way respectful of the geometry of the manifold, which can be achieved as follows. Given $\mathfrak{f}_\alpha(x,\tilde{x})$, we select arbitrarily a point $x_0 \in \mathscr{B}_t$ and we introduce an auxiliary function $\mathfrak{f}_\alpha^{(0)}(x_0,\,\cdot\,) : \mathscr{U}_t(x_0,\delta) \to \mathbb{R}$, such that, for an appropriate $\tilde{x}_0 \in \mathscr{U}_t(x_0,\delta)$, $\mathfrak{f}_\alpha^{(0)}(x_0,\tilde{x}_0) = \mathfrak{f}_\alpha(x,\tilde{x})$. In order for $\tilde{x}_0$ to be "appropriate", it has to depend on x and $\tilde{x}$ (and on x_0). This can be obtained by calling for the operator

$$\mathscr{T}_x^{x_0} := \exp_{x_0} \circ (\mathscr{P}_{x_0}^{x})^{-1} \circ \exp_x^{-1} : \mathscr{U}_t(x,\delta) \to \mathscr{U}_t(x_0,\delta). \tag{A.6}$$

  As anticipated above, for each $\tilde{x} \in \mathscr{U}_t(x,\delta)$, $\exp_x^{-1}$ returns a vector $\boldsymbol{v}_x$, such that $\|\boldsymbol{v}_x\| \leq \delta$. Then, $(\mathscr{P}_{x_0}^{x})^{-1}$ transports $\boldsymbol{v}_x$ parallely to x_0, so that

$(\mathscr{P}_{x_0}^{x})^{-1}\boldsymbol{v}_x = \boldsymbol{v}_{x_0}$. Finally, the operator $\exp_{x_0}$ maps $\boldsymbol{v}_{x_0}$ into $\tilde{x}_0 = \exp_{x_0}(\boldsymbol{v}_{x_0}) \in \mathscr{U}_t(x_0, \delta)$. Therefore, it holds that $\tilde{x}_0 = \mathcal{T}_x^{x_0}(\tilde{x})$, thereby explaining how $\tilde{x}_0$ depends on x and $\tilde{x}$, for a given x_0. More specifically, the action of $\mathcal{T}_x^{x_0}$ on $\tilde{x}$ permits to find the only $\tilde{x}_0$ such that Equation (A.2) becomes

$$\mathfrak{f}_\alpha(x, \tilde{x}) = \mathfrak{f}_\alpha^{(0)}\left(x_0, \mathcal{T}_x^{x_0}(\tilde{x})\right) = \mathfrak{f}_\alpha^{(0)}(x_0, \tilde{x}_0), \tag{A.7}$$

where the composition $\mathfrak{f}_\alpha(x, \cdot) = \mathfrak{f}_\alpha^{(0)}(x_0, \cdot) \circ \mathcal{T}_x^{x_0} : \mathscr{U}_t(x, \delta) \to \mathbb{R}$ is implied. The essence of this result is that the information on the non-locality of a given phenomenon between x and $\tilde{x}$, encompassed by $\mathfrak{f}_\alpha(x, \tilde{x})$, is "transported" to the pair of points x_0 and $\tilde{x}_0$ (see Fig. A.1).

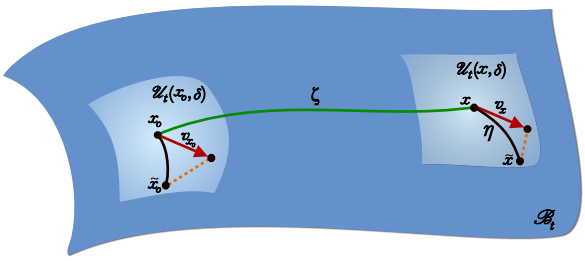

Figure A.1: The convolution on manifolds is defined by transporting $\mathfrak{f}_\alpha(x, \cdot) : \mathscr{U}_t(x, \delta) \to \mathbb{R}$ to every point of $\mathscr{B}_t$, while taking into account the manifold geometry. Thus, given a point $\tilde{x} = \eta(1) \in \mathscr{U}_t(x, \delta)$, the operation $\exp_x^{-1}(\tilde{x})$ returns the vector $\boldsymbol{v}_x = \eta'(0)$, which is parallel transported to $\boldsymbol{v}_{x_0}$ through a geodesic $\zeta : [0, s] \to \mathscr{B}_t$ connecting $x = \zeta(s)$ and $x_0 = \zeta(0)$, and the operation $\exp_{x_0}(\boldsymbol{v}_{x_0})$ returns the point $\tilde{x}_0 \in \mathscr{U}_t(x_0, \delta)$. In this way, $\mathfrak{f}_\alpha(x, \cdot)$ is transported from $\mathscr{U}_t(x, \delta)$ to $\mathscr{U}_t(x_0, \delta)$.

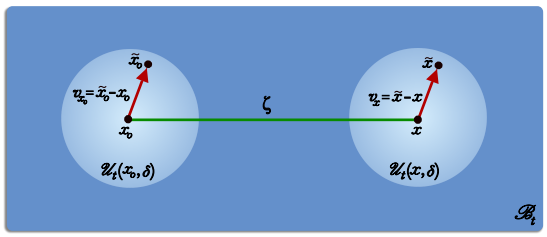

Figure A.2: In a flat subset of an affine space $\boldsymbol{v}_{x_0} = \tilde{x}_0 - x_0$ is equipollent to $\boldsymbol{v}_x = \tilde{x} - x$. Therefore, $\mathfrak{f}_\alpha(x, \tilde{x})$ and $\mathfrak{f}_\alpha^{(0)}(x_0, \tilde{x}_0)$ can be rephrased as $\mathfrak{f}_\alpha(x, \tilde{x}) = \hat{\mathfrak{f}}_\alpha(x - \tilde{x})$ and $\mathfrak{f}_\alpha^{(0)}(x_0, \tilde{x}_0) = \hat{\mathfrak{f}}_\alpha^{(0)}(x_0 - \tilde{x}_0)$.

To conclude, we notice that, in an affine space or, more generally, in a flat subset of an affine space, the procedure outlined above boils down to the determination of the unique point $\tilde{x}_0$ such that $\boldsymbol{v}_{x_0} = \tilde{x}_0 - x_0$ is equipollent to $\boldsymbol{v}_x = \tilde{x} - x$, for given x_0, x and $\tilde{x}$. Indeed, within this framework, $\mathcal{T}_x^{x_0}$

operates in such a way that $\boldsymbol{v}_{x_0} = \mathcal{T}_x^{x_0}(\tilde{x}) - x_0 = \tilde{x}_0 - x_0$ is parallel to $\boldsymbol{v}_x$ (because $\boldsymbol{v}_x$ is parallel transported along the geodesic —now, a straight line— connecting x with x_0) and $\|\boldsymbol{v}_{x_0}\| \equiv \|\tilde{x}_0 - x_0\| = \|\tilde{x} - x\| \equiv \|\boldsymbol{v}_x\|$. Moreover, $\mathfrak{f}_\alpha(x, \tilde{x})$ and $\mathfrak{f}_\alpha^{(0)}(x_0, \tilde{x}_0)$ can be rephrased as $\mathfrak{f}_\alpha(x, \tilde{x}) = \hat{\mathfrak{f}}_\alpha(x - \tilde{x})$ and $\mathfrak{f}_\alpha^{(0)}(x_0, \tilde{x}_0) = \hat{\mathfrak{f}}_\alpha^{(0)}(x_0 - \tilde{x}_0)$, respectively, and Equation (A.2), or Equation (A.7), is trivially satisfied. In this respect, we say that Equation (A.2) adapts the meaning of convolution from the case of an affine space to the case of a manifold (see Fig. A.2).

Bibliography

[1] F. Ben Adda. "La différentiabilité dans le calcul fractionnaire". In: *Comptes Rendus de l'Académie des Sciences - Series I - Mathematics* 326.7 (Apr. 1998), pp. 787–791. DOI: 10.1016/s0764-4442(98)80013-x.

[2] E. C. Aifantis. "On the microstructural origin of certain inelastic models". In: *Transactions on ASME Journal of Engineering Materials and Technology* 106 (1984), pp. 326–330.

[3] E. C. Aifantis. "The physics of plastic deformation". In: *International Journal of Plasticity* 3 (1987), pp. 211–247.

[4] E. C. Aifantis and J. B. Serrin. "The mechanical theory of fluid interfaces and Maxwell's rule". In: *Journal of Colloid and Interface Science* 96.2 (Dec. 1983), pp. 517–529. DOI: 10.1016/0021-9797(83)90053-x.

[5] G. Alaimo et al. "A fractional order theory of poroelasticity". In: *Mechanics Research Communications* 100 (Sept. 2019), p. 103395. DOI: 10.1016/j.mechrescom.2019.103395.

[6] G. Allaire and M. Briane. "Multiscale convergence and reiterated homogenisation". In: *Proceedings of the Royal Society of Edinburgh: Section A Mathematics* 126.02 (Jan. 1996), pp. 297–342. DOI: 10.1017/s0308210500022757.

[7] N. M. Allen et al. "Genetic potassium channel-associated epilepsies: Clinical review of the Kv family". In: *European Journal of Paediatric Neurology* 24 (Jan. 2020), pp. 105–116. DOI: 10.1016/j.ejpn.2019.12.002.

[8] G. Alotta et al. "A fractional nonlocal approach to nonlinear blood flow in small-lumen arterial vessels". In: *Meccanica* 55.4 (Mar. 2020), pp. 891–906. DOI: 10.1007/s11012-020-01144-y.

[9] D. Ambrosi and F. Mollica. "On the mechanics of a growing tumor". In: *International Journal of Engineering Science* 40.12 (July 2002), pp. 1297–1316. DOI: 10.1016/s0020-7225(02)00014-9.

[10] D. Ambrosi and L. Preziosi. "Cell adhesion mechanisms and stress relaxation in the mechanics of tumours". In: *Biomechanics and Modeling in Mechanobiology* 8 (2009), pp. 397–413. DOI: 10.1007/s10237-008-0145-y.

[11] D. Ambrosi and L. Preziosi. "On the closure of mass balance models for tumor growth". In: *Mathematical Models and Methods in Applied Sciences* 12.05 (May 2002), pp. 737–754. DOI: 10.1142/s0218202502001878.

[12] D. Ambrosi, L. Preziosi, and G. Vitale. "The insight of mixtures theory for growth and remodeling". In: *Z. Angew. Math. Phys.* 61 (2010), pp. 177–191. DOI: 10.1007/s00033-009-0037-8.

[13] D. Ambrosi, L. Preziosi, and G. Vitale. "The interplay between stress and growth in solid tumors". In: *Mech. Res. Commun.* 42 (2012), pp. 87–91.

[14] L. Anand, O. Aslan, and A. Chester. "A large-deformation gradient theory for elastic-plastic materials: Strain softening and regularization of shear bands". In: *International Journal of Plasticity* 30–31 (2012), pp. 116–143. DOI: 10.1016/j.ijplas.2011.10.002.

[15] L. Anand et al. "A one-dimensional theory of strain-gradient plasticity: formulation, analysis, numerical results". In: *Journal of the Mechanics and Physics of Solids* 53 (2005), pp. 1789–1826. DOI: 10.1016/j.jmps.2005.03.003.

[16] R. P. Araujo and D. L. McElwain. "A history of the study of solid tumour growth: the contribution of mathematical modelling". In: *Bulletin of Mathematical Biology* (May 2004). DOI: 10.1016/s0092-8240(03)00126-5.

[17] H. Askes and E. C. Aifantis. "Gradient elasticity in statics and dynamics: An overview of formulations, length scale identification procedures, finite element implementations and new results". In: *International Journal of Solids and Structures* 48.13 (June 2011), pp. 1962–1990. DOI: 10.1016/j.ijsolstr.2011.03.006.

[18] T. M. Atanackovic, S. Pilipovic, and D. Zorica. "A diffusion wave equation with two fractional derivatives of different order". In: *Journal of Physics A: Mathematical and Theoretical* 40.20 (Apr. 2007), pp. 5319–5333. DOI: 10.1088/1751-8113/40/20/006.

[19] T. M. Atanackovic and B. Stankovic. "Generalized wave equation in nonlocal elasticity". In: *Acta Mechanica* 208.1-2 (Nov. 2008), pp. 1–10. DOI: 10.1007/s00707-008-0120-9.

[20] T. Atanacković et al. "The Cattaneo type space-time fractional heat conduction equation". In: *Continuum Mechanics and Thermodynamics* 24.4-6 (Oct. 2011), pp. 293–311. DOI: 10.1007/s00161-011-0199-4.

[21] T. M. Atanacković et al. *Fractional Calculus with Applications in Mechanics: Vibrations and Diffusion Processes*. ISTE Ltd., Jan. 2014. 422 pp. ISBN: 1848216793.

[22] T. M. Atanacković et al. *Fractional Calculus with Applications in Mechanics: Wave Propagation, Impact and Variational Principles*. ISTE Ltd., Jan. 2014. 422 pp. ISBN: 1848216793.

[23] G. A. Ateshian. "On the theory of reactive mixtures for modeling biological growth". In: *Biomechanics and Modeling in Mechanobiology* 6.6 (2007), pp. 423–445. DOI: 10.1007/s10237-006-0070-x.

[24] G. A. Ateshian and J. D. Humphrey. "Continuum Mixture Models of Biological Growth and Remodeling: Past Successes and Future Opportunities". In: *Annual Review of Biomedical Engineering* 14.1 (Aug. 2012), pp. 97–111. DOI: 10.1146/annurev-bioeng-071910-124726.

[25] G. A. Ateshian and J. A. Weiss. "Anisotropic hydraulic permeability under finite deformation". In: *J. Biomech. Engng.* 132 (2010), pp. 111004-1–111004-7. DOI: 10.1115/1.4002588.

[26] J. L. Auriault. "Effective macroscopic description for heat conduction in periodic composites". In: *International Journal of Heat and Mass Transfer* 26.6 (June 1983), pp. 861–869. DOI: 10.1016/s0017-9310(83)80110-0.

[27] J.-L. Auriault, C. Boutin, and C. Geindreau, eds. *Homogenization of Coupled Phenomena in Heterogenous Media*. ISTE, Jan. 2009. DOI: 10.1002/9780470612033.

[28] J.-L. Auriault, C. Geindreau, and C. Boutin. "Filtration Law in Porous Media with Poor Separation of Scales". In: *Transport in Porous Media* 60.1 (July 2005), pp. 89–108. DOI: 10.1007/s11242-004-3649-7.

[29] J.-L. Auriault and J. Lewandoska. "Effective Diffusion Coefficient: From Homogenization to Experiment". In: *Transport in Porous Media* 27.2 (1997), pp. 205–223. DOI: 10.1023/a:1006599410942.

[30] D. Axelrod et al. "Mobility measurement by analysis of fluorescence photobleaching recovery kinetics". In: *Biophysical Journal* 16.9 (1976), pp. 1055–1069.

[31] D. Axelrod et al. "Mobility measurement by analysis of fluorescence photobleaching recovery kinetics". In: *Biophysical Journal* 16.9 (Sept. 1976), pp. 1055–1069. DOI: 10.1016/s0006-3495(76)85755-4.

[32] F. Baaijens, C. Bouten, and N. Driessen. "Modeling cartilage remodeling". In: *J. Biomech.* 43 (2010), pp. 166–175. DOI: 10.1016/j.jbiomech.2009.09.022.

[33] O. Baglieri et al. "Fractional Viscoelastic Modeling of Antirutting Response of Bituminous Binders". In: *Journal of Engineering Mechanics* 143.5 (May 2017). DOI: 10.1061/(asce)em.1943-7889.0001081.

[34] N. Bakhvalov and G. Panasenko. *Homogenisation: Averaging Processes in Periodic Media*. Springer Netherlands, 1989.

[35] J. Bear and Y. Bachmat. *Introduction to Modeling of Transport Phenomena in Porous Media*. Kluwer, Dordrecht, 1990.

[36] J. Bear, L. G. Fel, and Y. Zimmels. "Effects of Material Symmetry on the Coefficients of Transport in Anisotropic Porous Media". In: *Transport in Porous Media* 82.2 (June 2009), pp. 347–361. DOI: 10.1007/s11242-009-9430-1.

[37] N. Bellomo and L. Preziosi. "Modelling and mathematical problems related to tumor evolution and its interaction with the immune system". In: *Mathematical and Computer Modelling* 32.3-4 (Aug. 2000), pp. 413–452. DOI: 10.1016/s0895-7177(00)00143-6.

[38] A. Beltempo et al. "A numerical integration approach for fractional-order viscoelastic analysis of hereditary-aging structures". In: *International Journal for Numerical Methods in Engineering* 121.6 (Nov. 2019), pp. 1120–1146. DOI: 10.1002/nme.6259.

[39] L. S. Bennethum, M. A. Murad, and J. H. Cushman. "Macroscale thermodynamics and the chemical potential for swelling porous media". In: *Transport in Porous Media* 39.2 (2000), pp. 187–225. DOI: 10.1023/a:1006661330427.

[40] A. Bensoussan, J.-L. Lions, and G. Papanicolau. *Asymptotic Analysis for Periodic Structures*. Elsevier Science, Jan. 1978. 699 pp.

[41] X. Bi et al. "A novel method for determination of collagen orientation in cartilage by Fourier transform infrared imaging spectroscopy (FT-IRIS)". In: *Osteoarthritis and Cartilage* 13.12 (Dec. 2005), pp. 1050–1058. DOI: 10.1016/j.joca.2005.07.008.

[42] J. Bonet and R. D. Wood. *Nonlinear Continuum Mechanics for Finite Element Analysis*. Cambridge University Press, New York, 2008.

[43] H. Brezis. *Functional Analysis, Sobolev Spaces and Partial Differential Equations*. Springer New York, 2010. DOI: 10.1007/978-0-387-70914-7.

[44] M. M. Bronstein et al. "Geometric Deep Learning: Going beyond Euclidean data". In: *IEEE Signal Processing Magazine* 34.4 (July 2017), pp. 18–42. DOI: 10.1109/msp.2017.2693418.

[45] A. Bueno-Orovio et al. "Fractional diffusion models of cardiac electrical propagation: role of structural heterogeneity in dispersion of repolarization". In: *Journal of The Royal Society Interface* 11.97 (Aug. 2014), p. 20140352. DOI: 10.1098/rsif.2014.0352.

[46] R. Burridge and J. B. Keller. "Poroelasticity equations derived from microstructure". In: *The Journal of the Acoustical Society of America* 70.4 (Oct. 1981), pp. 1140–1146. DOI: 10.1121/1.386945.

[47] N. Burton-Wurster and G. Lust. "Fibronectin and proteoglycan synthesis in long term cultures of cartilage explants in Ham's F12 supplemented with insulin and calcium: effects of the addition of TGF-β". In: *Archives of Biochemistry and Biophysics* 283.1 (1990), pp. 27–33.

[48] V. A. Buryachenko. "On thermoelastostatics of composites with nonlocal properties of constituents I. General representations for effective material and field parameters". In: *International Journal of Solids and Structures* 48.13 (June 2011), pp. 1818–1828. DOI: 10.1016/j.ijsolstr.2011.02.023.

[49] H. Byrne and L. Preziosi. "Modelling solid tumour growth using the theory of mixtures". In: *Mathematical Medicine and Biology* 20.4 (Dec. 2003), pp. 341–366. DOI: 10.1093/imammb/20.4.341.

[50] H. M. Byrne and M. A. J. Chaplain. "Growth of nonnecrotic tumors in the presence and absence of inhibitors." In: *Mathematical biosciences* 130 (2 Dec. 1995), pp. 151–181. ISSN: 0025-5564. DOI: 10.1016/0025-5564(94)00117-3.

[51] H. M. Byrne and D. Drasdo. "Individual-based and continuum models of growing cell populations: a comparison". In: *Journal of Mathematical Biology* 58.4-5 (Oct. 2009), pp. 657–687. DOI: 10.1007/s00285-008-0212-0.

[52] S. Capuani et al. "Spatio-temporal anomalous diffusion imaging: results in controlled phantoms and in excised human meningiomas". In: *Magnetic Resonance Imaging* 31.3 (Apr. 2013), pp. 359–365. DOI: 10.1016/j.mri.2012.08.012.

[53] M. Carfagna and A. Grillo. "The Spherical Design Algorithm in the numerical simulation of biological tissues with statistical fibre-reinforcement". In: *Computing and Visualization in Science* (2017), pp. 1–28. ISSN: 1433-0369. DOI: 10.1007/s00791-017-0278-6.

[54] A. Carpinteri, B. Chiaia, and P. Cornetti. "Static–kinematic duality and the principle of virtual work in the mechanics of fractal media". In: *Computer Methods in Applied Mechanics and Engineering* 191.1-2 (Nov. 2001), pp. 3–19. DOI: 10.1016/s0045-7825(01)00241-9.

[55] A. Carpinteri, P. Cornetti, and A. Sapora. "A fractional calculus approach to nonlocal elasticity". In: *The European Physical Journal Special Topics* 193.1 (Mar. 2011), pp. 193–204. DOI: 10.1140/epjst/e2011-01391-5.

[56] A. Carpinteri and F. Mainardi, eds. *Fractals and Fractional Calculus in Continuum Mechanics*. Springer Vienna, Dec. 1997. 360 pp. ISBN: 321182913X.

[57] J. J. Casciari, S. V. Sotirchos, and R. M. Sutherland. "Mathematical modelling of microenvironment and growth in EMT6/Ro multicellular tumour spheroids". In: *Cell Proliferation* 25.1 (Jan. 1992), pp. 1–22. DOI: 10.1111/j.1365-2184.1992.tb01433.x.

[58] J. J. Casciari, Stratis V. Sotirchos, and R. M. Sutherland. "Variations in tumor cell growth rates and metabolism with oxygen concentration, glucose concentration, and extracellular pH". In: *Journal of Cellular Physiology* 151.2 (May 1992), pp. 386–394. DOI: 10.1002/jcp.1041510220.

[59] P. Cermelli, E. Fried, and M. E. Gurtin. "Transport relations for surface integrals arising in the formulation of balance laws for evolving fluid interfaces". In: *Journal of Fluid Mechanics* 544 (2005), p. 339. DOI: 10.1017/s0022112005006695.

[60] P. Cermelli, E. Fried, and S. Sellers. "Configurational stress, yield and flow in rate-independent plasticity". In: *Proc. R. Soc. Lond. A* 457 (2001), pp. 1447–1467. DOI: 10.1098/rspa.2001.0786.

[61] N. Challamel et al. "On the fractional generalization of Eringen's nonlocal elasticity for wave propagation". In: *Comptes Rendus Mécanique* 341.3 (Mar. 2013), pp. 298–303. DOI: 10.1016/j.crme.2012.11.013.

[62] M.A.J. Chaplain, L. Graziano, and L. Preziosi. "Mathematical modelling of the loss of tissue compression responsiveness and its role in solid tumour development". In: *Mathematical Medicine and Biology: A Journal of the IMA* 23.3 (Sept. 2006), pp. 197–229. DOI: 10.1093/imammb/dql009.

[63] G. A. Chauvet. "Non-locality in biological systems results from hierarchy". In: *Journal of Mathematical Biology* 31.5 (May 1993). DOI: 10.1007/bf00173887.

[64] A. S. Chaves. "A fractional diffusion equation to describe Lévy flights". In: *Physics Letters A* 239.1-2 (Feb. 1998), pp. 13–16. DOI: 10.1016/s0375-9601(97)00947-x.

[65] K. D. Cherednichenko, V. P. Smyshlyaev, and V. V. Zhikov. "Non-local homogenized limits for composite media with highly anisotropic periodic fibres". In: *Proceedings of the Royal Society of Edinburgh: Section A Mathematics* 136.1 (Feb. 2006), pp. 87–114. DOI: 10.1017/s0308210500004455.

[66] V. Ciancio et al. "Uniform materials and the multiplicative decomposition of the deformation gradient in finite elasto-plasticity". In: *J. Non-Equilib. Thermodyn.* 33(3) (2008), pp. 199–234. DOI: 10.1515/JNETDY.2008.009.

[67] P. Ciarletta, D. Ambrosi, and G. A. Maugin. "Configurational forces for growth and shape regulations in morphogenesis". In: *Bulletin of the Polish Academy of Sciences –Technical Sciences* 60(2) (2012), pp. 253–257. DOI: 10.2478/v10175-012-0034-5.

[68] P. Ciarletta, D. Ambrosi, and G. A. Maugin. "Mass transport in morphogenetic processes: A second gradient theory for volumetric growth and material remodeling". In: *J. Mech. Phys. Solids* 60 (2012), pp. 432–450. DOI: 10.1016/j.jmps.2011.11.011.

[69] P. Ciarletta, M. Destrade, and A. L. Gower. "On residual stresses and homeostasis: an elastic theory of functional adaptation in living matter". In: *Scientific Reports* 6.1 (Apr. 2016). DOI: 10.1038/srep24390.

[70] P. Ciarletta and G. A. Maugin. "Elements of a finite strain-gradient thermomechanical theory for material growth and remodeling". In: *Int. J. Non-Lin. Mech.* 46 (2011), pp. 1341–1346. DOI: 10.1016/j.ijnonlinmec.2011.07.004.

[71] P. Ciarletta et al. "Mechano-transduction in tumour growth modelling". In: *Eur. Phys. J. E* 36 (2013), p. 23. DOI: 10.1140/epje/i2013-13023-2.

[72] D. Cioranescu and P. Donato. *An introduction to homogenization*. Oxford University Press, 1999. ISBN: 0198565542.

[73] S. Cleja-Tigoiu and G. A. Maugin. "Eshelby's stress tensors in finite elastoplasticity". In: *Acta Mechanica* 139.1-4 (Mar. 2000), pp. 231–249. DOI: 10.1007/bf01170191.

[74] H. L. E. Coker et al. "Controlling Anomalous Diffusion in Lipid Membranes". In: *Biophysical Journal* 116.6 (Mar. 2019), pp. 1085–1094. DOI: 10.1016/j.bpj.2018.12.024.

[75] J. Collis et al. "Effective equations governing an active poroelastic medium". In: *Proceedings of the Royal Society A: Mathematical, Physical and Engineering Science* 473.2198 (Feb. 2017), p. 20160755. DOI: 10.1098/rspa.2016.0755.

[76] S. C. Cowin. "How is a tissue built?" In: *J. Biomech. Eng.* 122 (2000), pp. 553–569. DOI: 10.1115/1.1324665.

[77] S. C. Cowin and G. A. Holzapfel. "On the Modeling of Growth and Adaptation". In: *Mechanics of Biological Tissue*. Ed. by Holzapfel G. A. and Odgen R. W. Springer-Verlag, 2006, pp. 29–46.

[78] E. Crevacore, S. Di Stefano, and A. Grillo. "Coupling among deformation, fluid flow, structural reorganisation and fibre reorientation in fibre-reinforced, transversely isotropic biological tissues". In: *International Journal of Non-Linear Mechanics* 111 (May 2019), pp. 1–13. DOI: 10.1016/j.ijnonlinmec.2018.08.022.

[79] C. J. Cyron and J. D. Humphrey. "Growth and remodeling of load-bearing biological soft tissues". In: *Meccanica* 52.3 (June 2016), pp. 645–664. DOI: 10.1007/s11012-016-0472-5.

[80] D.Ambrosi et al. "Perspectives on biological growth and remodeling". In: *J. Mech. Phys. Solids* 59(4) (2011), pp. 863–883. DOI: 10.1016/j.jmps.2010.12.011.

[81] Y. Danyuo et al. "Anomalous Release Kinetics of Prodigiosin from Poly-N-Isopropyl-Acrylamid based Hydrogels for The Treatment of Triple Negative Breast Cancer". In: *Scientific Reports* 9.1 (Mar. 2019). DOI: 10.1038/s41598-019-39578-4.

[82] D. del-Castillo-Negrete. "Fractional diffusion models of nonlocal transport". In: *Physics of Plasmas* 13.8 (Aug. 2006), p. 082308. DOI: 10.1063/1.2336114.

[83] F. dell'Isola, A. Della Corte, and I. Giorgio. "Higher-gradient continua: The legacy of Piola, Mindlin, Sedov and Toupin and some future research perspectives". In: *Mathematics and Mechanics of Solids* 22(4) (2017), pp. 852–872. DOI: 10.1177/1081286515616034.

[84] Z.-Q. Deng, V. P. Singh, and L. Bengtsson. "Numerical Solution of Fractional Advection-Dispersion Equation". In: *Journal of Hydraulic Engineering* 130.5 (May 2004), pp. 422–431. DOI: 10.1061/(asce)0733-9429(2004)130:5(422).

[85] L. Deseri et al. "Power-law hereditariness of hierarchical fractal bones". In: *International Journal for Numerical Methods in Biomedical Engineering* 29.12 (July 2013), pp. 1338–1360. DOI: 10.1002/cnm.2572.

[86] A. Di Carlo and S. Quiligotti. "Growth and balance". In: *Mechanics Research Communications* 29.6 (Nov. 2002), pp. 449–456. DOI: 10.1016/s0093-6413(02)00297-5.

[87] M. Di Paola and M. Zingales. "Fractional differential calculus for 3D mechanically based non-local elasticity". In: *International Journal for Multiscale Computational Engineering* 9.5 (2011), pp. 579–597. DOI: 10.1615/intjmultcompeng.2011002416.

[88] M. Di Paola and M. Zingales. "Long-range cohesive interactions of non-local continuum faced by fractional calculus". In: *International Journal of Solids and Structures* 45.21 (Oct. 2008), pp. 5642–5659. DOI: 10.1016/j.ijsolstr.2008.06.004.

[89] S. Di Stefano et al. "Anelastic reorganisation of fibre-reinforced biological tissues". In: *Computing and Visualization in Science* 20.3-6 (June 2019), pp. 95–109. DOI: 10.1007/s00791-019-00313-1.

[90] S. Di Stefano et al. "Effective balance equations for electrostrictive composites". In: *Zeitschrift für angewandte Mathematik und Physik* 71.5 (Sept. 2020). DOI: 10.1007/s00033-020-01365-x.

[91] S. Di Stefano et al. "Self-influenced growth through evolving material inhomogeneities". In: *International Journal of Non-Linear Mechanics* 106 (Nov. 2018), pp. 174–187. DOI: 10.1016/j.ijnonlinmec.2018.08.003.

[92] L. Dormieux, K. Djimédo, and U. Franz-Josef. *Microporomechanics*. Chichester, West Sussex, England Hoboken, NJ: Wiley, 2006. ISBN: 9780470032008.

[93] N. J. B. Driessen et al. "A computational model for collagen fibre remodelling in the arterial wall". In: *J. Theor. Biol.* 226 (2004), pp. 53–64. DOI: 10.1016/j.jtbi.2003.08.004.

[94] W. Ehlers et al. "Inverse poroelasticity as a fundamental mechanism in biomechanics and mechanobiology". In: *Nat. Commun.* 1002(8) (2017), pp. 1–10. DOI: 10.1038/s41467-017-00801-3.

[95] A. J. Ellingsrud, C. Daversin-Catty, and M. E. Rognes. "A cell-based model for ionic electrodiffusion in excitable tissue". In: *Modeling excitable tissue - the EMI framework*. Ed. by Kent-Andre Mardal, Marie E. Rognes, and Aslak Tveito. 7. Springer, 2021. Chap. A cell-based model for ionic electrodiffusion in excitable tissue, pp. 14–27. URL: https://www.springer.com/gp/book/9783030611569.

[96] A. J. Ellingsrud et al. "Finite Element Simulation of Ionic Electrodiffusion in Cellular Geometries". In: *Frontiers in Neuroinformatics* 14 (Mar. 2020). DOI: 10.3389/fninf.2020.00011.

[97] N. Engheta. "Fractional curl operator in electromagnetics". In: *Microwave and Optical Technology Letters* 17.2 (Feb. 1998), pp. 86–91. DOI: 10.1002/(sici)1098-2760(19980205)17:2<86::aid-mop4>3.0.co;2-e.

[98] M. Epstein. "Self-Driven continuous Dislocations and Growth". In: *Mechanics of Material Forces. Advances in Mechanics and Mathematics*. Ed. by Maugin G.A. Steinmann P. Vol. 11. Springer, Boston, MA, 2005, pp. 129–139.

[99] M. Epstein. *The geometric language of continuum mechanics*. Cambridge University Press, 2010.

[100] M. Epstein and M. Elżanowski. *Material Inhomogeneities and their Evolution — A Geometric Approach*. 1st ed. Springer-Verlag Berlin Heidelberg, 2007. DOI: 10.1007/978-3-540-72373-8.

[101] M. Epstein and G. A. Maugin. "On the geometrical material structure of anelasticity". In: *Acta Mechanica* 115.1-4 (Mar. 1996), pp. 119–131. DOI: 10.1007/bf01187433.

[102] M. Epstein and G. A. Maugin. "Thermomechanics of volumetric growth in uniform bodies". In: *International Journal of Plasticity* 16.7-8 (June 2000), pp. 951–978. DOI: 10.1016/s0749-6419(99)00081-9.

[103] A. C. Eringen. *Electrodynamics of Continua I: Foundations and Solid Media*. New York, NY: Springer New York, 1990. ISBN: 9781461232261.

[104] A. Cemal Eringen. "Linear theory of nonlocal elasticity and dispersion of plane waves". In: *International Journal of Engineering Science* 10.5 (May 1972), pp. 425–435. DOI: 10.1016/0020-7225(72)90050-x.

[105] G. Estrada-Rodriguez, H. Gimperlein, and K. J. Painter. "Fractional Patlak–Keller–Segel Equations for Chemotactic Superdiffusion". In: *SIAM Journal on Applied Mathematics* 78.2 (Jan. 2018), pp. 1155–1173. DOI: 10.1137/17m1142867.

[106] G. Estrada-Rodriguez et al. "Space-time fractional diffusion in cell movement models with delay". In: *Mathematical Models and Methods in Applied Sciences* 29.01 (Jan. 2019), pp. 65–88. DOI: 10.1142/s0218202519500039.

[107] S. Federico. "Covariant formulation of the tensor algebra of non-linear elasticity". In: *Int. J. Nonlinear Mech.* 47 (2012), pp. 273–284. DOI: 10.1016/j.ijnonlinmec.2011.06.007.

[108] S. Federico and T. C. Gasser. "Non-Linear Elasticity of Biological Tissues with Statistical Fibre Orientation". In: *Journal of the Royal Society Interface* 7 (2010), pp. 955–966. DOI: 10.1098/rsif.2009.0502.

[109] S. Federico and A. Grillo. "Elasticity and Permeability of Porous Fibre-Reinforced Materials Under Large Deformations". In: *Mechanics of Materials* 44 (2012), pp. 58–71. DOI: 10.1016/j.mechmat.2011.07.010.

[110] S. Federico and W. Herzog. "On the Anisotropy and Inhomogeneity of Permeability in Articular Cartilage". In: *Biomechanics and Modeling in Mechanobiology* 7 (2008), pp. 367–378. DOI: 10.1007/s10237-007-0091-0.

[111] S. Federico and W. Herzog. "On the Permeability of Fibre-Reinforced Porous Materials". In: *International Journal of Solids and Structures* 45 (2008), pp. 2160–2172. DOI: 10.1016/j.ijsolstr.2007.11.014.

[112] L. Fel and J. Bear. "Dispersion and Dispersivity Tensors in Saturated Porous Media with Uniaxial Symmetry". In: *Transport in Porous Media* 85.1 (Mar. 2010), pp. 259–268. DOI: 10.1007/s11242-010-9558-z.

[113] N. Filipovitch et al. "Infiltration experiments demonstrate an explicit connection between heterogeneity and anomalous diffusion behavior". In: *Water Resources Research* 52.7 (July 2016), pp. 5167–5178. DOI: 10.1002/2016wr018667.

[114] G. Forgacs et al. "Viscoelastic Properties of Living Embryonic Tissues: a Quantitative Study". In: *Biophysical Journal* 74 (1998), pp. 2227–2234.

[115] R.A. Foty et al. "Surface tensions of embryonic tissues predict their mutual envelopment behavior". In: *Development* 122 (1996), pp. 1611–1620.

[116] Y. C. Fung. *Biomechanics. Motion, flow, stress, and growth.* Springer, New York, 1990.

[117] P. Fuschi, A. A. Pisano, and D. De Domenico. "Plane stress problems in nonlocal elasticity: finite element solutions with a strain-difference-based formulation". In: *Journal of Mathematical Analysis and Applications* 431.2 (Nov. 2015), pp. 714–736. DOI: 10.1016/j.jmaa.2015.06.005.

[118] N. Gal and D. Weihs. "Experimental evidence of strong anomalous diffusion in living cells". In: *Physical Review E* 81.2 (Feb. 2010). DOI: 10.1103/physreve.81.020903.

[119] D. Garcia et al. "A three-dimensional elastic plastic damage constitutive law for bone tissue". In: *Biomech. Model. Mechanobiol.* 8(2) (2009), pp. 149–165. DOI: 10.1007/s10237-008-0125-2.

[120] K. Garikipati et al. "A continuum treatment of growth in biological tissue: the coupling of mass transport and mechanics". In: *J. Mech. Phys. Solids* 52 (2004), pp. 1595–1625. DOI: 10.1016/j.jmps.2004.01.004.

[121] M. G. D. Geers, R. de Borst, and T. Peijs. "Mixed numerical-experimental identification of non-local characteristics of random-fibre-reinforced composites". In: *Composites Science and Technology* 59.10 (Aug. 1999), pp. 1569–1578. DOI: 10.1016/s0266-3538(99)00017-2.

[122] H. Gimperlein and J. Stocek. "Space–time adaptive finite elements for nonlocal parabolic variational inequalities". In: *Computer Methods in Applied Mechanics and Engineering* 352 (Aug. 2019), pp. 137–171. DOI: 10.1016/j.cma.2019.04.019.

[123] I. Giorgio et al. "Viscous second gradient porous materials for bones reconstructed with bio-resorbable grafts". In: *Extreme Mechanics Letters* 13 (2017), pp. 141–147. DOI: 10.1016/j.eml.2017.02.008.

[124] C. Giverso and L. Preziosi. "Modelling the compression and reorganization of cell aggregates". In: *Mathematical Medicine and Biology* 29 (2012), pp. 181–204. DOI: https://doi.org/10.1093/imammb/dqr008.

[125] C. Giverso, M. Scianna, and A. Grillo. "Growing avascular tumours as elastoplastic bodies by the theory of evolving natural configurations". In: *Mech. Res. Commun.* 68 (2015), pp. 31–39. DOI: http://dx.doi.org/10.1016/j.mechrescom.2015.04.004.

[126] A. Goriely. *The Mathematics and Mechanics of Biological Growth.* Springer New York, 2016. DOI: 10.1007/978-0-387-87710-5.

[127] A. Grillo, M. Carfagna, and S. Federico. "An Allen–Cahn approach to the remodelling of fibre-reinforced anisotropic materials". In: *Journal of Engineering Mathematics* 109.1 (Apr. 2018), pp. 139–172. ISSN: 1573-2703. DOI: 10.1007/s10665-017-9940-8.

[128] A. Grillo, M. Carfagna, and S. Federico. "Non-Darcian flow in fibre-reinforced biological tissues". In: *Meccanica* 52 (2017), pp. 3299–3320. DOI: 10.1007/s11012-017-0679-0.

[129] A. Grillo, S. Federico, and G. Wittum. "Growth, mass transfer, and remodeling in fiber-reinforced, multi-constituent materials". In: *International Journal of Non-Linear Mechanics* 47 (2012), pp. 388–401. DOI: 10.1016/j.ijnonlinmec.2011.09.026.

[130] A. Grillo, R. Prohl, and G. Wittum. "A poroplastic model of structural reorganisation in porous media of biomechanical interest". In: *Continuum Mech. Therm.* 28 (2016), pp. 579–601. DOI: 10.1007/s00161-015-0465-y.

[131] A. Grillo et al. "A study of growth and remodeling in isotropic tissues, based on the Anand-Aslan-Chester theory of strain-gradient plasticity". In: *GAMM-Mitteilungen* 42.4 (May 2019). DOI: 10.1002/gamm.201900015.

[132] A. Grillo et al. "Remodelling in statistically oriented fibre-reinforced materials and biological tissues". In: *Math. Mech. Solids* 20(9) (2015), pp. 1107–1129. DOI: 10.1177/1081286513515265.

[133] M. E. Gurtin. "Generalized Ginzburg-Landau and Cahn-Hilliard equations based on a microforce balance". In: *Physica D* 92 (1994), pp. 178–192.

[134] M. E. Gurtin. "On the plasticity of single crystals: free energy, microforces, plastic-strain gradients". In: *Journal of the Mechanics and Physics of Solids* 48.5 (May 2000), pp. 989–1036. DOI: 10.1016/s0022-5096(99)00059-9.

[135] M. E. Gurtin and L. Anand. "A theory of strain-gradient plasticity for isotropic, plastically irrotational materials. Part II: Finite deformations". In: *International Journal of Plasticity* 21 (2005), pp. 2297–2318. DOI: 10.1016/j.ijplas.2005.01.006.

[136] M. E. Gurtin, E. Fried, and L. Anand. *The Mechanics and Thermodynamics of Continua*. Cambridge University Press, 2010.

[137] K. Hackl and F. D. Fischer. "On the relation between the principle of maximum dissipation and inelastic evolution given by dissipation potentials". In: *Proceedings of the Royal Society A: Mathematical, Physical and Engineering Sciences* 464.2089 (Oct. 2007), pp. 117–132. DOI: 10.1098/rspa.2007.0086.

[138] R. H. Hardin and N. J. A. Sloane. "McLaren's improved snub cube and other new spherical designs in three dimensions". In: *Discrete & Computational Geometry* 15.4 (Apr. 1996), pp. 429–441. DOI: 10.1007/bf02711518.

[139] I. Hariton et al. "Stress-driven collagen fiber remodeling in arterial walls". In: *Biomech. Model. Mechanobiol.* 6(3) (2007), pp. 163–175. DOI: 10.1007/s10237-006-0049-7.

[140] K. Hashlamoun et al. "Fluorescence recovery after photobleaching: direct measurement of diffusion anisotropy". In: *Biomechanics and Modeling in Mechanobiology* 19.6 (June 2020), pp. 2397–2412. DOI: 10.1007/s10237-020-01346-z.

[141] S. M. Hassanizadeh. "Derivation of basic equations of mass Transp. Porous Med., Part 2. Generalized Darcy's and Fick's laws". In: *Adv. Water Resour.* 9 (1986), pp. 207–222. DOI: 10.1016/0309-1708(86)90025-4.

[142] S. Majid Hassanizadeh. "Derivation of basic equations of mass transport in porous media, Part 1. Macroscopic balance laws". In: *Advances in Water Resources* 9.4 (Dec. 1986), pp. 196–206. DOI: 10.1016/0309-1708(86)90024-2.

[143] S. Majid Hassanizadeh and Anton Leijnse. "A non-linear theory of high-concentration-gradient dispersion in porous media". In: *Advances in Water Resources* 18.4 (Jan. 1995), pp. 203–215. DOI: 10.1016/0309-1708(95)00012-8.

[144] P. Haupt. *Continuum Mechanics and Theory of Materials*. Springer, 2000.

[145] G. Helmlinger et al. "Solid stress inhibits the growth of multicellular tumor spheroids". In: *Nature Biotechnology* 15.8 (Aug. 1997), pp. 778–783. DOI: 10.1038/nbt0897-778.

[146] R. Hill. "Elastic properties of reinforced solids: Some theoretical principles". In: *Journal of the Mechanics and Physics of Solids* 11.5 (Sept. 1963), pp. 357–372. DOI: 10.1016/0022-5096(63)90036-x.

[147] A. L. Hodgkin and A. F. Huxley. "A quantitative description of membrane current and its application to conduction and excitation in nerve". In: *The Journal of physiology* 117.4 (1952), pp. 500–544.

[148] M. H. Holmes. *Introduction to Perturbation Methods*. Springer New York, 2013. DOI: 10.1007/978-1-4614-5477-9.

[149] M. H. Holmes and V. C. Mow. "The nonlinear characteristics of soft gels and hydrated connective tissues in ultrafiltration." In: *Journal of biomechanics* 23 (11 1990), pp. 1145–1156. ISSN: 0021-9290. DOI: 10.1016/0021-9290(90)90007-P.

[150] M. Hori and S. Nemat-Nasser. "On two micromechanics theories for determining micro–macro relations in heterogeneous solids". In: *Mechanics of Materials* 31.10 (Oct. 1999), pp. 667–682. DOI: 10.1016/s0167-6636(99)00020-4.

[151] Q. Huang, G. Huang, and H. Zhan. "A finite element solution for the fractional advection-dispersion equation". In: *Advances in Water Resources* 31.12 (Dec. 2008), pp. 1578–1589. DOI: 10.1016/j.advwatres.2008.07.002.

[152] T. J. R. Hughes. *The Finite Element Method: Linear Static and Dynamic Finite Element Analysis*. Dover Publications, 2000.

[153] J. D. Humphrey. "Towards a Theory of Vascular Growth and Remodeling". In: *Mechanics of Biological Tissue*. Ed. by Holzapfel G.A. and Ogden R.W. Springer-Verlag, 2006, pp. 3–15.

[154] R. Interian et al. "Tumor growth modelling by cellular automata". In: *Mathematics and Mechanics of Complex Systems* 5.3-4 (Oct. 2017), pp. 239–259. DOI: 10.2140/memocs.2017.5.239.

[155] R. K. Jain, J. D. Martin, and T. Stylianopoulos. "The role of mechanical forces in tumor growth and therapy". In: *Annual Review of Biomedical Engineering* 16 (2014), pp. 321–346. DOI: 10.1146/annurev-bioeng-071813-105259.

[156] C. Jiang et al. "The Anomalous Diffusion of a Tumor Invading with Different Surrounding Tissues". In: *PLoS ONE* 9.10 (Oct. 2014). Ed. by Maria G. Castro, e109784. DOI: 10.1371/journal.pone.0109784.

[157] A. Jüngel and I. V. Stelzer. "Entropy structure of a cross-diffusion tumor-growth model". In: *Mathematical Models and Methods in Applied Sciences* 22.07 (May 2012), p. 1250009. DOI: 10.1142/s0218202512500091.

[158] C.-S. Kim, C. Randow, and T. Sano, eds. *Hybrid and Hierarchical Composite Materials*. Springer International Publishing, 2015. DOI: 10.1007/978-3-319-12868-9.

[159] M. M. Knodel et al. "Synaptic bouton properties are tuned to best fit the prevailing firing pattern". In: *Frontiers in Computational Neuroscience* (2014). DOI: 10.3389/fncom.2014.00101.

[160] M. A. Konerding, E. Fait, and A. Gaumann. "3D microvascular architecture of pre-cancerous lesions and invasive carcinomas of the colon". In: *British Journal of Cancer* 84.10 (2001), pp. 1354–1362. DOI: 10.1054/bjoc.2001.1809.

[161] M. Köpf et al. "Anomalous diffusion of water in biological tissues". In: *Biophysical Journal* 70.6 (June 1996), pp. 2950–2958. DOI: 10.1016/s0006-3495(96)79865-x.

[162] R. Krishna and J.A. Wesselingh. "The Maxwell-Stefan approach to mass transfer". In: *Chemical Engineering Science* 52.6 (Mar. 1996), pp. 861–911. DOI: 10.1016/s0009-2509(96)00458-7.

[163] E. Kröner. "Allgemeine Kontinuumstheorie der Versetzungen und Eigenspannungen". In: *Archive for Rational Mechanics and Analysis* 4.1 (Jan. 1959), pp. 273–334. DOI: 10.1007/bf00281393.

[164] E. Kröner. "Elasticity theory of materials with long range cohesive forces". In: *International Journal of Solids and Structures* 3.5 (Sept. 1967), pp. 731–742. DOI: 10.1016/0020-7683(67)90049-2.

[165] E. Kuhl. "Growing matter: A review of growth in living systems". In: *J. Mech. Behav. Biomed. Mater.* 29 (Jan. 2014), pp. 529–543. DOI: 10.1016/j.jmbbm.2013.10.009.

[166] D. J. Lacks. "Tortuosity and anomalous diffusion in the neuromuscular junction". In: *Physical Review E* 77.4 (Apr. 2008). DOI: 10.1103/physreve.77.041912.

[167] L. D. Landau. *Electrodynamics of continuous media*. Oxford Oxfordshire New York: Pergamon, 1984. ISBN: 9780080302751.

[168] L. D. Landau and E. M. Lifshitz. *Fluid Mechanics*. Elsevier, 1987. DOI: 10.1016/c2013-0-03799-1.

[169] M. Lax and D. F. Nelson. "Maxwell equations in material form". In: *Physical Review B* 13.4 (1976), pp. 1777–1784. DOI: 10.1103/physrevb.13.1777.

[170] D. Le Bihan et al. "Diffusion tensor imaging: concepts and applications". In: *Journal of Magnetic Resonance Imaging* 13.4 (2001), pp. 534–546.

[171] H. A. Leddy and F. Guilak. "Site-specific molecular diffusion in articular cartilage measured using fluorescence recovery after photobleaching". In: *Annals of Biomedical Engineering* 31.7 (2003), pp. 753–760.

[172] H. A. Leddy, M. A. Haider, and F. Guilak. "Diffusional anisotropy in collagenous tissues: fluorescence imaging of continuous point photobleaching". In: *Biophysical Journal* 91.1 (2006), pp. 311–316.

[173] J. I. Lee et al. "Measurement of diffusion in articular cartilage using fluorescence correlation spectroscopy". In: *BMC Biotechnology* 11.1 (2011), p. 19.

[174] E. K. Lenzi et al. "Anomalous diffusion and transport in heterogeneous systems separated by a membrane". In: *Proceedings of the Royal Society A: Mathematical, Physical and Engineering Sciences* 472.2195 (Nov. 2016), p. 20160502. DOI: 10.1098/rspa.2016.0502.

[175] I. S. Liu. "Method of Lagrange multipliers for exploitation of the entropy principle". In: *Archive Rational Mech. Anal.* 46 (1972), pp. 131–148.

[176] B. Loret and F.M.F. Simões. "A framework for deformation, generalized diffusion, mass transfer and growth in multi-species multi-phase biological tissues". In: *Eur. J. Mech. A* 24 (2005), pp. 757–781. DOI: 10.1016/j.euromechsol.2005.05.005.

[177] N. F. Lori et al. "Diffusion tensor fiber tracking of human brain connectivity: aquisition methods, reliability analysis and biological results". In: *NMR in Biomedicine* 15.7-8 (2002), pp. 494–515.

[178] V. A. Lubarda and A. Hoger. "On the mechanics of solids with a growing mass". In: *International Journal of the Mechanics and Physics of Solids* 39 (2002), pp. 4627–4664.

[179] J. Lubliner. *Plasticity Theory*. Dover Publications, Inc., Mineola, New York, 2008.

[180] W. J. Lukiw. "Alzheimer's disease (AD) as a disorder of the plasma membrane". In: *Frontiers in Physiology* 4 (2013). DOI: 10.3389/fphys.2013.00024.

[181] I. Lunati, S. Attinger, and W. Kinzelbach. "Macrodispersivity for transport in arbitrary nonuniform flow fields: Asymptotic and preasymptotic results". In: *Water Resources Research* 38.10 (Oct. 2002), pp. 5–1–5–11. DOI: 10.1029/2001wr001203.

[182] V. E. Lynch et al. "Numerical methods for the solution of partial differential equations of fractional order". In: *Journal of Computational Physics* 192.2 (Dec. 2003), pp. 406–421. DOI: 10.1016/j.jcp.2003.07.008.

[183] P. Macklin, V. Cristini, and J. Lowengrub. "Biological background". In: *Multiscale Modeling of Cancer*. Cambridge University Press, 2010, pp. 8–23. DOI: 10.1017/cbo9780511781452.003.

[184] P. Macklin et al. "Multiscale modelling and nonlinear simulation of vascular tumour growth". In: *Journal of Mathematical Biology* 58.4-5 (Sept. 2009), pp. 765–798. DOI: 10.1007/s00285-008-0216-9.

[185] A. Madeo, F. dell'Isola, and F. Darve. "A continuum model for deformable, second gradient porous media partially saturated with compressible fluids". In: *Journal of the Mechanics and Physics of Solids* 61(11) (2013), pp. 2196–2211. DOI: 10.1177/1081286515616034.

[186] J. Marchena-Menéndez et al. "Macroscopic thermal profile of heterogeneous cancerous breasts. A three-dimensional multiscale analysis". In: *International Journal of Engineering Science* 144 (Nov. 2019), p. 103135. DOI: 10.1016/j.ijengsci.2019.103135.

[187] R. Marin. "The neuronal membrane as a key factor in neurodegeneration". In: *Frontiers in Physiology* 4 (2013). DOI: 10.3389/fphys.2013.00188.

[188] A. Maroudas. "Physicochemical properties of cartilage in the light of ion exchange theory". In: *Biophysical Journal* 8.5 (1968), pp. 575–595.

[189] J. E. Marsden and T. J. R. Hughes. *Mathematical Foundations of Elasticity*. Dover Publications, Inc., Mineola, New York, 1983.

[190] J. E. Marsden and T. J. R. Hughes. *Mathematical Foundations of Elasticity*. Dover Publications, Inc., Mineola, New York, 1983.

[191] P. Mascheroni et al. "An avascular tumor growth model based on porous media mechanics and evolving natural states". In: *Mathematics and Mechanics of Solids* 23.4 (June 2018), pp. 686–712. DOI: 10.1177/1081286517711217.

[192] P. Mascheroni et al. "Predicting the growth of glioblastoma multiforme spheroids using a multiphase porous media model". In: *Biomech. Model. Mechanobiol.* 15.5 (Jan. 2016), pp. 1215–1228. DOI: 10.1007/s10237-015-0755-0.

[193] G. A. Maugin. *Continuum mechanics of electromagnetic solids*. Amsterdam New York New York, N.Y., U.S.A: North-Holland Sole distributors for the U.S.A. and Canada, Elsevier Science Pub. Co, 1988. ISBN: 0444703993.

[194] G. A. Maugin and M. Epstein. "Geometrical material structure of elastoplasticity". In: *Int. J. Plasticity* 14(1-3) (1998), pp. 109–115. DOI: 10.1016/S0749-6419(97)00043-0.

[195] M. M. Meerschaert, J. Mortensen, and S. W. Wheatcraft. "Fractional vector calculus for fractional advection–dispersion". In: *Physica A: Statistical Mechanics and its Applications* 367 (July 2006), pp. 181–190. DOI: 10.1016/j.physa.2005.11.015.

[196] M. M. Meerschaert and C. Tadjeran. "Finite difference approximations for two-sided space-fractional partial differential equations". In: *Applied Numerical Mathematics* 56.1 (Jan. 2006), pp. 80–90. DOI: 10.1016/j.apnum.2005.02.008.

[197] A. Menzel. "A fibre reorientation model for orthotropic multiplicative growth. Configurational driving stresses, kinematics-based reorientation and algorithmic aspects". In: *Biomechan. Model. Mechanobiol.* 6(5) (2007), pp. 303–320. DOI: 10.1007/s10237-006-0061-y.

[198] A. Menzel. "Modelling of anisotropic growth in biological tissues — A new approach and computational aspects". In: *Biomechan. Model. Mechanobiol.* 3 (2005), pp. 147–171. DOI: 10.1007/s10237-004-0047-6.

[199] A. Menzel and E. Kuhl. "Frontiers in growth and remodeling". In: *Mechanics Research Communications* 42 (2012), pp. 1–14. DOI: 10.1016/j.mechrescom.2012.02.007.

[200] R. Metzler and J. Klafter. "The random walk's guide to anomalous diffusion: a fractional dynamics approach". In: *Physics Reports* 339.1 (Dec. 2000), pp. 1–77. DOI: 10.1016/s0370-1573(00)00070-3.

[201] M. Mićunović. *Thermomechanics of Viscoplasticity*. Springer New York, 2009. DOI: 10.1007/978-0-387-89490-4.

[202] G. W. Milton. *The Theory of Composites*. Cambridge University Press, 2002. DOI: 10.1017/cbo9780511613357.

[203] M. Minozzi et al. "Growth-induced compatible strains". In: *Math. Mech. Solids* 22.1 (Aug. 2017), pp. 62–71. DOI: 10.1177/1081286515570510.

[204] W. Mueller-Klieser, J. P. Freyer, and R. M. Sutherland. "Influence of glucose and oxygen supply conditions on the oxygenation of multicellular spheroids". In: *British Journal of Cancer* 53.3 (Mar. 1986), pp. 345–353. DOI: 10.1038/bjc.1986.58.

[205] W. F. Mueller-Klieser and R. M. Sutherland. "Oxygen tensions in multicell spheroids of two cell lines". In: *British Journal of Cancer* 45.2 (Feb. 1982), pp. 256–264. DOI: 10.1038/bjc.1982.41.

[206] I. Muha et al. "Effective diffusivity in membranes with tetrakaidekahedral cells and implications for the permeability of human stratum corneum". In: *Journal of Membrane Science* 368.1-2 (Feb. 2011), pp. 18–25. DOI: 10.1016/j.memsci.2010.10.020.

[207] T. Mura. *Micromechanics of defects in solids*. Springer Netherlands, 1987. DOI: 10.1007/978-94-009-3489-4.

[208] D. F. Nelson. *Electric, Optic, and Acoustic Interactions in Dielectrics*. Wiley & Sons, 1979. ISBN: 0-471-05199-3.

[209] S. P. Neuman and D. M. Tartakovsky. "Perspective on theories of non-Fickian transport in heterogeneous media". In: *Advances in Water Resources* 32.5 (May 2009), pp. 670–680. DOI: 10.1016/j.advwatres.2008.08.005.

[210] G. Nguetseng. "A General Convergence Result for a Functional Related to the Theory of Homogenization". In: *SIAM Journal on Mathematical Analysis* 20.3 (May 1989), pp. 608–623. DOI: 10.1137/0520043.

[211] K. Nishimoto. *Fractional Calculus: Integrations and Differentiations of Arbitrary Order*. University of New Haven Press, 1989.

[212] K. B. Oldham and J. Spanier. *The Fractional Calculus. Theory and Applications of Differentiation and Integration to Arbitrary Order*. Elsevier Science, 1974. ISBN: 0-12-525550-0.

[213] T. Olsson and A. Klarbring. "Residual stresses in soft tissue as a consequence of growth and remodeling: application to an arterial geometry". In: *Eur. J. Mech. A* 27(6) (2008), pp. 959–974. DOI: 10.1016/j.euromechsol.2007.12.006.

[214] M. Ostoja-Starzewski et al. "From fractal media to continuum mechanics". In: *ZAMM - Journal of Applied Mathematics and Mechanics / Zeitschrift für Angewandte Mathematik und Mechanik* 94.5 (Jan. 2013), pp. 373–401. DOI: 10.1002/zamm.201200164.

[215] P. Paradisi et al. "A generalized Fick's law to describe non-local transport effects". In: *Physics and Chemistry of the Earth, Part B: Hydrology, Oceans and Atmosphere* 26.4 (Jan. 2001), pp. 275–279. DOI: 10.1016/s1464-1909(01)00006-5.

[216] R. Penta and D. Ambrosi. "The role of the microvascular tortuosity in tumor transport phenomena". In: *Journal of Theoretical Biology* 364 (Jan. 2015), pp. 80–97. DOI: 10.1016/j.jtbi.2014.08.007.

[217] R. Penta, D. Ambrosi, and A. Quarteroni. "Multiscale homogenization for fluid and drug transport in vascularized malignant tissues". In: *Mathematical Models and Methods in Applied Sciences* 25.01 (Nov. 2014), pp. 79–108. DOI: 10.1142/s0218202515500037.

[218] R. Penta, D. Ambrosi, and R. J. Shipley. "Effective governing equations for poroelastic growing media". In: *Q. Jl Mech. Appl. Math* 67.1 (2014), pp. 69–91. DOI: 10.1093/qjmam/hbt024.

[219] R. Penta and A. Gerisch. "An Introduction to Asymptotic Homogenization". In: *Lecture Notes in Computational Science and Engineering*. Springer International Publishing, 2017, pp. 1–26.

[220] R. Penta et al. *Constitutive Modelling of Solid Continua*. Ed. by José Merodio and Raymond Ogden. Springer International Publishing, 2020. DOI: 10.1007/978-3-030-31547-4.

[221] R. Penta et al. "Porosity and Diffusion in Biological Tissues. Recent Advances and Further Perspectives". In: *Constitutive Modelling of Solid Continua*. Springer International Publishing, Nov. 2020, pp. 311–356.

[222] Raimondo Penta and Alf Gerisch. "Investigation of the potential of asymptotic homogenization for elastic composites via a three-dimensional computational study". In: *Computing and Visualization in Science* 17.4 (Aug. 2015), pp. 185–201. DOI: 10.1007/s00791-015-0257-8.

[223] S. Pezzuto and D. Ambrosi. "Active contraction of the cardiac ventricle and distortion of the microstructural architecture". In: *International Journal for Numerical Methods in Biomedical Engineering* 30(12) (2014), pp. 1578–1596. DOI: 10.1002/cnm.2690.

[224] I. Podlubny. *Fractional Differential Equations: An Introduction to Fractional Derivatives, Fractional Differential Equations, to Methods of Their Solution and Some of Their Applications (ISSN Book 198)*. Academic Press, 1998. ISBN: 9780080531984.

[225] A. Poulenard and M. Ovsjanikov. "Multi-directional geodesic neural networks via equivariant convolution". In: *ACM Transactions on Graphics* 37.6 (Dec. 2018), pp. 1–14. DOI: 10.1145/3272127.3275102.

[226] S. Preston and M. Elzanowski. "Material Uniformity and the Concept of the Stress Space". In: *Continuous Media with Microstructure*. Ed. by Bettina Albers. 1st ed. Springer-Verlag Berlin Heidelberg, 2010, pp. 91–101. DOI: 10.1007/978-3-642-11445-8.

[227] L. Preziosi, D. Ambrosi, and C. Verdier. "An elasto-visco-plastic model of cell aggregates". In: *J. Theor. Biol.* 262(1) (2010), pp. 35–47. DOI: 10.1016/j.jtbi.2009.08.023.

[228] L. Preziosi and G. Vitale. "A multiphase model of tumor and tissue growth including cell adhesion and plastic reorganization". In: *Math. Models Methods Appl. Sci.* 21.09 (Sept. 2011), pp. 1901–1932. DOI: 10.1142/S021820251-1005593.

[229] E. Pruchnicki. "Hyperelastic homogenized law for reinforced elastomer at finite strain with edge effects". In: *Acta Mechanica* 129.3-4 (Sept. 1998), pp. 139–162. DOI: 10.1007/bf01176742.

[230] H. Qian, M. P. Sheetz, and E. L. Elson. "Single particle tracking. Analysis of diffusion and flow in two-dimensional systems". In: *Biophysical Journal* 60.4 (1991), pp. 910–921.

[231] S. Quiligotti. "On bulk growth mechanics of solid-fluid mixtures: kinematics and invariance requirements". In: *Theoret. Appl. Mech.* 28-29 (2002), pp. 277–288.

[232] S. Quiligotti, G. A. Maugin, and F. dell'Isola. "An Eshelbian approach to the nonlinear mechanics of constrained solid-fluid mixtures". In: *Acta Mech.* 160 (2003), pp. 45–60. DOI: 10.1007/s00707-002-0968-z.

[233] T. M. Quinn and V. Morel. "Microstructural modeling of collagen network mechanics and interactions with the proteoglycans gel in articular cartilage". In: *Biomech. Model. Mechanobiol.* 6 (2007), pp. 73–82. DOI: 10.1007/s10237-006-0036-z.

[234] Y. Rabotnov. *Elements of Hereditary Solid Mechanics*. Mir, 1977.

[235] A. Ramírez-Torres, S. Di Stefano, and A. Grillo. "Influence of non-local diffusion in avascular tumour growth". In: *Mathematics and Mechanics of Solids* 26.9 (Jan. 2021), pp. 1264–1293. DOI: 10.1177/1081286520975086.

[236] A. Ramírez-Torres, V. Napoli, and A. Grillo. "Fractional versus fractal formulation of the Poisson–Nernst–Plack model for the propagation of the membrane potential in neurons". In: *(In Preparation)* (2022).

[237] A. Ramírez-Torres et al. "An asymptotic homogenization approach to the microstructural evolution of heterogeneous media". In: *International Journal of Non-Linear Mechanics* 106 (Nov. 2018), pp. 245–257. DOI: 10.1016/j.ijnonlinmec.2018.06.012.

[238] A. Ramírez-Torres et al. "Biomechanic approach of a growing tumor". In: *Mechanics Research Communications* 51 (July 2013), pp. 32–38. DOI: 10.1016/j.mechrescom.2013.04.006.

[239] A. Ramírez-Torres et al. "The role of malignant tissue on the thermal distribution of cancerous breast". In: *Journal of Theoretical Biology* 426 (Aug. 2017), pp. 152–161. DOI: 10.1016/j.jtbi.2017.05.031.

[240] A. Ramírez-Torres et al. "Three scales asymptotic homogenization and its application to layered hierarchical hard tissues". In: *International Journal of Solids and Structures* 130-131 (Jan. 2018), pp. 190–198. DOI: 10.1016/j.ijsolstr.2017.09.035.

[241] Ariel Ramírez-Torres, Raimondo Penta, and Alfio Grillo. "Two-scale, nonlocal diffusion in homogenised heterogeneous media". In: *Archive of Applied Mechanics* (Mar. 2021). DOI: 10.1007/s00419-020-01880-3.

[242] E. K. Rodríguez, A. Hoger, and A. D. McCullogh. "Stress-dependent finite growth in soft elastic tissues". In: *Journal of Biomechanics* 27 (1994), pp. 455–467. DOI: 10.1016/0021-9290(94)90021-3.

[243] R. Rodríguez–Ramos et al. "Computation of the relaxation effective moduli for fibrous viscoelastic composites using the asymptotic homogenization method". In: *International Journal of Solids and Structures* 190 (2020), pp. 281–290. DOI: 10.1016/j.ijsolstr.2019.11.014.

[244] J. P. Roop. "Computational aspects of FEM approximation of fractional advection dispersion equations on bounded domains in $\mathbb{R}^2$". In: *Journal of Computational and Applied Mathematics* 193.1 (Aug. 2006), pp. 243–268. DOI: 10.1016/j.cam.2005.06.005.

[245] T. Roose, S. J. Chapman, and P. K. Maini. "Mathematical Models of Avascular Tumor Growth". In: *SIAM Review* 49.2 (Jan. 2007), pp. 179–208. DOI: 10.1137/s0036144504446291.

[246] S. Sadik and A. Yavari. "On the origins of the idea of the multiplicative decomposition of the deformation gradient". In: *Mathematics and Mechanics of Solids* 22.4 (Oct. 2017), pp. 771–772. DOI: 10.1177/1081286515612280.

[247] S. Salsa. *Partial Differential Equations in Action: From Modelling to Theory*. New York: Springer, 2008.

[248] S. Salsa et al. "Elementi di analisi funzionale". In: *UNITEXT*. Springer Milan, 2009, pp. 259–324.

[249] S. G. Samko, A. A. Kilbas, and O. I. Marichev. *Fractional Integrals and Derivatives: Theory and Applications*. Gordon and Breach Science Publishers, 1993.

[250] E. Sanchez-Palencia. *Non-Homogeneous Media and Vibration Theory*. Springer Berlin Heidelberg, 1980. DOI: 10.1007/3-540-10000-8.

[251] A. Sapora, P. Cornetti, and A. Carpinteri. "Diffusion problems on fractional nonlocal media". In: *Open Physics* 11.10 (Jan. 2013). DOI: 10.2478/s11534-013-0323-0.

[252] A. Sapora et al. "Nonlocal Diffusion in Porous Media: A Spatial Fractional Approach". In: *Journal of Engineering Mechanics* 143.5 (May 2017). DOI: 10.1061/(asce)em.1943-7889.0001105.

[253] S. C. Schonsheck, B. Dong, and R. Lai. "Parallel Transport Convolution: A New Tool for Convolutional Neural Networks on Manifolds". In: *arXiv preprint* (May 2018).

[254] G. Sciarra, G. A. Maugin, and K. Hutter. "A variational approach to a micro-structured theory of solid-fluid mixtures". In: *Archive of Applied Mechanics* 73 (2003), pp. 194–224. DOI: 10.1007/s00419-003-0279-4.

[255] G. Sciumè et al. "A multiphase model for three-dimensional tumor growth". In: *New J. Phys.* 15.1 (Jan. 2013), p. 015005. DOI: 10.1088/1367-2630/15/1/015005.

[256] A. C. Scott. "The electrophysics of a nerve fiber". In: *Reviews of Modern Physics* 47.2 (1975), p. 487.

[257] M. Sen and E. Ramos. "A Spatially Non-Local Model for Flow in Porous Media". In: *Transport in Porous Media* 92.1 (Oct. 2011), pp. 29–39. DOI: 10.1007/s11242-011-9889-4.

[258] S. A. Silling. "Origin and effect of nonlocality in a composite". In: *Journal of Mechanics of Materials and Structures* 9.2 (May 2014), pp. 245–258. DOI: 10.2140/jomms.2014.9.245.

[259] J. H. Smith et al. "How neurons exploit fractal geometry to optimize their network connectivity". In: *Scientific Reports* 11.1 (Jan. 2021). DOI: 10.1038/s41598-021-81421-2.

[260] S. L. Sobolev. "Nonlocal diffusion models: Application to rapid solidification of binary mixtures". In: *International Journal of Heat and Mass Transfer* 71 (Apr. 2014), pp. 295–302. DOI: 10.1016/j.ijheatmasstransfer.2013.12.048.

[261] A. Solbrå et al. "A Kirchhoff-Nernst-Planck framework for modeling large scale extracellular electrodiffusion surrounding morphologically detailed neurons". In: *PLOS Computational Biology* 14.10 (Oct. 2018). Ed. by Ernest Barreto, e1006510. DOI: 10.1371/journal.pcbi.1006510.

[262] T. Stylianopoulos et al. "Causes, consequences, and remedies for growth-induced solid stress in murine and human tumors". In: *PNAS* 109(38) (2012), pp. 15101–15108.

[263] T. Stylianopoulos et al. "Coevolution of Solid Stress and Interstitial Fluid Pressure in Tumors During Progression: Implications for Vascular Collapse". In: *Cancer Research* 73.13 (Apr. 2013), pp. 3833–3841. DOI: 10.1158/0008-5472.can-12-4521.

[264] N. Svanstedt, J. Wyller, and E. Malyutina. "A one-population Amari model with periodic microstructure". In: *Nonlinearity* 27.6 (May 2014), pp. 1391–1417. DOI: 10.1088/0951-7715/27/6/1391.

[265] L. A. Taber. "Biomechanics of Growth, Remodeling, and Morphogenesis". In: *Appl. Mech. Rev.* 48.8 (1995), p. 487. DOI: 10.1115/1.3005109.

[266] V. E. Tarasov. "Electromagnetic field of fractal distribution of charged particles". In: *Physics of plasmas* 12.8 (2005), p. 082106.

[267] V. E. Tarasov. "Fractional vector calculus and fractional Maxwell's equations". In: *Annals of Physics* 323.11 (Nov. 2008), pp. 2756–2778. DOI: 10.1016/j.aop.2008.04.005.

[268] V. E. Tarasov and G. M. Zaslavsky. "Fractional dynamics of systems with long-range interaction". In: *Communications in Nonlinear Science and Numerical Simulation* 11.8 (Dec. 2006), pp. 885–898. DOI: 10.1016/j.cnsns.2006.03.005.

[269] A. Tomic, A. Grillo, and S. Federico. "Poroelastic Materials Reinforced by Statistically Oriented Fibres - Numerical Implementation and Application to Articular Cartilage". In: *IMA Journal of Applied Mathematics* 79 (2014), pp. 1027–1059. DOI: 10.1093/imamat/hxu039.

[270] T. J. Vaughan, C. T. McCarthy, and L. M. McNamara. "A three-scale finite element investigation into the effects of tissue mineralisation and lamellar organisation in human cortical and trabecular bone". In: *Journal of the Mechanical Behavior of Biomedical Materials* 12 (Aug. 2012), pp. 50–62. DOI: 10.1016/j.jmbbm.2012.03.003.

[271] A. S. Verkman. "Solute and macromolecule diffusion in cellular aqueous compartments". In: *Trends in Biochemical Sciences* 27.1 (2002), pp. 27–33.

[272] A. Visintin. "Towards a two-scale calculus". In: *ESAIM: Control, Optimisation and Calculus of Variations* 12.3 (June 2006), pp. 371–397. DOI: 10.1051/cocv:2006012.

[273] P. R. Wills, D. J. Scott, and D. J. Winzor. "Thermodynamics and Thermodynamic Nonideality". In: *Encyclopedia of Biophysics*. Ed. by G. C. K. Roberts. Springer, Berlin Heidelberg, 2013, pp. 2583–2589. DOI: https://doi.org.10.1007/978-3-642-16712-6_287.

[274] W. Wilson et al. "Prediction of collagen orientation in articular cartilage by a collagen remodeling algorithm". In: *Osteoarthr. Cartil.* 14 (2006), pp. 1196–1202. DOI: 10.1016/j.joca.2006.05.006.

[275] Y. Xia et al. "Diffusion and relaxation mapping of cartilage-bone plugs and excised disks using microscopic magnetic resonance imaging". In: *Magnetic Resonance in Medicine* 31.3 (1994), pp. 273–282.

[276] Y. Xia et al. "Self-diffusion monitors degraded cartilage". In: *Archives of Biochemistry and Biophysics* 323.2 (1995), pp. 323–328.

[277] K. Xylouris, G. Queisser, and G. Wittum. "A three-dimensional mathematical model of active signal processing in axons". In: *Computing and Visualization in Science* 13.8 (Dec. 2010), pp. 409–418. DOI: 10.1007/s00791-011-0155-7.

[278] K. Xylouris and G. Wittum. "A three-dimensional mathematical model for the signal propagation on a neuron's membrane". In: *Frontiers in Computational Neuroscience* 9 (July 2015). DOI: 10.3389/fncom.2015.00094.

[279] K. Xylouris and G. Wittum. "A three-dimensional model of a gap junction". In: *Il Nuovo Cimento C* 32 (2009), pp. 231–238. ISSN: 03905551, 03905551. DOI: 10.1393/ncc/i2009-10353-4.

[280] V. Želi and D. Zorica. "Analytical and numerical treatment of the heat conduction equation obtained via time-fractional distributed-order heat conduction law". In: *Physica A: Statistical Mechanics and its Applications* 492 (Feb. 2018), pp. 2316–2335. DOI: 10.1016/j.physa.2017.11.150.

[281] M. Zingales. "Fractional-order theory of heat transport in rigid bodies". In: *Communications in Nonlinear Science and Numerical Simulation* 19.11 (Nov. 2014), pp. 3938–3953. DOI: 10.1016/j.cnsns.2014.04.004.

This Ph.D. thesis has been typeset by means of the TEX-system facilities. The typesetting engine was pdfLATEX. The document class was `toptesi`, by Claudio Beccari, with option `tipotesi=scudo`. This class is available in every up-to-date and complete TEX-system installation.